Excerpts from

PROCESSES IN BIOLOGICAL VISION:

including,

ELECTROCHEMISTRY OF THE NEURON

This material is excerpted from the full β-version of the text. The final printed version will be more concise due to further editing and economical constraints. A Table of Contents and an index are located at the end of this paper.

James T. Fulton
Vision Concepts
jtfulton@neuronresearch.net

Updated November 20, 2018

Copyright 2001 James T. Fulton

14 Tertiary Processing--Signal Encoding, Transmission & Decoding [1]

This Chapter remains in editorial review at this time. However, the materials in some Sections are important and need to be available for comment as soon as possible. Since tertiary processing is applicable to all sensory, motor and CNS signaling, the chapter is being broadened to apply to all of these applications. Some sections will only be of interest to selected readers.

[xxx collect material from Sections 9.3.1 thru 9.3.6 and 10.8.7 into this chapter]

14.1 Introduction

This chapter will address the synapse, the modulatable driven multvibrator associated with the luminance and other monopolar signaling channels of vision, and the modulatable free-runnning multivibrators associated with the chrominance and other bipolar signaling channels of vision. While the synapse is the simplest form, it will be addressed last in order to establish the appropriate context first.

The primary reason for the existence of tertiary signaling is one of efficiency. The primary responsibility of tertiary signaling related to the afferent neural system is to connect the sensory neurons of each sensing modality in the peripheral nervous system to the central nervous system efficiently. It has a similar responsibility in connecting the CNS to the remote elements of the efferent neural system. In the higher animals, it also has a similar responsibility to interconnect the myriad, and widely dispersed, individual engines of the CNS efficiently.

Tertiary signaling consists of a group of mechanism that are closely related functionally but quite disparate technologically. At the top level, these mechanisms include:

1. Electro-magnetic signal propogation over specialized (myelinated) axons in place of the previously widely assumed transmission by electrical charge diffusion.

2. Computational anatomy, the spatial rearrangement of parallel neural signal channels, to achieve complex signal processing objectives without requiring transcendental calculations (such as a Fourier transform or other trigonometric calculations)

3. Signal route conservation through sophisticated signal path sharing and dispersed signal processing engines.

Much of the material in the initial sections of this Chapter may be unfamiliar to the reader. To understand the operation of the signal processing associated with signal projection within the neural system requires some knowledge of signaling theory, a subject far removed from conventional biology, is necessary. Some of the material may appear ethereal in the absence of the appropriate formal training. If the material in **Sections 14.2** through **Section 14.4** appears entirely foreign, the reader can proceed to **Section 14.5** which concentrates on the implementation of the signal projection circuits at a less abstract level.

The coding mechanisms used in biological vision are quite sophisticated. The variety of techniques used has only been rivaled in man-made systems introduced commercially and industrially during the 1990's. As an example, the system appears to employ diversity encoding to reduce the number of physical signal paths within the optic nerve to a number far below the number of photoreceptor cell outputs. Yet little information is lost that is important to the animals well being. Only less important information is lost. Diversity encoding has only recently appeared in commercial products under one of its subcategories, spread spectrum technology. Equally important, the visual system does not attempt to transmit stationary scene information to the brain repeatedly. It only transmits changes in scene details. This approach has recently been implemented in satellite-to-home television in order to transmit hundreds of television signals within the space usually used by only a few.

---

[1]Released: 20 November 2018

2 Processes in Biological Vision

14.1.1 Original perspective of chapter

The initial focus of this Chapter was to be on the character of the signaling path between the signal processing elements of the retina and the central nervous system. It was originally described as Stage 3 in the visual system because of its sequential position following the signal processing within the retina, Stage 2. This signaling path is the dominant, although not exclusive, constituent of the morphological feature generically known as the optic nerve. However, it soon became clear that this type of signaling path had much wider utilization within the visual and nervous systems. It is the method of choice wherever it is necessary to project signals over distances greater than a few millimeters. Thus the signaling techniques used in the optic nerve are the same as those used in the commissure connecting various engines within the central nervous system (CNS). They are also the same as those used in both the efferent and afferent paths of the peripheral nervous system (PNS). In the general case, the label Stage 3 can be used to generically describe any signal projection circuit within the nervous system. In the hierarchal sense, the label applies to the signaling originating with the ganglion cells of the retina and terminating with the stellate cells of the CNS. However, all of the commissure and all of the signal paths of the PNS share this same topology, although different morphological names are frequently assigned to the originating and terminating circuits (neurons). In all of these channels, the label Node of Ranvier is used to describe the signal regenerating features found along these signal paths.

There is a significant problem in comparing the proposed performance of Stage 3 circuits with the available literature. First, no data could be found that actually isolated only the Stage 3 circuits and quantified their performance. The data has traditionally been obtained by stimulating the visual system with light and recording a stream of action potentials at some location in the visual system. The resulting data represents the response of Stage 1, Stage 2 and Stage 3 circuits (and sometimes Stage 4 circuits) in cascade. Second, the selection of the recording point has generally been opportunistic. Either the retina, the LGN or a location in the occipital cortex has been probed until a pulse stream was located. The response of this pulse stream to imaging light has then been determined, generally using broad band spectral filters that did not isolate an individual spectral channel. Third, lacking an adequate model of the visual system, the recorded pulse streams have not been adequately identified as to their purpose or to the signal manipulations preceding their recording. This has led to discussions focusing on selected signals from a matrix of center-surround concepts where the center and the surround may vary both spatially and spectrally (in an uncontrolled manner). Fourth, many investigators have impaled a ganglion (or eccentric) cell in the region forward of the hillock. The waveforms recorded at such a site is very complex. It frequently shows one or more action potential pulses superimposed on the analog waveform causing the action potentials. The data of Purple & Dodge discussed below illustrates this format well. Their data does not illustrate the detailed performance of Stage 3. However, it can be further deconvolved to give a clearer insight. Care is required in interpreting these waveforms. As a result of these problems, data in the literature may be interpreted differently based on the model proposed in this work than it was in the original publication.

Fortuitously, the signals recorded by probing the axonal segment of ganglion (and eccentric) cells exhibit both the output signal, F1, from the circuit superimposed on an amplified version of the input signal, E', driving the circuit (the notation is explained below).

Most of the earlier investigators have shied away from recording luminance channel information because of the difficult in locating channels that do not produce a continuous stream of action potentials. After locating a continuous stream of action potentials, the investigators frequently note that the input stimulus either causes an increase or a decrease in the frequency of the action potential stream. They have then spoken of an on- or off-signal, in terms of whether it causes an increase or a decrease in this frequency, without any reference to the intervening signal processing creating the pulse stream. As a result, confusion has been inherent in attempting to describe these signals. This framework of terminology has not contributed to an understanding of the operation of the visual system.

It will be shown here that continuous action potential pulse streams are inherently associated with bipolar signals (not bipolar cells) resulting from signal processing in Stage 2. It is important to determine whether these signals are created in the first lateral matrix, the second lateral matrix or as part of a diversity encoding matrix associated with Stage 3 before attempting to characterize them. Only in this way can the appropriate designation be applied to them..

14.1.2 Plan of discussion EXPAND

The signal encoding and decoding function in animal vision has not received the attention it deserves in the field of vision research. This is due to three reasons:

1. The physical difficulty of accessing the individual elements of the system for signal recording purposes. While it is relatively easy to penetrate the axonal membrane (axolemma) and contact the axoplasm with an electrical probe, it is much more difficult to access a dendroplasm or podaplasm.

2. The failure of the biological community to recognize the intrinsically electrolytic nature of the nervous system.

3. The relative sophistication of the encoding schemes--which has not been recognized in the past by the typical biological investigator who had no training in signal and modulation theory.

In general, the purpose of Stage 3 signal processing (subsequently to be described as signal projection) is straight forward:

1. Encode all of the information received by the input neurons in as compact a form as possible compatible with efficient recovery of the data at the output neurons using simple realizable circuits.

2. Provide a signaling method that insures minimal signal loss (and signal distortion) over the signaling path lengths required.

3. Provide adequate signaling circuit reliability over the life span of the animal.

This chapter will develop the details associated with each of the above purposes.

14.1.3 Background (using vision as a framework)

14.1.3.1 Fundamental physical architectures of the Phylogenic Tree

[xxx move this material to PBV chap 1 or 2?]
The visual system in each phyla exhibit a different fundamental physical (morphological) architecture. The form of this architecture can be related generally to the functional requirements dictated by the environment occupied by the animal. These requirements are hierarchal and begin at a very basic level. They include requirements related to:

+ The circadian rhythm (if any) of the illumination found in the local environment.

+ The operating cycle of the animal (generally associated with its internal temperature environment).

+ The life expectancy of the animal.

+ The location of the eyes relative to the remainder of the body.

+ The distance between the retinas and the nearest subsequent signal processing functions (engines).

+ The flexibility between the eyes and the local portion of the body

As in other features found within a Phylogenic Tree, there is frequently a large variety of mechanisms and modifications introduced within different species to optimize their functionality within their environmental niche. In some primitive and transitional types, it becomes difficult to separate the circuit elements into clearly defined stages. Limulus is a clear example of the merging of the signal processing and signal projection functions within a single neural circuit. The following discussions are designed to highlight the nominal architecture of the different phyla and do not attempt to describe all of the variations therein.

14.1.3.1.1 Architecture of Arthropoda

The simplest visual and neural architecture beyond the photospots of *Annelida* appears to be that of *Arthropoda*. Gouras has provided an architectural plan and other information for the visual system of honey bee[2]. As shown in **Figure 14.1.3-1**, the retina of the eye is immediately adjacent to, or a subsection of, the brain. All of the axons of the photoreceptors are very short and synapse directly with the neurons within the Lamina, LA. The length of these

[2]Gouras, P. (1991) The Perception of Colour. Volume 6 of Vision and Visual Dysfunction. Boca Raton, FL: CRC Press. pp 276-277

axons is normally measured in microns. Gouras makes no note of any tonic signals between the photoreceptors and the Lamina. He does note tonic signals being passed between the feature extraction engines of the brain, primarily between the medulla, ME and the lobula, LO. There are no eyelids or other muscle-controlled features associated with the eyes that would require signals to be fed back to the eyes from the brain.

It is proposed that there is no Stage 3, involving signal projection by action potentials, between the retina and the first signal extraction engine of the brain in most if not all of *Arthropoda*.

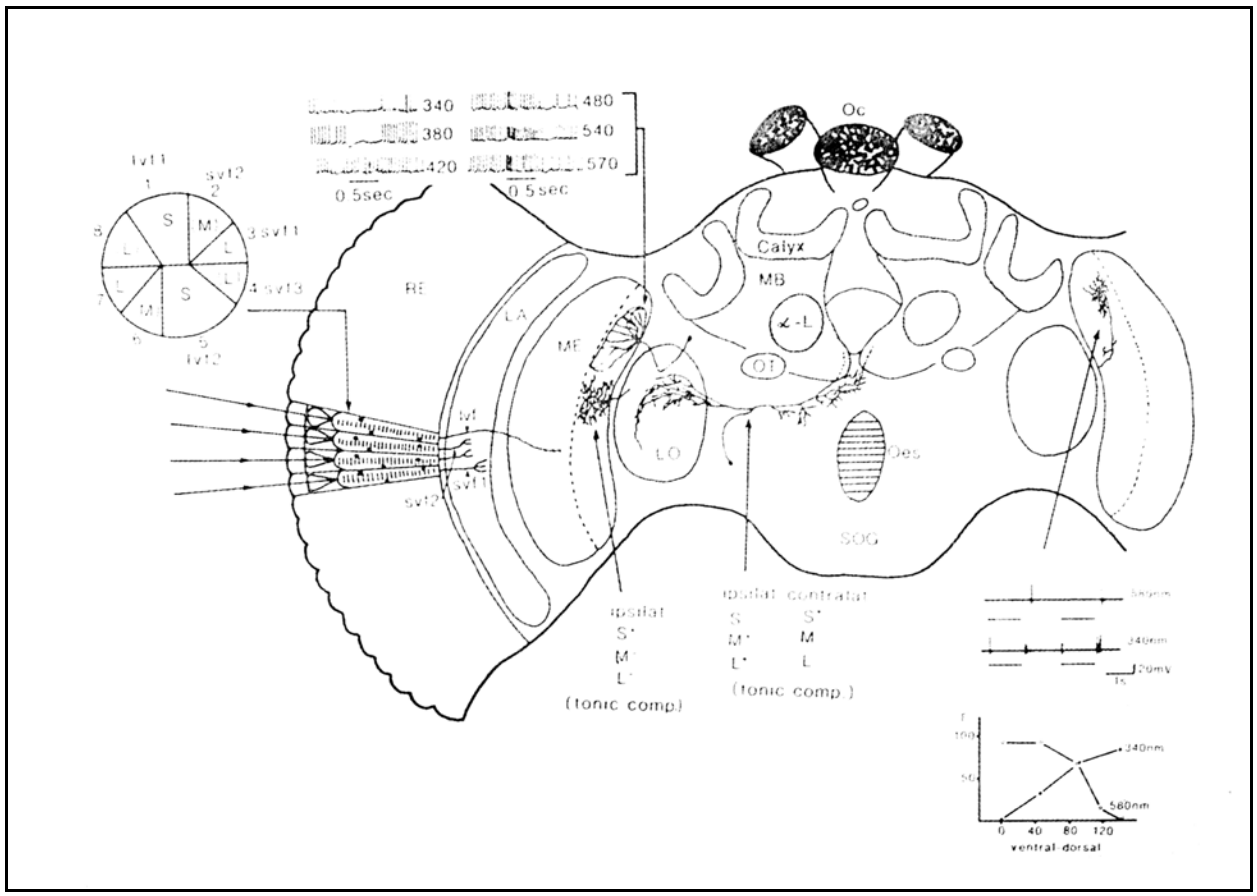

Figure 14.1.3-1 Architecture of the visual system of *Arthropoda* , specifically the honey bee. Note the notation referring to the tonic component of the neural signals leaving but not entering the lamina, LA. See the source for the details related to this figure. From Gouras, 1991.

14.1.3.1.2 Architecture of *Mollusca*

The physical architecture found in (particularly the higher members of) *Mollusca* is quite different from *Arthropoda*. As seen in **Figure 14.1.3-2** from Young, there is a much cleared differentiation between the neurons of the retina and the neurons of the first feature extraction engines of the brain. While the distances remain short in many smaller species, they can become substantial in the larger *Cephalopods*. Furthermore, to effectively occupy its environmental niche, *Cephalopods* have a need to image their surroundings without relying on external motions. This is most effectively accomplished by moving the eyes relative to the head. Thus, there is a need to hinge the eyes relative to the head of the animal, at least relative to one axis. This functional need appears to account for the crossing of the neural paths between the retina and the brain (that only occurs relative to one axis of vision). As a result, the line of fixation of the eye can be made to oscillate in one plane relative to the scene. While the motion only amounts to a small fraction of a degree, it is commensurate with the magnitude of the tremor found in *Chordata*. In the architectural context, the extended length of the axons of the photoreceptors and their crossing on the way to the brain in *Mollusca* is analogous to the optic nerves and optic xxx in *Chordata*. The literature reports a different method of packaging of the axons within the optic nerve of *Mollusca* compared to that in *Chordata*. In the nominal case, the axons of *Mollusca* are not myelinated. Myelination of individual axons plays an important role in reducing the capacitance per unit length of axons. To overcome this shortcoming, the optic nerves of Mollusca frequently employ another capacitance reducing mechanism. The axons are closely packed.

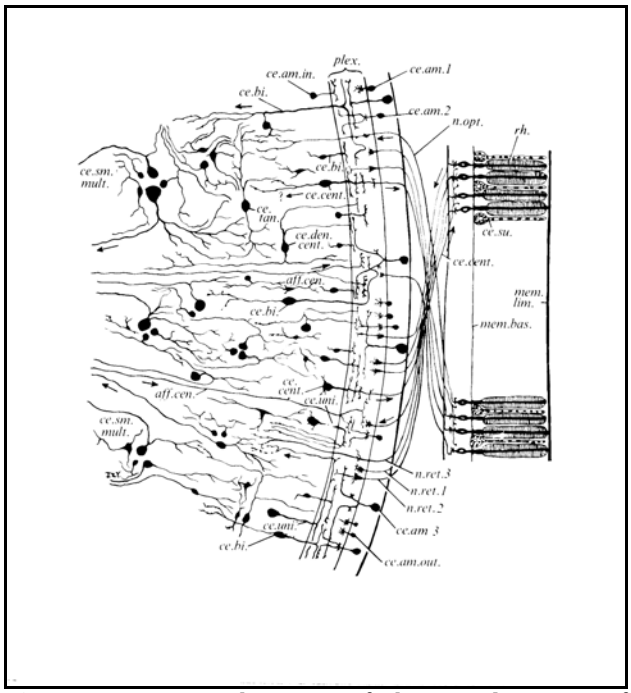

Figure 14.1.3-2 Architecture of the visual system of *Mollusca.* From Young (1971).

14.1.3.1.3 Architecture of *Chordata*

The physical architecture of *Chordata* has been designed to provide maximum rotational flexibility between the eye and the eye socket. When combined with the potential rotational flexibility between the head and the body, this flexibility leads to a very flexible system for surveying (and searching) a very wide total field of view. In the case of some chordates, the eyes operate independently. This allows even greater flexibility in surveying essentially a complete spherical object space. This capability requires considerable lengthening of the optic nerve between the retina and the initial feature extraction engines of the brain, particularly in the larger members of the phylum.

Virtually no research has been reported concentrating on the length of the optic nerve in *Chordata,* or more specifically in humans. **Figure 14.1.3-3** provides a simple plan view of the visual path in humans designed to emphasize the required length of the optic nerve, and more importantly the individual axons from the photoreceptor cells. The minimum axon length is typically xxx mm and the longest may exceed xxx mm when the circumferential length of the retinal cup is considered. These distances place a requirement on the visual system to minimize signal deterioration when projecting signals over these distances. The requirement relates to even longer distances in other species. It is this requirement that initially led to the use of myelinated axons, the introduction of pulse encoding and finally the introduction of Nodes of Ranvier in *Chordata*.

When viewed from a three dimensional perspective, the eyes of the human have been placed very close to the midbrain in order to minimize the distance between the retina and the initial feature extraction engines located in the midbrain. Similarly, the distance between the superior colliculus and the oculomotor neurons has also been minimized.

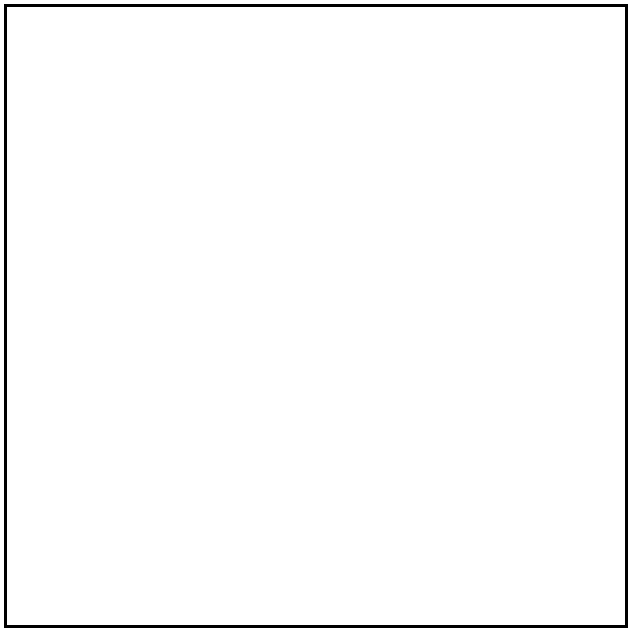

Figure 14.1.3-3 Architecture of the visual system of *Chordata*. Empty xxx

14.1.3.3.2 Description of the signal projection paths in *Chordata*

By examining an overall block diagram of the visual system of *Chordata*, the signal projection paths are easily highlighted. These paths include both the afferent signal paths associated with sensing and the efferent signal paths associated with pointing, focus and light intensity control. These paths are highlighted in **Figure 14.1.3-4**. The path leading to the original definition of a Stage 3 functional circuit is shown in the upper left. However, all of the enumerated signal projection circuits exhibit the same functional characteristics as this initial path. The original stage definitions were listed in **Section 1.5.1.2.2** and detailed in **Section 11.1.4.2**.

As discussed and illustrated in Chapter 15, there are hundreds, if not thousands, of commissure within the brain. These are all signal projection circuits with operational characteristics virtually identical to the projection circuits within the optic nerve. There are also inputs from other sensory systems that all arrive at the brain via signal projection circuits. All of the efferent signals from the brain leave via signal projection circuits similar to those defined for Stage 3 visual circuits.

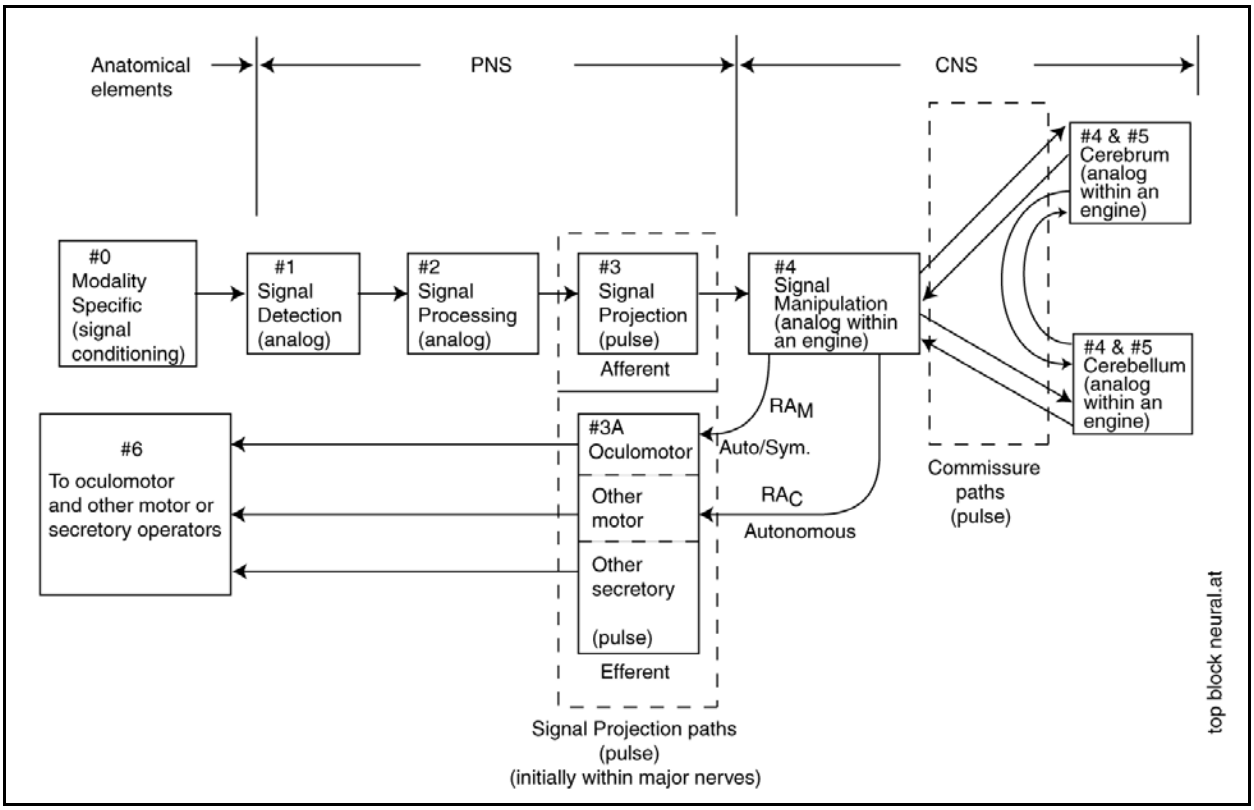

Figure 14.1.3-4 Top neural block diagram of the visual system of Chordata highlighting the signal projection paths (within the dashed boxes).

14.1.3.3.3 Detailed architecture of the initial Stage 3 paths in *Chordata*

Figure 14.1.3-5 repeats the architecture of the signaling paths developed in Section 2.8. It illustrates the technical challenge involved in achieving the high degree of structural freedom between the eyes of *Chordata* and the brain and skeletal systems. All of the important information collected by the retina must be transmitted to the brain over the minimum possible number of individual signaling channels (axons). The number of channels is approximately one million in human vision. To achieve the necessary physical circuit reduction (from the initial 10^8 channels associated with the photoreceptors), it appears the system employs diversity encoding where feasible. This technique will be discussed briefly latter.

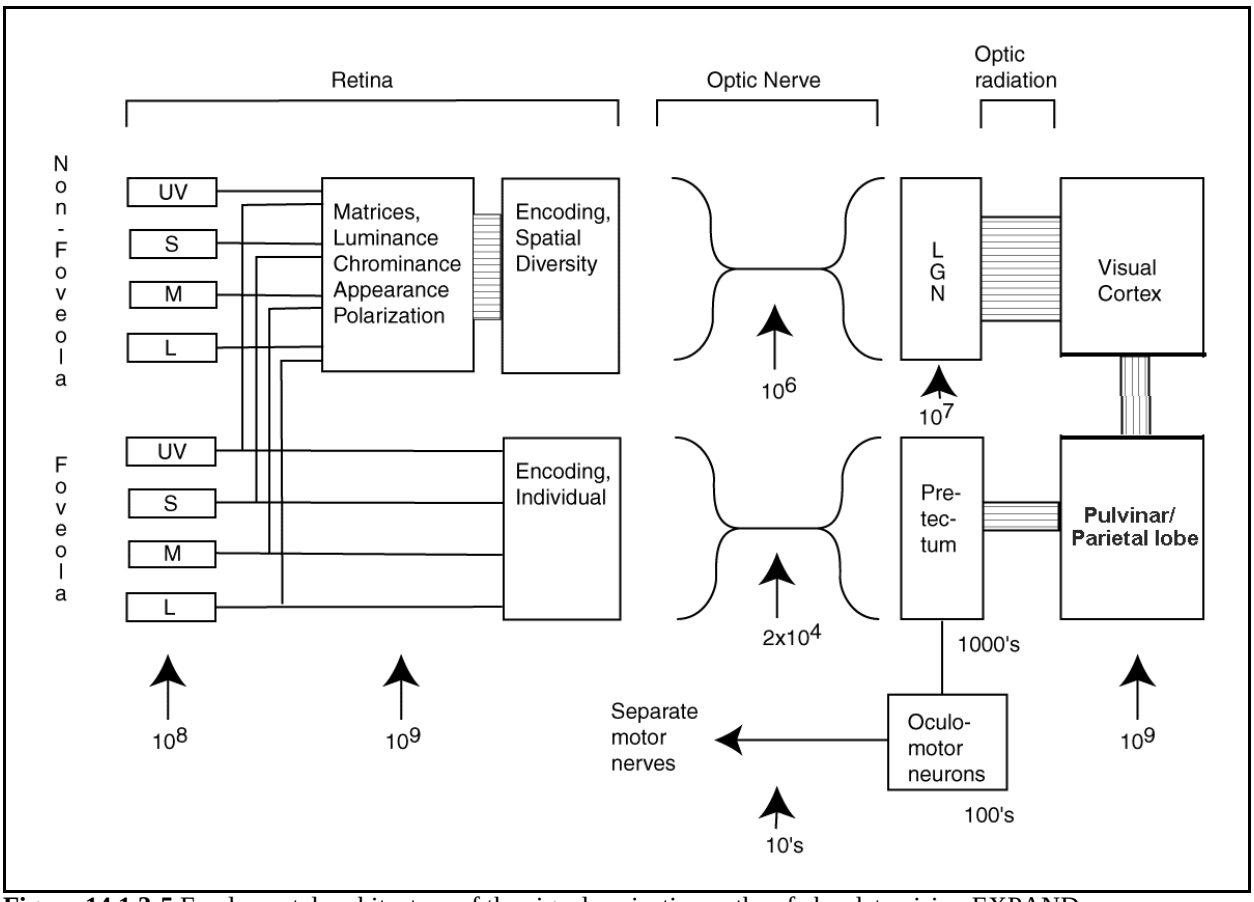

Figure 14.1.3-5 Fundamental architecture of the signal projection paths of chordate vision EXPAND.

14.1.4 Introduction focused on hearing

The hearing modality employs the same circuit topology within Stage 3 as does vision. Because of the nominal one dimensional character of the hearing signals associated with one ear, it is simpler to interpret and illustrate the fundamental features of the Stage 3 signal paths in hearing. These paths

The subject of this chapter is the transmission of signals between node E' (the emitter terminal of the Activa within the encoding neuron) and node G (the collector terminal of the decoding neuron) of the auditory system as shown in **Figure 14.1.3-6**. Frame A provides a block diagram of where Stage 3 circuits are found in the neural system. Frame B provides a fundamental Stage 3 circuit configuration. This circuit includes one or more Nodes of Ranvier. It is important to note that Nodes of Ranvier associated with the spiral ganglia, within the cochlear nerve, may occur before or after the soma of the neuron. This hints at the lack of a neural role for the soma. Its role within the neuron is limited to homeostasis and growth.

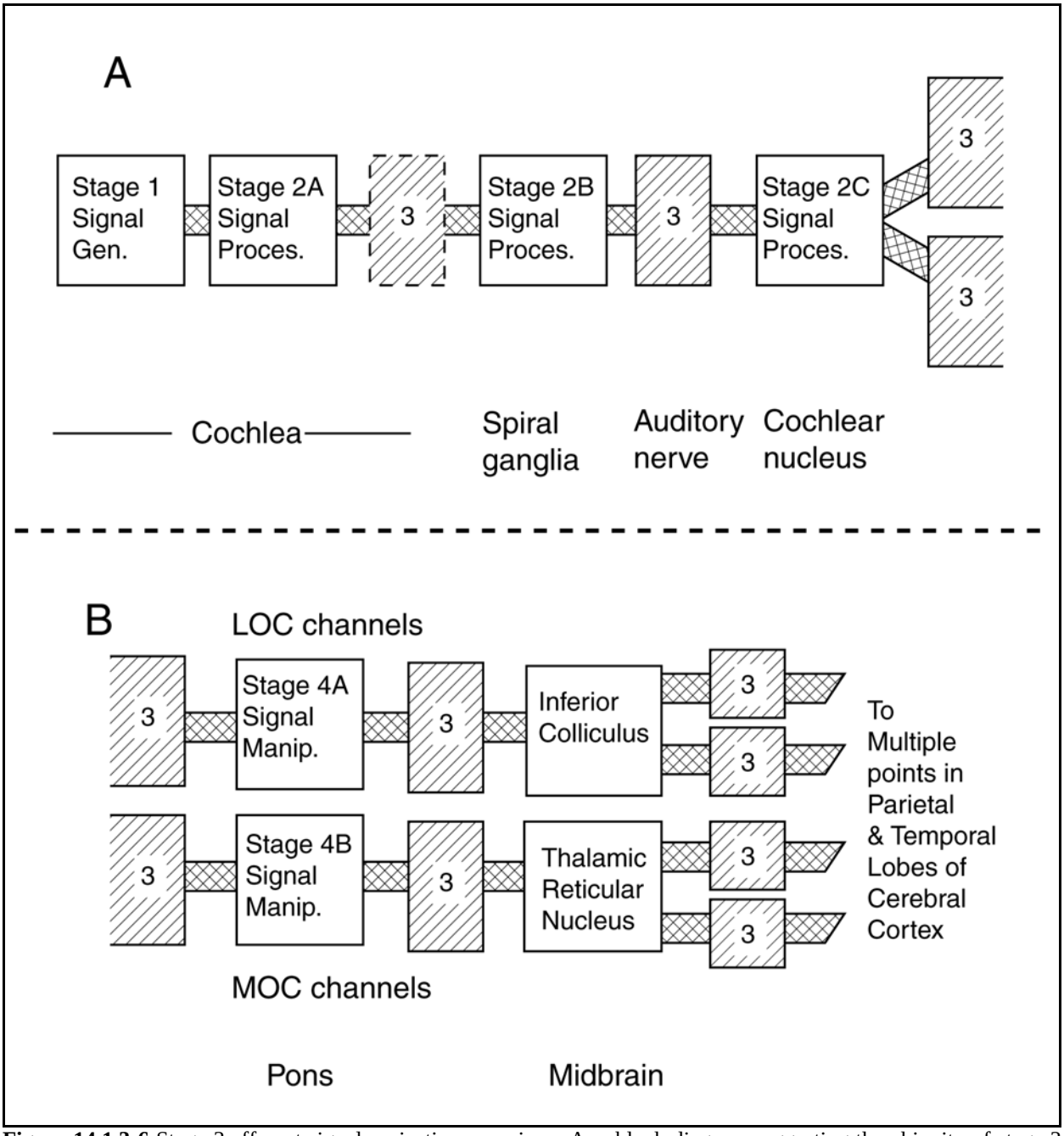

Figure 14.1.3-6 Stage 3 afferent signal projection overview. A; a block diagram suggesting the ubiquity of stage 3 circuits. The crosshatched paths represent the highly parallel circuits within an individual channel. Each of the crosshatched segments contains multiple synapses in parallel. The segments between Stages 1 & 2 represent Type N & B neurons. The segments between Stage2 & 4 contains multiple numbered signal types, including Types I through V. Each of the multiple projection neurons within each Stage 3 segment contain multiple Nodes of Ranvier. LOC = channels originating within the lateral superior olive. MOC = channels originating within the medial superior olive.B; the fundamental, end-to-end Stage 3 circuit. C; variants related to the stellate decoding neurons of hearing.

[xxx Provide word picture of above figure. i. e. TRN contains both PGN & MGN., etc.
[xxx not all nodes (engines or lesser ganglia) of the auditory system between the trapezoidal body and the mid brain

are shown

Figure 14.1.3-7

The Stage 3 encoding neuron is generally described morphologically as the ganglion neuron if it occurs orthodromic to the sensory neurons in hearing. However, this same functional neuron occurs at the output of every signal extraction engine of Stage 4 (and nearly all the engines of Stage 5 as well). The signal decoding neurons are frequently described morphologically as stellate neurons in vision. They have been similarly described by a long list of the leaders in the hearing community[3]. Unfortunately, these functional neurons have taken on a variety of whimsical names in the recent literature, particularly those within the cochlear nucleus. In this work, the stellate cell is the generic name for all neurons receiving pulse signals from more than two millimeters distant and decoding the information carried by those pulse streams into analog signal information. This is a more appropriate description than the less precise variant in Manis, et. al. The decoding mechanism is also more complex than described by Manis, et. al. and their reference to Young et. al[4]. Describing these mechanisms is a major goal of this chapter.

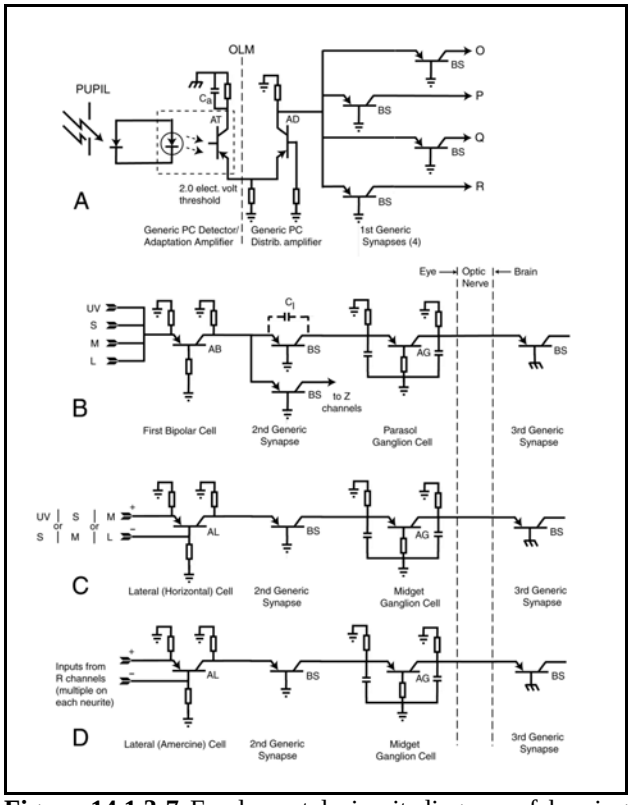

Figure 14.1.3-7 Fundamental circuit diagram of hearing EDIT labels to show hearing instead of vision From 11.7.2.1 in vision. May combine with previous figure.

Frame C provides an initial description of the variants of the Stage 3 stellate cell decoding circuits used in hearing. These variants are designed to decode both the monopolar amplitude signals and the time-delay modulated difference signals (which support the awareness mode of operation), and provide detection of the first action potential within a stream of action potentials. This action provides the earliest possible signal to the Alarm mode of the system.

The role and characteristics of the signals employed in stage 3 signal projection have not been studied systematically in the auditory system. Most of the activity has been relate to recording the time of the leading edge of the pulses in a pulse train and plotting the results as a "period histogram."

14.1.4.1 Background literature from hearing

[xxx check whether Liberman & Kiang contribute to this chapter]
Most of the data related to stage 3 projection neuron signals in hearing have related to the cochlear nerve (or auditory nerve) emanating from the spiral ganglia. Frequently the signals from the IHC to the spiral ganglia are

[3]Manis, P. Marx, S. & White, J. (1996) Integrative mechanisms of ventral cochlear nucleus stellate cells *In* Ainsworth, W. Evans, E. Hackney, C. *eds.* Cochlear nucleus: structure and function in relation to modeling. Vol. 3 Part A of Advances in Speech, Hearing and Language Processing. Greenwich, Ct: JAI Press. Pp 213-229

[4]Young, E. Robert, J-M. & Shofner, W. (1988) Regularity and latency of units in ventral cochlear nucleus: *J Neurophysiol* vol. 60, no. 1, pp 1-29

called type I neurons and those from the OHC are called type II neurons. To avoid later confusion, these afferent neuron types will be labeled type B (broadband) and type N (narrowband) respectively in this work. Following the cochlear nerve, the various signal types, of which there are many will be identified by type number using roman numerals.

Schwartz has reviewed the morphological characteristics of the neurons of the spiral ganglia[5]. She has provided statistical data on the size of these neurons in the albino rat. She has also divided them into two morphological classifications. The first consists of larger myelinated neurons with the second consisting of smaller unmyelinated neurons. No discussion was presented concerning the spontaneous rate of action potential generation between these two classes. A figure is presented attempting to interpret the data available concerning the innervation of the sensory neurons over time. The idea that the two types of primary auditory neurons have two different peripheral innervation patterns was refined by Kiang, et. al, 1982). Brown & Ledwith have discussed two classes of afferent neurons as well as two classes of efferent neurons related to the spiral ganglia based on morphology[6]. They discuss (in text) both the process synapsing with the sensory neurons and those synapsing with neurons within the cochlear nucleus. They did not summarize the properties of these neurons in a clear and concise table. Much of their material relates to the imminent Stage 4 signal processing within the cochlear nucleus.

Brown & Ledwith describe the orthodromic axons of the cochlear nerve. The type N axons "are typically thin and unmyelinated, making it likely that impulses are conducted slowly along them." The type B processes synapsing with the IHC are generally myelinated. They assert the dendrites (peripheral processes) synapsing with the OHC along the outer spiral fibers (the type N spiral ganglion neurons) are separable into three classes. "In the basal turn, outer spiral fibers usually contact only one of the three rows of outer hair cells and show increasing numbers of terminals from the innermost row (row 1) to the outermost row." They identified swellings at frequent intervals along the lengths of many neurons. Whether these are Nodes of Ranvier or electrostenolytic power sources is unknown. Brown & Ledwith offered no explanation for the purpose of these swellings.

[xxx discuss the tonotopic character of the cochlear nerve. Show cross-section. Must address both the broadband and narrowband (roman numeral) distribution of axons within the nerve.

Much of the available data was originally presented based on the phase of one or other characteristic relative to the stimulus. While several papers have described the term absolute phase, this is an oximoron. Phase is by definition relative to some reference event. Frequently this phase is computed in angular measure, degrees or radians without recognizing there may be a large component in the measurements due to the delay of the signal along an acoustic or neural path. This delay is due to the limited travel velocity of the signal and is frequency independent. While this delay component can be described in angular units at a given frequency, this description becomes frequency dependent. It is frequently preferred to describe such delays as a separate expression, that frequently can be described as the latency of the overall circuit relative to the stimulus.

Within Stage 3 circuits, each Node of Ranvier introduces a fixed delay that is not related to frequency response of the channel or the frequency content of the signal in any way. Describing this time delay in angular measure usually serves no useful purpose.

[xxx re-outline and re write paragraph]
Stage 3 employs two distinct classes of neural signaling channels, those which respond to monopolar input signals and generate trains of action potentials based on a "driven" oscillator, and those that respond to a bipolar input signal and generate trains of action potentials based on a "free-running" oscillator. In both hearing and vision, the application of these two classes is quite distinct and obvious. The driven oscillators exhibit a spontaneous rate, SR, that is equal to zero (except in the presence of extraneous noise). The spontaneous rates (center frequencies in the absence of input signal) of the free-running oscillators exhibit a nominal value near xxx pulses per second with a small standard deviation. When presented in a histogram, the mean SR is frequently combined with a broadband noise component.

In hearing, the ensemble of signals occurring within Stage 3 circuits may be more complex than in vision. It appears

---

[5]Schwartz, A. (1986) Auditory nerve and spiral ganglion cells: morphology and organization *In* Altschuler, D. Hoffman, D. & Bobbin, R. *ed*. Neurobiology of Hearing: The Cochlea NY: Raven Press pp 1-21

[6]Brown, M. & Ledwith, J. (1990) Projections of thin (type-II) and thick (type I) auditory-nerve fibers into the cochlear nucleus of the mouse *Hear Res* vol. 49, pp 105-118

to be more difficult to insure near zero input conditions. Additional signal processing may also be occurring within Stage 2 of hearing that is not currently understood or clearly documented.

The fact that all action potentials are positive going waveforms has inhibited some investigators from clearly interpreting their data. The common statement that no stimuli were found that inhibited action potential generation shows this lack of understanding of the encoding environment used. The problem has been compounded by the non-rectilinear "rate" histogram frequently found in the literature.

As noted by Geisler[7], the dynamic range of signals following stage 1 within the auditory system "are functionally limited to approximately two orders of magnitude." This work uses a slightly larger and more specific value of 200:1. In the case of Stage 3 signals, this range is expressed as a difference in action potential pulse rates, not pulse amplitudes. Recognition of this dynamic range limit has a major impact on the interpretation of many neural "tuning curves" (**Section 5.x.x**).

14.1.4.2 Importance of synchronous data recording

Much of the data in the literature does not provide an adequate description of the time characteristics of recorded signals relative to the temporal description of the initial stimulus. In the absence of such data, it is difficult to allocate the time delays associated with various portions of the sensory modality and to define the temporal performance of individual circuit elements.

[xxx pick up from PBV or neuron manuscripts]

Evans noted that the action potential pulse trains he measured in guinea-pig frequently extended beyond the duration of the stimulus. This was particularly true at frequencies below 2 kHz. "In particular, mult-peak histograms were obtained in fibres of characteristic frequency below 2 kHz. The envelopes of these histograms had decay times of 4—6 msec. In some cases, as many as 8 peaks were resolved." He noted that Tasaki (1954) had observed the same phenomenon. The reason for these peaks will become obvious during the discussion in this chapter.

14.1.5 Requirements in future test protocols and equipment configurations

This chapter will introduce considerable new material concerning the operation of the neural system. This material will call for the use of new experimental techniques, particularly in the areas of data collection and data interpretation.

Temperature has a major impact on the chemical and electrical parameters associated with the electrolytics of neural operation. The significant variations in neural system performance as a function of temperature have not been widely recognized by the neural community in the past. Variations of a factor of xxx are encountered between 20 C and 37 C. For reproducible research, it is important to record the temperature of the specimens to at least ±0.5 Celsius accuracy. An accuracy of ±0.1 Celsius should be the goal. Neumcke has provided an enlightening graph of the effect of temperature on the quiescent voltages of the neural system in the rat[8].

A new theoretical analysis will demonstrate that many of the histogram techniques used in the past are not compatible with an accurate interpretation of the data collected. By using modified data collection and analysis techniques, a much more precise and simpler interpretation of the operation of the neural system becomes available. Two different types of histogram will be introduced that are appropriate when examining summation signal and difference signal channels. These techniques will be addressed in **Section xxx**.

The addition of some simple electronic circuitry will allow any investigator to decode the signals being transmitted over Stage 3 Signal Projection circuits. As a result, comparisons will be available on a dual trace oscilloscope or other recording media, between the stimulus signal and the equivalent signal being transmitted past a given point over a specific portion of the neural system. The use of this new circuitry will become obvious during the development of the chapter. The key fact is that the information transmitted over the neural system does not use amplitude of frequency modulation. A clearer understanding of the modulation techniques used will lead to a better understanding of the equipment needed to interpret those signals. The key requirement is that the experimenter

---

[7]Geisler, C. (1998) From sound to synapse. NY: Oxford Univ. Press page 17 and chapter 12

[8]Neumcke, B. (1983) The myelinated nerve: Some unsolved problems. *Experientia*, vol. 39, pp 976

differentiate between signals being transmitted using delta-modulation encoding and time-delay modulation encoding. The result of using the wrong decoder techniques is illustrated by the confusion in the current journal and textbook literature. The details related to the new circuitry will be developed in **Section xxx**.

14.2 Neural coding: architecture, modes & mechanisms

The circuits of Stage 3 Signal Projection are used throughout the neural system, regardless of sensory modality and whether the paths are afferent or efferent. They are used in a variety of methodologies in order to achieve the desired degree of optimization called for by the operational requirement. Stage 3 signaling paths involve both signal coding and decoding, as well as route conservation techniques and computational anatomy. These approaches will be addressed in reverse order.

While these techniques appear to be used throughout the neural system, their application is most obvious in the visual and auditory systems. Examples from these two systems will be described briefly below.

The implementation of these techniques within the neural system are not compatible with a variety of previous concepts of neural operation, in both vision and hearing, developed without recognizing the presence of mechanisms using these techniques. These old concepts cannot be used as a counter to the theoretical models presented in this work that recognize these mechanisms.

14.2.1 The utility of conformal transforms in information analysis

Figure 14.2.1-1 provides a top level description of the concepts of both spatial and temporal conformal transformations as applied to neural information extraction. The top frame of this figure concentrates on the basic spatial conformal transform. Sensory neural paths inevitably originate in the periphery (on the left) at a spatially definable surface. These neural paths are assembled into physical groups (defined as individual nerves) as part of the afferent signaling paths of the neural system.. When a portion of the system is stimulated, the signals related to that stimulus generate a spatial pattern within one or more of these nerves. Near the sensory neurons, these patterns are frequently recognizable in terms of the stimulus. Such patterns are described as retinotopic in vision, tonotopic or cochleotopic in hearing, etc. As part of the information extraction process (the core purpose of the afferent neural system), the patterns associated with a given nerve become more abstract and eventually exhibit no relationship to the spatial pattern of the original stimulus.

The conformal transformation concept is shown in the figure using the cross-over symbols. Such cross-overs appear repeatedly along the afferent neural paths. Following a conformal transformation, the signals are usually processed algebraically (along with additional correlative processes) within one or more signal processing (signal manipulation) engines as shown prior to the passing of the signals to the next engine. The pattern of the signals in this orthodromic nerve frequently undergo additional conformal transformation prior to arriving at the next engine.

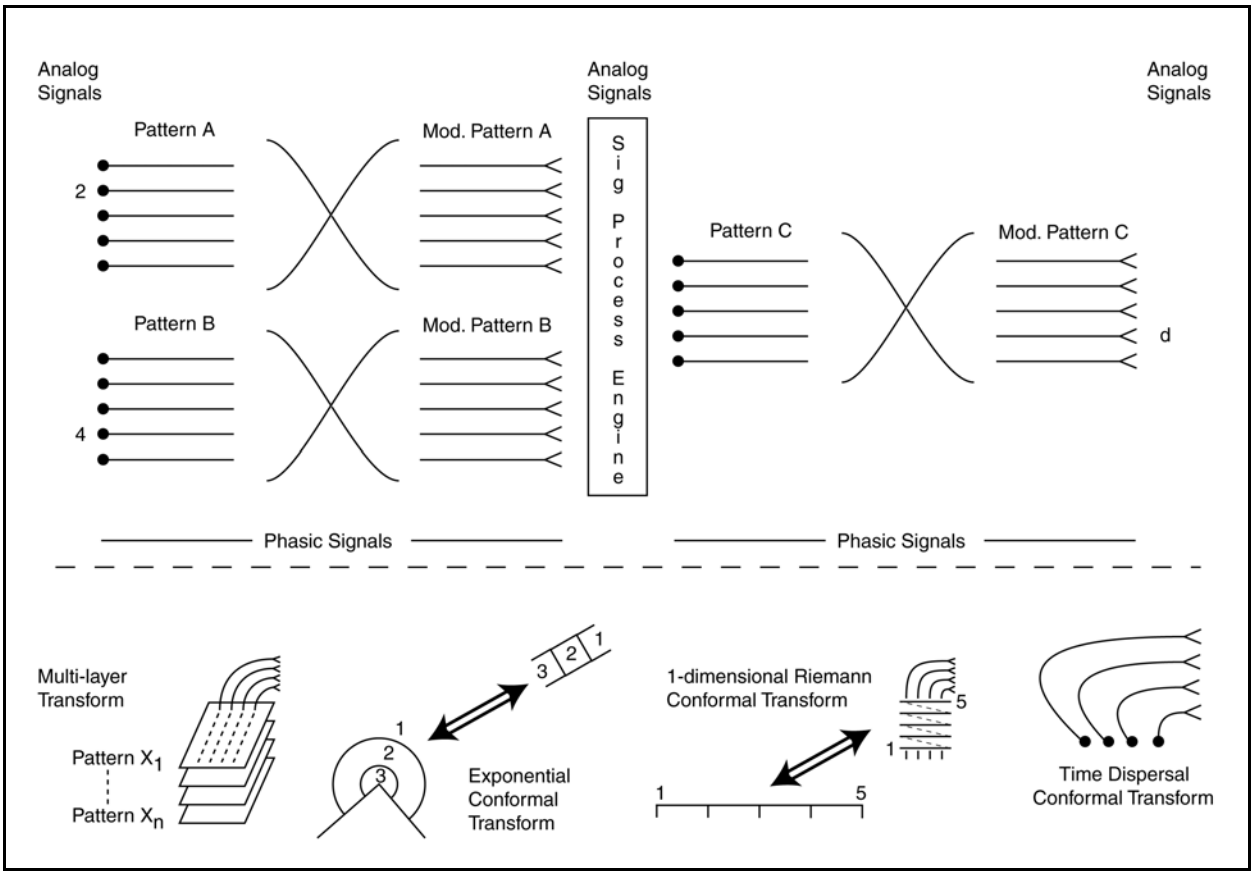

Figure 14.2.1-1 Top level description of tertiary signaling. Top; simple spatial conformal transformations. The spatial patterns of multiple signaling channels are frequently transposed during propagation between two points. Note numeric labels on the extreme left and letter label on the extreme right. Lower left; a simple conformal transformation involving stacking of groups of neural terminations. Lower left center; a complex exponential conformal transformation. Lower right center; a complex spatial conformal transformation by Riemann. Lower right; conformal transformation introducing differential time delay.

This gradual loss of retinotopic or tonotopic organization occurs in two phases. The most obvious phase involves the mathematical manipulations performed within the feature extraction engines of the neural system. However, an equally important phase is that related to the conformal transformations carried out by the groups of neurons passing between one engine and the next. It is the necessity of performing a variety of mathematical computations within the neural system without employing transcendental mathematics that calls for these transformations. A remarkable range of computations can be performed through the use of conformal transformations coupled with simple algebraic manipulations along with one other manipulation. The neural system is intimately related to the exponential transform. The ubiquity of the non-dimensional exponential transform (found within every functional element of every neuron) provides an easy method of performing division–and conceptually multiplication. Two- and three-dimensional transforms are used very effectively also. While the mathematical manipulations are carried out primarily within the other stages of the neural system, the conformal transformations are a feature of the tertiary signal processing stage. These transformations can easily be seen at the gross level in the combination of the optic nerves and the chiasm of the visual system. The transforms associated with the optic nerve are primarily spatial transforms. However, the transforms associated with Meyer's Loops and their conjugates, Reyem's Loops, perform a conformal transformation with respect to time. The concept is illustrated at the lowr right in the above figure. Reyem's loops are formed by the spherical ganglion neural paths of the retinal layer of each oculus. They present a time-dispersed pattern to the lateral geniculate nuclei that is invaluable in computing the position of a stimulus within the field of view of the eyes. However, this time dispersal is deleterious to further processing of the image information. Therefore, Meyer's Loops are used to remove this time dispersal prior to further processing in the occipital lobe of the cerebral cortex (**Section xxx** in xxx).

14.2.1.1 The arrangement of planes for purposes of coincidence detection and correlation

At the next level of complexity, the luminance and chrominance channels found within the two optic nerves must be combined into a single neural image of the environment before optimum feature extraction can be undertaken. This merging of information occurs both in the lateral geniculate nuclei (for the left and right peripheral fields of view) and the perigeniculate nuclei (a single physiological entity although possibly recognizable superficially as two morphological structures). The concept is illustrated in the lower left frame of the above figure. The implementation of the process is different for the peripheral retinas and the foveola.

One set of sensing neurons is designed to detect angular separation between signals related to a given stimulus as they occur in eyes that have not converged on the stimulus in the scene. Because of the lack of proper convergence, the error messages generated for different individual stimuli may not agree. The process employs a weighted summation process to give the best possible coarse convergence signal.

Subsequently, a second set of sensing neurons is responsible for merging the converged image information. Many of these sensing neurons only access a particular pair of layers (the two luminance layers or individual pairs of the O, P, Q layers). Their output is the sum of the information provided in the pair of layers. These sensing neurons are used to carry the information on to area 17 of the occipital lobe for initial feature extraction and interp generation.

In the case of the central retinas, the process consists of arranging the raw spectral channel data (that has not been encoded within the retina) into a two-layer stack within the perigeniculate element that can be accessed by sensing neurons. These sensing neurons are arranged perpendicular to the plane of the stack. As in the case of the LGN, the sensing neurons of the PGN are responsible for performing an error analysis designed to provide a fine convergence error signal and also to combine the information from each retina into a single retinal map. The output of the latter sensing neurons are directed to the pulvinar for initial feature extraction and interp generation.

14.2.1.2 The more complex conformal transformations used in vision

Because of the spherical arrangement of the far-field of vision and the highly curved retina of mammals, feature extraction should require the performance of very complex mathematical manipulations for imagery outside of the retina. However, through the use of conformal transformations, this requirement is avoided. There are many examples of such transformations within the neural system. The most famous of these representations is that of the surface area of the skin of a human projected onto a representation of the brain where the surface area is weighted by the density of somatosensory neurons (xxx refer.). The representation is at a very coarse level but it demonstrates the concept. At the more detailed level, the mathematical advantage becomes more obvious. As illustrated at the lower left center, a specific exponential conformal transformation is used to convert circular features in object space into straight lines when projected onto the surface of area 17 of the occipital lobe[9]. As a result of this transformation, sensing neurons with long straight dendritic structures can be used to sense circular features in object space. ***This example of a conformal transformation shows how the neural system avoids a wide variety of requirements to perform transcendental mathematical calculations***.

14.2.1.3 The more complex Riemann conformal transform in hearing

In hearing, a more complex mathematical transform is performed by using computational anatomy. Riemann has developed the mathematical principles required to describe the transform of a continuous line or surface into a set of discontinuous lines or surfaces[10]. The technique is described by the Principle of Analytic Continuation. In the case of hearing, the human ability to appreciate music leads to the realization that the continuous mapping of the auditory frequency spectrum generated in the cochlear partition is transformed into a discontinuous mapping as described in the lower right center frame of the above figure. In the case of hearing, each octave length (factor of two in frequency) segment of the cochlear spectrum is separated and placed in an individual layer of a correlation stack. The layers are aligned so that harmonically related frequencies are aligned along a vertical slice through the stack. These vertical slices are actually occupied by sensing neurons. Each of these neurons is used to summate the harmonically related signal components from each octave of the overall spectrum into a single channel. The signals

---

[9]Kober, H. (1957) Dictionary of Conformal Representations. NY: Dover Publications, Catalog S160. pp 27 & 87 LOC Call: QA646 .K73 1957

[10]Guillemin, E. (1949) The Mathematics of Circuit Analysis. NY: John Wiley & Sons. pp 288-315

from these sensing neurons constitute the output pattern delivered to the pulvinar for initial feature extraction and interp generation. While this procedure would be extremely difficult to perform mathematically, it is almost trivial using computational anatomy. ***When performed in conjunction with the frequency dispersing mechanism of the cochlear partition, this mechanism entirely eliminates the need to perform any transcendental calculations (such as a Fourier Transform) within the auditory neural system. These combined mechanisms also avoid the need to implement any resonant or "tuned" circuits within the auditory system.***

14.2.2 Route conservation as a major tool in neural systems

The general layout of the neural systems associated with vision and hearing have been described elsewhere in this work (**Section xxx**). The feature to note here is the parsimony employed in those arrangements. Information being passed by signals from the peripheral to the central nervous system is extracted sequentially according to the performance requirements. This is most easily seen in the block diagrams of vision and hearing (where alarm-mode information is extracted from the signals prior to analytical-mode information). Morphologically, the higher importance of alarm-mode information is seen by the distribution of the feature extraction engines of hearing. Those engines related to the detection of strong impulse responses are found in the trapezoidal body and their outputs are passed directly to the motor system for override operation of the neck and other body muscles as well as the oculomotor and eyelid muscles of the eyes. They do not proceed to the diencephalon or cerebral cortex before implementation. These muscle groups react before the higher level perceptual and cognitive engines have processed the information. A similar situation is found in the various lower level reflex arcs (those frequently and routinely tested by a physician). In these cases, the muscle response occurs before the higher level awareness mode processing and cognition can occur.

Both the sequence and hierarchy of information extraction are easiest to recognize in the dispersed engines of the auditory system. Much of the original short duration impulse information associated with the alarm-mode of auditory operation never reach the diencephalon and cerebral cortex. These signals are processed within the trapezoidal body. Following processing, commands are sent directly to the appropriate muscle signaling nodes (like the xxx within the visual system) and only a supervisory signal is sent to the higher brain. Similar information associated with source location based on tonal information is extracted (probably in or near the inferior colliculus) and the relevant less important information is sent to the higher brain centers. Following cognition, commands may or may not be given to turn the organisms attention to the source. (As an example, at a party or group conversation, the subject does not turn its head to follow each individual speaker. Instead, it attempts to obtain maximum information by perusing the environment more widely.

At a lower levels within the neural system, individual sensory paths may be combined to conserve signal projection assets. This appears to be a common feature of the somatosensory system where the complete interpretation of the character of the stimulus may require correlation of data from other sensory channels. A simple example is when someone is told heat is going to be applied to a small area of his skin and a low temperature stimulus (ice) is actually applied. In the absence of vision, the subject will frequently respond as though he had been burned. An interesting example of route conservation is the subject of acupuncture. When certain sensory neurons, particularly those associated with touch, are stimulated, the neural system frequently perceives a stimulation at a different location. There is clearly a convergence of some neural channels. In these cases, at least one portion of the neural signaling channel is shared between two distinct sensory neurons. Ambiguities introduced by such sharing is frequently resolved at a higher level of the neural system by employing multiple sensory system correlation.

14.2.3 The translation of the analog information into the phasic domain by encoding

Virtually no information could be found in the biological literature discussing the operational reasons for the existence of the neurons associated with signal projection. These neurons are generally known as ganglion neurons (cells) and stellate neurons (cells) in vision. Ganglion neuron is also a common name associated with the encoding neurons of the spiral ganglia in hearing. However, the term stellate neuron has been less widely used in discussing the decoding neurons of the trapezoidal body in hearing. Neither ganglion or stellate neurons has been used consistently when speaking of the encoding and decoding neurons of the CNS.

The above lack of uniformity in naming based on physiological function, rather than morphology, has retarded development of the field of research in both vision and hearing.

In larger animals, the distance between individual engines (particularly between the peripheral source and the central nervous system) can be considerable, up to several meters. Transmitting a neural signal over these distances by charge diffusion requires prohibitive amounts of energy (power over a period of time). To alleviate this problem, the

neural system employs pulse transmission techniques that rely upon a technique that has not been previously documented in the biological literature. The phasic signals, consisting of streams of action potentials, are propagated (as opposed to diffused) over typically myelinated axons just as they are within a man-made coaxial cable. The equations of Maxwell describe this electro-magnetic propagation over the neuron. This is in contrast to previous assumptions that the signals are transmitted based on Lord Kelvin's diffusion equations, as asserted subsequently primarily by Herman and by Rall. The detailed discussion concerning these competing high level concepts is found in **Section xxx**.

Figure 14.2.1-2 shows the top level Stage 3 signal path formed by a single pair of ganglion and stellate neurons within a larger nerve. All of the signals applied to the input of the Stage 3 signal path are analog (electrotonic). Similarly, all of the output signals from the path are analog. The ensemble of neural paths at the entrance to a Stage 3 segment forms a spatial pattern at a given instant of time. Similarly, the ensemble of neural paths at the exit forms a spatial pattern at a given instant. As noted previously, these two patterns may be grossly different. However, the elements of each signal path remains the same. Between the elements of a Stage 3 segment, the signal is propagated as a phasic signal.

Each of the neural paths within a signal propagation nerve consist of three critical components as shown in this figure. Each path can be described as consisting of a ganglion neuron that is used to encode the analog information into a phasic signal and a stellate neuron that is used to decode the phasic signal in order to recover the original analog signal prior to additional algebraic processing. Nodes of Ranvier, NoR, are frequently found between these elements multiple. Often multiple NoR are found between a single pair of ganglion and stellate neurons. Each of these NoR are used to regenerate the action potential pulse stream at regular intervals of between one and two millimeters.

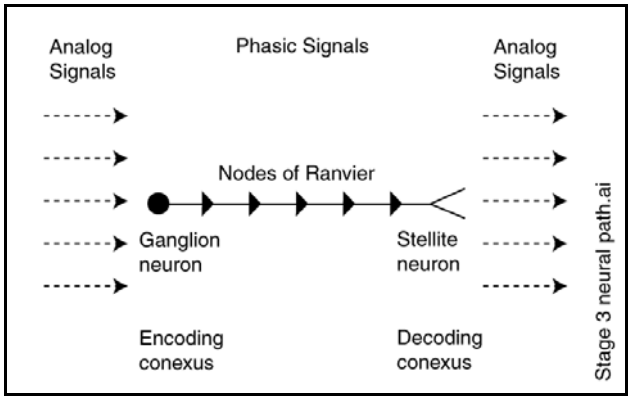

Figure 14.2.1-2 Top level description of the Stage 3 signal path.

A critical feature of this neural path has caused unnecessary errors in the literature. The Nodes of Ranvier introduce a fixed delay into the neural path as they regenerate the individual action potentials. The more NoR associated with a given length of a neural path, the greater the fixed delay introduced into the path. When experimentalists attempt to calculate the velocity of neural signal propagation, they frequently overlook this delay and consider the total delay as representative of the velocity of propagation over a given distance. The resulting calculation correctly describes the effective or average velocity of propagation. However, the instantaneous velocity of neural signal propagation along an axon is considerably higher (**Section xxx**).

The method of signal encoding and decoding used in the neural system is discussed in detail in **Sections 14.4** & **14.5 xxx**.

14.3 The actual codes used in signal propagation

There has long been a debate as to whether the action potential pulses are deterministic or probabilistic in character. As van Drongelen noted, the electrophysiologist easily demonstrates the action potentials are deterministic following their stimulation[11]. However, the neurophysioloogists have routinely asserted the action potentials are probabilistic because they can not achieve repeatable results in their experiments. The difference is clearly due to their inadequate understanding of the circuits within a stage 3 neuron. The stage 3 neuron is completely capable of incorporating a lead lag network of sufficient complexity prior to the pulse generating Activa to cause the problems encountered by the neurophysioloogist.

As an aside, the conceptual sketch of a nerve fiber in figure 14.1 of van Drongelen shows

[11]van Drongelen, W. (2007) Signal Processing for Neuroscientists. NY: Elsevier pg 220

he does not appreciated that there is no "vertical" membrane current through the axon segment of a stage 3 myelinated neuron.

Bershadskii has recently provided a series of papers describing the *in-vitro* operation of selected neurons operate in a chaotic (deterministic via a complex function) model[12,13]. He suggests his neurons are excited by random noise. He did not show the actual output waveforms of any neuron but made computations based on a correlation function ostensibly representing a series of action potentials recorded *in-vitro*. Although noting the nominally equal height of the action potentials from a single neuron *in-vivo*, he did not indicate the amplitude for his action potentials. Specifying this height is critically important in determining whether a pulse stream is a real set of action potentials from a stage 3 neuron or merely the result of forced oscillation in a neuron due to an intentional or incidental bias change associated with the probe protocol.

Wikipedia provides a nice brief overview of the correlation function and its variants. Although unsigned, the material does reference a recent text[14]. It does develop the inconsistency of notation among scientific disciplines at even this late date. "Different fields of study define autocorrelation differently, and not all of these definitions are equivalent. In some fields, the term is used interchangeably with autocovariance."

Much of what Bershadskii asserts is correct from a mathematical perspective. However, he is unable to show that his responses are valid under *in-vivo* situations or to describe the actual limitations on the application of his findings. He did not address the actual encoding algorithm of the neural system although his results are compatible with the neural algorithm. This algorithm is developed below. His correlation function suggests his neuron was synchronously excited rather than by a random input. It exhibits an initial pulse followed by a long tail with a ripple suggestive of the presence of a harmonic component (probably due to the nonlinear mechanisms present).

As recently as 2005, Ventriglia & Di Maio[15] have asserted the neural code presumably associated with the peripheral neural system was unknown. "The problem of the code used by brain to transmit information along the different cortical stages is yet unsolved. Two main hypotheses named the rate code and the temporal code have had more attention, even though the highly irregular firing of the cortical pyramidal neurons seems to be more consistent with the first hypothesis." Their discussion does not address the details and options utilized in stage 3 signal projection. They do not identify the requirement of any useful (intensity–related stimulus) code to identify clearly the time of the initial event.

This section will describe the phasic code actually used in the stage 3 neural system and how the information encoded by the ganglion neuron can be recovered by a stellate neuron, including a series of examples demonstrating the solution to the above neurophysiologists' problems.

14.3.1 The Neural Code used in the magnacellular (brightness) and other monopolar pathways

The optimum parasol type (monopolar input) ganglion neuron should show maximum sensitivity to stimuli without introducing significant noise into the neural pathway. This condition calls for the quiescent emitter (dendrite) voltage, Ven(quiescent), to be more negative than but as close as practical to the cutoff voltage labeled point 2. This maximizes the dynamic range available for the signal, between cutoff and saturation and accepts the generation of an occasional

---

[12]Bershadskii, A. (2011) Prime numbers and spontaneous neuron activity http://arxiv.org/abs/1103.1167v1

[13]Bershadskii A. (2010 Broken chaotic clocks of brain neurons and depression http://arxiv.org/abs/1012.1611v2

[14]Dunn, P. (2005) Measurement and Data Analysis for Engineering and Science, New York: McGraw–Hill, ISBN 0-07-282538-3

[15]Ventriglia F., Di Maio V. (2005) Neural Code and Irregular Spike Trains. In: De Gregorio M., Di Maio V., Frucci M., Musio C. (eds) Brain, Vision, and Artificial Intelligence. BVAI 2005. Lecture Notes in Computer Science, vol 3704. Springer, Berlin, Heidelberg

extraneous action potential due to analog noise.

The pulse train(s) generated by parasol type (monopolar input) ganglion neurons are described in the engineering literature as representing time-delay encoding or modulation. This type of modulation is characterized by packing more information into a given signal space than nearly any other form of modulation. Time-delay encoding is a more sophisticated form than a simple rate-based code. It is a place code. Time-delay encoding generates an initial pulse that occurs earlier the more intense the stimulus. Subsequent pulses occur closer together for higher intensity stimuli, as in rate-based coding.

The time-delay code used in the neural system is a (temporal) place code and not a rate code. The time of occurrence of the first pulse is relevant and provides important information related to the intensity of the stimulus. The time interval before the next pulse is linearly proportional to the stimulus amplitude during the that interval. The reciprocal of this interval, the pulse rate, is not linearly related to the stimulus and is in fact asymptotic.

If the lead-lag network of a ganglion neuron creates a flat frequency pass band from the sensory neuron to the ganglion Activa, the first action potential departs from its quiescent level immediately upon the input exceeding the threshold level of the circuit. This initial pulse is used as an alarm mode signal in the subsequent circuits of stage 4. Subsequent pulses occur with a decrease in time delay that is linearly proportional to the amplitude of the stimulus above threshold.

In typical laboratory experiments, the probe impedance is usually many megohms (compared to the synapse impedance of about 0.25 megohms (**Hearing, figure 3.6.2-1**). As a result, parametric excitation of a ganglion neurons usually employs a constant current source that charges the input capacitor, C. The result is an emitter to ground voltage that is a linear ramp up to the threshold level. The capacitor is discharged during the pulse interval and the ramp begins again. This is the condition seen between points 5 and 2 in the above dendrite potential waveforms.

More details related to time-delay modulation in monopolar neural circuits can be found in Section 14.2.2 of "Processes in Biological Vision[16]."

If care is taken in experiment design, it is possible to ensure a simple bandlimited step input to the encoding portion of the stage 3 ganglion neuron(s) associated with monopolar signals (such as brightness). The absolute voltage levels relative to the neural matrix and the polarity of the step are significant. The transient performance will vary with this polarity.

14.3.1.1 The IRIG description of the code

The code used in monopolar neural signaling was categorized by the Inter Range Instrumentation Group (IRIG, a for-runner of NASA) during the 1950's in Standard 106-96. The monostable pulse stream is described as a return-to-zero (RZ) type of code. It is described as an analog representation in the pulse domain of an analog signal. The actual time-delay code is described as a pulse position modulation (PPM) code.

> In the IRIG and in the neural PPM code, the time of the first pulse is associated with when the event took place and the interval between subsequent pulses describes the intensity of the stimulus at the start of that interval. This type of code is also known as a "phase code" or a "place code."

The instrumentation industry has moved on with the advent of the digital computer and the emphasis of the IRIG today is totally on pulse code (rather than pulse position) modulation. All of the files of the IRIG are in a repository at the University of Arizona Libraries.

---

[16] Fulton, J. (2004) Processes in Biological Vision http://neuronresearch.net/vision/pdf/14Tertiary.pdf

14.3.1.1.1 An IRIG encoder compatible with a stage 3A neuron

Figure 14.3.1-1 illustrates a circuit used in a typical IRIG encoder of 1965[17]. The circuit configuration within the dashed line is the fundamental oscillator, based on a commercial NPN transistor, 2N3553. The circuit is essentially identical to that in the figure of Section 9.xxx. Only the polarity of the power supply is reversed to accommodate conventional telemetry practice. This requires use of an NPN transistor instead of its PNP equivalent.

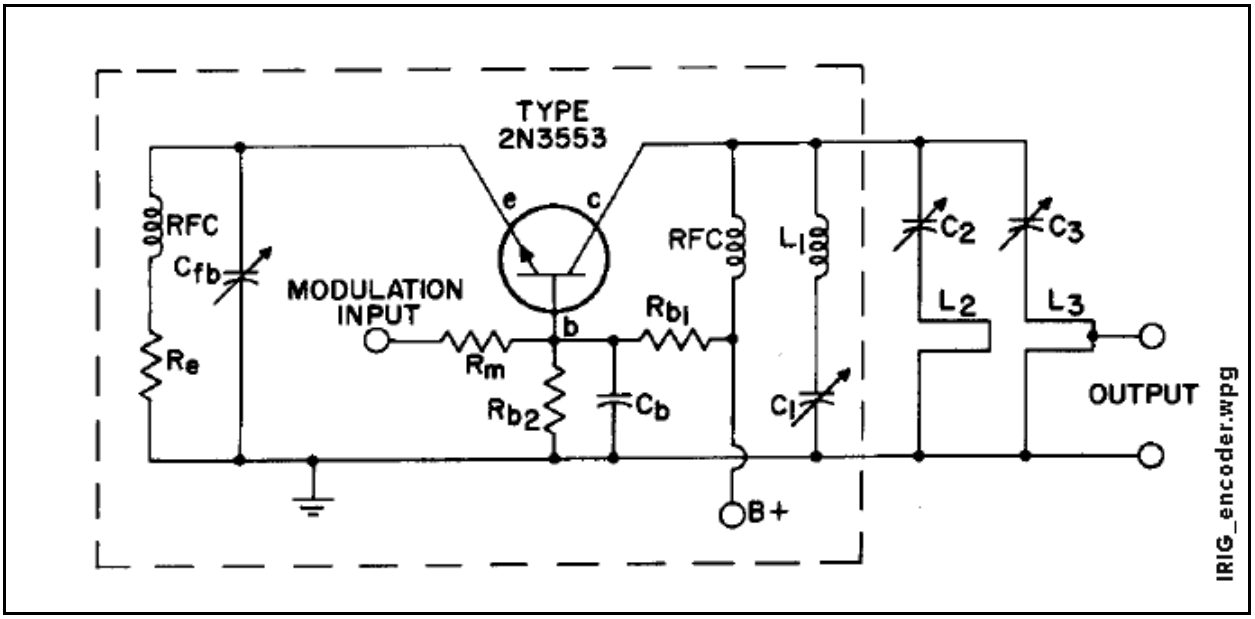

Figure 14.3.1-1 A typical encoder circuit satisfying the IRIG Standard 106-96 using an NPN type instead of a PNP type semiconductor device. The circuit outside of the dashed box is used to raise the frequency of the output pulse train. It is not needed in the neural application of this circuit. It can be replaced by a coaxial cable or in the neural case, by a myelinated axon. RFC; radio frequency choke. See text. From D'Elio & Poole of RCA, 1965.

In this example of a commercial encoding circuit, the analog signal is introduced at the base (b) or inverting terminal of the transistor. It could just as easily be introduced at the emitter (e) terminal.

The RFC employed on the right in the figure is used to prevent pulses formed in the collector circuit from leaking back into the base circuit. This RFC will prevent the analog waveform from being contaminated by the pulses in the collector circuit. In neural circuits, whether such an RFC is present is important. When a oscilloscope probe is attached intra-cellularly to the soma with the RFC present, the recorded waveform will be pure analog. If it is attached in the absence of the RFC, the recorded waveform may show the summation of the analog driving waveform and the pulse output waveform. It is up to the investigator to understand this choice and take it into account when discussing his data.

The complimentary, PNP, type to be used in emulating a biological neuron or Node of Ranvier consists of the 2N2904 series of discrete devices.

As discussed in the earlier subsection, this circuit can be made to generate pulses continuous, modulated by the analog signal input OR made to only generate pulses in response to the analog input by varying the values of R_{b1} and R_{b2}.

---

[17] D'Elio, C. & Poole, J., [RCA] (1965) Single-Transistor, L-Band Telemetering Transmitter. University of Arizona Libraries http://hdl.handle.net/10150/578467

14.3.2 The Neural Code used in the parvocellular (chrominance) and other bipolar pathways

The optimum midget type (bipolar input) ganglion neuron should accomodate the largest amplitude bipolar signal without causing significant distortion. This condition calls for the quiescent emitter (dendrite) voltage, Ven(quiescent), to be in the middle of the dynamic range between the emitter cutoff and saturation voltages. As a result, the same ganglion circuit as used for the magnocellular pathways is biased to provide a continuous series of action potentials that can be phase modulated to encode the amplitude information associated with the bipolar analog stimulus.

Being a place code, the action potential stream generated by the ganglion neuron will exhibit a discontinuity very near the time of any major change in the stimulus. However the value of that change may not be apparent until the next clearly defined time-delay interval (between the subsequent two pulses). This fact has long been recognized in the electrical engineering community and it is memoriallized in both the NTSC and PAL analog color television standards. As in these systems, the neural system uses the positive region of the bipolar signal to encode "green" information and the negative region to encode either "blue" or "red" information (there are two chrominance channels in the large mammals).

If care is taken in experiment design, it is possible to ensure a simple bandlimited step input to the encoding portion of the stage 3 ganglion neuron(s) associated with bipolar signals (such as chrominance). Being a bipolar channel, the absolute starting and ending voltage levels of the step relevant to the neural matrix are significant. It is frequently desirable to generate a monopolar stimulus starting from the nominal quiesecent level of the input circuit.

14.3.3 The Transfer Functions for the Sum & Difference Neural Codes

The following figure shows the nominal transfer function for the ganglion neuron; biased for monopolar operation on the left and for bipolar operation on the right. Note the linearity of the transfer function with respect to time delay interval. Conversely, the transfer function is highly nonlinear (in fact assymptotic) with respect to the rate of action potential generation.

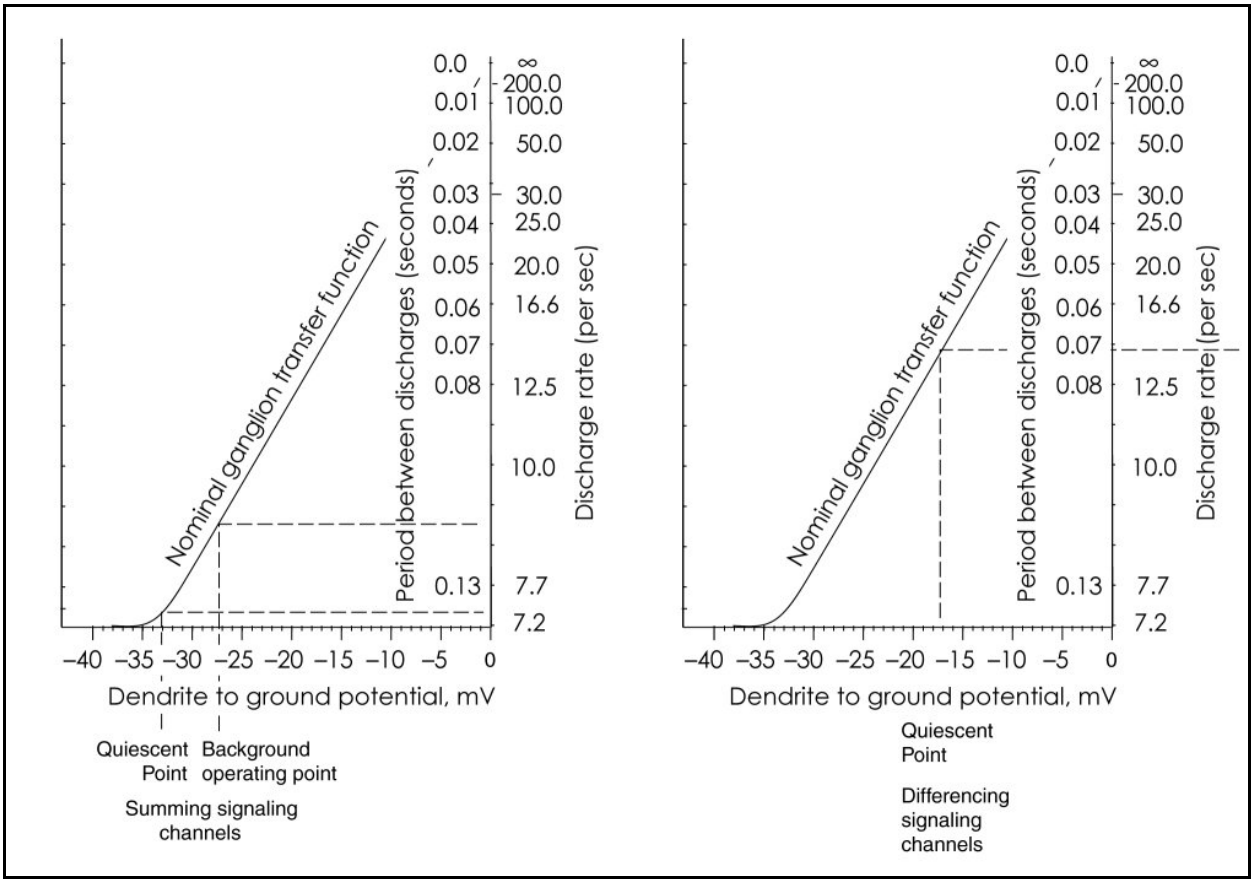

Figure 14.3.3-1 The steady state transfer functions of the stage 3A encoding neurons. Left; the steady state transfer function of the monopolar (summing channel) encoding neurons. The neuron is biased to generate less than 8 pulses per second in the absence of stimulation. The generated pulses are frequently irregular when measured *in-vitro* due to extraneous signals. Right; the steady state transfer function of the bipolar (differencing channel) encoding neurons. The circuit is typically biased to generate about 15 pulses per second in the absence of stimulation. The pulses are equally spaced under *in-vivo* conditions. Note the linear vertical scales for intervals between pulses as opposed to the logarithmic vertical scales for the frequency generated for a static dendrite to ground potential. Cutoff typically occurs near –32 mV dendrite to ground potential.

14.3.4 Examples of sound encoding

The following figure provides simple examples of signal encoding. The left frames show the typical quiescent condition at the top (output above the related input), a phasic signal resulting from stimulus by a constant amplitude analog signal, and a phhasic signal resulting from a higher amplitude analog signal. In both cases, both analog signals cause a first phasic action potential very near the start of the analog signal.

The right frames show a more complex situation. The top frame shows a constant phasic signal in the absence of any analog input stimulus. The middle frame shows the phasic response to a two-step positive-going analog stimulus, while the lower frame shows the response to a two-step negative-going analog stimulus. In both cases, a change in the pulse spacing occurs with the start of the analog waveform. Note that large negative going analog signals can drive the resulting phasic signal to very long pulse-to-pulse spacings. These long intervals greatly restrict the transfer of information by the system.

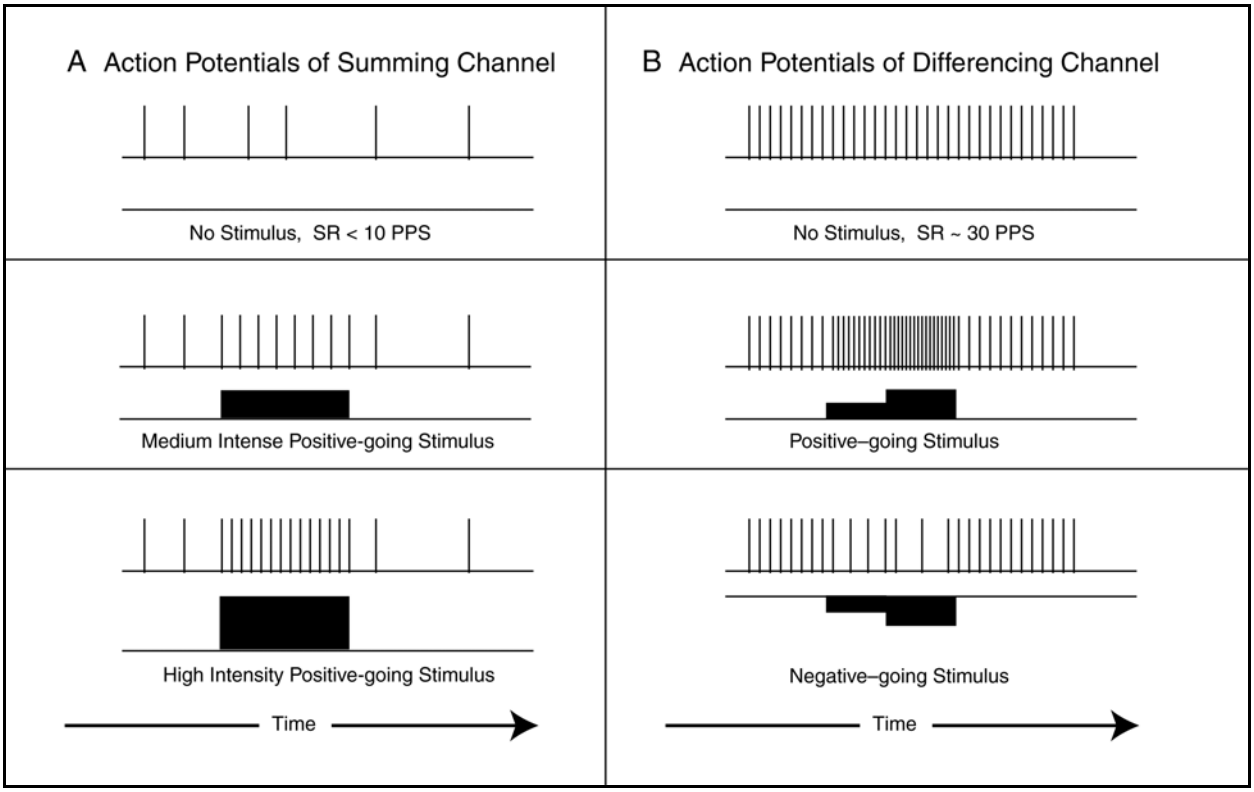

Figure 14.3.3-2 Examples of the place code used in the neural system. The code is the same but its application to the summing (A) and differencing (B) channels is fundamentally different. In A (top) only random noise spikes occur in the absence of stimulation. Stimulation causes the generation of an organized set of spikes with their spacing indicative of the intensity of the stimulation. In B (top), a set of equally spaced spikes are created in the absence of stimulation. Upon stimulation by positive-going stimuli, the interval between spikes decreases in proportion to the amplitude of the stimulus. Conversely, negative-going stimulation causes a proportionate increase in the interval between spikes in proportion to the intensity of the stimulus.

The maximum action potential pulse rate is difficult to specify. Under *in-vivo* conditions, the maximum rate reported in the literature is typically above 200 but less than 500 pulses per second. Under *in-vitro* conditions, and particularly parametric excitation conditions, rates up to 900 pps have been reported. However, it is not clear that these high rates are significant and can be decoded without distortion by the stellite neurons discussed in the following pages of this subject set.

- - - -

XXX Vision related stuff

The goal of the signal coding architecture used in the visual system is to deliver the essence of the scene, presented to the eyes in object space, to the brain in the most efficient manner possible. The resulting coding architecture is highly dependent on the detailed requirements placed on the visual system of a given species. These requirements vary immensely within the phylogenic tree. They even vary between man and the other upper primates of *Hominoidea*. This section will concentrate on the complete architecture found in man. The simpler architectures used in virtually all lower forms can be seen within this most global architecture.

There are two major aspects to the subject of architectural coding relative to vision. One is the question of the

coding architecture related to the spatial aspects of the retina. The second has to do with the methods of coding the information generated by the photoreceptors of the retina for efficient transmission to the brain. Both of these aspects are impacted by the bottleneck caused by the optic nerve. This bottleneck is imposed by a functional requirements associated with *Chordata*. A subsidiary of these two aspects is the coding employed to translate the spatial frequencies associated with certain features in the scene into a more compact signature. A review of the visual system shows there are a variety of coding methods used to optimize the system. The adoption of these coding schemes is another example of form following function.

Once the overall coding architecture of the visual system is defined, it becomes apparent that the same architecture is used within the cortex itself. The techniques used within Stage 3 of the visual system, directly related to the optic nerve, are found to also apply to all of the commissure within the brain. They are also found to apply to the signal projection circuits of the peripheral nervous system.

The techniques of mapping and encoding employed in vision are sophisticated and relatively obscure. They are not normally encountered in biological research. However, they are critical to an understanding of the operation of the visual process. This section will discuss the highlights and a number of examples of the architecture of visual coding. It will be followed by Section 14.3 discussing the functional aspects of coding and providing generic examples of the coding used in vision. Sections 14.4 will then develop the detailed circuits actually used within the visual system to implement this architecture.

14.2.1 Field mapping in vision

To set the stage for the following discussion, it is important to resolve certain issues. Contrary to the position taken in many lower level texts, the retina consists of an extensive array, on a highly curves surface, of photoreceptors of only one size (within a factor of two) as shown by Pirenne and others (see **Section 3.2.2.1**). The pitch of the photoreceptor cells does not play a significant role in the loss of spatial resolution with field angle relative to the line of sight. It is also important to re-emphasize that the form of the sensory system in human vision is not that of an imager. It is fundamentally a change detection system. Because of this fact, the human eye is frequently characterized as achieving “super-resolution,” resolution beyond that calculated for a pixel based imager.

As discussed earlier in **Chapter 2**, the mapping of the object field onto the retina of a complex eye is a very nonlinear geometrical process. The lens/cornea combination is a very sophisticated “thick lens” system employing graded index materials. The back focal length of the system is a strong function of the field angle with respect to the optical axis. The result is a very high degree of geometric distortion. Although the photoreceptors of the retina are all of nearly equal diameter, resulting in an essentially constant resolution in retinal space, the geometric performance of the optics results in a much poorer limiting resolution in the periphery of object space. Because the effective aperture of the optical system varies with field angle also, the resulting F/# of the system is nearly constant. As a result, the illuminance of the resulting image relative to the scene illuminance is almost constant with field angle.

It is the limited resolution of the optical system in man, rather than the limiting resolution of the photoreceptor array, that is usually reported in the literature.

The detailed mapping of the object space of a given visual system into retinal space requires a complete ray trace of the optical system. Because of the complexity of the human optical system, such a ray trace will not be provided within this work.

14.2.1.2 Retinal field mapping

When discussed in the literature, the relationship between the retinal map and both the neural paths of the optic nerve and of the cortical projections are usually spoken of conceptually. There is little material describing the mathematical (or geometrical) transformations employed. In most cases, the authors speak of the degree of convergence needed between the number of photoreceptors in the retina and the number of nerve fibers in the optic nerve. This ratio is usually given as between 100 and 150 based on the assumption that the neural paths in the optic nerve are individual hardwired circuits dedicated in time to a specific photoreceptor channel. This is an overly simplistic assumption.

Understanding the operation of the pointing and shutter system leads to an understanding of the spatial encoding by the retina and subsequent decoding by the cortex that allows such excellent spatial discrimination capability to be performed using only the limited number of neural fibers found in the optical nerve bundle. This capability employs

two separate techniques; a short term memory storage capability similar to the full frame memory storage used in modern digital television transmission, and an encoding system of the n-ary type. The advantage of the full frame short term memory is obvious, the retina need only transmit changes in the scene that have occurred within the last frame interval, an interval known to be less than 1/20 second in most cases and closely related to the fusion frequency of the eye.

> As an incidental note, it can be pointed out that the nominal pulse interval of the midget ganglion cells associated with the differential chromatic channels of vision, is 1/30 second.

14.2.1.2.1 Retinal mapping requirements in man

The system requirement applicable to a specific animal can be subdivided into a small group of individual top level requirements. These requirements are most easily related to the modes of operation of the eye, which are in turn related to the phylogeny of the animal and its environmental niche. A catolog of the operating modes of the human visual system will be developed in **Section 15.2.5**. For the human, the number of top level operating modes are two, the awareness mode (shared with other animals) and the analytical mode (most highly developed in man). One of the primary purposes of the awareness mode is to develop alarm signals correlated with the dangers perceived by the animal. These perceptions are based heavily on learning. How these alarm signals are processed is highly species dependent.

The awareness mode– In the awareness mode, the eyes have the responsibility of reporting significant changes within their instantaneous field of view to the CNS promptly. If the characteristics of these changes form a small set, it is possible for the system to extract these characteristics early and reduce the volume of data that must be sent to the CNS. Similarly, if some of these characteristics are only required to exhibit a certain accuracy, the volume of data can be controlled appropriately.

In humans, and most chordates, the awareness mode is not required to describe the nature of an object in the peripheral field in spatial detail. The detailed parameters are obtained in conjunction with the analytical mode and the ability of the system (eyes, neck and torso) to swing the line of sight to concentrate on individual areas sequentially.

The alarm path– Except for the fovea, the system requirement is that the brain receive information as to the location of a change in the illuminance of a pixel within the retina, and, if a sustained change, the relative change in amplitude of the illuminance. There is no requirement that there be an individual direct connection between a neuron of the optic nerve and a photoreceptor. The requirement is more closely related to the "packet" transmission mode of the INTERNET than the continuous circuit mode related to a leased telephone line. In developing the detailed performance of the retinal mapping system, it is important to appreciate this difference.

The Analysis mode– Following an alarm, the line of fixation is normally made to coincide with the line between the aperture of the eye and the source of the alarm. The system requirement is that the line of fixation be made to scan the source of the alarm in order to ascertain the nature of the object causing the alarm and its probable intent. This requirement calls for relatively intense utilization of the signal paths between the fovea and the higher cognitive centers. It is likely that the neural pathways between a small group of foveal photoreceptors and the cognitive centers are analogous to the "leased line" analogy mentioned above. These appear to be the neural circuits that go to the pretectum area of the brain. By going to this location, the neurons provide the least possible circuit delay around the servo loop that includes the muscles performing the physical scanning function.

The missions of both of the above modes can be accomplished using only luminance information. However, they can be performed better if chrominance information is also available. It is therefore likely that the chrominance circuits parallel the luminance circuits in some sense in both modes. Determining the relative importance of the chrominance and luminance circuits, especially in terms of field position, is one of the most difficult in psychophysics.

An additional underlying requirement is that the reliability of the system not be degraded by the mapping operation.

The subject to be addressed is then; how are the signals associated with the awareness and analytical mode, and any auxiliary alarm signals coded for transmission to the brain. The fundamental question is best understood by examining the awareness mode first.

Other authors have divided the visual function into focal and ambient sections[18]. It appears their ambient division is similar to the above awareness mode. Their focal division appears to encompass many of the elementary functions of the analytical mode.

14.2.1.2.2 Retinal mapping requirements of the awareness mode

As noted above and earlier in this work, the visual system (in the absence of tremor) is a change detection system. This is due to the presence of a zero in the frequency response of the transfer function of the adaptation amplifiers of the photoreceptor cells. In animals not exhibiting tremor (*Arthropoda*, most *Mollusca* and lower *Chordata*), this greatly simplifies the awareness task. The animal does not "see" anything in its visual field of view that is not associated with changes in illumination level at the pixel level. The problem resolves into a simple one of specifying where in the field the change occurred. For very simple animals, this reduces to the problem of specifying which simple eye (or photospot) sensed the change. In some of these animals, the output of the photoreceptor cell is connected directly to a muscle and flight is the immediate response. In more advanced animals, triangulation, based on the information from several photospots, several simple eyes or several ommatidia within a compound eye, may be used to determine the direction of the threat prior to flight.

> The reader should be cautious, any motion of the line of sight of the animal relative to object space will cause a change in the illumination level at most of the photoreceptors in its visual system. Thus any sudden motion of the animal will generate an "image" of object space for a short interval. Rhythmic motions can generate a quasi continuous "image." These motions are frequently adequate for species identification, mating and other functions.

An important conclusion can be drawn from the electophysiology of all animals. No example of calculations involving transcedental functions (trigonometry) by animals could be found in the literature. The calculations are made based on two or more perpendicular axes. The calculations are based on tangents and cotangents and not on radial coordinates such as magnitude and angle. This is a significant architectural observation. It suggests the retinas of more advanced animals are subdivided into Cartesian sectors for purposes of computing the alarm path signals. As discussed below and in **Chapters 7** and **15**, this is clearly the case in humans.

The primary requirement with regard to the awareness mode of vision is that signals be produced in the retina that describe the location of any change in illuminance in the field of view . In all but the simplest animals, these signals are transmitted to the CNS. As the complexity of the visual system increases, a second requirement becomes the projection of the signals to the CNS in the most compact form available. As the size of the animal increases, the requirement that the transmission be accomplished in a timely manner also becomes important. This latter requirement is a major reason for the implementation of Stage 3, the specialized signal projection circuits of vision, in the higher animals.

An additional requirement on the visual system not related to signaling is for a memory element. As the sophistication of the animal increases, there is a need to memorize certain patterns in object space that define food, other members of the same species, and particularly virulent enemies. Such a memory element located within the CNS can greatly enhance the performance of the overall system. In conjunction with the above memory, the performance of the system may be enhanced by a facility for recognizing specific simple intensity patterns in time. These can greatly aid in the computation of the relative velocity of threatening elements in object space. Such facilities, if located within the retina, can further reduce the overall signal processing task of the visual system and may simplify the task of signal conversion to meet the limited channel capacity of the optic nerve.

The architecture of the visual system associated with the awareness mode in man appears to be designed to meet a number of requirements within several constraints. The major constraint is the significant spatial dispersion in the photon flux associated with a given change in illumination in the peripheral retina compared to the same signal in object space. To all of the above requirements, several separate signaling paths are used.

For purposes of alarm reporting, the signals from the photoreceptors of the retina (exterior to the foveola) are grouped together into Cartesian (rectilinear) sectors of approximately the same diameter, in object space, as the desired circle of error associated with centering an image within the foveola. Based on this work, the bipolar cells

---

[18]Stone, J. (1983) Parallel Processing in the Visual System. NY: Plenum pg 354

performing this function (there may be more than one per sector operate in a linear summing mode. However, the ganglion cell(s) supporting an individual sector operates with a very low threshold in order to generate an action potential to report the lowest feasible signal change within the sector. This mechanism of aggregating many low level signals before applying the signal to a threshold circuit effectively recovers the signal deterioration caused by the optical system. The resulting alarm signals are passed as directly as possible to the superior colliculus in order to engage both the oculomotor system and the skeletal locomotion systems. Since these circuits are hard wired, it is not necessary to provide a position label to the signal packet. The position label is associated with the point of arrival of the signals within the midbrain. The oculomotor system proceeds to rotate the eyes and thereby image the presumed threat onto the foveola. This allows the POS to perform a more detailed threat analysis (both pre and post avoidance action by the skeletal system).

For purposes of general awareness, the same aggregation of signals associated with each sector can also be used to perform a coarse update of the general saliency map (see **Chapter 15**) associated with the awareness mode. After discussing the mapping requirement of the analytical mode, a higher performance operating procedure for updating the saliency map at higher resolution.

14.2.1.2.3 Retinal mapping requirements of the analytical mode

This section will concentrate on the analytical mode of man. This mode is far more complex than the simple pattern comparison capability of simpler animals.

The analytical mode of vision, as defined in this work, is closely tied to the electrophysiological feature known as a foveola. This feature may or may not be coincident with the morphological feature known as the fovea, depending on the species and its location within the phylum, *Chordata*. In the human, the foveola is generally the central disk of 1.2 degrees diameter within the larger fovea (about 6.2 degrees in diameter). It is this central disk that is responsible for the ability of man to analyze the content of a scene to a degree unheard of in other species. The photoreceptors contained within this disk appear to be connected by individual neural paths to the pretectum of the midbrain. It is also closely tied to the oculomotor system since the requirement in the next paragraph is a full time one. It cannot be achieved by a change detector in the absence of motion. Nor can it rely upon the relatively slow motion achievable by large animals purposely moving their eyes, head and torso.

The requirements placed on the analytical mode of the visual system of man, with regard to the foveola, are unique. The primary task is to extract the features of a scene imaged onto the foveola with an unprecedented degree of detail in a timely manner. The level and flexibility desired in this feature extraction mechanism is not compatible with any preliminary processing within the retina. Thus, no requirement is placed on the system to minimize the number of neural paths between the photoreceptors of the foveola and the midbrain. There are approximately 23,000 such neural paths. However, a major requirement is placed on the pretectum of the midbrain. The pretectum is tasked with extracting the features (which may be essentially random) associated with a visual field of approximately 175 photoreceptors in diameter.

The number of potential patterns that can be imaged within an array of 175 cells in diameter is mind boggling.

Timely manner is underlined in the previous paragraph. It imposes two sub requirements. First, the extraction of the features must be accomplished within small multiples of 50 msec. Second, the extraction must be accomplished in the absence of any intrinsic variation of illumination in object space. Thus an artificial motion, between the scene and the line of sight, must be provided by the analytical system. This is the requirement that gives rise to the tremor associated with oculomotor system of human vision. Without this capability, an animal is unable to image a scene continuously. Without this capability, the resolution capability of the visual system is limited to that of a pixilated retina.

The above requirement leads to the architecture of the Precision Optical System incorporated within the visual system of man (and possibly other *Hominoidea* to a degree). This system is outlined in [**Figure 15.2.5-3**] and detailed in **Sections 7.3** & **7.4**.

The resulting architecture is based on a two dimensional parallel processor, optimized for binary changes in illumination level among the elements within its processing array, and operating at a cycle interval of 50 msec. The individual outputs (correlation factors related to a specific image of the scene applied to the foveola), defined as interps. These interps are summed sequentially to form percepts that are compared with and/or stored in the cerebellum prior to any subsequent cognitive activities associated with the cerebral cortex. Simultaneously, these interps (or percepts) are analyzed with respect to the alarm signaling path criteria. If appropriate, signals are issued immediately to the efferent neural system (via the command path) to take appropriate defensive action.

14.2.1.2.4 Routine upgrading of the saliency map

Although discussed more fully in Chapter 15, there is a need to upgrade the saliency map (full frame memory of the environment surrounding an animal) at high resolution on a variable time frame basis. The conventional procedure is to use the oculomotor system to generate large and medium saccades that effectively scan the total field of view of the visual system (possibly augmenting this field using the skeletal system to increase the total effective field of view) and sequentially map this field at high resolution. This mode of operation relies upon the full field memory to store the acquired data over the long term. The control of this mode may involve both a volition mode based on signals from the cerebellum as well as a second possible semi random saccade generator.

14.2.1.2.5 The role of color data in the awareness and analytical modes

The requirement placed on the visual system and therefore the need for a specific architecture is more difficult to define than the requirement regarding changes in illumination (which are frequently generated by changes in the spatial position of objects). While substituting the spectral absorption of individual photoreceptors for another absorption may create a broader overall spectral response, it can only do this at the expense of average sensitivity since the integrated spectral absorption per unit area of the retina remains unchanged. A case can be made that the chromatic characteristics of a scene are important in determining threats to the animal. However, the electrophysiology of the system suggests that the alarm system largely ignores chromatic content in the interest of saving time. Alternately, the chromatic content of the scene can be considered important in determining the edibility of food (at least among some species) and possibly for selecting a mate. The requirement for chromatic performance based on these criteria are less time critical.

In developing the requirement, the trend appears to be toward a chromatic capability more as a convenience than a necessity. If this is so, the requirement on chromatic fidelity is probably less than otherwise. This appears to be the case based on electrophysiology and many psychophysical tests. This would account for the fact that the architecture of the visual system exhibits both less resolution and less timeliness with regard to chrominance than it does with regard to luminance information. This is achieved by employing a larger degree of signal convergence between the photoreceptor cells and the lateral cells of the chrominance channels of vision than in the luminance channels. It is also achieved by requiring less fidelity in the chrominance information projected to the brain. It appears that this is particularly true with regard to the short and long wavelength spectral channels.

The architecture of the visual system introduces a high degree of convergence relative to the chrominance data projected to the brain. It is also less demanding with respect to fidelity in the chrominance channels than with regard to the luminance data.

14.2.1.3 Mapping theory

This work does not propose that the visual system uses a high level diversity encoding scheme to reduce the number of neurons in the optic nerve of *Chordata*. However, further research may show that the extremely complex arborization of the ganglion neurons of the retina employ such a coding architecture. It appears clear that such a system is not used with regard to the signaling channels related to the foveola. However, one may be used to support the peripheral retina. This section will document some of the principles of such a system.

The successful implementation of such an architecture may require compromises in the timing available to specific signals being transported over the optic nerve.

14.2.1.3.1 Background

Mapping theory is a highly developed mathematical field. In telephony, it is frequently called addressing theory. In the human case, the optic nerve contains a nominal one million individual neural fibers. The retina contains a nominal 150 million individual photoreceptors. The basic question is how many neural fibers are needed to provide adequate addressing for the photoreceptors. As an initial boundary condition, one million neural fibers can provide $2^{1,000,000}$ unique addresses using only two binary states. This is an astronomically high number. Only 28 neural fibers, 2^{28} states, are needed to provide an individual address for each of 268 million photoreceptors. Neglecting the reliability issue, addressing is not a major problem in human vision. There is no need for any convergence as the term is used in the vision literature.

There are a variety of methods of providing higher reliability than the simple addressing scheme using only 28

neural fibers. The simplest is to provide 56 fibers operating in a redundant mode, two neural circuits for each channel. However, this mode can lead to ambiguity. Using three neural circuits for each channel, only 84 neural fibers, allow voting. This technique is the simplest form providing error correction following a signaling failure or a signaling conflict.

From the perspective of mapping theory, these modes can be described as n-ary--a term defined in the next section. The first case is 1-28ary, the second is 2-56ary and the third is 3-84ary.

14.2.1.3.2 Nominal architecture

Many investigators have been struggling with the ideas of convergence and divergence within the retina for a long time. They have relied on the premise that the neurons in the optic nerve are hardwired in a simple topological manner to the various photoreceptors. The results based on this premise have not been fruitful. There is an alternate premise, that the photoreceptors are hardwired to the optic nerve in a very complex but deterministic manner. An n-ary system is of this type. The n-ary encoding technique has been used in high performance communications systems since the 1960's or earlier where it was necessary to send as much data as possible over a narrow communications channel. It is a type of diversity modulation. The name is generic and indicates that each information element is transmitted as a symbol. Each symbol is associated with n particular states taken from a set of -ary states. The expression -ary is taken from the simplest such set, the binary set. A larger set might be tertiary, quaternary, etc. A specific type used by the author for satellite communications was a 2-nonary or 2-9ary system. The symbols can take any form. In radio communications involving a one dimensional signal, the symbols are frequently the phase of the carrier frequency relative to a reference phase, which may be the phase of the previous symbol. In the transmission of two dimensional material, the principle is the same. In the visual system, the symbols can be individual small groups of nerve fibers. Using simple combinatorial analysis, it was shown above that only 84 neural fibers were required to provide individual addresses for each of the 150 million photoreceptors of the retina with sufficient reliability to allow minimal error correction, i.e., a 3-84ary system. These simple calculations are usually used to demonstrate realizability in an addressing system. The actual addressing architecture of vision is still unknown. However, it is clear that the optic nerve is not a bottleneck with respect to retinal mapping.

---
with approximately one million individual nerves in the optic nerve, it is possible to encode essentially all of the 100-150 million pixels of the retina using no more than YYY nerves per symbol. The required system is therefore no more complex than a YYY-millionary system[19]. In the actual visual system, the order of the encoding system is unknown. This simple calculation contradicts the occasional soothsayer in the literature that says the optical fiber bundle is severely limited in its data transmission capability. In fact, it has adequate if not excess capacity. This calculation also provides an introduction to the reason for the complex interconnections found in the inner plexiform layer of the retina.

In the cortex, the decoding follows the same mathematical (or geometrical) rules as the encoding in the retina. Notice that diversity modulation using an YYY-millionary system does not require any analog to digital convertors, even though such devices are frequently employed in man-made systems of this type.

The architecture of the human visual system, with the “direct fibers” associated with the fovea going to the Pretectum, suggests that there may be a subdivision of the optic nerve fiber bundle. The nerves associated with this subdivision may employ a different symbol table. However, this is probably unnecessary in light of the capacity involved. In fact, it is quite possible that the full symbol table is used to transmit all of the visual field to the LGN’s and an additional area of the symbol table transmits selected data to the Pretectum. This would provide a limited amount of redundancy to the cortex. It could also account for the frequent observation of limited acuity among certain types of color deficient patients.

> In code breaking, it is common practice to develop the symbol map as an aid to determining relationships between the information transmitted before the full code is broken. Such a symbol map would be very useful in understanding the spatial encoding used in the retina. It would be suggestive of the spatial summation and spatial differencing techniques sought by various vision investigators. It might also suggest whether the nerves going to the Pretectum use the same

---

[19]Care must be observed here. The word millenary is related to a thousand in British English. The intent is to specify one million degrees of freedom.

symbol table or a more specialized table.

14.2.1.4 Role of physiological optics in retinal mapping

There have been very few investigations of the circuits of Stage 3 to date. As these types of experiments are undertaken, it will be important to model the visual system properly. This modeling must include the physiological optics as well as the neural circuits. This will be particularly important as the desired precision in the results is raised.

Recently, interferometric techniques have come into use in vision research. They offer a very high level of precision compared to earlier techniques. They also offer a flexibility in stimulus pattern generation, orientation and positioning on the retina not easily obtained with other techniques. However, it is a very early day and the capabilities and limitations of some of the test sets have not been completely understood. See the **Addendum**, Interferometry in Vision Research for a more complete discussion of this technique.

14.2.1.5 Delay as a factor in retinal mapping

A little recognized but important factor in the visual process is the relative time a signal takes to reach the cortex from a given location in the retina. As will be discussed in Chapter 15, Meyer's loop is a significantly more important feature from a functional perspective than it is from a morphological perspective. There is an equivalent structure to Meyer's loop in the retina. It is the distance that the axon of a ganglion cell must travel to reach the blind spot of the retina and the entrance to the optic nerve. The physical distances involved in the retina are smaller than those associated with Meyer's loop. However the electrical distances are essentially identical. This is because of another practical consideration. To avoid additional scatter of light due to the ganglion cell axons in the neural layer, the portion of the ganglion axon prior to reaching the optic nerve are not myelinated[20]. This lack of myelination results in a lower phase velocity of signals along the axon and a longer effective electrical length for this portion of the axon.

14.2.1.5.1 Delay associated with Meyer's loop EMPTY

[xxx discuss length and subsequent delay associated with Meyer's loop as enumerated in Chapter 15, part I section 15.2.2.1 and in part II, section 15.6.7.2. Discuss both average and differential delay to restore phase cohenece between neural signals arriving at the occipital lobe.]

14.2.2 Signal coding

Obtaining recordings of action potentials at different locations along the signal paths to the brain is relatively easy. However, the farther from the retina, the more highly encoded (or processed) the data is that the signals carry This leads to signals with frequency (or pulse-to-pulse time intervals) as a function of spectral frequency that may not be easily interpreted. The DeValois & DeValois paper cited below includes a discussion of the ambiguities in the data and analyses of various investigators in this area. The signals recorded at the optic nerve are typically simpler and less ambiguous than some recorded at the LGN. By the time the signals reach area 17, they begin to lose their recognizable features with respect to both spectral wavelength and spatial location. Recording signals at the PGN and at the pulvinar appear currently to be beyond the state of the electrophysiological art.

The fundamental coding architecture used in the retina is shown in **Figure 14.3.4-1** with a focus on the peripheral retina and leading to the LGN/occipital couple (Section xxx). The signal pathways to the foveola vary slightly in that no signals relating to the middle pathway extend to the PGN/pulvinar. Instead, individual neurons are provided between each spectrally sensitive sensory neuron of stage 1 and the stage 3B decoding neurons of the PGN/pulvinar couple via stage 3A encoding ganglion neurons (that have not been given formal names).

---

[20]Black , J. & Waxman, S. (1988) The perinodal astrocyte. GLIA, vol. 1, pp. 169-183

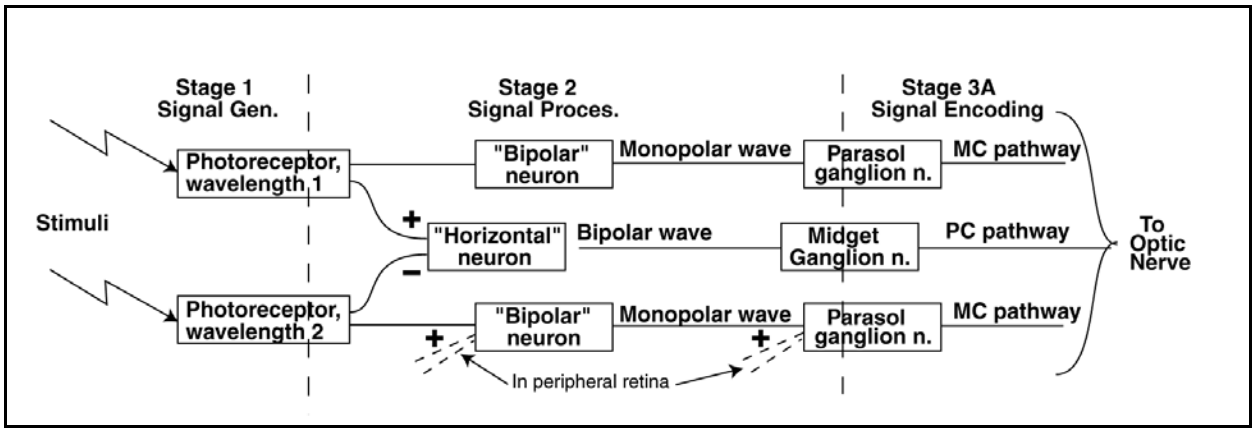

Figure 14.3.4-1 Fundamental coding architectures used in the peripheral retina. The upper and lower pathways relate to magnocellular pathways representing R–channel data throughout the retina and "Y" signals (individual UV–, S–, M –, and L–channel signals found only in the foveola and projecting to the PGN/pulvinar couple. The middle pathway processes differential signals of the O = S – UV, P = S – M, and Q = L – M types. The dashed lines along the lower pathway are suggestive of the high level of summation that may be found in the peripheral areas of the retina involving sensory receptors of a single spectral type. See text.

The stage 1 and stage 2 signals of the retina are all analog signals. The R–channel signals destined to the LGN/occipital couple are encoded by parasol ganglion neurons into Magnocellular type signals found within the neurons associated with the magnocellular pathways as suggested by the lower pathway. The chrominance signals are processed by the middle pathway beginning with the stage 2 differencing step by horizontal neurons and sometimes by the input neurite structures of the midget ganglion neurons themselves. In either case, the output of the stage 3A midget ganglion neurons are typically "free-running" (action potential) pulse streams associated with the parvocellular pathway. These pulse streams are encoded on a pulse-to-pulse interval basis. Additional details regarding these individual paths and circuits will be provided below.

Figure 14.3.4-2 shows the next level of detail of the coding architecturs used in the retinas. A; shows the detailed circuitry connecting a stage 2 circuit to an encoding stage 3A ganglion neuron, including n Nodes of Ranvier. It delivers an encoded analog signal via a stream of monopulses (action potentials) to a stage 3B decoding stellate neuron (see definition in **Sections 14.2.3 & xxx**) that outputs an analog replica of the input signal. B; the equivalent circuit of the input synapse acting as an "active diode." The impedance, Z, is essentially a perfect electrical diode that can be represented by a fixed impedance over a limited signal amplitude range. It is shunted by a capacitor. The value of P is chosen to insure an output that is a duplicate of the positive going input signal with essentially an amplification of 1.000 but a change in DC amplitude between the input and output terminals. The circuit of frame A incorporating the equivalent input of frame B is typically used to pass R–channel and G–channel signals between engines of the complete neural system. C; an alternate stage 3A showing two distinct inputs that eliminate the need for the horizontal neuron of the previous figure.. The upper input synapse passes a unity gain copy of the analog input to the non-inverting input of the stage 3 ganglion Activa. The lower input synapse passes a unity gain copy of the analog input to the inverting input of the stage 3A ganglion Activa. The impedance in the base lead of the Activa insures the negation at the base of the Activa exhibits the same amplification factor as the amplification factor of the non-inverting circuit. The upper input can consist of an S– or L–channel signal. The lower input can consist of an UV– or M – channel signal. Any of these signals can be the summation of multiple individual input signals of the selected chrominance signals (not shown) The summations are accomplished by bipolar cells. With these assignments, the stage 3A ganglion can deliver an encoded output representing, O = S – UV, P = S – M or Q = L– M chrominance signals based on the choice of nomenclature shown in **Section 17. 3**. This circuit configuration can also process N –channel polarization signals (usually containing difference signals generated by two sensory neurons. of the same, but not necessarily, chrominance type but with different physical orientation in the regina). D; The equivalent circuit of the output synapse connecting the last axon segment to a stage 3B decoding stellate neuron. The synapse acts the same as the input synapse of frame B. The stellate cell delivers a faithful band-limited version of the input signal (whether it is a monopolar or bipolar signal) by proper selection of the impedance, P. **Figure 1.7.5-4** provides a similar figure summarizing the above signal processing. **See Section 14. xxx** for additional details concerning biasing by the voltage source labeled E and C throughout the generic stage 3 circuit.

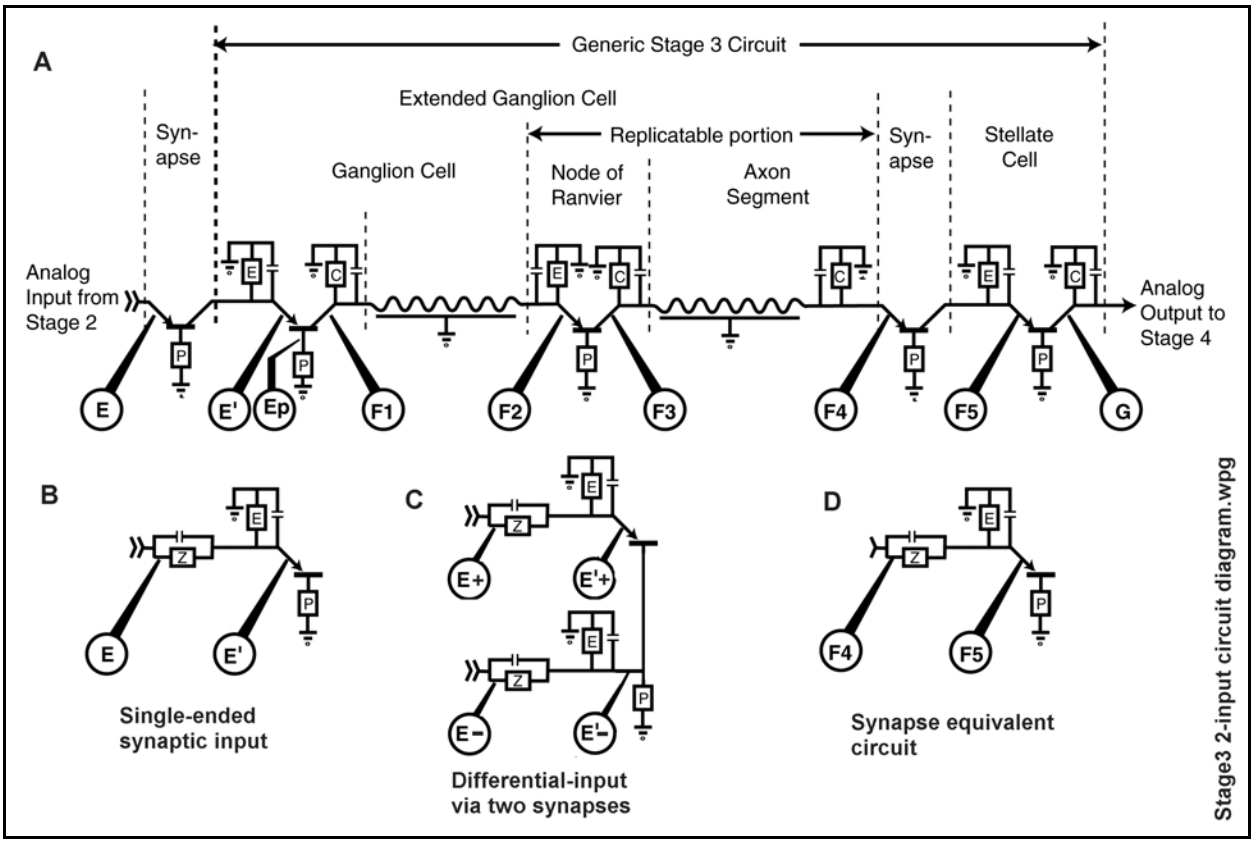

Figure 14.3.4-2 Details of the coding architecture used in the retinas. A; the generic stage 3 circuit propagating streams of monopulses (action potentials. B; Equivalent circuit of the input synapse acting as an "active diode". C; alternate input structure of the ganglion neuron providing two inputs in a differential configuration. See text. D; the output of the stage 3A (encoding) ganglion neuron connected to the stage 3B (decoding) xxx neuron by the equivalent circuit of the synapse acting as an "active diode."

Destexhe et al. discuss "the active properties of dendrites and how they convey discrete synaptic inputs to the soma." Unfortunately, their interpretation of these phenomena are based on their archaic concept of a two-terminal electrolytic neuron. See **Section 14.6.3.7**. However, their data is readily, and more effectively, interpreted using the three-terminal neuron incorporating the Activa (**Chapter 8**).

14.2.2.1 Introduction to signal encoding and modulation

It will be shown that the losses associated with the propagation of low level analog signals over distances exceeding a few millimeters is excessive at the impedance levels of neural circuits. Therefore, as in similar man-made circuits, it becomes desirable to adopt a different signaling method in those cases. There are two widely recognized methods of accomplishing this. Both involve a translation of the signals out of a low frequency region of the temporal spectrum that includes zero frequency to a higher frequency region. This results in signaling channels that are narrower relative to their central frequency. It is much easier to maintain good signal integrity in narrower frequency channels.

To achieve the translation described above, signaling theory would suggest either of two techniques:

1. The sampling of the baseband signal information at intervals and generating a series of pulses that describe the information in the original signal. This technique is generally defined as encoding.

2. Using the baseband signal information to cause the parameters of a continuous series of pulses to vary in a

manner that describes the information in the original signal. This technique is generally defined as modulation.

Both of the above techniques are use in the neural circuits of vision. The encoding mechanism is used for monopolar signals typified by the luminance information derived from the scene. The modulation mechanism is typically used to project bipolar signals derived from the scene, such as those associated with chrominance, polarization and appearance.

The fundamental signal encoding scheme used in animal vision is classified as time-delay modulation, a form of phase modulation. As will be developed in this chapter, the modulation is a function of both the elements of the scene presented to the eye and also, at least in the case of the higher vertebrates, to the small physical oscillation of the eye, known as continuous tremor. This type of modulation is characterized by packing more information into a given signal space than nearly any other form of modulation. Appendix C provides more details on this type of modulation.

The chrominance information is encoded using the same type of time delay modulation. However, the encoding devices, the ganglion cells, operate in a different temporal mode. Whereas the luminance channel ganglion cells only generate action potentials "on demand," i.e., in response to a monopolar electrotonic input signal, the chrominance channel ganglion cells generate a continuous stream of action potentials whose pulse to pulse interval is modulated by a bipolar electrotonic input signal.

14.2.2.1.1 Frequency versus phase modulation

[xxx reorient to include AM & comment on poor use of terms related to modulation and encoding techniques]

There is a problem in the different use of the expression frequency modulation in the vernacular and the technical literature. While the term frequency modulation is commonly used with reference to one type of commercial radio transmission, the actual modulation used in that system is not frequency modulation. It is a hybrid of the phase modulation type designed to obtain certain performance features. However, phase modulation systems are plagued by pink noise. This noise is characterized by higher energy density at higher frequencies in the recovered baseband signal. To overcome this problem, an additional pair of circuits are introduced. The encoding circuit at the transmitter consists of a phase modulator and a pre-emphasis circuit. At the receiver, a demodulator circuit is followed by a de-emphasis circuit. The pre-emphasis circuit is a form of the more general lead-lag electrical circuit used in many man-made electronic systems. The basic modulator is a phase modulator. It changes the phase of the carrier of the transmitter in response to the baseband (typically audio) input signal. The de-emphasis circuit at the receiver decreases the output signal as a function of frequency. This de-emphasis circuit suppresses both the pink noise associated with the technique as well as the signal information. To counter the loss in signal information, a pre-emphasis circuit is introduced at the transmitter. As a result, the overall input output characteristic of the system is flat with baseband signal frequency but the potential pink noise interference is suppressed.

The biological neural system employs phase modulation as its primary technique associated with signal projection. However, there is a small amount of experimental data suggesting that pre-emphasis circuits are found associated with some ganglion cells. This data must be examined carefully to assure the observed effect is due to pre-emphasis in the ganglion cell and not due to the frequently observed peaking associated with the leading edge of the generator potential from the photoreceptor cells. Whether the analog circuitry associated with the pre-emphasis and de-emphasis circuits are considered part of Stage 3 is largely arbitrary. However, functionally, they are closely associated with Stage 3.

14.2.2.1 Luminance coding

14.2.2.1.2 Luminance coding at the LGN

DeValois & DeValois have provided the characteristics of a variety of R-channel signals as a function of wavelength recorded at the LGN. The subjects were macaque monkeys. The probe locations within the LGN were not specified with great precision. They primarily made measurements in response to incremental changes in stimulation. Thus, they recorded both positive going changes from a baseline illumination and negative going changes. These were recorded from what they describe as spectrally nonopponent cells. These waveforms typically show a familial relationship to the overall spectral sensitivity function of the eye. The precise form of the waveform may indicate the state of adaptation of the eye during the test. They recorded signals where the frequency rose and signals where the frequency fell in response to positive increments of stimulation. This would suggest that there recordings were not of signals as received from the ganglion cells of the retina. The maximum pulse frequency reported was 45-50

Hz.

14.2.2.2 Chrominance coding EMPTY

[xxx develop fact, the coding of chrominance information is bipolar and applied to a carrier **]**

14.2.2.2.1 Chrominance coding in the optic nerve

The most recent direct observation of the chrominance encoding function is by Troy & Lee[21] and by Troy & Robson[22]. They looked at a variety of X and Y cells in cat (1992) as well as cells associated with the magnocellular (MC) and parvocellular (PC) pathways of macaque monkeys (1994). As predicted by this work, they observed continuous action potentials generation in the X and Y cells (presumably associated with the chrominance channels) in the presence of continuous and uniform illumination. They labeled these pulses as a maintained discharge. They observed that signals in the PC-pathways (presumably originating from midget ganglion cells) discharge in a sustained fashion while MC-pathway cells (presumable originating from parasol ganglion cells) discharged transiently to stimulation with lights of all wavelengths at moderate contrast levels. If the above presumptions are correct, their results are in excellent agreement with this work. Wilson has also noted the conflict between the anatomical and physiological literature with regard to the designations (p)arasol and (m)idget cells connecting to the (m)agnocellular and (p)arvocellular channels respectively[23]. However, his explanation relates to bipolar cells and appears awkward.

Their 1992 study used a P-31 phosphor light source. In their 1994 study, they used two individual narrow band illumination sources. One had a dominant wavelength of 554 nm (half amplitude width of 18 nm) and the other a dominant wavelength of 638 nm (half amplitude width of 23 nm). They mixed these lights to form a "Yellow" light. The method they used to control the mixture is not supported by this work.

In the absence of a functional model of the process they were exploring, they used statistical techniques to ascertain power densities and other statistical attributes. In particular, they introduced the assumption that the pulses were due to a "renewal process." They describe a renewal process as one that generates a series of events in which the intervals between them are identically and independently distributed. This stochastically based assumption appears inappropriate for a clearly deterministic process such as the pulse interval between pulses in a chromatic channel where the interval is directly controlled by the DC potential between the emitter and base of an Activa. The design of their experiment did not call for the control of the adaptation state of the photoreceptors. It is not clear whether it called for the recording of all of their data as a function of absolute time. If it did, the data could be re-examined with the intent of determining the change in pulse interval with time, independent of all other variables. This process may separate their apparently stochastic data into a more complex series of parameters due to individual deterministic processes.

In 1992, they described the rate of this discharge as moderate but indicated its mean inter-pulse interval was not steady. This was probably due to changes in the adaptation state during their measurements. They also collected data using a series of stationary one dimensional sinusoidal gratings produced on a P-31 phosphor screen as test patterns. Since this type of phosphor excites photoreceptors of multiple spectral types, it is important to understand the state of adaptation of each of these types during the experiments. This subject was not addressed in the above papers. As a result, their data for ensembles of typically 20 to 100 cells show a significant statistical variation. One of their interesting observations was that the standard deviation of the pulse interval was a direct function of the mean interval. In general agreement with this work, the mean intervals, collected over unspecified durations, were typically 18-60 ms in their 1992 study (a variation of 3:1). In their 1994 study, the variation has decreased to 20-30 impulses per second (a variation of only 1.5:1). The 1994 study also paid more attention to variations in rates with time within their data. It concluded there were *statistically* significant trends in the rate of maintained discharges although they were generally small. This appears consistent with the adaptation process which has time constants on the order of minutes.

Merigan & Maunsell have noted the critical nature of the P pathway within the optic nerve[24], "Perhaps the most dramatic effect of P pathway lesions is an apparently complete loss of color vision (Figure 2C) (Merigan 1989;

---

[21]Troy, J. & Lee, B. (1994) Steady discharges of macaque retinal ganglion cells. Visual Neurosci. Vol. 11, pp. 111-118

[22]Troy, J. & Robson, J. (1992) Steady discharges of X and Y retinal ganglion cells of cat under photopic illuminance. Visual Neurosci. Vol. 9, pp. 535-553

[23]Wilson, H. (1997) A neural model of foveal light adaptation and afterimage formation. *Visual Neurosci.* vol. 14, pp 403-423 (pg 407)

[24]Merigan, W. & Maunsell, J. (1993) How parallel are the primate visual pathways? *Annu. Rev. Neurosci* vol 16, pp 369-402

Merigan et al 1991b; Schiller et al 1990a).” They note separately, “The physiological responses of cells in the P and M pathways are virtually identical on some dimensions and profoundly different on others. The most striking difference is sensitivity to color. P pathway neurons show color opponency of either the red/green or blue/yellow type, which means that they respond to color change regardless of the relative luminance of the colors (Derrington & Lennie 1 984). M neurons, on the other hand, are considered insensitive to color, because they have virtually no response to color alternation when the luminance of the color is balanced.”

Merigan & Mausell clearly demonstrate the M & P pathways are subpathways of the LGN-occipital pathway. They do not appear to address the PGN-pulvinar pathway.

One of their concluding statements is very useful, “ Many readers may wonder how our conclusions can differ so much from the view of parallel subsystems that has reached such prominence. The explanation lies partly in overly enthusiastic acceptance of the notion of parallel subsystems. Few ideas in neuroscience have achieved anything approaching the acceptance that this proposal has received in the six years since it first appeared in print. Two factors have fueled its rapid acceptance. First, it promised to simplify greatly the vast collection of data on visual system organization, thus providing a rationale for the physiological differences between the M and P pathways and between the parietal and temporal pathways. However, simple ideas are not always robust. A relevant example is that the simple and long-standing model of orientation hypercolumns in VI required fundamental revision following the discovery of cytochrome oxidase blobs. Second, the proposal of parallel subsystems was consistent with an impressively large collection of observations. Although none of those observations is conclusive, their number would make a strong case if each supported parallel subsystems independently. Unfortunately, they do not.” They followed with “We expect that the question of parallel pathways will continue to generate intense interest, and it is likely that our understanding will be refined in coming years. Whatever consensus emerges in the future, clearly the simple description that has held sway in recent years is, at best, a rough approximation of the truth.” [xxx add more information]

A re-analysis of the above works based on the framework provided by this work appears very profitable.

14.2.2.2.2 Chrominance coding at the LGN

DeValois & DeValois have provided the spectral characteristics related to a variety of action potentials measured at the LGN[25]. The subjects were macaque monkeys. The probe locations within the LGN were not specified with great precision. Some of the characteristics appear to be directly related to the P– & Q–channels. They correctly assumed that the signals were carrying color information. However, the data is plotted as a frequency shift versus stimulus wavelength. As discussed above, the information is actually carried by the pulse to pulse time interval, a form of phase (as opposed to frequency) modulation. There published figures were not sufficiently precise to allow replotting on a time interval basis. However, the figures do demonstrate the change in pulse to pulse interval as a function of saturation in the P–channel signals illustrated. It is also perfectly clear in these waveforms that the L-channel exhibits a peak absorption near 625 nm. The nominal carrier frequency in their figures was 7.5 cycles per second. This frequency appears too low to represent raw signals arriving from the eye. The nominal carrier frequency could be associated with a spectral wavelength of 570-580 nm.

14.2.3 Coding theory applicable to neural systems

While highly developed in the communications world, coding theory as it applies to the neural system has not been explored methodically in biology. Coding theory as it applies to the neural system is generally concerned with the modulation of a carrier system (typically a series of action potential pulses) with an information carrying component (typically an electrotonic signal created initially by the sensory neurons).

The modulation of a carrier system can be accomplished in a great variety of ways. At the most fundamental level, it involves the multiplication of two signal waveforms. This multiplication can occur in one of two ways. First, the amplitude of the carrier system can be varied in a way that describes the modulating signal. While sounding simple, there are at least six different ways of varying the amplitude of the carrier. Second, the time between the cycles of the carrier system can be varied. Here also, there are considerably more than six ways of achieving such

[25]DeValois, R. & DeValois, K. ((1975) Neural coding of color. *In* Carterette, E. & Friedman, M. *eds*, Handbook of Perception, Vol. 5: Seeing, NY: Academic Press pp 117-166 *also in* Byrne, A. & Hilbert, D. *eds*, Readings in Color, Vol. 2, Chapter 4

modulation. Rather than speaking of absolute time differences, it is more general to speak of the time difference relative to the nominal time between adjacent cycles of the carrier system and use circular notation. As a result, the two major methods of modulation are known as amplitude and angle modulation[26]. These two fundamental methods can both be expanded to include both linear and exponential forms of modulation.

While the amplitude modulation and frequency modulation of a carrier (consisting of an action potential stream) have been discussed conceptually in the biology literature, neither of these types of modulation are actually used within the neural system.

To avoid confusion, it is important to delineate distortion within the analog circuits of the neural system and modulation as used within the phasic circuits of the system. Both phenomena can generate "sidebands" that are distinctly different than the original undistorted or unmodulated signal. Distortion is caused by a nonlinear mechanism within the signal path. It generates "sidebands" that are harmonically related to the original baseband signal. A baseband signal is one that is described as beginning at, or as symmetrical about, zero frequency. The generated sidebands share this relationship with zero frequency. Modulation also generates sidebands. However, they are of a fundamentally different type. In modulation, the information carrying sidebands are formed at frequencies that are symmetrical about the fundamental frequency of the carrier system. They are not symmetrical about zero frequency. While the sidebands resulting from modulation are the fundamental means of signal transmission within the neural system, those due to distortion interfere with successful signal transmission. In most cases, the extraneous signals due to distortion are pathological in origin. They are frequently caused by excessive stimulus amplitude being applied to an auditory system during laboratory investigations.

Two types of angle modulation are commonly employed in the neural system. Both involve varying the time delay between adjacent action potential pulses in a stream of such pulses. In the first case, the stream of pulses does not exist in the absence of a modulating input signal. The stream of pulses is therefore described as "driven" by the presence of the modulating signal. In the second case, the stream of pulses occur at regular intervals in the absence of any modulating signal. As a result, this form of pulse stream is known as "free-running."

14.2.3.1 The unique features of the action potential EMPTY

14.2.3.2 The driven stream of action potentials

The ganglion neurons of Stage 3 signal projection associated with the luminance channels are of the driven oscillator type. This type of modulation is uniquely suited to support both the awareness and alarm modes of vision. The initial pulse in the action potential pulse stream is a unique indicator of a change in the environment sensed by the organism. Regardless of the amplitude of the stimulus, the occurrence of a single initial pulse within the signaling channel can be used to cause an alarm mode reaction. The occurrence of subsequent pulses within the signaling channel can be used to quantify the magnitude of the stimulus for later determination as to its level of threat, or for other purposes.

In the luminance channel, the amplitude of the monopolar stimulus is encoded into a series of pulses. As a general rule, only one pulse signifies a very low level stimulus. However, a series of closely spaced pulses can represent a very high amplitude stimulus. Where the stimulus is not stationary with time after its initiation, the structure of the series of pulses created within the driven signaling channel may be very complex.

The form of modulation used in the summation channels of the neural system is best described as a time-delay mode of angle modulation. The time delay between adjacent pulses decreases as the modulating signal intensity is increased. While this type of modulation may appear to be frequency modulation when examined as a response to a sinusoidal input signal, its characteristics are quite different when examined as a response to a ramp input. The change in frequency of the carrier is the reciprocal of that expected in frequency modulation. This difference can be shown by expanding Panter's figure 7-2 to include a ramp input signal and a time-delay modulated output signal.

Time delay modulation is particularly easy to implement using a relaxation oscillator circuit. It is merely necessary to vary the input bias level of the oscillator circuit.

---

[26]Panter, P. (1965) Modulation, Noise and Spectral Analysis. NY: McGraw-Hill Chapters 1, 5 & 7

14.2.3.3 The free-running stream of action potentials

The ganglion neurons of Stage 3 signal projection associated with the chrominance, polarization and other differencing circuits are of the free-running oscillator type. Since there is no initial pulse in a continuous stream, there is no information to support an alarm mode of neural operation. However, the free-running stream offers a capability not shared with the driven pulse stream. It can be modulated by a bipolar signal such as a type N, O, P or Q difference signal. It can also be used to support the bipolar signals generated by the amercine neurons that are not addressed in detail in this work.

The fact that a change in the modulating signal can occur at any time relative to the start of a pulse within the pulse stream shows that the modulated signal cannot carry any information about the time of occurrence of the initial change. The modulated signal can only describe the change in modulating signal over a period of several pulses. Such information is generally of lesser precision than that carried by the driven pulse stream channels.

As in the case of the driven stream of action potentials, the form of modulation used in the differencing channels of the neural system is best described as a time-delay mode of angle modulation. The time delay between adjacent pulses decreases as the modulating signal intensity is increased. While this type of modulation may appear to be frequency modulation when examined as a response to a sinusoidal input signal, its characteristics are quite different when examined as a response to a ramp input. The change in frequency of the carrier is the reciprocal of that expected in frequency modulation.

14.2.3.4 Relevant data EMPTY

14.2.4 Functional Encoding

The field of action potential creation and measurement has long been a mystery to the electrophysiology community. This has largely been due to the continual attempts to consider the neuron as a two terminal, fundamentally chemical device. It has been aggravated by the empirical approach usually taken when investigating the neurons and action potentials[27]. When it is realized the neuron is a three terminal electrolytic device containing an active semiconductive element, the Activa, the picture becomes much clearer. The generation of action potentials becomes obvious (See Section xxxx). In addition, the method of encoding also becomes obvious.

[edit xxx]
After one or more neural stages, the output signals from the Inner Nuclear Layer are presented to the ganglion cells of the Ganglion Cell Layer as voltages. These voltages modulate the binary (not analog) output signal of the ganglion cells.

In man made electronic oscillator circuits of the relaxation type, it is typical to think in terms of an input voltage as controlling the time interval between output pulses. However, the active device (the amplifier) in these circuits usually senses a voltage on a capacitor used as a summing node. in the retina, it is probably easiest to think of the last bipolar cell depositing a charge on the input capacitance of the ganglion dendrite. This charge, when summed algebraically with a current generated internally by the ganglion cell determines how frequently a pulse appears on the axon of the ganglion cell. The resulting train of binary output pulses is clearly of the time delay modulation type. This will be shown later

14.3.2 Encoding

As developed in Chapter 13, the analog signal processing section of the retina delivers two types of signals to the ganglion cells of the retina;

---

[27]Levick, W. (1973) Discharge in the visual system and its role for information processing. *In* Handbook of Sensory Physiology, Vol VII, No. 3, Jung, R. *ed*. NY: Springer-Verlag, pp 577-583

+ a monophase signal relative to a quiescent signal level generally related to the input from a single photoreceptor, or group of photoreceptors of the same spectral type

+ a biphase signal relative to a quiescent signal level generally related to the difference in input between two, or three, different photoreceptors or photoreceptor groups based on spectral classification or geometrical location. This biphase signal may be triphasic in spectral character, i. e. exhibiting two peaks of one polarity normally separated by one peak of opposite polarity when examined after stimulation of the photoreceptors by a spectrographic input signal.

The electrophysiological and morphological literature combined represent that the monophasic signal is processed by a parasol type of ganglion cell while the biphasic signals are processed by midget type ganglion cells. The functional difference is that the monophasic signal is translated into a pulse signal that only exists when the signal exceed a critical threshold relative to its quiescent signal level. The interpulse duration for this signal channel ranges from **XXX to XXX**. The biphasic signal is translated into a pulse signal that has a variable time duration between pulses. The nominal time duration between pulses is 0.2 seconds[28] **[[seems to low, check this]]** when the input signal is at its quiescent value. The extremes of this duration are about **XXX to XXX**.

[[question of whether two ganglion channels are needed to provide output from a monophasic channel in order to obtain edges for black going white and white going black.]]

Record is one of the few who have attempted to compare the electrotonic and phasic neural signals in the same figure[29]. Although his terminology is imprecise, the idea is correct. The electrotonic signal associated with the photoreceptors and bipolar cells is not a modulated signal, it is merely an electrical waveform characterized by its variation in amplitude. The electrotonic signal is modulated onto the phasic pulse stream by the ganglion cells. The resulting signal looks like it contains frequency modulation. It is in fact a more sophisticated type known as phase modulation.

14.3.2.1 Details of the encoding of the monophase signal EMPTY

[xxx show single ended input circuit from stage 2.

14.3.2.2 Details of the encoding of the biphase signal EMPTY

[xxx show differential input circuit from stage 2.

14.3.3 Transmission

[see Dyke Thomas, 3rd edition xxx]

14.3.4 Decoding

[xxx referenced in **Section 15.4.3.1.3** see Millman pg 575-577 ref. in 15.4.3.1.3]
This section is placed here to follow the thematic context of this Chapter. However, much of the discussion relies on the data associated with later Chapters, particularly Chapters 16 and 17 to justify the positions taken. The reader may prefer to examine those Chapters before reviewing this material.

From an engineering point of view, there are a variety of methods for recovering the data encoded by a phase modulation system of the time delay type. It would serve no purpose to review all of these here. However, there are two specific cases that need to be examined. The next section will address the question of recovering a signal proportional to the signal at the ganglion cell input. A following section will address recovery circuits capable of handling phase modulated signals where it is important to recover the first pulse and the interval between only two pulses. This capability is not usually available in conventional frequency discriminator types of decoders.

---

[28]Guyton, A. (1976) Textbook of Medical Physiology. Philadelphia, PA: W. B. Saunders pp. 812

[29]Records, R. (1979) Physiology of the Human Eye and Visual System NY: Harper & Row, pg 324

the number of methods available when it is desired to recover both the absolute delay of the first pulse relative to a reference pulse as well as the interpulse delays that follow it are more limited. A simple method capable of this level of performance will be described below as a putative model to aid researchers in the laboratory.

14.3.4.1 Linear versus antilogarithmic decoding

In Chapter 16, the question will be addressed as to whether the stellate cells recover a signal directly and linearly proportional to the voltage applied to the Activa of the ganglion cell or whether they recover a signal proportional to the antilogarithm of that signal. In general, linear detection of the information associated with the interpulse interval of an action potential stream can be recovered by a simple diode rectifier. A better design employs an active amplifier exhibiting amplification but biased to act as a rectifier of signals above a specific amplitude. This second form is easily achieved with the conventional type of neuron where the signal is applied to the dendritic input, the poditic input is held to the desired threshold level and a capacitance is placed between the axon plasma and local ground. No feedback or other circuitry is necessary. By properly sizing the capacitor, the axoplasm potential can be made proportional to the time interval between action potential pulses.

On the other hand, it may be desirable to recover a signal that is the antilogarithm of the signal applied to the Activa of the ganglion cell. This would be the case in the luminance channel where a signal proportional to the actual scene illuminance was desired. Such a circuit can be achieved using a simple modification of the above circuit. If the input impedance of the preceding synapse is adjusted appropriately and a diode is provided between the axoplasm and the dendroplasm, the axoplasm potential will have a value proportional to the antilogarithm of the potential applied to the synapse by the axoplasm of the previous neuron.

Both of the above circuit configurations are easily achieved in neurons. More details on these circuits are readily available on any text on analog microcircuits[30].

14.3.4.2 Details of the decoding of the monophase signal

The decoding of a monophasic time delay modulated signal is relatively simple. The goal is to measure a difference between the time of a reference signal (related to the tremor command sent to the eye muscles and compensated for the time delay related to both the neuromotor path and the “straight through” signal path) and the time of the information signal. Furthermore, if multiple signal pulses are sensed during the pulse to pulse interval of the reference signal, different interpretations may be applied to the signal. If only one pulse is received, and it is at a similar time delay as a similar pulse in the previous tremor period, the recovered analog value most likely represents the position of a sharp transition in the field. If more than one pulse is received during the tremor period, an integration with time is performed and the recovered analog value is more likely to be a representation of a change in (the relative) illumination in the field relative to the (relative)illumination reported during the previous tremor period.

Basically, the recovered signal consists of a flag indicating the most probable nature of the recovered signal and an analog representation of the analog signal originally presented to the associated ganglion cell in the retina. **Figure 14.3.9-1 Figure 14.3.5.1-1** illustrates these modes of operation. [xxx How does this differ from 14.5.4-4 alternate sig recovery]

[30]Millman, J. & Halkias, C. (1972) Integrated Electronics: Analog and Digital Circuits and Systems. NY: McGraw-Hill pp 575-577

14.3.4.3 Details of the decoding of the biphase signal

The decoding of a biphasic time delay modulated signal is also relatively simple. In this case, the goal is to measure the time difference between adjacent pulses in the signal being received from the associated ganglion cell in the retina (the modulator) and subtract from this time interval the expected time interval of the ganglion cell pulses under quiescent (no signal from cells distal to the ganglion cell) conditions.
The total tremor period is nominally 0.0125 seconds, corresponding to a frequency of 80 Hertz.

The result is a signal that can be either positive or negative and is a replica of the signal impressed on the input to the ganglion cell which carried the hue information associated with either the L - M or the S-M channel. In this case, each time interval is compared to the reference value to provide hue information. The number of pulse received during a given tremor interval becomes an indication of the saturation of the color information. **[[is this right]]** **Figure 14.3.5.2-1** illustrates these modes of operation**.**

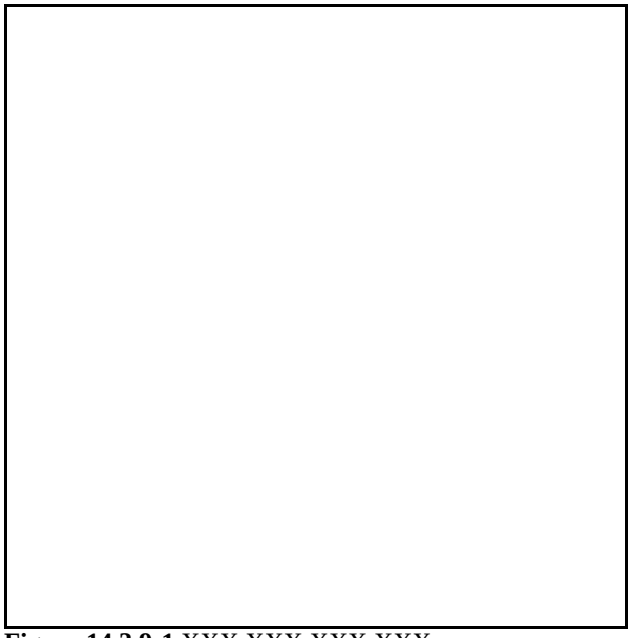

Figure 14.3.9-1 XXX XXX XXX XXX

14.3.5 Form of the decoded information

[[show a temporal baseline]]
[[phase detection versus vibration motion]]
[[don't develop Hering signals, etc.

In summary, the decoded data from each channel of the optical system, defined in basic form above, can be described as follows;

+

14.3.5.1 Luminance related signals

Sperling, et. al. have shown that the perceived luminance signal has the same spectral properties as the luminance channel within stage 2 and stage 3 circuits of the visual system measured electrophysically[31]. They did this by measuring the luminance signal at the thalamus (using elements of both the pulvinar and lateral geniculate nucleus).

14.3.5.1.1 Form EMPTY

14.3.5.1.2 Motion EMPTY

14.3.5.1.3 Brightness EMPTY

14.3.5.2 Chrominance related signals

14.3.5.2.1 Hue

Based on the description of the signals generated by the ganglion cells of the chrominance channels and the

[31]Sperling, H. Crawford, M. & Espinoza, S. (1978) Threshold spectral sensitivity of single neurons in the lateral geniculate nucleus and of performing monkeys *Mod Probl Ophthal* vol. 19, pp 2-18

demodulation techniques discussed in **Section 14.3.5.2**, the two chrominance channels present a pair of signals to the higher perceptual centers that are biphase in nature and indicative of the L – M and S – M hue difference signals formed in the signal processing part of the retina after individual spectral channel adaptation to the input illumination level.

> This processing chain accounts for why a red and white check table cloth will still look red and white under a pinkish light, as long as there is still a blue and a green component in the pinkish light. The situation is entirely different under a laser or a sodium vapor lamp.

These biphase hue signal exhibit a zero or null value at the nominal wavelengths of 494 nm and 572 nm in humans under nominal white light illumination conditions. **Figure 14.3.9-2** illustrates this situation and compares it to the measured data of Wright & Pitt.

14.3.5.2.2 Saturation

[[Wright & Pitt show minima at 493 nm & 592 nm.]]

14.3.5.3 Composite information map in vector space

As a result of the decoding process, the brain is presented with information, in vector format, to update its current database representing its perceptual visual field. This vector information is still in a field space that is not directly related to the external world. The information is in a spatial format that includes the effects of;

+ spatial distortion due to the physiological optical system
+ spatial distortion due to the non-homogeneity of the photoreceptor field of the retina
+ spatial distortion due to the various convergent signal processing paths in the retina

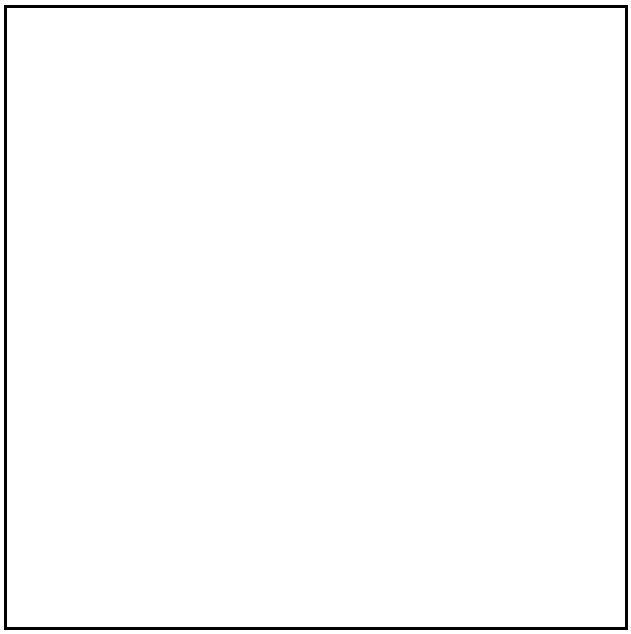

Figure 14.3.9-2 XXX XXX XXX XXX

Each vector contains a time and address tag, either implicitly or explicitly, and information about;

+ the presence or absence of an edge at its nominal location **or both**

+ the change in illuminance at that location from a previous value
+ the change in hue of that location relative to a previous value

As seen above, if the vector is representing an edge, the data associated with both the luminance channel and the hue channel may be distorted or irrelevant and should be ignored. In the absence of an edge in the luminance channel, both the luminance and chrominance channel provide valid data.

14.3 Overview of Stage 3 operation and performance norms

Yost has given the most recent textbook interpretation of a ganglion (encoding and projection) neuron within the auditory system[32]. His figure emphasizes the morphology of the cell. His use of the term neurolemma (as opposed to a plasmalemma), to describe a membrane exterior to the myelin sheath will not be used here. Functionally, there are two neurolemmas other than the axolemma. **Figure 14.4.1-1** adapts his figure to show additional detail related to the inside of the soma, or cell body. It is of interest because it shows the phasic signal conversion occurring

[32]Yost, W. (2000) Fundamentals of Hearing, 4th Ed. NY: Academic Press pg 289

initially outside of the soma (presumably at the dendrite/axon boundary). This is the situation believed to exist in the Stage 3 neurons of the cochlear nerve. It may occur at any Stage 3 neuron since the role of the soma is only supportive. Technically, the soma may or may not contain a connexus.

In this modification, the axon is shown passing through the soma until it reaches the connexus within the hillock. The nucleus, cytoplasm and remainder of the soma plays no functional role in neural signaling. These elements are concerned with homeostasis and cell growth. The phasic neural signal is regenerated at each connexus, whether it is external to the soma and usually called a Node of Ranvier or internal to the soma. In accordance with this work, the phasic signal is transported along the neuron by propagation as shown, and not by his designation conduction. The fact that the signaling pathway is physically interrupted, and conduction is blocked, at each Node of Ranvier is indicated by the black line forming a barrier at each connexus.

[xxx see Oertel, et. al. 1990]

[xxx add material and figure for stellate (decoding) neurons]

14.3.1 Types of encoding used in vision, hearing, etc.

[xxx rewrite]
[xxx basically same as in vision, and probably other sensory modalities as well.]

[xxx discuss ganglion and stellate neurons as transition elements, between tonic (analog) and phasic (pulse) signaling paths.

[xxx reference or consolidate with other material on encoding and modulation]

14.3.1.1 Evidence of differential encoding in hearing

Hind, et. al. have provided clear evidence for differential encoding in the squirrel monkey[33]. Their figure 9 shows the results of a two-tone test wherein the pulse rate was reduced when a second tone was introduced following introduction of a first tone. With a 1200 Hz tone at 50 dB and a 1900 Hz introduced at 90 dB, the number of spikes at the axon of an auditory nerve fiber was driven to near zero.

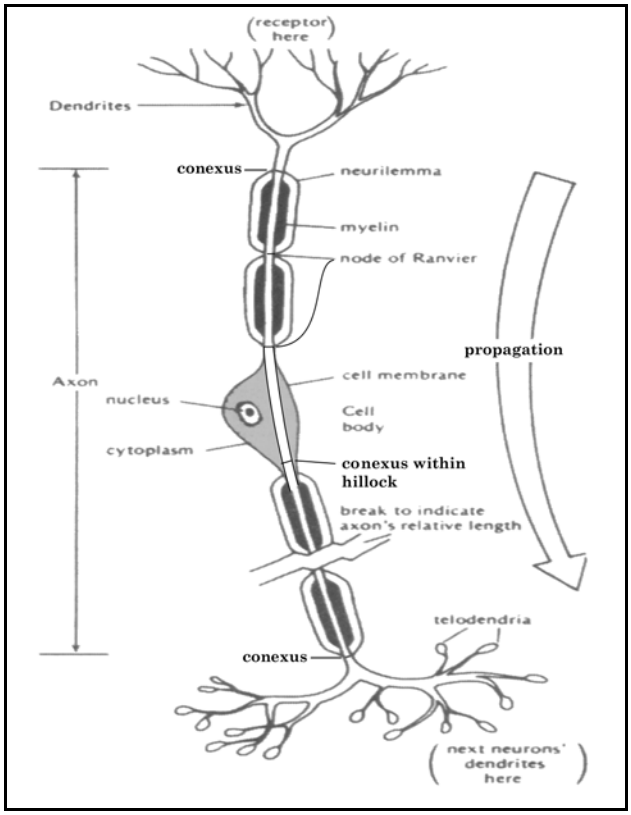

Figure 14.4.1-1 Basic structure of a ganglion projection neuron as found in the auditory system. Note the connexus separating the dendrites from the start of the axon. The cell body, nucleus and cytoplasm play no role in neural operation. Compare to Yost, 2000.

14.3.2 Details of the projection neuron circuits EMPTY

14.3.2.1 Details of the stage 3 encoding circuits EMPTY

[xxx fill in from vision work]
Figure 14.4.2-1 describes the transfer function of a ganglion neuron (configured for relaxation oscillation).

---

[33]Hind, J. Anderson, D. Brugge, J. & Rose, J. (1967) Coding of information pertaining to paired low-frequency tones in single auditory nerve fibers of the squirrel monkey *J Neurosci* vol 30, pp 794-816

[xxx time delay is a function of intensity, both mono and bipolar changes. plot to highlight the frequency change is hyperbolic and difficult to measure in the bipolar case since the frequency change becomes small.]

[xxx Include both analog and pulse (timing) outputs at stellate cell]

14.3.2.2 The action potential (AP) versus pseudo-action potentials

[xxx differentiate clearly between action potential and generator potential]
The hearing literature, and the neurology literature in general, frequently speaks of action potentials in the vernacular. While the above section defines the features of the action potential in relation to the operation of the Stage 3 neurons, it does not address the other concepts, or descriptors, found in the literature. The subject of negative-going action potentials is not uncommon in the literature when in fact all action potentials are positive- going[34].

[xxx show NoR like circuit before soma]

[xxx rework to differentiate between action potential and generator potential]
[xxx figure should not show cuticular plate or be labeled OHC or IHC if its stage 3.]
Figure 14.4.2-2 provides a multi-frame description of the waveforms, and their origins, associated with phasic neuron (within both ganglion cell soma and their associated Nodes of Ranvier). The left frame shows a cytological sketch of the neuron. The middle frame shows a simplified circuit diagram of the neuron. The right frame shows typical waveforms found in the laboratory. In order to maintain a positive voltage up orientation, it has been necessary to draw the circuit diagram of the neuron inverted in the middle frame. Thus the base is shown above the emitter and collector terminals.

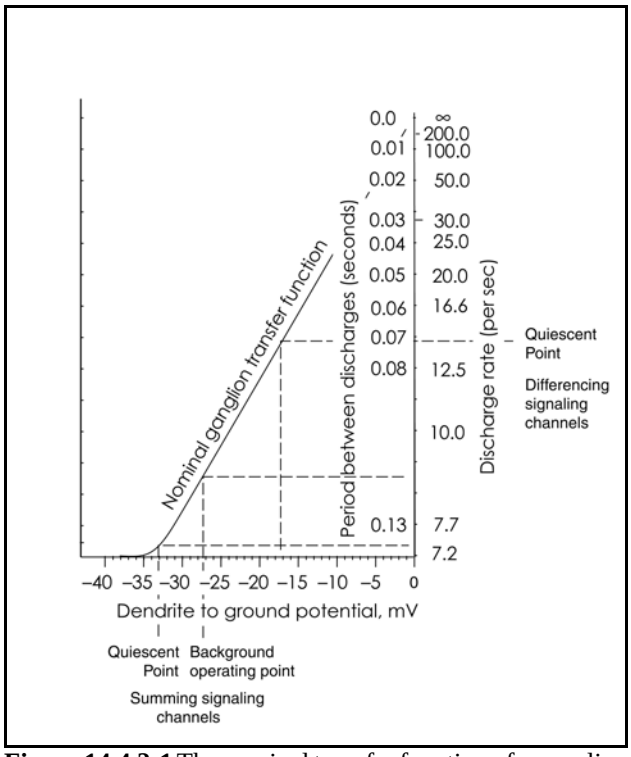

Figure 14.4.2-1 The nominal transfer function of a ganglion neuron. The response shown contains two different operating conditions. Those labels along the bottom indicate the preferred operating points when encoding summation channels (monopolar signals). The labels on the right indicate the preferred operating points when encoding differencing channels (bipolar signals).

[34]Kohlloffel, L. (1974) Recording from spiral ganglion neurones In Zwicker, E. & Terhardt, E. eds. Facts and Models in Hearing. NY: Springer-Verlag pg 194

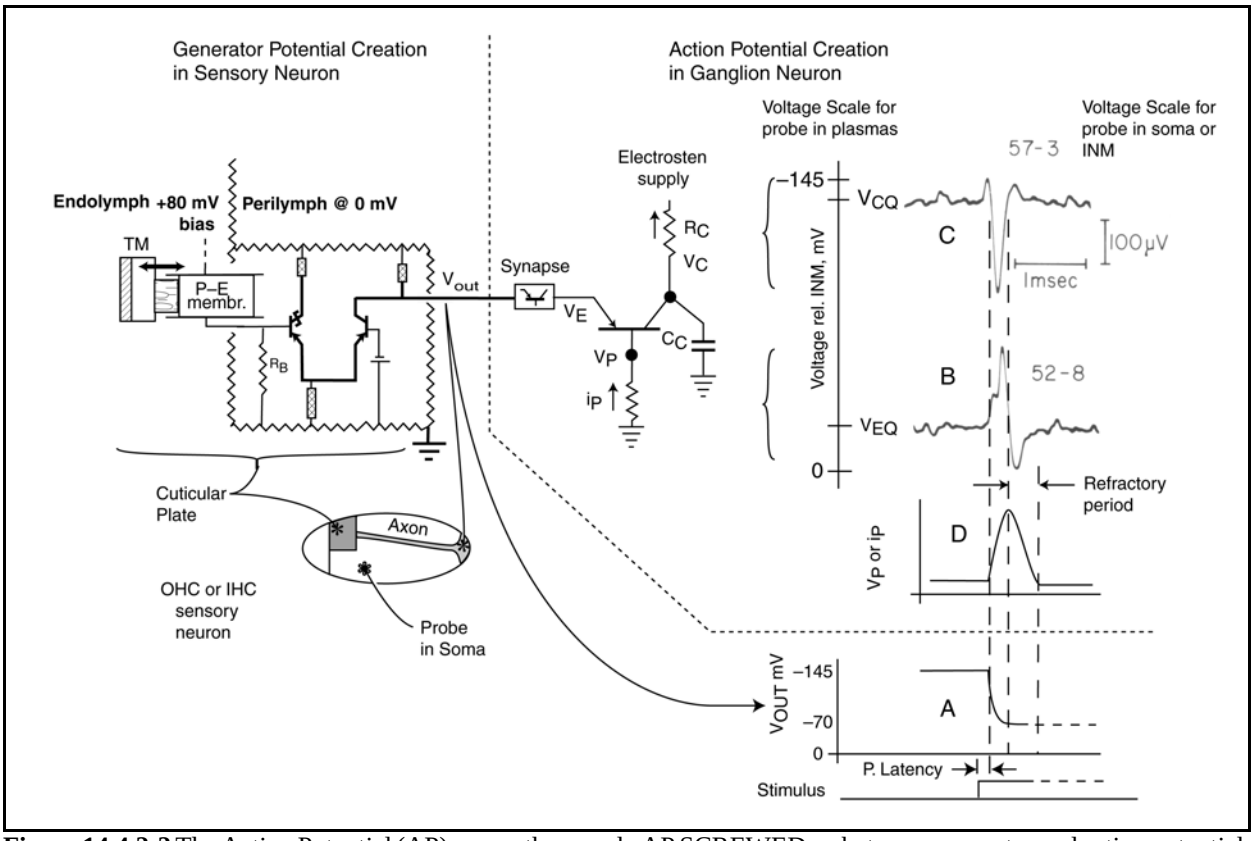

Figure 14.4.2-2 The Action Potential (AP) versus the pseudo AP SCREWED up between generator and action potential. Note the two voltage scales. Action potentials are positive-going millivolt level waveforms within the axoplasm. Microvolt level signals are usually measured within the soma of the neuron or in the INM. See text. Waveforms from Kohlloffel. 1974.

The Activa within a neuron is composed of the juxtaposition of two bilayer membranes. The total thickness of the Activa is less than 35 microns. Thus it is virtually impossible to locate except through electron-microscopy. Attempts to probe the neuron to locate the Activa usually contact either the chamber of the cell containing the podaplasm of the Activa or the larger dendroplasm and axoplasm volumes. Frequently, only the cytoplasm of the cell associated with growth and homeostasis is contacted. As shown in the figure, the voltages associated with the operation of the neuron are millivolt level signals while the signals obtained by probing the cytoplasm are usually in the microvolt range. The microvolt level signals reflect the capacitive coupling between the neural plasmas and the cytoplasm. These signals frequently exhibit artifacts (such as the negative going overshoot) as shown in waveform A. There are additional artifacts due to making measurements using bandpass filters. The waveforms in the figure were acquired using a 80 Hz to 10 kHz bandpass filter. Measuring the DC potentials at the probe location is a sure method of differentiating between true action potentials and other waveforms. A true action potential (waveform A) is measured in the axoplasm of a Stage 3 ganglion neuron. It begins from a voltage near –140 mV and rises to a voltage near –40mV (giving a positive going excursion of about 100 mV). This voltage change is caused by the operation of the neuron as a one-shot multi-vibrator-type oscillator. Notice the step in the rising portion of the waveform. To the left of the step, the circuit is operating as an amplifier below the threshold for oscillation. To the right of the step, the circuit is operating above threshold as an oscillator.

There are two current paths shown in the figure. Current i_p is the current through the base of the Activa in response to the signal applied to the emitter (terminal with the arrowhead). It passes through the resistance, R_P, generating the voltage V_P. This voltage is shown at upper right. It

exists for the duration of the positive portion of waveform A and is drawn from the charge stored on capacitor, C_C. As charge is removed from this capacitor, the electrostenolytic supply begins to replace this charge. This results in the current i_C through the resistor R_C. The waveform at lower right shows this current and the equivalent voltage across R_C.

The voltage waveform in A is the action potential generated within the neuron (frequently in the hillock) and propagated along the axon. It is positive going during its rise in potential. The voltage waveform in B is frequently described as a negative-going action potential. It is not known to propagate along the axon and ***the waveform in B is in fact a pseudo-action potential***. It does not exhibit the step or shoulder so characteristic of real action potentials and it is negative-going. It is acquired by probes penetrating into or near the podaplasm of the neuron. The magnitude of the voltage defines which situation applies. The voltage shown in the lower right waveform is also occasionally mistaken for an action potential, even though it is typically wider in time than an action potential. It does not exhibit a step or shoulder but is positive going.

Each of the currents described above is well represented in the literature. In fact they form the foundation for the chemical theory of the neuron that is not accepted here. The current forming waveform A, i_p, is frequently described as an ingoing current. Hodgkin & Huxley immortalized this current by calling it by the acronym, "the sodium current.[35]" The current forming the waveform at lower right, iC, is frequently described as the out-going current. Hodgkin & Huxley labeled this current using the acronym, "potassium current." ***The currents passing into and out of a neuron have nothing to do with ions of the alkali metals.*** They were selected based entirely on the relative concentration of these ions within and outside of the in-vivo neurons they studied. They did not evaluate these neurons in-vivo nor did they demonstrate that these ions were able to penetrate the lemma of the neuron. It is now widely recognized, following endless experiments to demonstrate that they do, that these ions do not pass through the lemma of neurons (**Section xxx**). Hodgkin & Huxley did not study the cytology of their neurons, and the active semiconductor device, transistor or Activa, had not been discovered in their time. They did not recognize the separation of the dendroplasm and axoplasm by the podaplasm. As a result, they had to invent a concept explaining why their positively charged sodium ions and potassium ions moved in opposite directions in the face of a unidirectional electrical field, the plasma to INM potential.

The voltages described above and in the figure are relative to the inter neural matrix, INM, surrounding the neuron. In the case of the Stage 3 ganglion neurons of hearing, this INM is the endolymph. It exhibits significantly different potential than the perilymph and other fluids of the body. This difference must be considered when measuring the DC voltages related to these ganglion cells.

[35]Hodgkin, A. & Huxley, A. (1952) xxx

14.3.2.2 Details of the stages 3B & 3BP decoding circuits EDIT

[xxx discuss time delay, summation decode, differencing decode, leading pulse detection and coincidence detection]
]xxx discuss irrelevance of SR in summation and differencing decoding.]

This section will develop the various forms the nominal stage 3B decoding circuit may take in its role for recovering information in the form of a series of words in series where each word consists of a series of action potentials. This configuration of information transmission is described in computer sciences as in the word serial/bit serial format. The word serial/bit serial format is that used throughout a majority of the neural system. It appears to be used exclusively in the peripheral neural system (PNS). The decoding circuits supporting this type of stage 3 propagation will be labeled stage 3B circuits.

There is an alternate configuration that may play an important role within the central nervous system (CNS), at least that of the higher animals and particularly the primates. It consists of words passed forward in serial format but utilizing multiple parallel chains of neurons, each carrying a separate bit of the word. This word serial/bit parallel format offers a much higher speed of information transmission and appears to be used by the commissure (groups of parallel myelinated neurons) of the CNS. Decoding word serial/bit parallel information may require slightly more complex circuits than used for stage 3B decoding. These will be known as stage 3BP (P for parallel) circuits.

Figure 14.4.2-3 illustrates a variety of signal recovery circuits that can be used in the stage 3B analog information recovery process. Some of the recovered signals may represent pulse information derived from such analog signals.

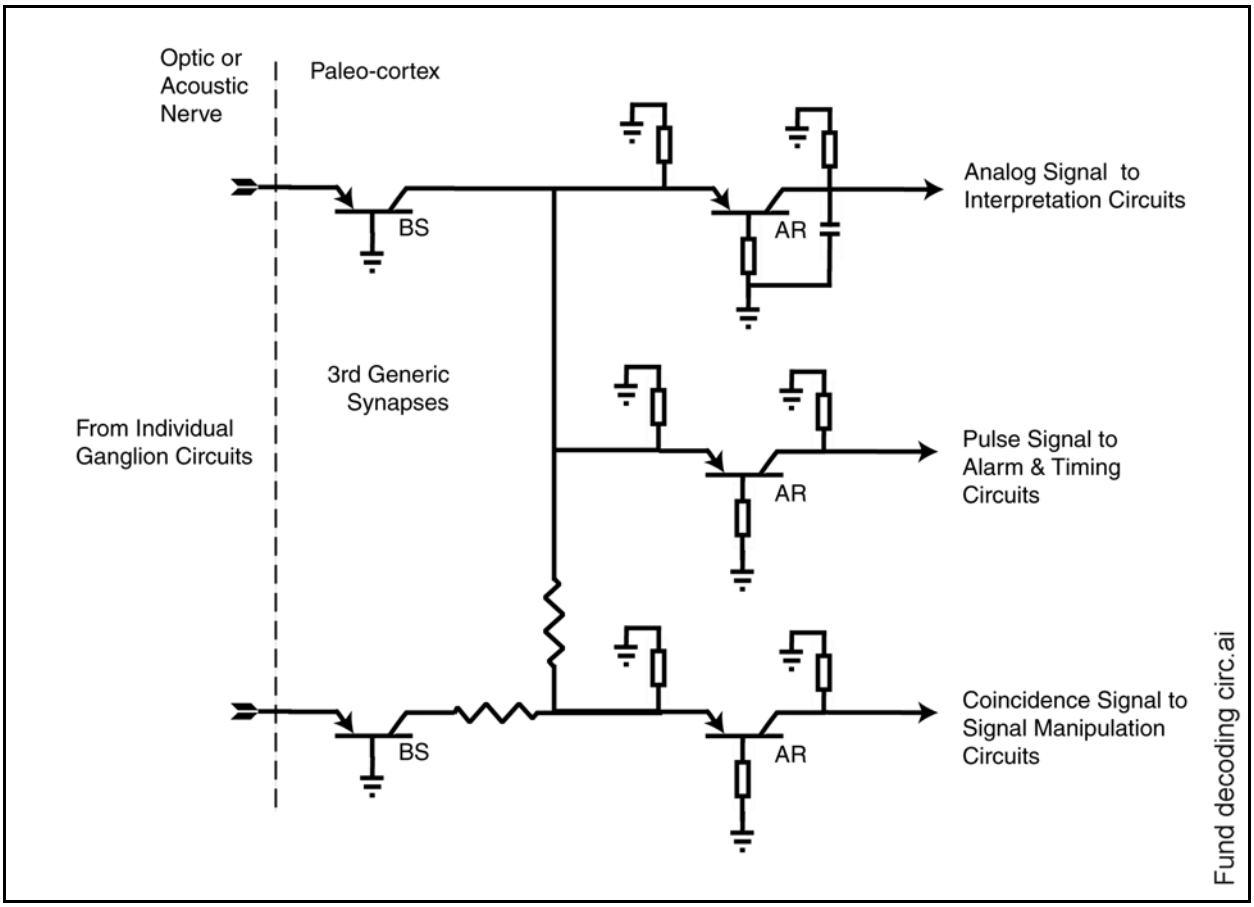

Figure 14.4.2-3 Generic stage 3B decoding circuit of the neurological system EXPAND to include coincidence circuit. Used in the LGN, the PGN and the cortex (cerebrum and pulvinar). The labels BS and AR are used for bookkeeping purposes and indicate Activa of different intrinsic capacities.

Figure 14.4.2-4 shows a modification of the previous figure proposed to be used to transmit information in word serial/bit parallel format in order to achieve an order of magnitude higher information capacity over a given signal path within a unit time interval. A separate voltage reference source is used to achieve noise free summation of the analog outputs related to a given word, or to accurately represent a set of analog values associated with different nodes of a multi-dimensional signal.

Bringing all of the base (poditic) circuit leads to a common point is a critical feature in noise reduction strategies in man-made electronic circuits. Further definition of the reference voltage source has not been achieved at this time. As part of that activity, it should be noted that the noise generally described by VS sufferers appears to be of the "pink" type, i.e., exhibiting an excess of high frequency components compared to more conventional "white" noise. White noise exhibits a flat noise power spectrum as a function of frequency.

The phenomenon of synaesthesia (a misperception of a sensory input as arising from a different sensory modality), the frequent occurrence of visual snow and tinnitus in the same subject, and the organization of the conceptual saliency map of [Figure xxx] might suggest that the neurons of significant areas of the saliency map (or the neurons/engines near the output of nearby association areas) might share a common reference voltage source.

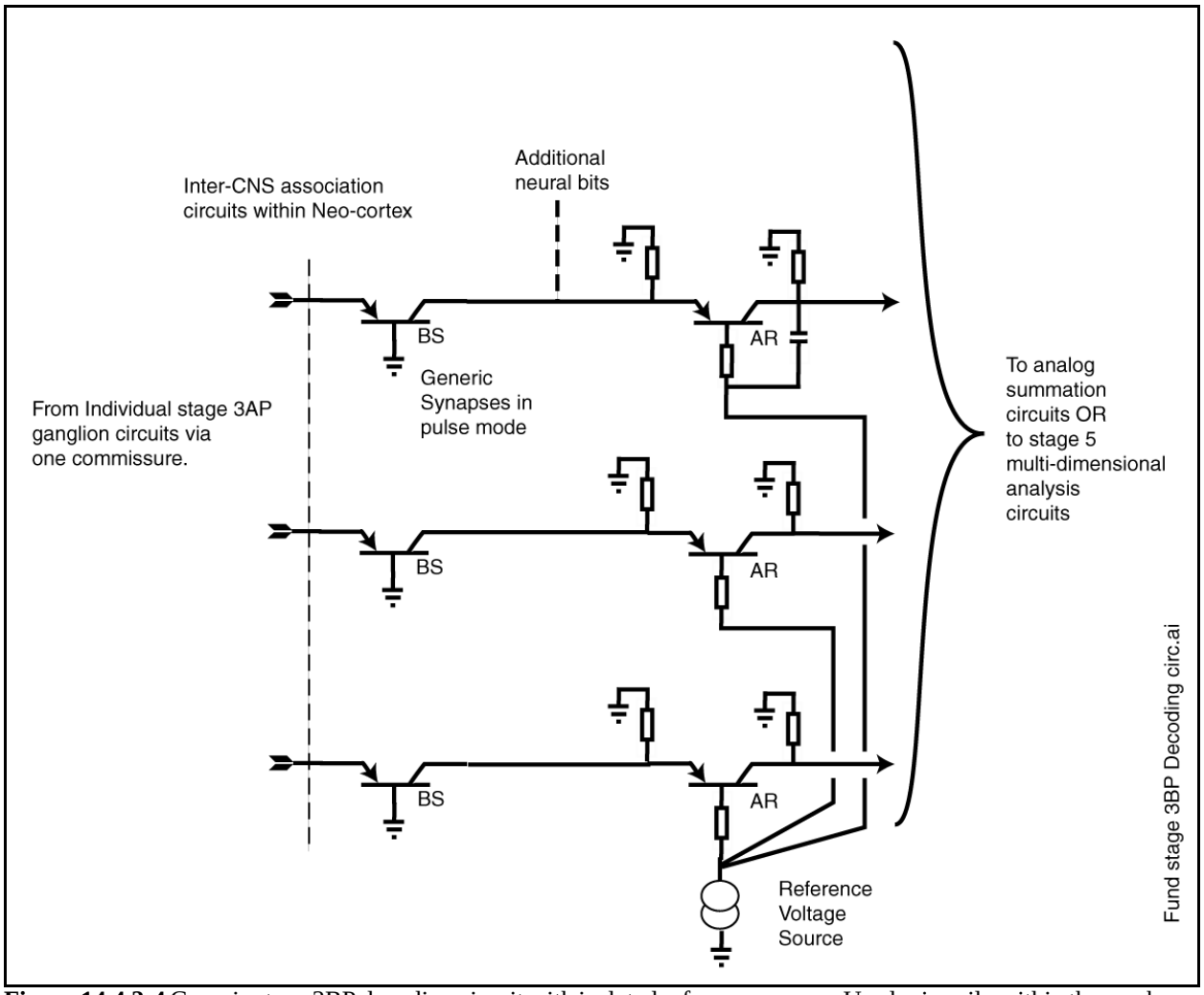

Figure 14.4.2-4 Generic stage 3BP decoding circuit with isolated reference source. Used primarily within the cerebrum and TRN of the thalamus for passing information in word serial/bit parallel format. As indicated at the top of the figure, the number of bits employed remains unknown.

14.6.1.6 The waveforms at the pedicle of the stellate cell

Figure 14.4.2-5 shows the signals typically associated with the stellate cell. By varying the bias point associated with the circuit elements on the output side of its conexus, a variety of signals can be decoded. The output signals can be optimized for monopolar, bipolar or pulse operation.

[xxx The stellate cell can operate in close coordination with the orthodromic stage 4 signal processing neurons. To optimize this coordination, the stellate cell may act as an analog decoder or it can act as an event detector. In the later case, the output of the stellate cell may be a pulse that can be easily processed by a coincidence detector.

Konig et. al. have recently addressed the options available in stage 3 ganglion cells and other stage 4 signal

processing neurons without the availability of a detailed model[36]. Their work is necessarily abstract and attempts to draw conclusions from a series of simple psychophysical experiments. There thesis is intriguing. "Here, we argue that coincidence detection, rather than temporal integration, might be a prevalent operation mode of cortical neurons. We base our arguments on established biophysical properties of cortical neurons and on particular features of cortical dynamics." Their introduction suggests they only considered the operation of phasic neurons and performed little literary research before formulating their psychophysical concepts. They criticize their sources for suggesting that the cortical neural circuits operate on a time cycle of less than 15 ms, suggesting that their work indicates a time scale of a few milliseconds. This work, and a great deal of other work has shown that many cortical subsystems, particularly those concerned with ocular pointing operate on a time scale shorter than that in order to achieve close loop servo performance at 100 Hertz or better (including the delays associated with the oculomotor muscles). Thus, as many as 10,000 neurons may be operating simultaneously, in a combined series and parallel channel environment, that produces an output in less than a few milliseconds.

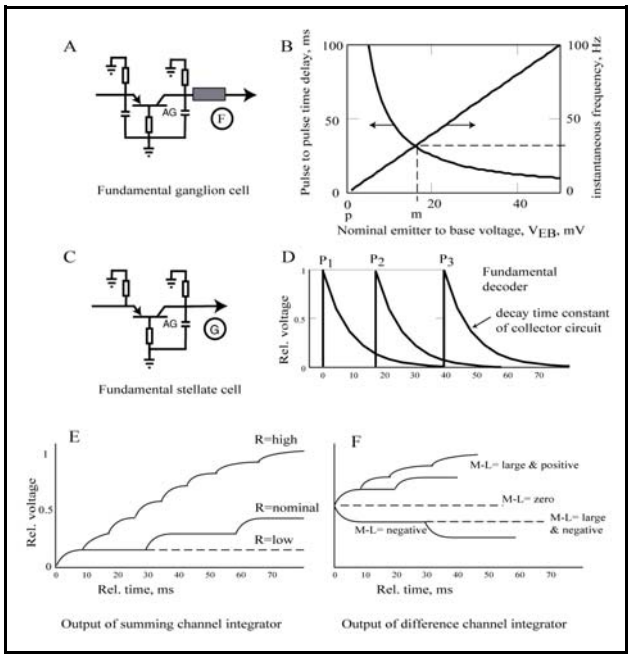

Figure 14.4.2-5 Signals recovered from the output of signal projection circuits.

Konig, et. al. use only simulated phasic neurons to present their case. While some of the cortical neurons undoubtedly operate in the coincidence mode, as suggested above for some of the stage 3 stellate cells, the vast majority of the cortical neurons do not do so using action potentials as input s signals. The coincidence function appears to occur after significant prior processing in the electrotonic mode. It is also likely to occur immediately before the process of memory implanting. Their sweeping proposal appears unsupportable. The subject of cortical signal processing will be addressed more fully in **Chapter 15**. **Chapter 7** has addressed the operation of the oculomotor servomechanisms in detail.

The symptom of "snowy vision" discussed in **Section 18.8.2** provides a rough estimate of the height of the individual steps in the recovered waveform shown in **D**, **E** and **F** of the above figure. Snowy vision appears to be caused by the generation of extraneous individual action potentials by the ganglion cells of the retina. When decoded at the brain, they result in an instantaneous change in amplitude estimated to be near 20% by only a few subjects. The sufferers describe the pulses as causing a "dark-going" noise pulse that is most obvious against a light background. The pulses appear to relate predominantly to the luminance channel as changes in color are reported much less frequently than changes in contrast. These suffers also confirm that the visual system operates as an AC coupled system. The noise pulses remain prominent in pitch darkness because of the neutral gray signal level achieved in the visual system (see Yarbus, 1967).

14.3.2.3 The end-to-end transfer function for a Stage 3 circuit

By combining the operating characteristics of the ganglion encoders and the stellate decoders described above, the overall operating performance of the Stage 3 projection circuit can be obtained.

Figure 14.4.2-6 illustrates the analog and pulse waveforms obtained in a conventional stage 3 neural circuit. The upper frame (**A**) illustrates a nominal analog input received from a stage 2 signal processing engine. Frames **B**

[36]Konig, P. Engel, A. & Singer, W. (1996) Integrator or coincidence detector? The role of the cortical neuron revisited *TINS*, vol. 19, no. 4, pp 130-137

through **C** illustrate the non-equally spaced pulses recorded from different locations along the axon segments of the encoding (ganglion) neuron. The lower frame (**D**) illustrates the performance of the decoding (stellate) neuron during signal recovery of the original analog signal.

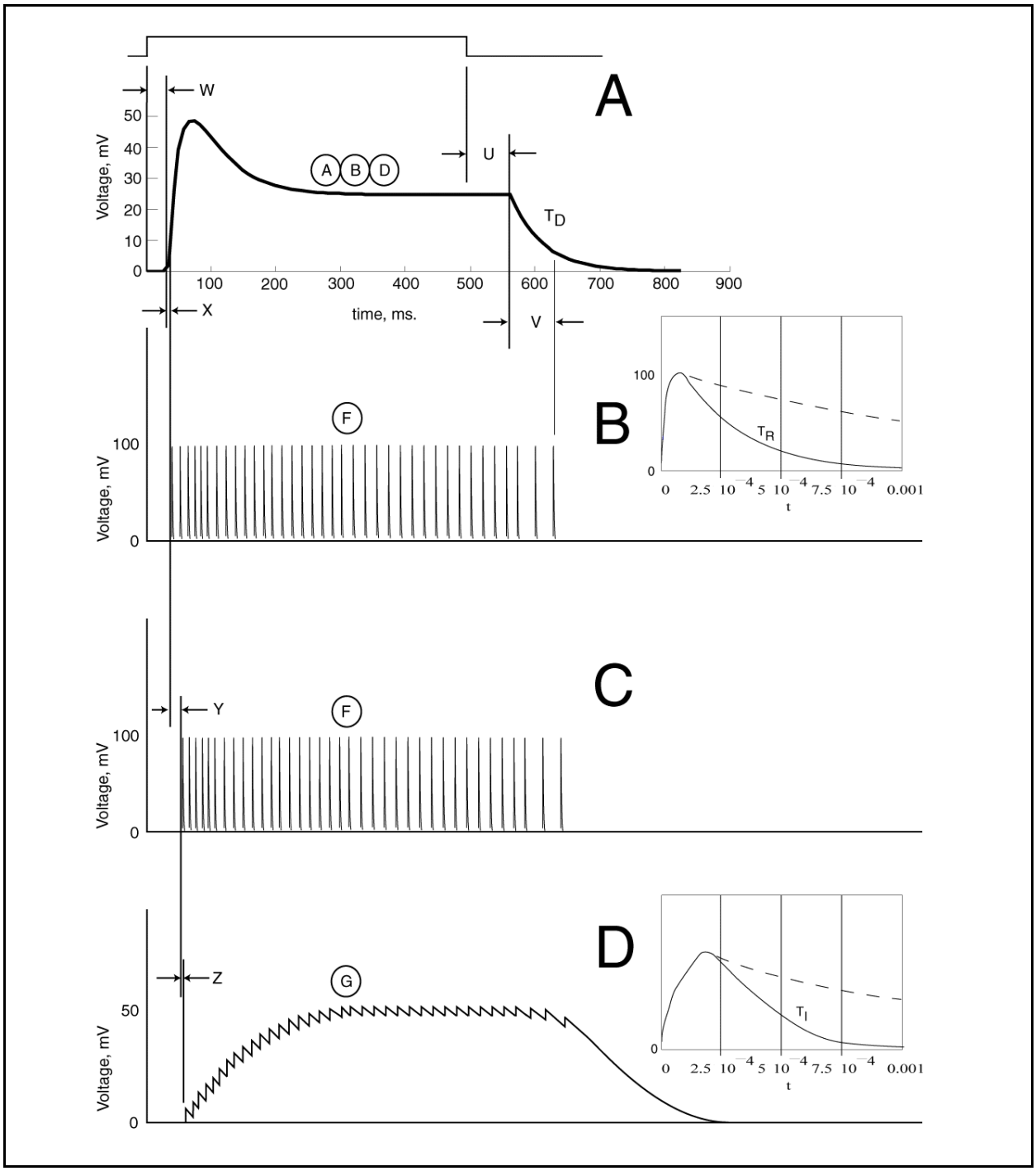

Figure 14.4.2-6 The performance of a combined ganglion cell and stellate cell of stage 3. **A**; the stimulating waveform typically received by a stage 3A encoding neuron (or ganglion cell). **B**; the non-equally spaced pulse train generated in response to the stimulation. X represents the delay introduced by the encoding neuron. **C**; the non-equally spaced pulse train received at the stage 3B stellate neuron after being delayed by regeneration by multiple Nodes of Ranvier (Y). **D**; the recovered analog waveform at the stage 3B stellate neuron before any filtering. Z shows the additional delay associated with the stellate neuron. The encircled letters refer to the equivalent encircled letters in previous figures in this Chapter.

Figure 14.4.2-7 shows an ideal overall transfer function of a Stage 3 projection circuit. The input excitation can be of either the monopolar or bipolar type. However, the intrinsic absolute bias point is set differently in the two situations. The vertical scales shown in the figure are nominal. They can be multiplied by a constant to obtain different operating ranges as required by the situation. The maximum pulse rate of auditory signal projection circuits are frequently higher than the equivalent visual circuits.

A parasol ganglion neuron is optimized for monophase signal processing when its quiescent point is near the negative most extent of its operating range. In the absence of any signal, its action potential generation rate will be near zero. Upon excitation, it will generate action potentials with a time period between pulses proportional to the change in excitation potential.

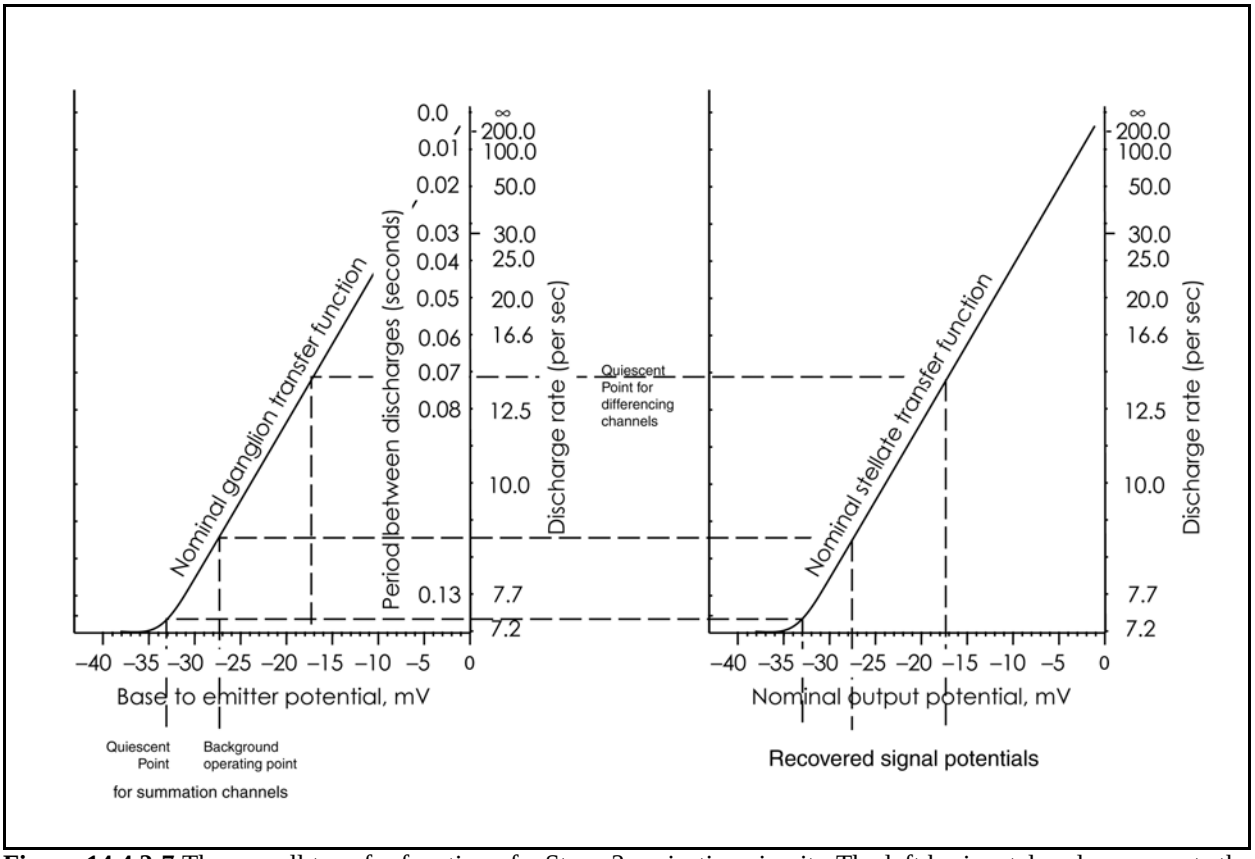

Figure 14.4.2-7 The overall transfer function of a Stage 3 projection circuit. The left horizontal scale represents the absolute emitter to base (dendrite to podite) potential of the ganglion encoder circuit. The right horizontal scale represents the equivalent (but relative) voltage scale for the output of a stellate decoder circuit. The entry points for a monopolar input signal are shown at lower left. In the absence of any signal, the quiescent operating point of the parasol type ganglion neuron is shown as –33 mV. The nominal background operating point is shown as –27 mV. Under large signal conditions, the signal extends from near –33 mV to near zero mV. Under ideal conditions, one form of the stellate decoding circuit will reproduce these voltages perfectly as shown by the dashed lines proceeding to the lower right. For a bipolar input signal, the midget ganglion neuron is typically biased to – 17 mV. The excitation can drive this potential over the range of –32 mV to about –2 mV. Under ideal conditions, the pulse rate generated is shown by the vertical scales. These scales can be multiplied by a constant to cover different operating ranges. The pulse interval is linearly related to the excitation potential. The actual pulse frequency is reciprocally related to the excitation. As for the monopolar signal, an ideal bipolar stellate decoder will generate an output potential that is a faithful replica of the input excitation. See text.

14.3.2.3.1 The transfer function supporting the Alarm mode

14.3.2.3.2 The transfer function supporting the Awareness mode

14.3.3 The quiescent operating conditions associated with Stage 3 EMPTY

14.3.3.1 The quiescent DC potential at the Stage 3 Alarm mode EMPTY

14.3.3.1.1 The quiescent DC potential at the Stage 3 Alarm mode EMPTY

14.3.3.1.1 The quiescent DC potential at the Stage 3 Awareness mode EMPTY

14.3.3.2 The quiescent noise conditions associated with stage 3 EMPTY

14.3.3.2.1 Comparison of the noise in the visual and hearing systems EMPTY

14.3.4 How temporal signal asymmetry is handled in vision

Because of the significant asymmetry in the temporal response of the Stage 3 projection circuits, it is to be expected that specific choices will be made as to the operation of the system. The result of these choices have been measured. The results are as expected. The choices made were optimal.

14.4 Specific coding applications by sensor modality

This section will develop the general architecture of coding used in the sensory system and then explore the special adaptations introduced to optimize a specific sensory modality.

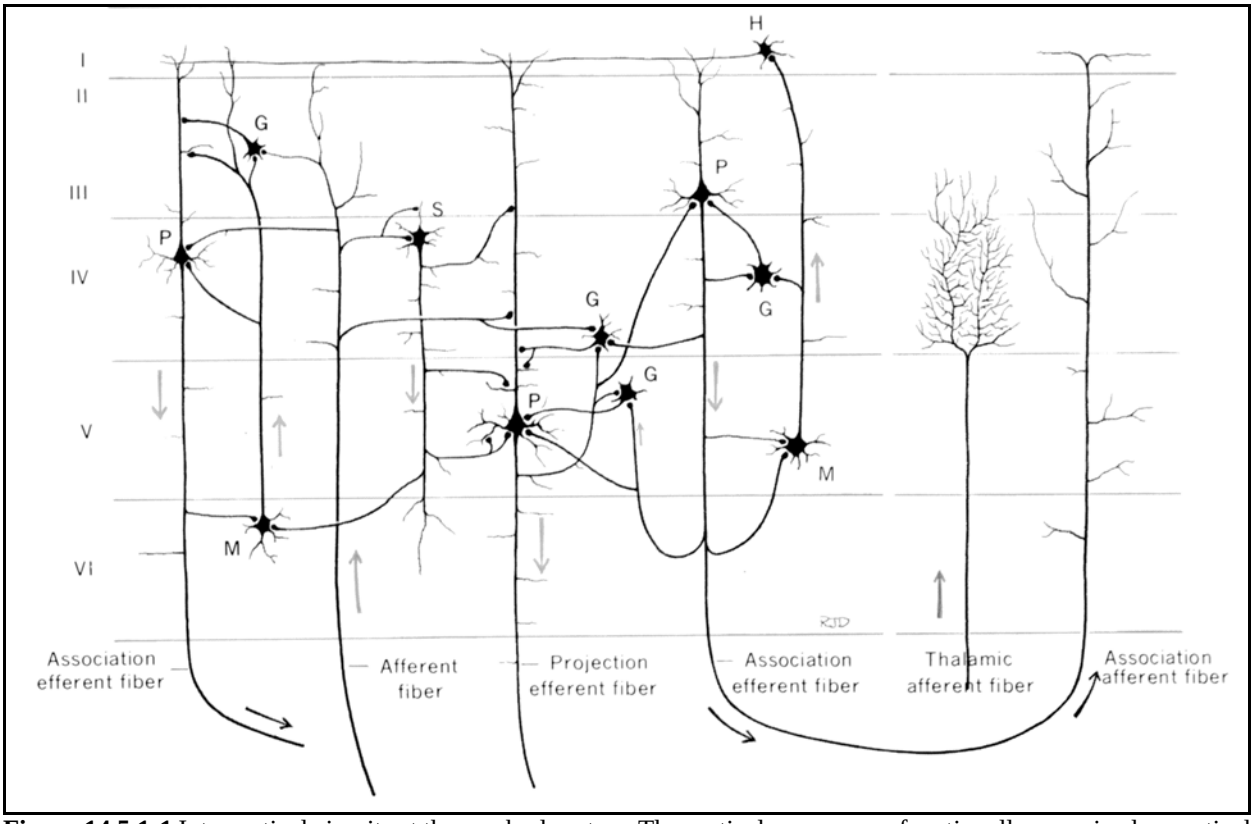

Figure 14.5.1-1 Intracortical circuits at the cerebral cortex. The cortical neurons are functionally organized as vertical columns oriented perpendicular to the cortical surface. See Text. From Noback, 1967.

14.4.1 Coding architectures used by all sensory modalities

14.4.1.1 Spatial encoding for purposes of temporal (frequency filtering)

While there is considerable discussion in the literature concerning conceptual circuits in the visual system tuned to various spatial frequencies, there are no tuned circuits in the technical sense. A tuned circuit involves a resonant circuit, generally described by an inductance and a capacitance (or their analogs). Such circuits are not found in neurology. The effect of spatial tuning is achieved in the temporal domain by summing signals from different photoreceptor channels after introducing the appropriate time delays between the signals. This mechanism is illustrated in **Figure 14.5.1-2**. Xxx words of explanation.

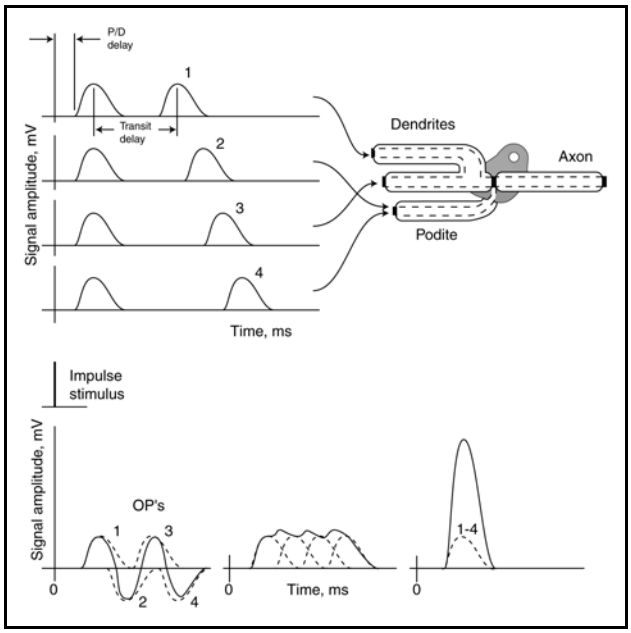

Figure 14.5.1-2 Diversity summing in time to achieve spatial filtering in image space on the retina.

14.4.1.2 Spatial encoding for purposes of Optic Nerve minimization–Phantom circuits

xxx introduce phantom circuits as a simple example. Note their applicability to the alarm operating mode and the peripheral retina.

14.4.1.3 Many to one versus many to a few

There are many references in the literature to the immense number of inputs to a single ganglion cell of the retina. There are similar references to the input structures of typical bipolar cells. Considerable data is also available on the tangled arrangement of the arborization of adjacent ganglion and adjacent bipolar cells. Based on the first observation, it is frequently suggested that there is an immense reduction in the number of signal paths due to the reduction in the number of outputs of the typical ganglion cell versus its number of inputs. This is frequently described colloquially as the many-to-one feature of the neural architecture[37]. However, if one looks at the combination of the convergence of signal paths from multiple preceding cells to more than one ganglion cell due to the above entanglement, it becomes obvious that the colloquial expression should not be many-to-one but more appropriately many-to-several. This difference in concept has a significant impact on the signal projection capability of the system. Instead of a simple signal summation as implied by the many-to-one analogy, the many to several analogy leads to the conclusion that the system may be employing spatial encoding to reduce the number of neurons in the optic nerve. This process is known as n-ary encoding and is widely used in low error rate signal transmission systems developed by man. The optic nerve is a choke point in the signal projection capability of the animal eye in higher mammals particularly. As in the typical computer, it is advantageous to reduce the number of signal paths between the CPU and the external world. By arranging the signals passing over a set of signal leads in both time sequence and a spatial pattern, the data associated with a large number of individual inputs can be funneled through a smaller set of signal leads and still be decoded at a latter point without significant loss related to individual input signals. This is the process of signal encoding introduced into the signal projection stage of the visual system of chordates. It is particularly highly developed in the higher mammals with ocular globes exhibiting a high degree of angular capability.

14.4.2 The architecture of spatial encoding relative to vision

The reader should be familiar with the work of Yarbus[38] and/or Ditchburn[39] (See **Sections xxx**) before studying the details of this chapter and particularly the sections concerned with decoding. These authors have presented substantial material on the dynamic operation of the visual system under operational conditions that is frequently overlooked or ignored by investigators exploring under static conditions or dynamic conditions that are not related to operational conditions, i. e. very short duration pulsed illumination. Yarbus is more physiologically oriented while Ditchburn is more behaviorally oriented. They stress (1) the mandatory requirement for motion between objects in the image plane and the retina for vision, and (2) the importance of the continuous tremor of the eye as the source of this motion in human vision. (1) leads to the perceptual recognition of an image element in the total image plane, (food in the case of a frog) and (2) leads to the perceptual recognition of the complete image plane (desired by higher mammals for navigation if not esthetic purposes. The overlay of the continuous tremor on the line of fixation does not eliminate the perception of independent image elements in the image plane; it adds the new capability of "imaging" to the more primitive capability of image element motion detection.

Working more recently with humans, Kelly[40], put it more succinctly, "Our results suggest that retinal image motion is the ***sine qua non*** of vision". Amen.

The visual system takes maximum advantage of the redundancy in a typical scene in its choice of coding algorithms. The investigator who attempts to apply steady state excitation to a visual system and then measure the signals within the system will encounter great difficulty, regardless of the time regime he explores. The visual system is not designed to transmit any steady state information to locations orthodromic to the adaptation amplifiers within the

---

[37]Boker, S. (1995) http://www.nd.edu/~sboker/ColorVision2/node11.html

[38]Yarbus, A. (1967) Eye movements and vision. NY: Plenum Press

[39]Ditchburn, R. (1973) Eye-movements and visual perception. Oxford: Clarendon Press

[40]Kelly, D. (1979) Motion and Vision. *J. Opt. Soc. Am.* vol. 69, no. 9, pp. 1266-1274 & vol. 69, no. 10, pp. 1340-1349

photoreceptor cells.

14.4.2.1 The architecture of spatial encoding relative to the retina EMPTY

14.4.2.2 The spatial encoding as presented to the LGN EMPTY

14.4.2.3 The spatial encoding as presented to the pretectum EMPTY

14.4.2.4 Spatial encoding remote from the retina

[xxx not relative to retina.]
Hubel and many others have provided architectural drawings of the interface between the neurons of the optic nerve and the initial structures of the brain. One of the few figures showing the details of the neurological interconnections at the cerebrum is from Noback[41]. **Figure 14.5.2-1** describes the conventionally defined six layers of the cerebrum. The individual layers will be discussed in Chapter 15. Noback points out that the cells are arranged in circular columns of finite diameter. It is these columns that are defined as engines in this work. They frequently include a million individual neurons. This is the complexity of a man-made computer microcircuit chip of 1990-92.

The important individual features in this figure are the horizontal cells of Cajal (H), the pyramidal cells (P) and the stellate cells (S). The caption of Noback's figure group the granule cells (G) with the stellate cells. These are the cells involved in projection of signals between areas of the brain. The horizontal cells of Cajal are analog cells used to transmit information over short distances, typically less than one millimeter. The pyramid cells (P) of this figure are known as ganglion cells elsewhere. They are analog to pulse converters that create action potentials that can be used to project information efficiently, and error free, over long distances. They begin a signal path described morphologically as a commissure. These commissure, labeled an association fiber here, can be of indefinite length (assuming there are Nodes of Ranvier spaced along each neural fiber). The commissure terminates at a stellate cells (S). The stellate cells, a.k.a. large pyramid cells, are integrating circuits used to recover the analog information from the action potential pulse stream. Thus, a combination of a pyramid (ganglion) cell and a stellate cell compose a stage 3 signal projection circuit. All of the other cells shown are involved in analog signal processing within one feature extraction or command generation engine. The P and S (including G) cells are usually found in layers IV and V. However, layer II frequently contains G and small P cells. They are sufficiently different from those of layer IV & V to be assigned to adjective small.

14.4.3 The architecture of acoustic frequency encoding relative to hearing EMPTY

14.4.3.1 The coding of neural signals in hearing EMPTY

14.4.3.1.1 Coding concepts applicable to hearing

The analysis of the coding principles used in hearing can be attacked exactly like any other messaging system. The basic principles of code-breaking apply. The **first** step is to perform a traffic analysis to determine where the messages are originating (and terminating). This is the role of morphology in this situation. The **second** step is to determine the character of the transmission channel. Is it a single channel serial data stream, or does it consist of multiple parallel channels with the data transmitted in parallel across these channels synchronously. In hearing, the signals at the cochlear nerve are clearly individual channels transmitting serial data streams. However, they clearly represent a large number of parallel data streams. The correlation between these streams is to be determined. However, the presence of correlation is clear. The major task of the CNS is to extract information about the sound source based on this correlation. Cursory examination of the signal routings (based on the morphological studies) shows multiple parallel paths (nerves) that each contain multiple individual neural circuits (projection neurons).

---

[41]Noback, (1967) XXX fg. 16-3

The **third** step is to determine the mode of signaling in the individual channels. Histograms can be very helpful in this step of the process. It is also helpful for the analyst to have broad experience in the potential methods of encoding used in similar systems. Such experience quickly shows the commonly used rate histogram is usually inappropriate (unless SR = 0).

> This step was the principle concentration of the team at Bletchley Park tasked with breaking the Enigma code of the Germans during World War II. The source of the traffic was well known. Based on the directional characteristics of the transmitters used and the subsequent actions by local units, the destination of the traffic was well known. At that time in history, only single streams of serial data were transmitted (although the Japanese did sectionalize and transpose the sections in their last proposal to President Roosevelt at the start of World War II in the Pacific).

The **fourth** step in code breaking is to determine the precise code used in a given transmission so that the underlying information can be obtained.

Brugge has provided a discussion similar to the above related to hearing[42]. He divides the methods of coding into four;

1. Labelled Line Code– Based on the Place Principle of Hearing. This corresponds to step 1 above, determining the source of the traffic. By determining the spatial position of the source within the cochlea, the expected frequency range can be determined for that signal (equivalent to determining which office originated the message in military communications).

2. Temporal Code– and 4. Ensemble Code– The Volley Theory of Hearing. Roughly equivalent to step 2 above. These two designations are related to the degree of parallel signaling employed and the degree of time synchronism between them.

3. Rate Code– Equivalent to step 3 above, determining the code used in an individual neural channel.

The hearing research community has not yet reached the level of step 4 above, the actual description in deterministic terms, of the code(s) used in hearing. This is partly because of the definition used by Brugge. "The term 'code' as applied to the auditory system, is simply a way of describing the manner in which information about sound is represented in such neural activity." This work will take the next step. It will go beyond describing the manner of encoding to describing the specific codes used in detail. It will also show how to read the code.

Brugge did use the term neural computation to describe the operation of the neural system in a global sense. This term can be further divided between computation within an "engine" (a major node of the neural system containing at least one million individual neurons) and computation accomplished by the rearrangement of the neural channels spatially. This latter technique will be called computational anatomy. Computational anatomy plays a major role in the sensory modalities of the neural system.

14.4.3.2 The coding of simple signals within stage 3 EMPTY

[xxx reflect on solving the coding of visual material coding of visual material

14.4.3.3 The coding of complex signals within stage 3 EMPTY

There has been very little material reporting a successful understanding of the code used in encoding complex material (in either stage 3 or stages 4 & 5).

[42]Brugge, J. (1992) An overview of central auditory processing In Popper, A. & Fay, R. (1992) The Mammalian Auditory Pathway: Neurophysiology. NY: Springer-Verlag pp 3-6

Moller presented a paper based largely on statistical analysis of stage 3 signals in 1980[43].

14.4.3.4 Ensemble coding

The investigators current ability to access multiple neurons simultaneously is in its infancy. No ability exist currently to locate and access a specific set of parallel neurons carrying messages, *en suite* (parallel data transfer), is currently zero. Papers discussing this capability are largely limited to making a variety of assumptions about the *en suite* channel operations. The results tend to be highly conceptual and statistically oriented. An example is the paper by Harper & McAlpine[44].

14.4.4 The architecture of spatial encoding relative to somatosensory performance RESERVED

14.4.5 The architecture of spatial encoding relative to taste and smell RESERVED

14.4.6 The use of histograms to interpret neurological signals BRIEF

As shown in Section xxx, the neurological system does not employ frequency modulation. Instead, it employs time-delay modulation. This difference appears insiginificant to an untrained eye looking at an oscilloscope or oscilloscope recording. However, it has a profound impact on the interpretation of the signals being conveyed by a pulse stream. **All of the data in the previous neurological literature presented in histogram form requires reinterpretation due to this profound difference**.

14.4.6.1 The use of histograms to interpret auditory data

[xxxUse style of Young, Robert and Shofner to explain histograms]
[xxx dress up the figure to show sine wave as well and envelope of sine wave above "phase-locking"]

Figure 14.5.6-1 provides a fundamental histogram as frequently used in hearing research[45]. Notice the action potentials in the "spike train" are in sequential order in the temporal plots. However, in the resulting histogram, they are hopelessly jumbled and pulses #6 and #11 are lost completely. While convenient in pedagogy, a histogram exhibits a serious problem when used in research. The histogram cannot be unfolded to reproduce the actual pulse stream representing the encoded analog signal.

---

[43]Moller, A. (1980) Coding of complex sounds in the auditory nervous system *In* Syka, J. & Aitkin, L. *ed.* Neuronal Mechanisms of Hearing. NY: Plenum Press pp 87-103

[44]Harper, N. & McAlpine, D. (2004) Optimal neural population coding of an auditory spatial cue *Nature* vol. 430, pp 682-685

[45]Young, E. (1988) xxx

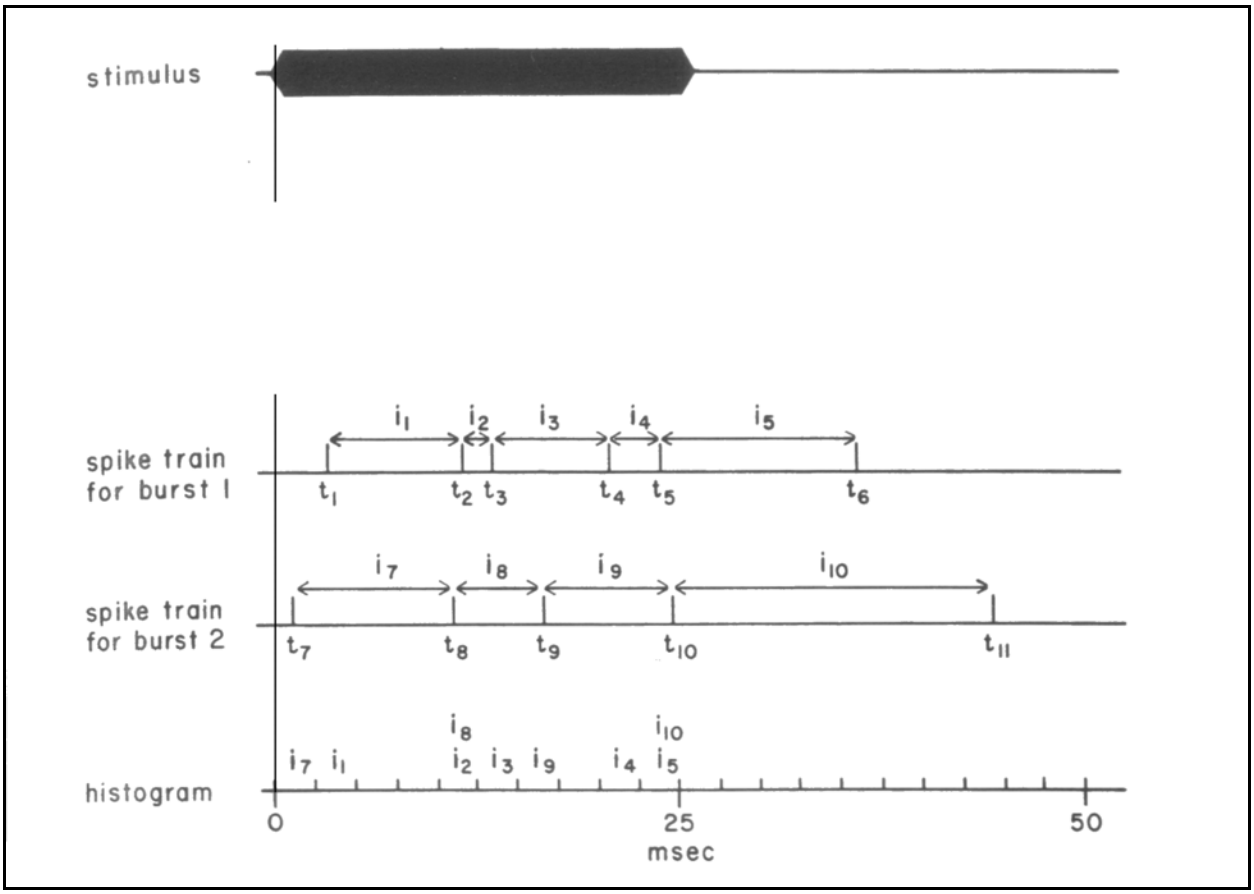

Figure 14.5.6-1 The form of a simple histogram ADD. From Young, 1988.

Succinctly, the convolution employed in a histogram cannot be deconvolved without significant external information relating to the test protocol and equipment.

Figure 14.5.6-2 from Johnson illustrates the above assertion. The integrated number of AP generated in response to the 0.809 kHz tone rises monotonically with intensity during the duration of one period of the tone. However, the time of occurrence of the pulses varies over a major fraction of one-half of the 1.23 ms period during the 15 second data accumulation phase. With a typical interval of 1.6 ms between AP at their maximum rate, there is little chance of two AP occurring within one period of 1.23 ms in this histogram.

The same thing cannot be said for the histograms for 0.353 kHz. The duration of the histogram is now 2.83 ms. As the intensity of the stimulus rises, the left hand pulse group represents the pulses initiated to define the presence of a electrical signal at node E (or E') that is above threshold for the ganglion neuron. At –60 dB (equivalent to 55 dB SPL–and within the phonotopic range), an additional pulse group begins to appear. This pulse group is not related to any particular phase of the stimulus tone. As will be developed in this chapter, it is the second pulse generated by the delta-modulation encoding scheme used in Stage 3 neurons of the neural system. It is part of the phasic signal describing the amplitude of the stimulus. The same form of second pulse group appears at high stimulus intensities in the 0.454 kHz histograms. However, the time between the two pulse groups appears to have lengthened. In fact, this is because the lenth of the time base has been reduced from 2.83 ms to 2.2 ms.

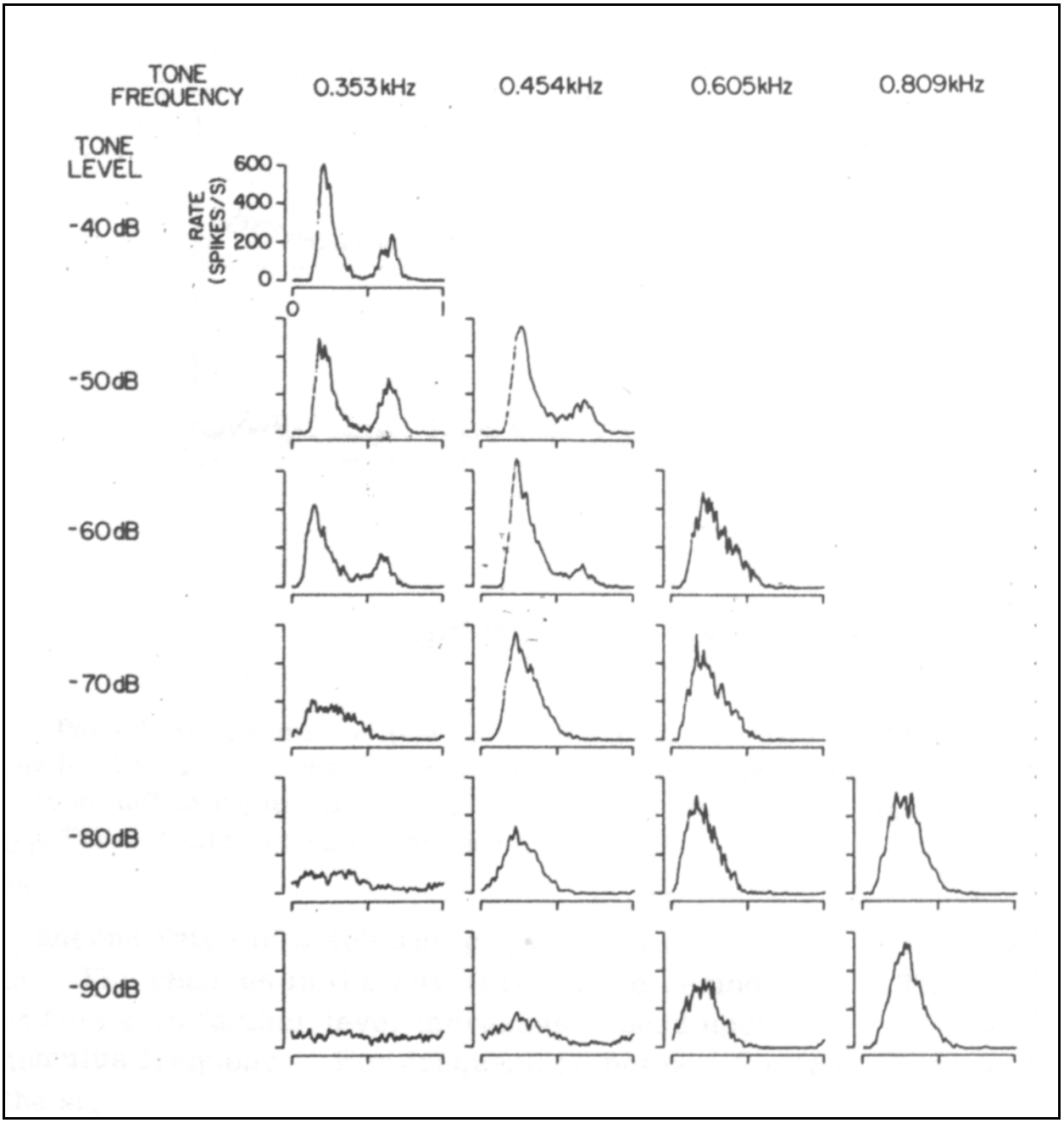

Figure 14.5.6-2 A period histogram prepared from the discharge pattern of a ganglion cell in response to single tones. The reference tone level was 115 dB SPL. Each histogram extends for the duration of one cycle of the stimulus. The reference phase for each column of histograms is the same. However, the phase varies between columns in order to reflect an order that is illusory. The SR for this ganglion cell fiber was 60 AP/sec. The CF of the associated sensory neurons was 0.8 kHz. Abstracted from a figure by Johnson, 1980.

Several investigators have attempted to relate the second pulse group to the opposite half cycle of the stimulating tone rather than to the encoding scheme of the Stage 3 ganglion neurons.

14.4.6.2 A new, revised histogram for hearing research BRIEF

As neurological research moves from the exploratory stage to the applied stage, it is important that future investigators present their data in a clearer histogram format. This section will identify such a histogram based on the physiology of hearing. It is based on the time delay encoding of fundamental sensory data as measured at node F and on stage 2 signal summation data, also measured at node F. This revised format can also be used to re-interpret old data presented in discharge rate histograms.

A great deal of the information concerning the operation of the auditory system is obtained using histograms displaying the rate of action potential generation as a function of time. The collected data, appearing random in character. To quantify this information, the time scale is generally divided into bins and the number of pulses acquired during that time interval is averaged within the bin.

Past histograms have been based on the assumption that the action potential pulses occurring at the axon of a auditory nerve fiber represent the stimulus when encoded using frequency modulation, a form of phase modulation. This chapter will show that this is incorrect. The encoding process employs time-delay modulation which is a different form of phase modulation. ***The primary feature of true phase modulation is that the first pulse in the series carries significant information***, This is not true in frequency modulation.

Xxx

Figure 14.5.7-1 shows the new rate histogram derived from the underlying time-interval histogram.
[xxx use inset from previous derivation in chapter 5]
[xxx bring all or selected material from from chapter 5.]

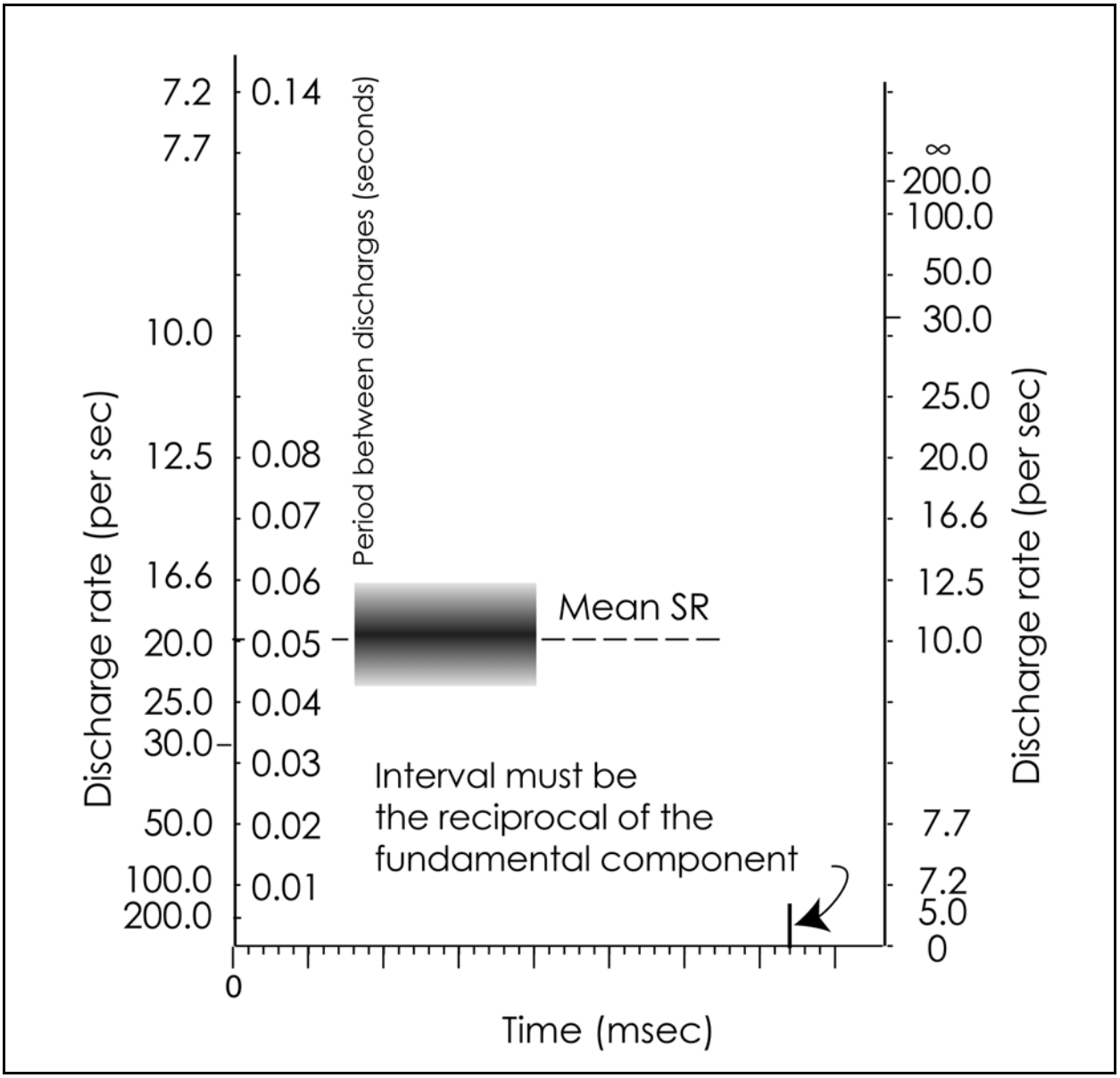

Figure 14.5.7-1 The revised rate histogram applicable to auditory research. The space within the axes is rectilinear. Note the background noise associated with the spontaneous rate (SR) is shown as a bi-phasic signal. The time scale on the left is shown only for orientation. Either the left or right discharge rate scales can be used (but not both). The scale on the right results in a histogram with a familiar orientation but a greatly expanded scale at low discharge rates. To obtain a stationary, equally weighted histogram, the time interval used must be a multiple of the reciprocal of the fundamental frequency in the data stream and a sub-multiple of the total signal acquisition time. See text.

14.4.6.3 Transformation of older histograms to the revised format EDIT

[xxx edit following to eliminate redundancy. take out references to chapter 7]

Several investigators have been influenced by other investigators use of the term rectifier and

have provided less than precise diagrams comparing the output histogram (measured at Stage 3) to the input signal of a sensory neuron[46,47]. Investigators have traditionally prepared a histogram plotting the number of pulses in a bin as a function of bins formed along the time axis. This histogram has compressed one half of the response until the histogram is used to support the conventional wisdom that the sensory neurons operate as rectifiers. The problem is a fundamental one. A lack of understanding the code used to encode the analog output of the sensory neurons onto a phasic action pulse carrier. The conventional assumption has been that the pulse rate of the action pulses is indicative of the signal information being transmitted. Unfortunately, this is not correct, at least for the OHC neurons which have been of most interest to investigators. It is the pulse interval that carries the information (the reciprocal of the pulse rate).

Figure 14.5.7-2 shows the process for converting old rate histograms into the revised format if the tabular data is not available. In most cases, even the tabular data may not be precise enough in critical areas and some approximations must be made. A template is shown in frame E of the figure that is the same as that introduced above. The space within the axes of the template is rectilinear as are the time interval (ordinate) and time (abscissa) scales.

[46]Hind, J. Andereson, D. Brugge, J. & Rose, J. (1967) Coding of information pertaining to paired low-frequency tones in single auditory nerve fibers of the squirrel monkey *J Neurophysiol* vol. 30, pp 794-816

[47]Brugge, J. Anderson, D. Hind, J. & Rose, J. (1969) Time structure of discharge in single auditory nerve fibers of the squirrel monkey in response to complex periodic sounds *J Neurophysiol* vol. 32, pp 386-401

This graph takes the conventional rate histogram (these from Brugge, et. al, 1998 based on their work in 1969) shown at lower left and converts it to a pulse-interval histogram. In the original histograms shown at lower left, the length of the time base was taken as a multiple of the interval associated with the fundamental frequency of 266 Hz and the third and fourth harmonics were combined and used as a stimulus. This is a necessary condition when collecting data for longer than the duration of one cycle of the fundamental frequency. Otherwise, averaging of the signal over the entire bin structure (see frame A_2, B_2 and E_1 in figure 3 in Hind, et. al. 1967). Brugge, et. al. fitted the analog waveform used to generate each histogram and obtained the apparent rectifying action they expected. They phased their analog waveforms to provide a best fit to the statistical data. This phasing was based on the assumption that the histogram represented a direct encoding of the data on a frequency modulation basis. Unfortunately, the neural encoding being discussed here, and relevant to at least the OHC of hearing, uses a time delay method of encoding. The Brugge, et. al. waveforms also appear to have assumed no attenuation within the hearing system as a function of frequency between the stimulus and the individual axons of the auditory fiber. This condition is not achieved in practice.

It is interesting to note a relationship inherent in the use of sine wave tones in these experiments. The derivative of the stimulus has the same shape as the original waveform. Thus, the same stimulus can be differentiated and re-phased to overlay the histograms just as well as the undifferentiated waveform. The dashed lines overlaying the Brugge, et. al. data are the integrals of the curves drawn with solid lines. It is incumbent on the investigator to know the precise nature of the signal processing (both acoustic and neural) involved in his experiments before he analyzes the data and draws conclusions. The Hind, et. al paper of 1967 reflects their assumption that is common to all of these papers, "Our findings with regard to discharge rates, which are presumably intensity functions of the stimulus. . . ." This statement implies that the rate is proportional to the stimulus. While the rates do exhibit a relationship to the original stimulus, it is not a simple one and these functions are not proportional.

The instantaneous pulse rate is the reciprocal of the instantaneous pulse interval. However, it is the pulse interval that describes the signal encoded onto the phasic action potential stream. The use of a nomograph is the best way to perform this conversion graphically. The conversion process is described at upper left. The curved line is a hyperbola expressing the equation $T = 1/f$ over the pulse rates of interest (zero to maximum pulse rate encountered). The minimum pulse rate is just as important as the maximum pulse rate. By using the same time period for data collection on both the old and the new histograms, the pulse rate can be transferred to the pulse interval histogram easily. This is done by projecting a line upward from the value in a given time bin until it intersects the conversion line. A line from that point can then be projected horizontally until the line intersect the same time bin in the new histogram. The process results in a new time-interval histogram that describes the shape of the original signals faithfully. Frames A, B & C at upper right correspond to the same frames at lower left. This type of time-interval histogram has been used by Hind, et. al. and Rose, et. al. but for a different purposes[48,49].

The resulting graph shows the average time interval between all of the pulses in a given bin. The curves shown at upper right represent the theoretical histogram describing the action potential inter-pulse interval for pulse streams with zero bin widths. Actual data will reflect the jagged form usually found for histograms with finite bin width. The curves also represent the stimulus waveform in the absence of any saturation in the signaling channel. ***No hint of rectification is found in these curves.*** However, the actual data can be expected to show both adaptation and saturation at higher stimulus intensities. Adaptation will appear as a symmetrical reduction in the excursions in the histograms over that expected in response to the stimulus level expected in the absence of adaptation. Saturation will appear as a reduction in amplitude of either the upper or lower excursion of the larger pulse patterns. This will be observed as compression of either the upper or lower excursion depending on the polarity of the output signal at the sensory neuron with

---

[48]Hind, J. Anderson, D. Brugge, J. & Rose, J. (1967) Coding of information pertaining to paired low-frequency tones in single auditory nerve fibers of the squirrel monkey *J Neurosci* vol 30, pp 794-816, fig 10

[49]Rose, J. Brugge, J. Anderson, D. & Hind, J. (1967) Phase-locked response to low-frequency tones in single auditory nerve fibers of the squirrel monkey *J Neurosci* vol 30, pp 769-793, figs 1, 3 & 4

respect to the stimulus. [xxx say what this polarization is after developing the sensory neuron polarity in this chapter and then the encoding polarity in chapter 7].

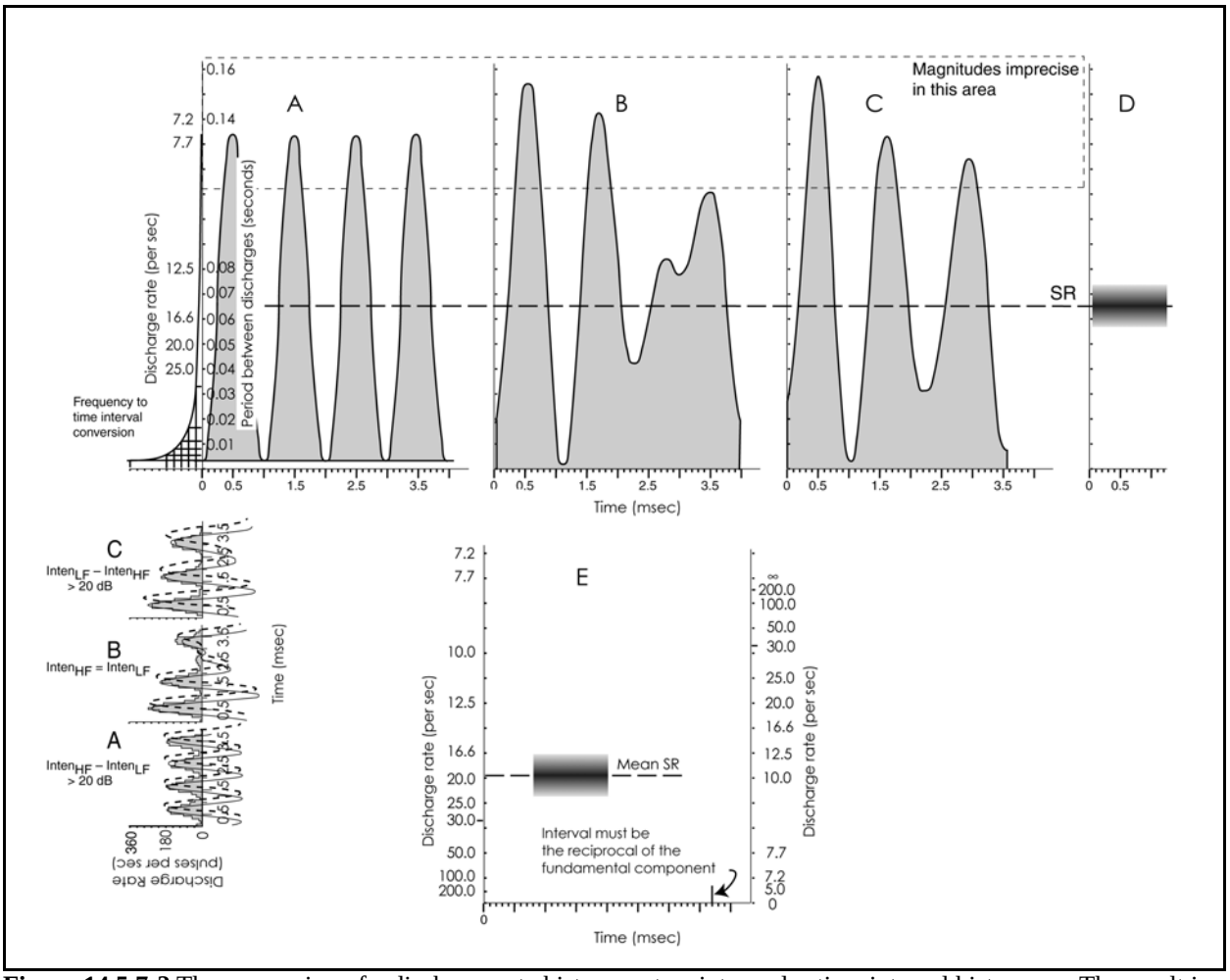

Figure 14.5.7-2 The conversion of a discharge rate histogram to a inter-pulse time interval histogram. The result is a clearer understanding of the Stage 3 signal encoding process. The data at lower left has been converted into the theoretical asymptotes for the same data in upper right by taking the reciprocal of the pulse rate, using the upper left quadrant. See text for a critical discussion of this figure. Data from Brugge, 1998.

The shape of the curves near the top of the figure cannot be obtained with precision from the rate histogram because of the compression in that part of the figure. The shape could be determined if the raw tabular data were still available.

Frame D shows the spontaneous rate now appears as a biphase waveform due to background or internal noise. This noise is normally additive with the signal, and becomes dominant in the kaumotopic regime (below 15 dB SPL). It is significant in the mesotopic regime (from 15 to 45 dB SPL) but negligible at higher intensities.

Frame E shows a template that can be used by any investigator. Two separate scales are

shown. Either of the two scales may be used (but not both). Use of the scale on the right leads to a conventional-looking histogram with the zero pulse rate at the bottom. The area within the scales is rectilinear although the discharge rate scales are not. The scales can be changed by multiplying all of the values on either scale by an integer to reflect the acquisition interval as a function of the presentation duration. It is important that the duration of the histogram be the reciprocal of the fundamental frequency in any tone based tests. Otherwise, the folding of the recorded data from the total acquisition interval will not form a stable histogram. If the interval is not based on the reciprocal of the fundamental, the histogram will change depending on the interval used and the initial interval in the folding operation.

In the future, investigators can continue to report the number of pulses in a narrow bin (a rate histogram) as long as they use the nonlinear pulse rate scale shown on either the left or right of the new interval histogram template. By re-scaling the histograms in Kiang[50], the analysis of his three-tone test data can be interpreted more effectively.

In their discussion, Rose, et. al. assert that "Our main finding is that the spiral ganglion neurons apparently transmit information regarding the frequency of a low tone by producing discharges as intervals grouped around the value of the period or its integral multiples." In essence, they concur that the signal information is transmitted within Stage 3 using a time delay modulated action potential stream where the time intervals between the pulses describe the stimulus, as a function of time. They describe this coding as involving a period-time code. While they describe what they call the cadence of a pulse stream, they did not uncover the relationship between the analog stimulus frequency and intensity, and the time intervals between the phasic action potential pulses.

14.4.6.4 Theoretical and real tone-test representations using the revised histogram

Figure 14.5.8-1 describes the revised (time-interval based) histogram in more detail as it applies to the sensory data measured at nodes F of the neural system, in the absence of any Stage 2 signal processing.

[xxx discuss relative location of SR, can it be this high in a fundamental channel?]
[xxx discuss tradeoff between pedestal height and sine wave versus frequency]

14.4.6.4.1 Test data applicable to the primary signaling channels

[xxx primary signaling channels do not include any stage 2 signal processing between the acoustic stimulus and node F.

14.4.6.4.2 Test data applicable to the additive signal processing channels

Additive signaling channels include stage 2 signal processing between the acoustic stimulus and node F.

MERGE Two-tone test data shown in

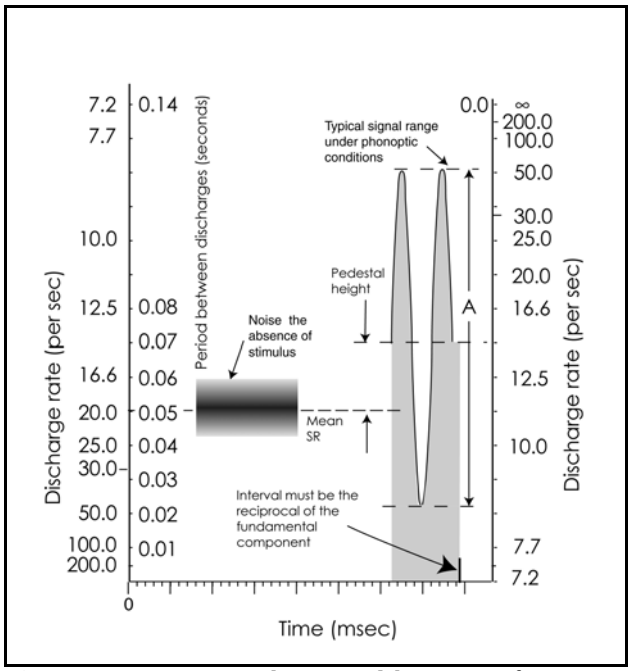

Figure 14.5.8-1 Using the revised histogram for type B (IHC) and type N (OHC) sensory channel data. Only one and one-half cycles of the response to the stimulus are shown representing a fundamental signaling path. Earlier responses involve a transient moving from the SR level to the pedestal level. Following the termination of the stimulus, the pedestal will decay back to the SR level. See text.

[50]Kiang, N. (1990) Curious oddments of auditory-nerve studies *Hear Res* vol. 49, pp 1-16

histograms of additive channels

[xxx could be both narrowband and broadband but most likely narrowband.

14.4.6.4.3 Test data applicable to the subtractive processing channels

Subtractive signaling channels include stage 2 signal processing between the acoustic stimulus and node F.

MERGE Two-tone test data shown in histograms of subtractive channels

14.4.6.5 More complex signal processing prior to node F

There is no limitation on stage 2 signal processing prior to the axons of auditory nerve fibers. In fact, the three tone tests of Kiang, discussed below, may have produced confirming data of such signal processing. Alternately, many more neurons leave the auditory nerve than there are sensory neurons. It is possible there is signal decoding, stage 4 signal manipulation and subsequent signal encoding. This possibility, for which little data is available to confirm (xxx unless I can find more morphology of the auditory nerve), must remain a fertile region for further exploration.

14.4.6.6 Three-tone test data shown in histograms

[xxx Kiang has some good data in 1990 paper that needs replotting. Without replotting it is virtually impossible to determine whether a given channel is the result of summation or differencing]

14.4.6.7 The use of histograms to interpret cumulative data in mammals SHOW

[xxx show old and new side by side.]

14.4.6.7.1 Background EMPTY

14.4.6.7.2 Examples from squirrel monkey (showing phase shift)

Anderson, et. al. have provided histogram data on the squirrel monkey[51]. The histograms were prepared to stress the change in phase of the data in the histograms as a function of frequency. The data is clear and also provides an estimate of the time delay (latency) between the stimuli and the response at the selected auditory nerve fibers. [xxx expand on this It may be useful to reference it in Chapter 9]

14.4.6.7.3 Examples from cat

Johnson has provided a large set of period histograms for one auditory fiber in the cat when using stimuli introduced into a closed ear canal[52]. While overly broad, his introduction suggests he was working only with OHC sensory neurons. His stated purpose was to study the relationship between the average spontaneous discharge rate and the synchronism between the time of stimulus and the time of the resultant action potentials. While his conclusion was that more

---

[51]Anderson, D. Rose, J. Hind, J. & Brugge, J. (1970) Temporal position of discharges in single auditory nerve fibers within the cycle of a sine-wave stimulus frequency and intensity effects *J Acoust Soc Am* vol. 49(4), pt 2, pp 1131-1139

[52]Johnson, D. (1980) The relationship between spike rate and synchrony in responses of auditory-nerve fibers to single tones *J Acoust Soc Am* vol. 68(4), pp 1115-1122

investigation was required, his data is useful in other contexts. The caption to his figure 1 carefully defines the reference phases for each histogram and notes that they each extend over a time interval corresponding to one cycle of the frequency shown. The frequency however, varies by a factor of four. For the higher frequency tone stimuli, the binning used suggests the presence of individual action potentials. The effect is less clear in the histograms from lower frequency stimuli. The average spontaneous rate for this axon was 60 spikes per second in the absence of stimulation. Under stimulation, the rate went as high as 600 spikes per second and as low as zero.

His figure 2 gives similar data for an axon of a channel with a CF of 3 kHz. The spontaneous rate was 37 spikes/second. The peak spike rate was less than 400 and the minimum again went to zero for intense stimuli. [xxx expand on Johnson's material]

14.4.6.7.4 Examples from guinea-pig

Palmer & Russell have provided extensive sets of period histograms from the afferent Stage 3 neurons of the guinea-pig in response to an unspecified method of stimulation (references to other papers were given).

14.5 Operation of the Stage 3, Signal Projection circuits

This section draws heavily on the discussion of the morphology, electrophysiology (both topography and topology) of the neurons found in **Chapters 8, 9** and **10**. This section will first examine the electro-cytology of a Stage 3 signal-encoding projection neuron (typically labeled a ganglion cell). It will then proceed to examine the circuit analogs useful in describing the operation of such a ganglion cell.

14.5.1 The Activa within a neuron

The Activas found within various neurons have not been studied as entities before their discovery and definition in this work. As indicated in the previous sections of this Chapter, the Activas exist in several different configurations within the various major types of neurons. Hersch & Peters[53] have provided a well-defined electron-micrograph of the Activa in a pyramidal cell of a rat, **Figure 14.6.1-1**. Note their designation of two separate and distinct neurites, the apical dendrite(conventional) and the basal dendrite (or podite as defined in this work). The four major elements concerning signaling are clearly shown, the apical dendrite, the basal dendrite (the podite), the Activa (within the hillock) and the axon. They are shown within the cell membrane but external to the nucleus in the area generally described as the cell body. The cell membrane and other features are not well resolved at only x5000 magnification. At higher magnification, imaging a different plane through the cell would probably be necessary to show the actual location of the "7-layer" membrane forming the actual Activa. Absent this level of detail, the above figure clearly shows the *location* of the podite or base region of the Activa between the apical dendrite and the axon. The Activa is in the region described as the initial segment of the axon. This is a subregion of the hillock and is not covered by myelin. The figure also shows the access of each of these areas to the external surface of the cell membrane for electrical and other purposes. Higher levels of magnification using the electron-microscope would also delineate areas of higher electron charge density that could be correlated with the bio-energetic materials providing electrical power and possibly interfaces with other nearby neurons.

[53]Hersch, S. & Peters, A. XXX in Shepherd 1988

Figure 14.6.1-2 is a caricature of the above figure shown with several additional synapses for purposes of discussion. Note the nucleus is shown surrounded by the dendritic conduit in this 2-dimensional view of a 3-dimensional object. For purposes of signaling, the nucleus is irrelevant and can be omitted entirely. For purposes of growth and maintenance, the nucleus has direct access to the surrounding fluids via the third dimension. The critical area of this neuron is the space within the dotted box. This area includes the two internal membranes separating the dendroplasm and the axoplasm. Usually, the distance between these two membranes is inconsequential. However, in a small region (not shown at this scale), they are only separated by about 100 Angstrom (10 nm.). The resulting 7-layer region forms the physical location of the Activa. The Activa is only found in the region where the two bi-layer membranes are separated by less than 100 Angstrom (but more than a critical minimum amount). They are not in physical contact from a semiconductor physics perspective.

[[The areas of bio-energetic activity are shown similarly to those seen in other cells at this magnification. (b) shows the putative electrical circuit overlay appropriate to (a). The location of the bio-energetics and the electronic overlay presentation is similar to that used in subsequent sections.]]**[not shown currently]**

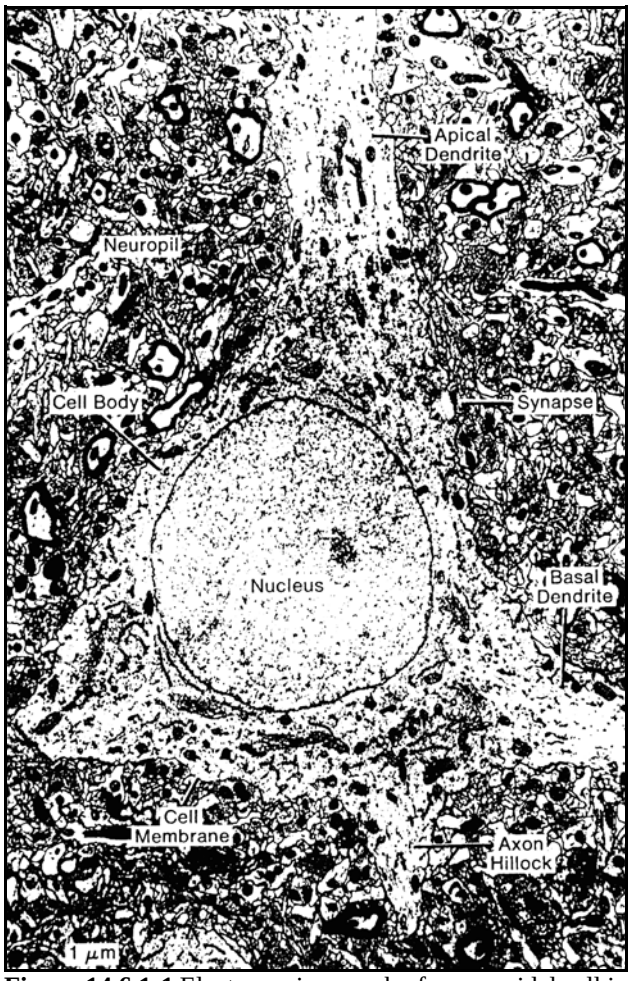

Figure 14.6.1-1 Electron micrograph of a pyramidal cell in the visual cortex of the rat. Magnification, approximately x5000 when printed five inches wide. From Hersch & Peters

Afifi & Bergman[54] have discussed the podite contact with the surrounding medium under the morphological designation, initial segment. They describe the base region of the Activa within this region as of 200 Angstrom (20 nm.) thickness and consisting of a dense layer of granular material. It is proposed that higher magnification imagery, and more careful selection of the slice location, would show the actual perinodal area to be essentially identical to the constricted axon segment, CON, region described by XXX [Waxman] and discussed in **Section 10.4.** At this gap width, it is proposed that the so-called dense granular material occupying the perinodal gap is, in fact, a liquid crystal of hydronium.

Hersch & Peters show a structure in the lower left of their figure that is not labeled. It may be an additional dendritic branch that is not well represented in the slice of the cell imaged in this electronmicrograph. This is the assumption made in the caricature which shows two distinct dendritic roots (both truncated for purposes of this discussion). The caricature also shows a series of synapses, labeled A through F. Synapses A through D all contact the dendritic plasma membrane and are by that definition axodendritic synapses. The synapses at E (and F as described below) contact the podite plasma membrane and are more properly labeled axopoditic synapses. This more precise definition stresses the need for a tabulation comparing the synapse from a morphological and electrophysiological perspective. **Table 9.2.5-1** is provided to aid in the more precise interpretation of the different types of synapses.

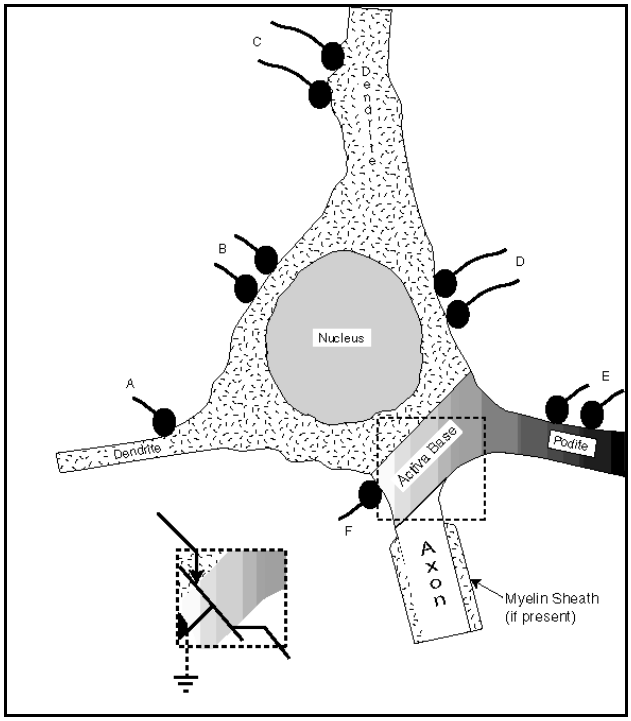

Figure 14.6.1-2 Caricature of the rat pyramidal cell based on the previous figure from Hersch & Peters.

14.5.1.1 DC potentials within a ganglion cell

Only a few investigators have attempted to measure the potentials within the dendrites of bipolar and horizontal cells. Copenhagen, Ashmore & Schnapf have provided point measurements reflecting the response of the photosensing system to light[55]. Guyton has provided an electrical potential mapping of a neuron of the pyramidal type[56]. A modified version of that figure is shown in **Figure 14.6.1-3**. Note the higher potential in the upper (poditic) arm of the neuron than found in the bulk of the neuron. The poditic arm is normally 15-25 mV more negative than the dendrites in order for the dendritic terminal of the Activa to be forward biased relative to the base terminal. Note also the voltage gradients in the various arms. This is exactly what would be expected by the current passing through the arms and creating a voltage drop. The voltage gradient is determined by both the current entering the neuron and the diameter of the arm at a given location that controls its local impedance. Although Guyton considered the various junctions shown to be either excitatory, the ones on the two left arms, or inhibitory, generally the ones on the top arm, these labels have been omitted. In this work, it is the Activa circuit within the neuron and its input circuits represented by the neurites that determines whether the output is the same or opposite polarity as the input signal. The circuit and the overall neuron is an analog device as illustrated by the smooth potential gradients within the neuron. The upper poditic arm is the inverting input terminal. The dendrites on the left are non-inverting input terminals. The axon potential was not provided in the original figure. It was probably near -120 mV (necessarily between -75 and -150 mV.) because of the large voltage difference between the dendrites and the podite and because of the considerable current flow present.

---

[54]Afifi, D. & Bergman, R. (1998) Functional Neuroanatomy NY: McGraw-Hill pg. 21

[55]Copenhagen, D. Ashmore, J. & Schnapf, J. (1983) Kinetics of synaptic transmission from photoreceptors to horizontal and bipolar cells in turtle retina, Vision Res. vol. 23, pp 363-369

[56]Guyton, A. (1976) Textbook of medical physiology. 5th edition Philadelphia, PA: W. B. Saunders pg. 622

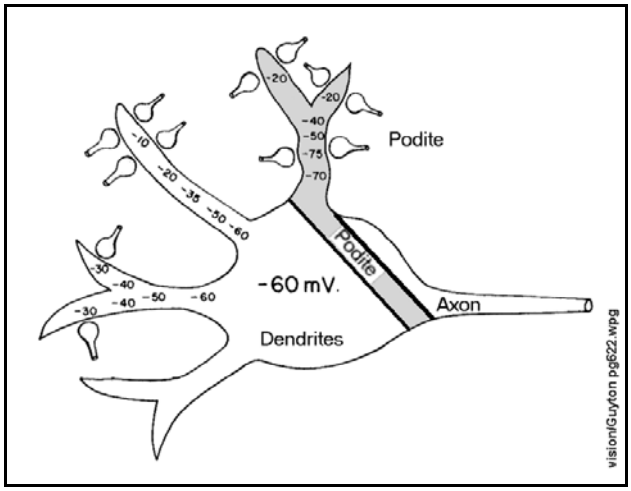

Figure 14.6.1-3 A potential map of a pyramidal type neuron showing the higher negative potential in the podite arm than in the bulk of the neuron representing the dendritic arm. Note the potential gradient along the arms due to current flowing within them. Modified from Guyton (1976).

14.5.1.2 AC potentials within a ganglion cell

Figure 14.6.1-4 reproduces (with only a minor change) a composite drawing from McGeer, Eccles & McGeer that they attribute to several investigators[57]. The figure has been modified to incorporate the shaded area representing the Activa.

—

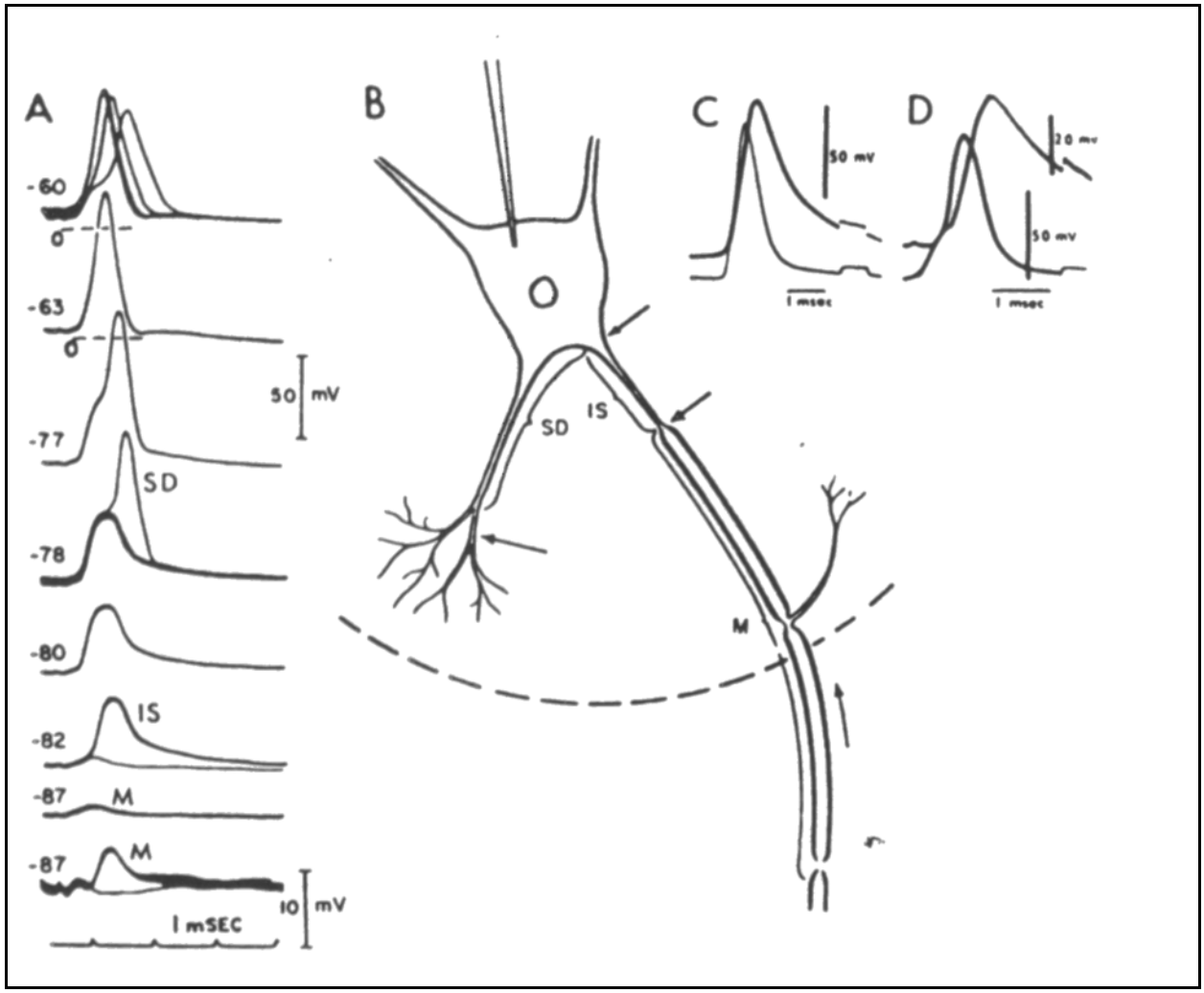

Figure 14.6.1-4 Intracellular responses evoked by an antidromic impulse relative to the "membrane potential." (A) The initial membrane potential (indicated to the left of each record) was controlled by the application of intracellularly applied currents. Initial resting potential was – 80 mV. The bottom record was obtained after increasing the amplification by 4.5:1. (B) A schematic drawing of the motorneuron showing neurites (only the one defined here as the poditic tree shown with branches), the soma, the initial segment of the axon (IS) and the medullated axon (M) with two Nodes of Ranvier (including one axon collateral) and a synapse with a subsequent neuron. See text for discussion of the arrows. (C) & (D) Simultaneous intracellular traces of neuritic and soma spike potentials from the same motorneuron. From McGeer, et. al., 1987.

---

[57]McGeer, P. Eccles, Sir J. & McGeer, E. (1987) Molecular Neurobiology of the Mammalian Brain. NY: Plenum Press, pp 70-72

Dowling has illustrated the decreasing excitability of a ganglion cell as a function of distance from the axon hillock (the location of the Activa)[58]. Unfortunately, he does not show the inverse phase relationship between the signals applied to the dendrites and the podites.

14.5.2 Block diagrams for the Stage 3, Signal Projection circuits

Stage 3 of the visual system is the simplest stage. While circuits with the same configurations and functionality appear in both the optic nerve, the various commissure and in the peripheral nervous system, they can all be considered members of Stage 3 of the neural system. They receive analog signals, propagate a coded facsimile of the signals over long distances and deliver a recovered copy of the original signal to the orthodromic circuits. The recovered copy must satisfy the quality of reproduction standards required for the operational portion of the neural system being supported. **Section 10.10** discusses these electrophysical requirements in more detail. Wherever a significant circuit delay is shown in the block diagrams of this work, one can assume it is caused by the physical delay introduced by the finite group velocity of signals projected by Stage 3 circuits.

14.5.3 Circuit elements critical to Stage 3, Signal Projection circuits

Figure 14.6.3-1 shows the fundamental signal processing path associated with stage 3 neural signaling. Stage 3 performs the critical function of coding the electrotonic signals from stage 2 into phasic form and decoding the phasic signals back into electrotonic form. The purpose is to allow the more efficient transmission of the signals using the mechanism of propagation rather than conduction. The signal encoding neuron is known generically as a ganglion cell in this work. The associated signal decoding neuron is known generically as a stellate cell.

The vertical black boxes at each end of the signal chain, and at the bottom of the ganglion cell, are electrotonic synapses. The vertical black boxes within the shaded stage 3 area are Nodes of Ranvier.

The single ganglion cell shown may consist of any number of Nodes of Ranvier. To maintain high operational efficiency at an acceptable error rate, these Nodes are generally placed every two millimeters or closer.

[58]Dowling, J. (1992) Neurons & Networks. Cambridge, MA: Harvard Univ. Press, pg 108

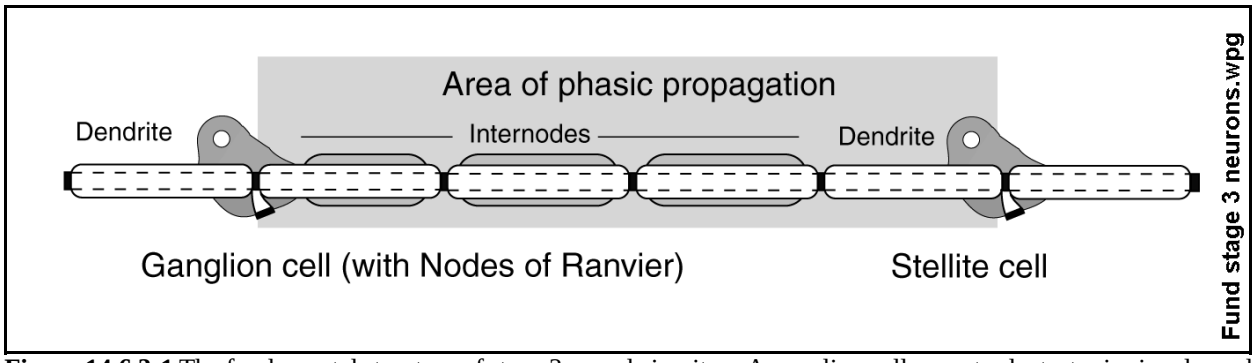

Figure 14.6.3-1 The fundamental structure of stage 3 neural circuitry. A ganglion cell accepts electrotonic signals, and encodes them into phasic form for propagation. A stellate cell accepts the phasic signals and decodes them into electrotonic signals similar to those received by the ganglion cell.

The following two figures are reproduced from Chapter 10. They are reproduced here to provide a bridge between the morphological description of certain elements of the neural system and the electrophysiology of the same elements. The figures may appear out of sequence because they were originally prepared from a discussion based on a different perspective.

Figure 14.6.3-2 describes a series of segments of an axon in communication with adjacent axonal or dendritic segments. The bulk figure with stippling and hatching describes the cell morphologically. The overlaying heavy solid lines describe the electrophysiological circuitry of the same cell. In each case, the symbol between the sections of conduit represents an electrolytic semiconductor device known as an Activa. The left half of the figure can be used to describe the amplifier circuit found within any neuron generating action potentials at a location antidromic to the hillock of the neuron. Alternately, the left half can be used to describe the Node of Ranvier between two axon segments. The right half can be used to describe either a Node of Ranvier or a synapse leading to a subsequent neuron. The difference between these cases revolves primarily around where the central axon segment receives its metabolic support and whether the region between the axon segments is in direct electrical contact with the surrounding INM. If the impedances, Z_b are located within the INM, the circuit at that point is defined as a synapse. If the impedance, Z_b, is located within the outer lemma of the neuron, the circuit is defined as a Node of Ranvier or the first (unnamed) Activa of the neuron located between its input dendroplasm and the axon (or first axon segment) of the neuron.

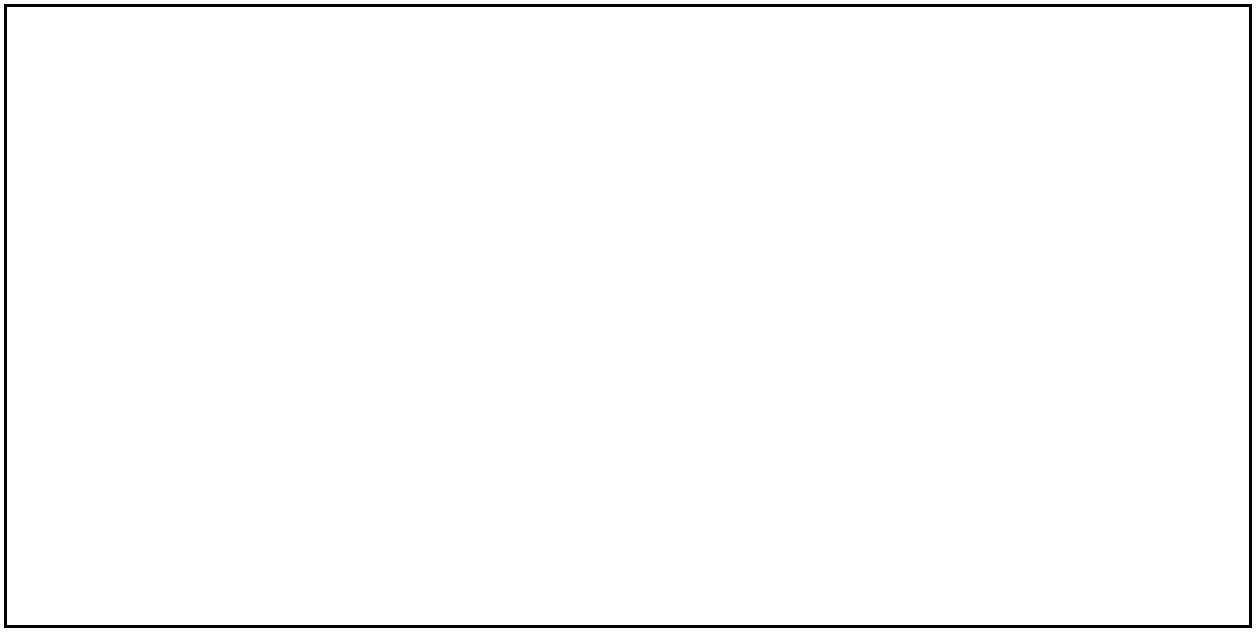

Figure 14.6.3-2 EMPTY The simple concept of a ganglion neuron as a series of conduits separated by regenerative amplifiers.

For purposes of this Chapter, the figure can represent either of two types of cells (and three configurations).

TABLE 14.5.2-1
Alternate configurations of the previous figure

Segment	As used in Ganglion Cell	As used in Stellate Cell	As used in a long axon of a ganglion cell
Left	dendrite	dendrite	previous axon segment
Middle	first axon segment	axon	axon segment
Right	2nd axon segment	following dendrite	subsequent axon segment

In the case of a ganglion cell, the left most conduit will be considered the dendroplasm of a ganglion cell. The first Activa will be involved in the generation of action potentials. The middle conduit can be considered the first section of the axon of such a cell. The right-most conduit can then be considered either an orthodromic axon segment or the dendrite of a orthodromic neuron.

In the case of a stellate cell, the left most conduit will be considered the dendroplasm of a the cell. For signals above a certain amplitude, the first Activa acts as a pulse rectifier. The middle conduit can be considered the axon of the nerve where the axolemma forms a very high capacitance between the axolemma and the INM. The resultant circuit acts as a pulse integrator and effectively recovers the analog information associated with the pulse to pulse interval along the pulse stream. The right-most Activa and conduit can then be considered a synapse and the dendrite of a orthodromic neuron.

Figure 14.6.3-3 illustrates the third case in greater detail. The central conduit is merely one of many replicated section along an axon separated from other conduits (axon segments) by Nodes of Ranvier. The conduit is designed to propagate a narrow pulse (action potential) along its length as efficiently as possible. Between sections of conduit are Nodes of Ranvier. Each Node contains an Activa in a circuit designed to regenerate the received action pulses and pass them to the next conduit section. The overall circuit is optimized to support these functions in a variety of ways. First, the current flow within the conduits is largely restricted to the volume between the dashed lines. By

providing a myelin coating on the exterior of the axolemma in the region labeled y, the capacitance between the axoplasm within this region and the INM is greatly reduced. As a result, this cylindrical axon segment forms a coaxial transmission line of very low capacitance relative to its intrinsic inductance. This results in a relatively high propagation velocity and a relatively low phase dispersion (the reason for the loss of signal amplitude) along the length of the conduit. Because the impedance of this transmission line is not well matched electrically to the Activa circuit at each Node, the sections labeled x and z are unmyelinated and act as impedance matching sections between the Nodes and the line. The section labeled x acts as a postnodal dendroplasm while the section labeled z acts as a prenodal axoplasm. The fluid is actually continuous between these two sections. However, the electrical potential and impedance of this fluid varies along the length of the conduit.

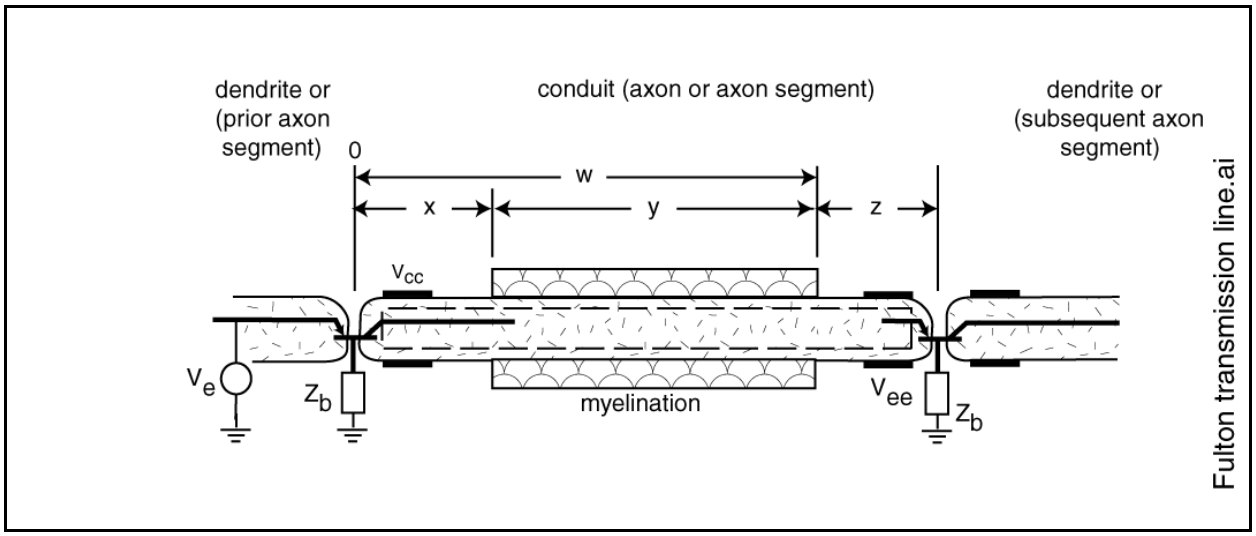

Figure 14.6.3-3 The morphology and topology of an axon segment ADD.

Figure 14.6.3-4 is designed to provide a simpler symbology for the axon segment of the above figure. The upper portion describes the morphology and some features of the cytology of only a single axon segment as it is found between two Nodes of Ranvier. The dashed line represents a foreshortening of the axon segment. In actuality, its length exceeds its diameter by at least fifty to one. The lower portion stresses the distributed LC (inductance-capacitance) character of the transmission line and the lump constant nature of the circuit forming the Node of Ranvier.

> The topological form describing the axon segment reinforces the fact that the axon segment is not represented by an RC cable. Based on its cylindrical morphology, it is properly described as a coaxial cable. It is correctly represented by an LC cable. Such a cable is dominated electrically by its inductance and capacitance. The physical resistances associated with such a cable are inconsequential.

The three lumped impedances are labeled to relate to the **E**mitter terminal, the **C**ollector terminal and the Base or **P**odoplasm terminal of the Activa.

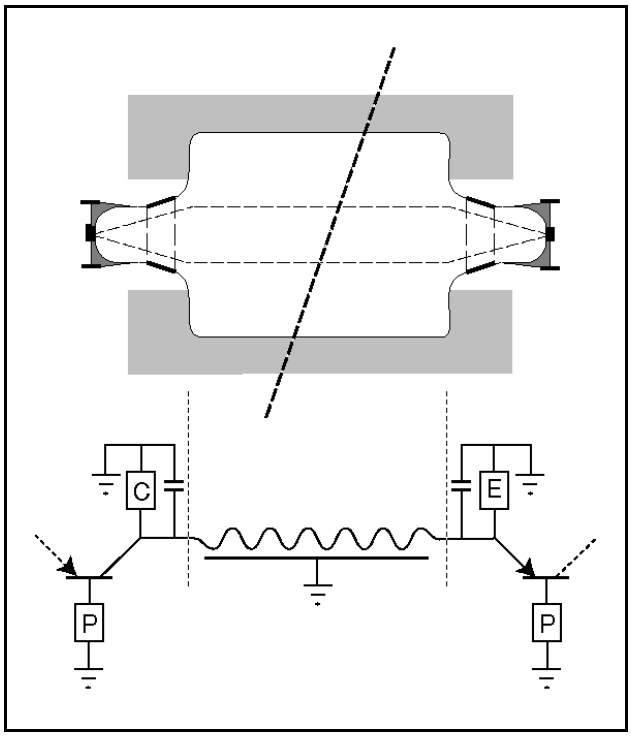

Figure 14.6.3-4 The topography and topology of an axon segment.

14.5.4 Circuit diagrams for the Stage 3, Signal Projection circuits

Figure 14.6.4-1 reproduces the overall circuit diagram of the visual system from its stimulation by photons to the reception of signals within the brain to aid in orienting the reader. It was presented and discussed in more detail in **Section 1.7.5.** The area within the solid-lined rectangle is the area of primary interest in this Chapter. It involves only phasic signals (usually described colloquially as action potentials). However, the following figure will expand this rectangle to include the analog circuits associated intimately with the phasic area. It will expand to include the 2nd generic synapse because of its role in a potential pre-emphasis circuit. Similarly, it will expand the rectangle to include the synapse and input circuit of the next neuron to the right of the stellate cells in order to account for a potential de-emphasis circuit. Note the remarkable similarity between the circuits in **Frame B** and **Frame C**.

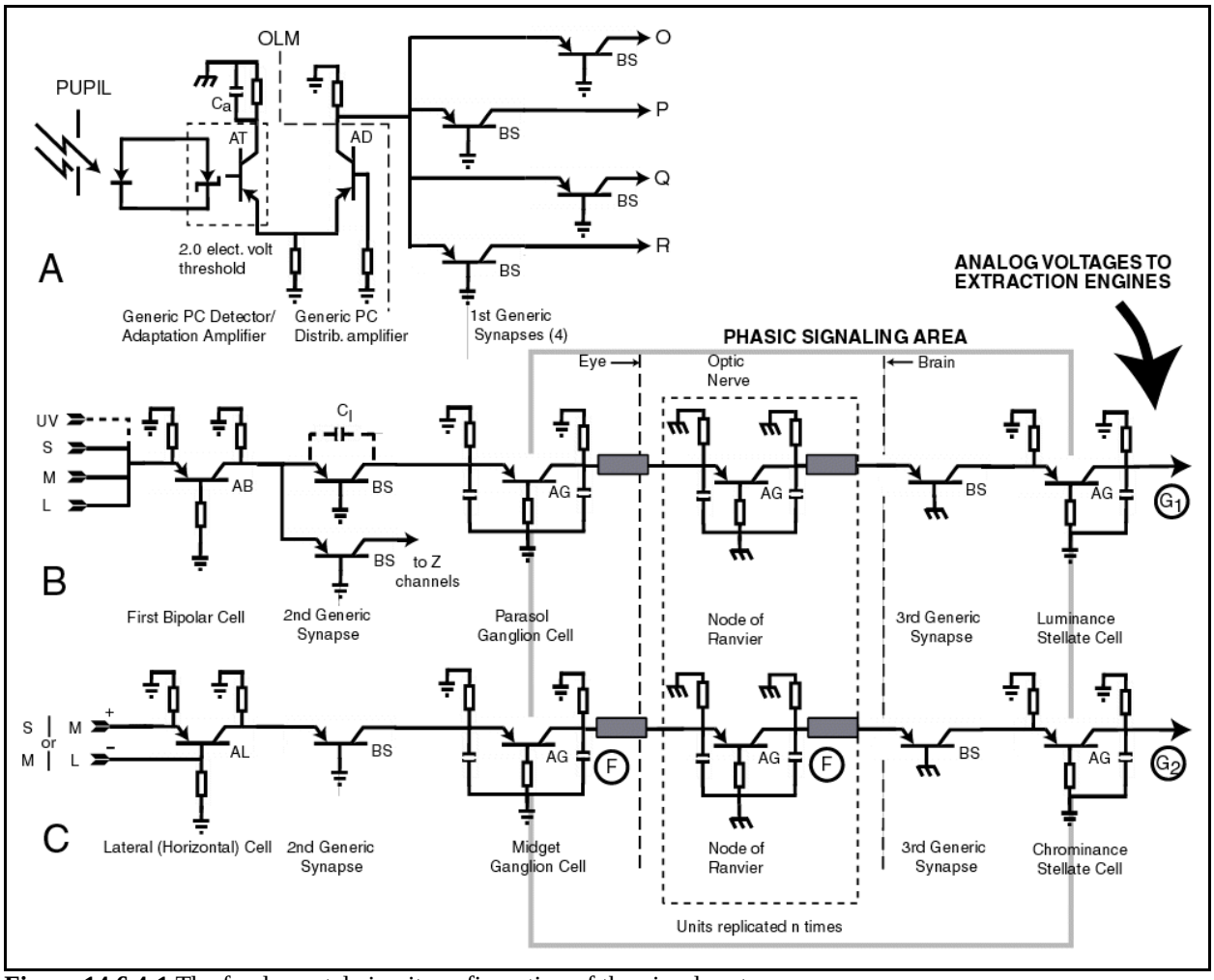

Figure 14.6.4-1 The fundamental circuit configuration of the visual system xxx.

There are only two operational differences between them. The first involves the way the various signals are applied to the 1st Bipolar cell and the Lateral cell. The second involves the bias potential on the emitter of the ganglion cells. This change in bias converts the driven monopulse oscillator of **Frame B** into a free-running phase modulated pulse oscillator of **Frame C**. As a result of these changes, the character of the signal at the outputs labeled G_1 and G_2 are fundamentally different. The signal at G_1 is monopolar in its deviation from a quiescent value. It typically represents a luminance channel signal that describes the relative brightness of the input stimulus. The signal at G_2 is fundamentally different. It is a bipolar waveform that describes the difference between the two signals applied to the inputs of the lateral cell. This difference is provided relative to the quiescent level of G_2. While the stellate cell associated with G_2 is labeled a chrominance type cell, the channel is identical to that used to convey polarization and appearance signals. The solid boxes shown as circuit elements in the figure will be expanded to a more detailed level in the following figure.

The signal projection function is accomplished in vision using a single (generic) circuit to connect the signal processing of the retina with the midbrain. However, the generic circuit is biased in two distinctly different ways to accomplish two apparently different signal projection functions. The first task is to transmit monopolar signals on a "demand basis." The second is to transmit bipolar signals on a continuous basis.

Figure 14.6.4-2 xxx decide which of these to show.

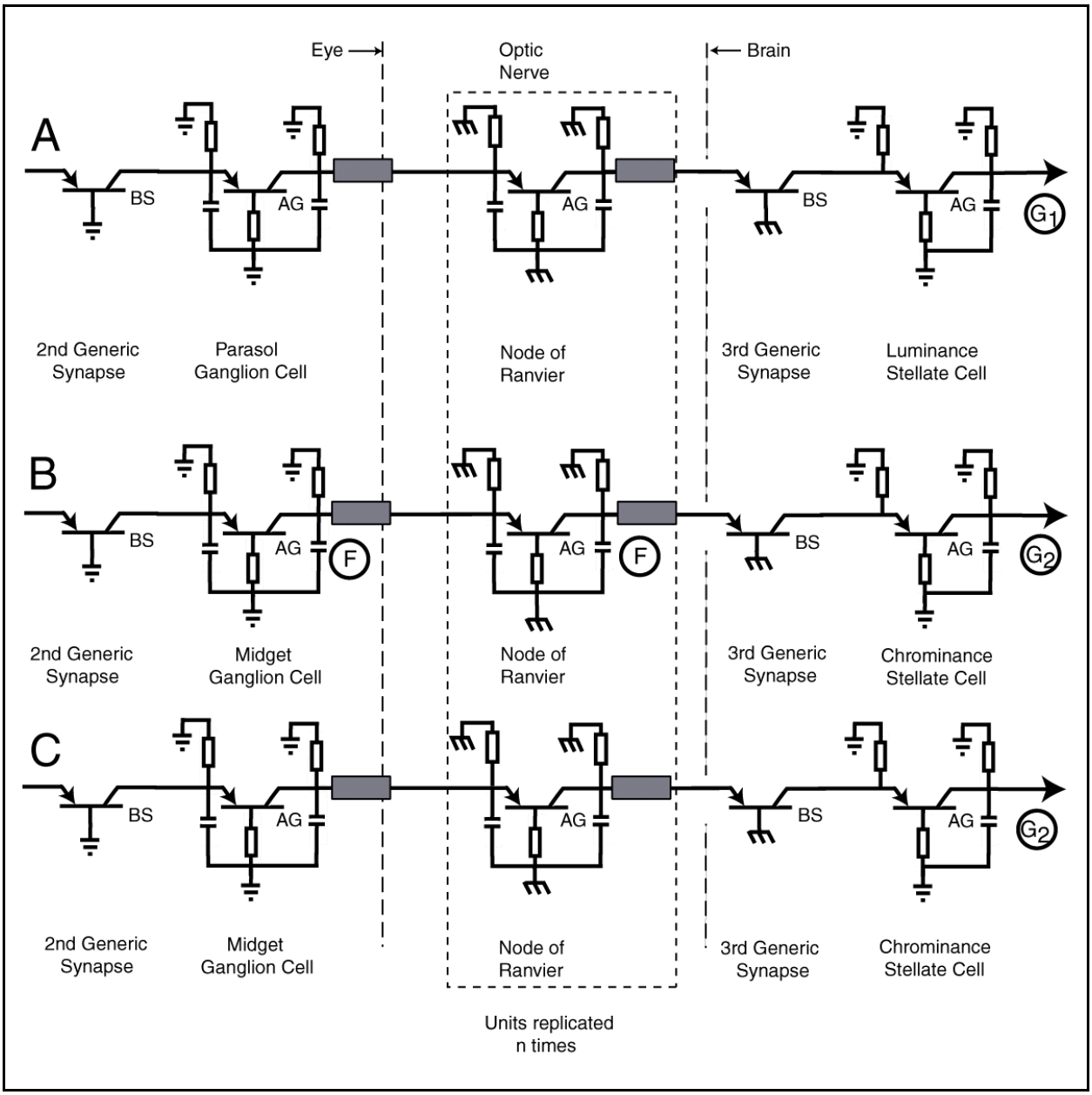

Figure 14.6.4-2 Optional circuit diagram.

The generic circuit of only signal projection, Stage 3, is shown in **Figure 14.6.4-3**. As discussed earlier, the circuit is shown including both a pre-emphasis and a de-emphasis circuit. These can be considered portions of Stage 2 and Stage 4 respectively. However, their intimate relationship to the overall signal projection function makes it important to include them here. The equivalent lead-lag networks forming the pre-emphasis and de-emphasis circuits are shown below the main circuit diagram. They are created by recognizing that both the synapses and the input circuits of the respective neurons can be described in terms of a parallel combination of a capacitance and the resistive component of an impedance. In the case of the synapse, the impedance is the transfer impedance between its emitter and collector terminals (when properly biased for the synapse to act as a diode). In the case of the orthodromic neuron, the impedance is the input impedance of the Activa (also represented by a diode when properly biased). The characteristics of the resulting lead-lag networks are determined by the ratios between the various

circuit elements. Speaking generally, a large series capacitance leads to a lead network while a large shunt capacitance leads to a lag network. If the series and parallel networks have identical phase angles, the resulting lead-lag network is merely a voltage divider exhibiting zero phase shift.

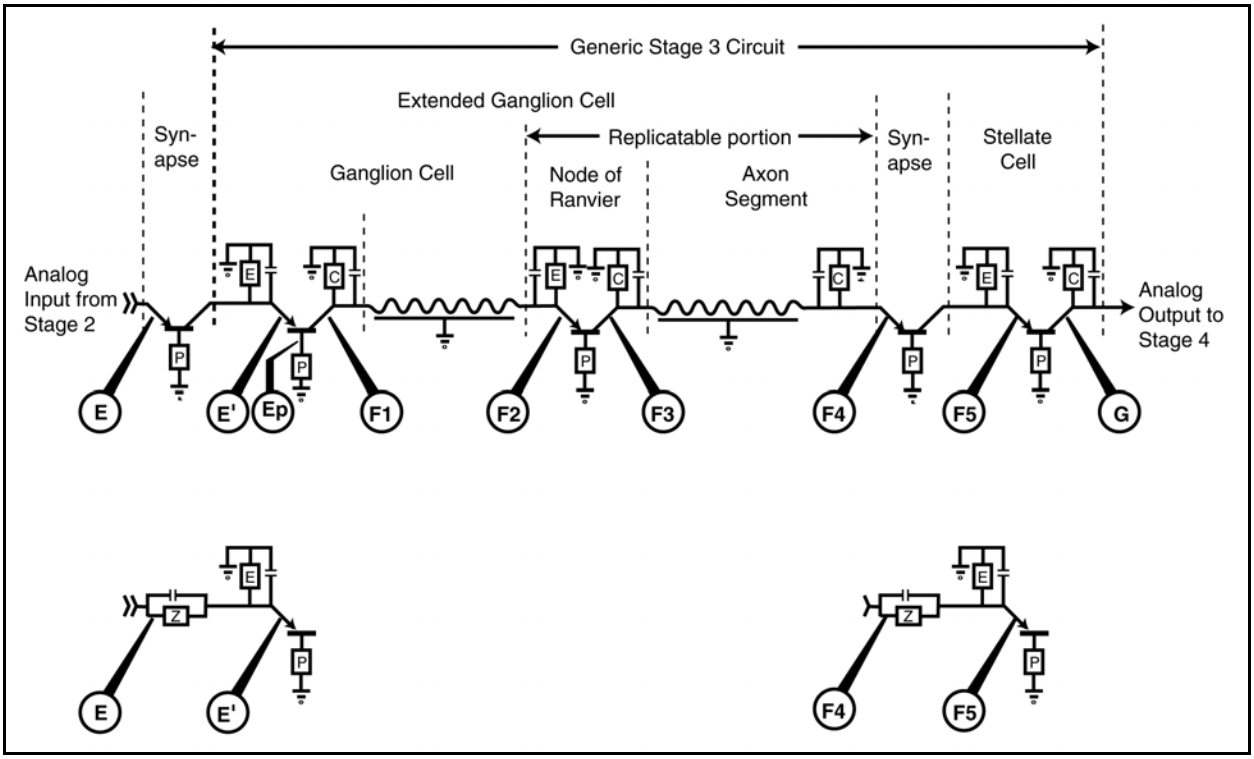

Figure 14.6.4-3 Generic Stage 3 circuit diagram. The lead-lag nature of the synapse-ganglion and synapse-stellate circuits are shown in the lower portion of the figure. See text.

In the main diagram, the impedances with letters within the boxes are complex. They contain both electrostenolytic power sources as well as diode impedances representing the lemma of the appropriate plasma conduit. The letters represent impedances at the **E**mitter (dendroplasmic) terminal of the Activa, at the base (**P**odoplasmic) terminal, and at the **C**ollector (axoplasmic terminal). **Z** is used to represent the simpler forward transfer impedance of the synapse. The role of these impedances is developed in **Section 9.3**.

In accordance with the more detailed discussion in **Chapter 9**, the ganglion cell is shown as consisting of an amplifier circuit and a nominally loss free LC transmission line. The morphological demarcation between these two elements is the Hillock leading to the axon. The electrical and cytological characteristics of this LC transmission line are essentially identical to the axon segment following the Node of Ranvier. By recognizing the LC nature of the coaxial axon and axon segment portions of the neuron, it is possible to accurately calculate the signal propagation velocity of the axon segments as well as their other electrical characteristics. These characteristics include both the amplitude loss and phase shift parameters as a function of distance along the axon. The amplitude loss is not due to resistive attenuation of the signal passed down the axon segment It is primarily due to the phase shift associated with such a simple (uncompensated) LC transmission line.

The shape and dimensions of the hillock and the feathered ending of the myelination near the hillock suggest that these features form an “impedance matching filter section” between the nominally constant impedance of the LC transmission line and the highly variable impedance of the oscillator circuit. A similar situation at the input to the Node of Ranvier suggests a similar section at that location. Such a section would reduce reflections from the Node back along the line toward the ganglion amplifier.

The generic Stage 3 circuit is a very good representation of the circuit conveying spectrally specific luminance signals from the photoreceptors of the foveola to the midbrain. The circuit is also a good representation of the Stage

3 circuits connecting the peripheral photoreceptors to the midbrain if the additional complexity introduced by potential diversity encoding is ignored.

As also discussed in **Section 9.3**, the amplifiers associated with the ganglion cells are biased to act as driven monopulse oscillators if they are relaying monopolar input signals. Alternately, they are biased as free-running oscillators if they are relaying bipolar signals. In this case, their pulse rate is a function of the potential applied to their input terminals. In both cases, the amplifiers associated with the Nodes of Ranvier are all biased to act as driven monopulse oscillators. They generate a new pulse in response to each (supra-threshold) pulse applied to their input. As in the case of the monopolar driven ganglion cell, the regenerated pulse is delayed considerably in time relative to the exciting pulse. This regeneration delay multiplied by the number of Nodes of Ranvier (plus one to account for the ganglion cell itself) associated with a given ganglion cell accounts for the majority of the signal delay in generic stage 3 circuits.

While the amplifier within the stellate cell exhibits an identical circuit configuration to both the amplifier of the ganglion cell and the Nodes of Ranvier, its performance is different because of the relative values of the various circuit elements. Here again, the bias potential between the emitter and base terminals of the Activa is the primary determinant of the operating mode of the circuit. It is usually set like that of a Node of Ranvier. The Activa delivers no current to the output circuit until an action potential is received that exceeds threshold. The secondary determinant is the value of the collector capacitance. While not large enough to support oscillation in the circuit, it acts as a pulse-to-pulse integrator. By integrating the charge associated with each received pulse, it generates an output signal that is a replica of the input signal applied to the overall Stage 3 circuit.

14.5.4.1 Circuits for conveying monopolar (primarily luminance) signals

[xxx see previous figure and discussion]

14.5.4.2 Circuits for conveying bipolar (primarily chrominance) signals

[xxx see previous figure and discussion]

14.5.4.3 Signals recovered from the projection circuits

Figure 14.6.4-4 illustrates three alternate signal decoding circuits that have been identified within the neural system.. They can be considered prototypical of more complex decoding circuits. While they are shown connected to a single synapse at upper left, this is only for illustrative convenience. A specific signaling channel may use any one or more of the prototypical circuits. The circuits vary in three respects. Different electrostenolytic supply potentials may be supplied to the different terminals of the Activa. The various complex impedances may exhibit different time constants. Finally, the internal impedances of the Activa may be different (controlled primarily by their physical size).

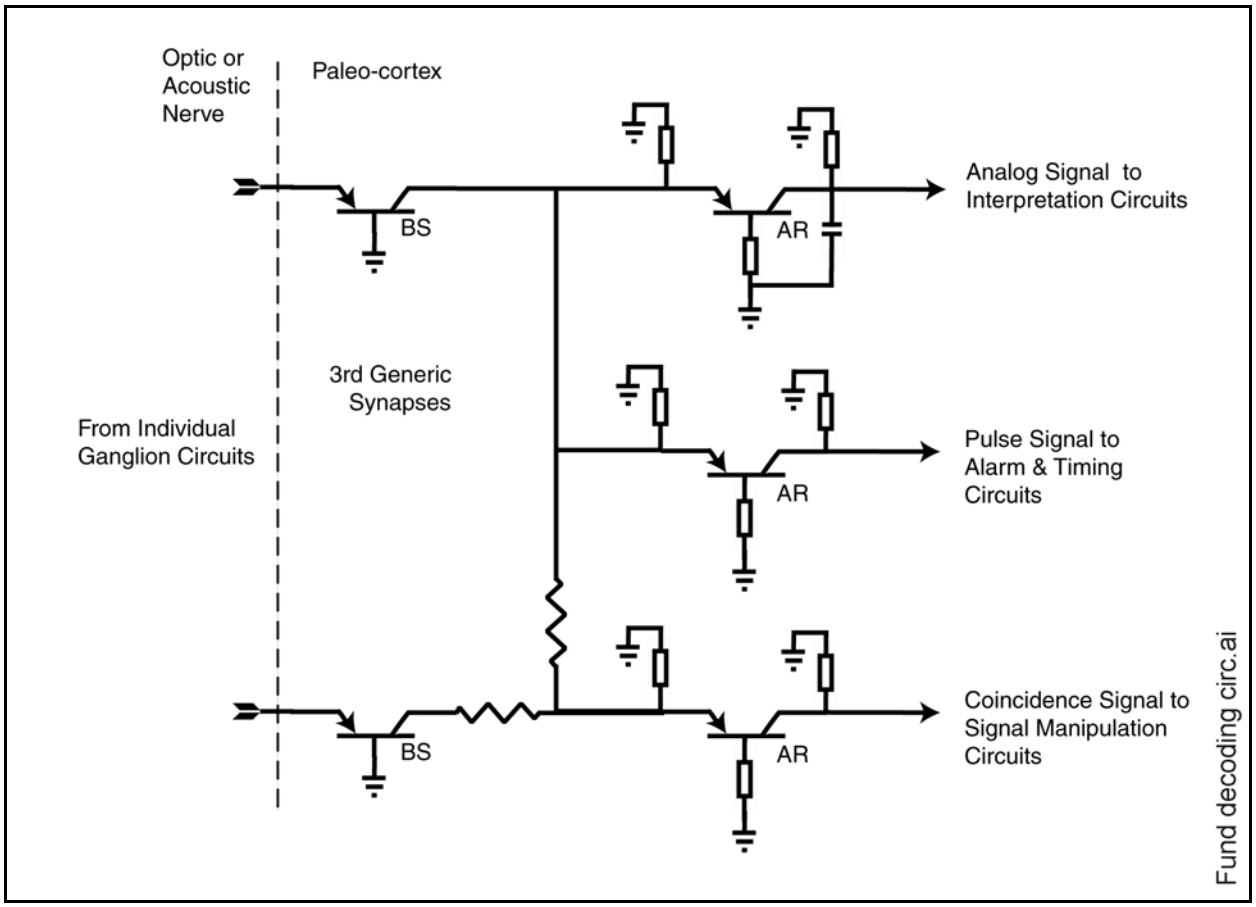

Figure 14.6.4-4 Alternate signal recovery circuits of Stage 3 signal projection channels. The rectangles consist of both RC circuits and electrostenolytic potential sources. The individual circuits (connexuses) vary in their input circuit biases and their output circuit time constants. The resistive elements shown may be incorporated in the output impedance of the synapse circuits. See text.

When used in summation channels, the upper stellate circuit has an input circuit bias that is near cutoff. It draws little or no current through the collector circuits in the absence of an action potential received via the synapse. It produces a pulse of current into its collector circuit upon receipt of each action potential via the synapse. The upper stellate cell has a long time constant collector circuit that integrates the pulse train as in the earlier example and provides a recovered analog equivalent to the original monopolar signal (typically the brightness of a scene element or the loudness of a narrowband aural frequency stimulus). This signal is passed to the interpretative and perceptual signal processing circuits of Stage 4. When used in the differencing channels, the upper stellate circuit has an input circuit bias that is also near cutoff. It operates very similarly to the summation channel but operates at a slightly different quiescent output potential in the absence of any input action potentials (an unreal situation normally). This places the quiescent output potential at the desired value in the presence of a continuous unmodulated action potential stream at its input and generates a bipolar output potential that emulates the original modulating signal.

The middle stellate cell is also biased so that its average collector current is very low. It has a shorter time constant collector circuit that does not integrate the signal. It passes the original pulse train along to subsequent circuits concerned with the timing of the leading edge of the luminance or loudness variation (and possibly their rate of change). This information is most useful to the alarm and timing circuits of Stage 4.

The lower stellate circuit is used to detect the time coincidence between two input signals. The input circuit is biased so that it will not produce any current in the collector circuit if only one action potential is received at its

input at a given time. However, if two action potentials are received simultaneously, their summed voltage will be sufficient cause a pulse of current to appear in the collector circuit. If the collector circuit exhibits a short time constant, the output signal will be a pulse having similar characteristics to the original action potentials. This appears to be the type of circuit used successfully in the source location circuits of the auditory system. It may also be used within the LGN of the visual system where the temporal coherence of the visual signals plays an important role.

14.5.4.4 Commissure circuits EDIT

[xxx edit]
As suggested in the introduction to this Chapter, the discussion of Stage 3 circuits can be applied equally well to any signaling tracts that are used to project analog information from one CNS engine to another more than 2 mm distant. Historically, the commissure have been defined histologically based on their appearance as matter, without regard to their functional importance. The "white matter" consists of the myelinated axons of stage 3 propagation neurons. The structureless myelination at the molecular level contributes to the scattering of all wavelengths of visible light, which results in their white appearance. Chapter 5 of the recent text by Williams et al. provides considerable new material with regard to the structure of the human brain[59].

As in the current brief Wikipedia description, the commissure have been described as fibers, implying a single neuron chain rather than as a group of fibers ala the label nerve used outside of the CNS.

In another *archaic* description based on histology rather than function,

> "The commissural fibers or transverse fibers are coherent white-matter structures that connect the two hemispheres of the brain. In contrast to commissural fibers, association fibers connect regions within the same hemisphere of the brain, and projection fibers connect each region to other parts of the brain or to the spinal cord. The commissural fibers include:
> • the transverse fibers of the corpus callosum
> •the anterior commissure
> •the posterior commissure
> •the lyra or hippocampal commissure."

This listing is unspecific and incomplete. Each of the tracts annotated are histologically described as commissure, even those also labeled as forming the corpus callosum. The coronal radiation from the thalamus and the tracts within the internal capsule (the thalamus) are not included.

[59]Williams, (Xxx) The Human Brain. [xxx found while searching Wikipedia related to marijuana]

This work will make a different interpretation based on the functional role of the fibers and fiber bundles within the CNS, and based on the recent provision of vivd images of the actual neural paths within the brain based on diffusion MRI techniques by Van Weeden and others, **Figure 14.6.4-5**. As described in an abstract by Weeden and associates[60], "Recent studies with diffusion MRI have shown new aspects of geometric order in the brain, including complex path coherence within the cerebral cortex, and organization of cerebral white matter and connectivity across multiple scales. The main assumption of these studies is that water molecules diffuse along myelin~sheaths of neuron axons in the white matter and thus the anisotropy of their diffusion tensor observed by MRI can provide information about the direction of the axons connecting different parts of the brain."

The investigations using this technique are being described as tractography[61]. "magnetic resonance imaging ("MRI") methods, such as diffusion MRI, have been developed to map major fiber pathways in a single brain. Diffusion MRI now affords a means by which to map the connectional anatomy of a single brain in its entirety." Such maps are becoming known as connectomes.

It will define the commissure as any fiber *bundle* within the CNS and equivalent to nerves (bundles of neurons as opposed to single neurons) within the PNS. In both cases, the nerves and commissure consist of bundles of nerves that are all myelinated.

Within the CNS, the vast majority of the white matter will be considered commissure (based on their function as myelinated stage 3 signal propagation neurons). Such commissure can be described as transverse commissure or longitudinal commissure.

The transverse commissure include:
•the major transverse commissure known as the corpus callusum
and the minor transverse commissure which includes;
- the anterior commissure,
- the posterior commissure,
- the lyra or hippocampal commissure and
- the commissure of the internal capsule (the thalamus).

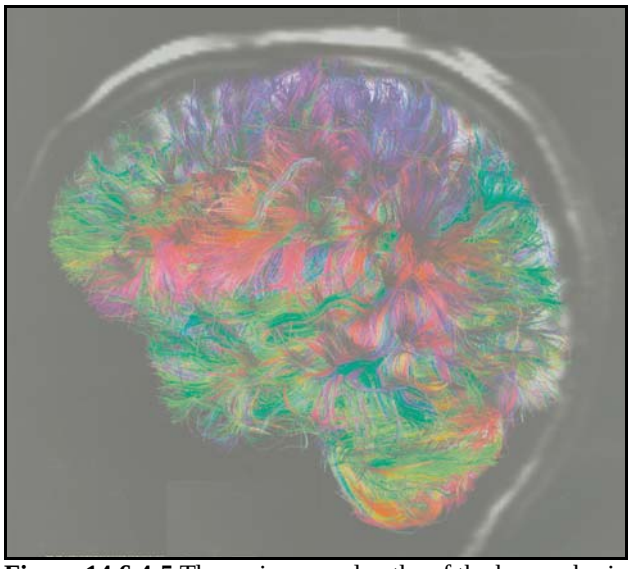

Figure 14.6.4-5 The major neural paths of the human brain based on diffusion MRI imaging technology. The image has been colorized to accentuate some of the paths to different cytoarchitectonic locations. See text. From Weeden, 2013.

The longitudinal commissure include:
- [xxx various paths within the CNS after initial processing of the sensory modalities by one engine or another.

The thalmo-cortical radiation is not well described using the terms transverse and longitudinal since the neurons and commissure from the thalamus radiate out to the cortex from a central location.

There is a technical difference involving how they are myelinated. The neurons in the nerve bundles are typically myelinated by individual glial cells (Schwann cells) associated with each neuron and extending over a significant length of the nerve. The neurons in the commissure bundles within the CNS are typically myelinated by sharing one glial cell (an astrocyte or oligodendroglia) among the neurons within a short section of the commissure. **Figure 14.6.4-6** illustrates these differences.

---

[60]Levy, A. Cwilich, G. Buldyrev, S. & Weeden, V. (2012) Modeling fluid diffusion in cerebral white matter with random walks in complex environments Abstract: Q41.00007 : APS March Meeting vol 57(1)

[61]Weeden, V. (2013) Systems and methods for improved tractographic processing US Patent Application 13/635,575

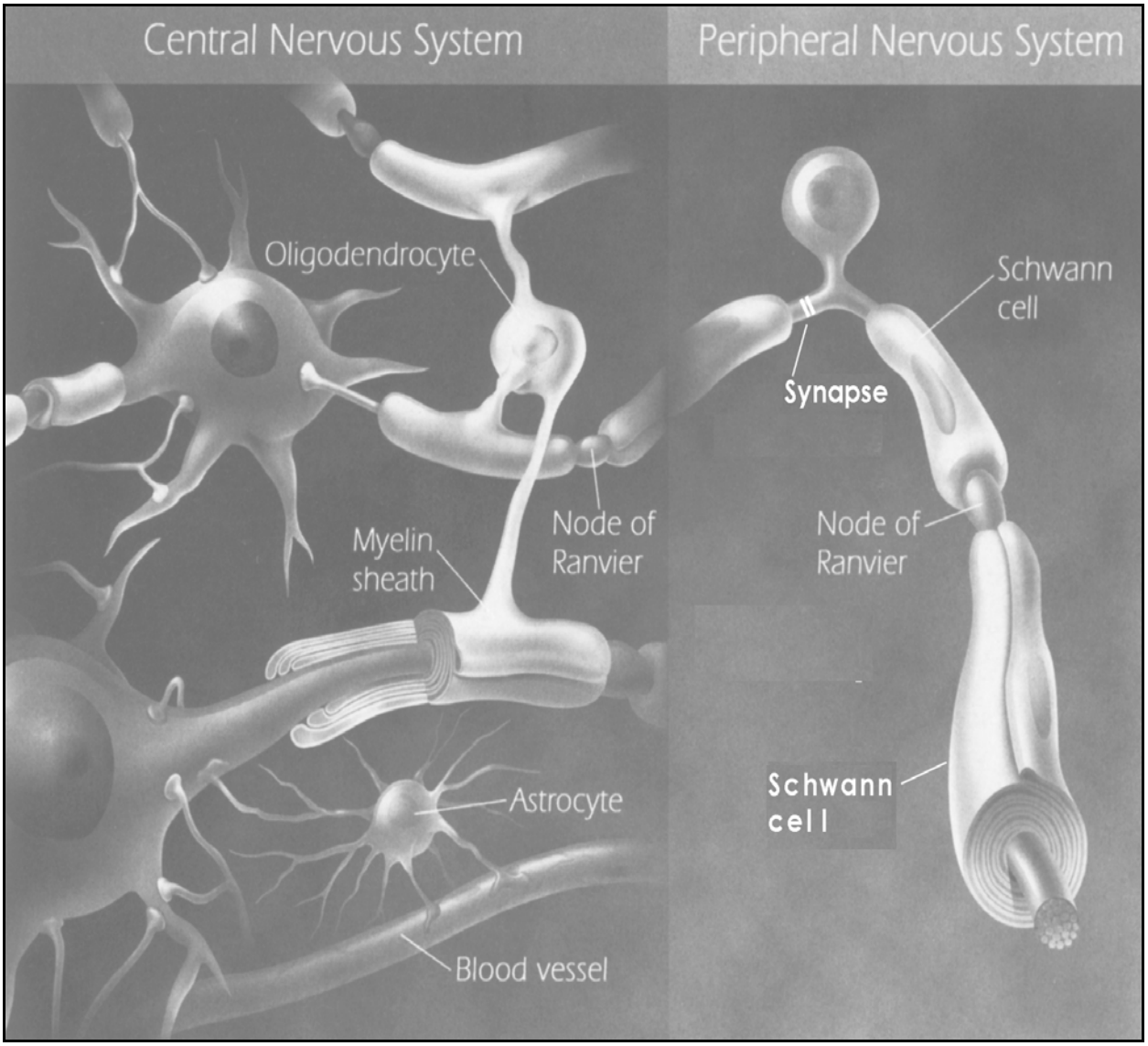

Figure 14.6.4-6 Difference in myelination between neurons of the commissure of the CNS and nerves ADD of the PNS. The artwork is of excellent quality. However, the contacts shown between the astrocyte and both the blood vessel and the neuron suggests an inadequate communication between the artist and the neuroscientist. It is probable that the structure labeled "astroctye" is actually another neuron. The demarcation between the CNS and PNS is clearly illustrative. It is suggested that the three axons within the CNS and served by one oligodendrocyte constitute all or part of one commissure. The one neuron shown within the PNS may or may not be grouped within a "nerve." See text. From Fields, 2010.

This work considers the signal paths from the eyes, ears and nose to be nerves rather than commissure because they are not integral *within* the confines of the CNS (within the blood-brain-barrier) when the brain is inflated and presented as a single contiguous sheet of neural tissue. The means of myelination appear to support this description of the nerves and commissure supporting the sensory modalities (see **Section xxx** in "The Neuron and Neural System" showing the myelination means).

The optic nerve is an example of a nerve exterior to the CNS whereas Meyer's Loops are fundamentally longitudinal

commissure between engines within the CNS. The optic nerve is fundamentally unidirectional. Most of the sensory modalities exhibit stage 2 signal processing engines prior to the transfer of the signals to the stage 3A signal encoding and projection engines, neurons and nerves for delivery to the stage 3B decoding engines and stage 4 information extraction engines of the CNS.

14.5.4.4.1 Commissure histograms EMPTY

A histogram of the number of individual neuron axons in a given commissure would contribute significantly to the understanding of stage 3 signal propagation within the CNS. The data for small commissure would be particularly useful. To date, such data has not appeared.

14.5.4.5 Other efferent neural circuits

As suggested in the introduction to this Chapter, the discussion of Stage 3 circuits can be applied equally well to any efferent circuits that are used to project analog information from an engine of the CNS to any terminus of the PNS located more than 2 mm distant. XXX needs words.

14.5.5 Transfer functions for Stage 3 Circuits

Figure 14.6.5-1 describes the nominal transfer functions of both a ganglion neuron (configured for relaxation oscillation) and a stellate neuron of Stage 3. For the correct choice of biasing potentials within the stellate recovery circuit, the recovered waveform can have the same DC and AC potentials as the original signal. If the input signal is of very high amplitude, the quality of the recovered signal can be degraded. For very large amplitude signals, the recovered signal will be distorted at low frequencies by the low action potential discharge rate. This low rate will restrict the low frequency response in the recovered signal. Since the discharge rate is asynchronous with respect to the input signal, the output will be distorted in a statistically non-stationary manner.

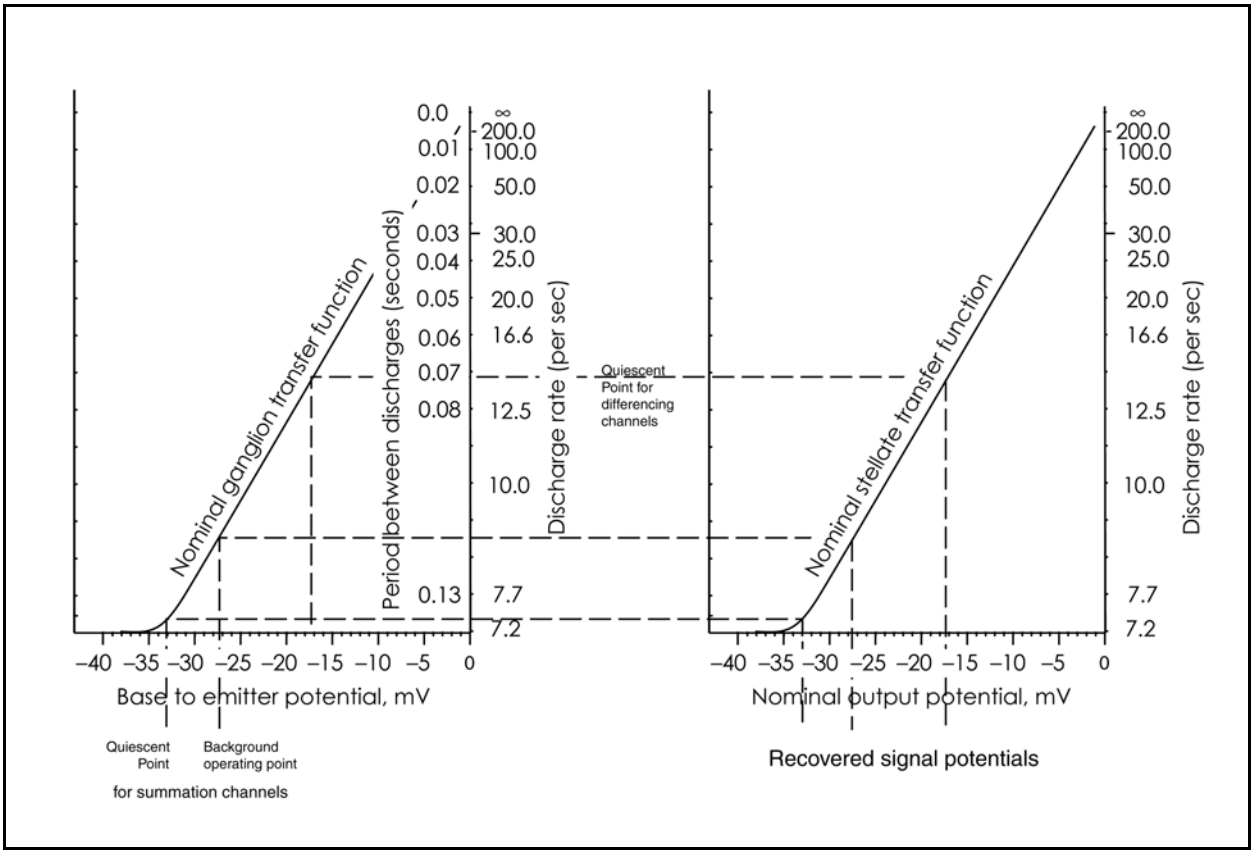

Figure 14.6.5-1 The nominal transfer function of Stage 3 ganglion & stellate neurons ADD. By proper biasing of the stellate neuron, the output signal has the same DC and AC properties as the input signal (for frequency components at least three times the minimum discharge rate encountered). By proper biasing of the ganglion neuron, either monopolar (summation) or bipolar (differencing) signals can be processed efficiently.

14.6 Performance of Stage 3 circuits

The available literature on the operation of the signal projection circuits is sparse. Most of the available data on Stage 3 circuit performance is based on stimulation of the complete visual system by light and the recording of a phasic signal stream at an arbitrary convenient location depending on the species examined. The analysis of the resulting waveforms can be complicated because of the many circuits and circuit variables involved in such an experiment. Experiments with Limulus have been particularly attractive because of the primitive nature of the overall visual system in this species. In Limulus, the signal processing and signal encoding functions associated with Stage 2 and Stage 3 appear to be merged and performed by a single "eccentric cell." This cell is located within the cartridge of the ommatidium and receives signals from one or more photoreceptor cells. Many of the experiments have not been sufficiently controlled to be completely clear about the interconnection(s) between the photoreceptor cells and the eccentric cell.

This section will describe several potential operating modes for the signal projection circuits and then compare the predicted modes with the experimental literature. In most cases, the predicted performance must include the predicted performance of the Stage 1 and Stage 2 circuits of the visual system combined with the Stage 3 circuits.

The performance of the generic Stage 3 circuit can be predicted based on [**Figure 14.5.4-2**]. The performance is most easily presented by discussing the individual waveforms found at each of the probe points described by the circled symbols. For the purposes of this section, the waveform presented to the input of stage 3 will be considered a true generator waveform as found at the pedicle of an individual photoreceptor. This assumption avoids any

complications due to the summing and differencing functions of, and any distortion introduced by, the circuits of stage 2.

It should be mentioned that many of the ganglion cells associated with the foveola and in the feature extraction engines of the cortex are used to generate a single action potential. The time of occurrence of this action potential is highly significant when compared to the similar signals in parallel signaling channels. It may constitute one dot in a binary retinotopic map or it may represente one bit in a “machine language” vector within the cortex.

The predicted performance of the generic stage 3 circuit compares favorably with the measured performance as indicated in **Section 14.6.3**. **Section 14.6.4** will expand the predicted performance to account for a variety of asymmetries found in human vision.

Fuortes[62] and Frank & Fuortes[63] have provided good data on Limulus. Barlow & Levick have provided some interesting data for the cat[64,65]. Their data must be examined carefully because design of the overall experiment was quite complex. Some of the data applies to luminance channels and some to chrominance channels. Their on-center data generally applies to luminance channels while their off-center data generally applies to chrominance channels. When speaking of off-center signals, they are really describing on-center signals that are applied to the inverting terminal of a lateral cell prior to being passed to a ganglion cell of Stage 3. Care must be taken to differentiate between foveola signals and peripheral signals in their data. In some cases, their peak pulse frequencies are lower than the normally accepted maximum values. However, the range of their rates, 70 pulses per second (pps) max and 1 pps minimum, appear representative.

Some of the best available data appears to be from Purple & Dodge[66]. The design of their experiment was much simpler than in the above case.

14.6.1 Predicted performance of the individual circuits

The theoretical performance of the generic stage 3 circuit is best described by first describing the waveforms found at each point in the circuit as the result of application of a simple generator waveform at the input. In some cases, it is important to consider both the impulse and the pulse response of the circuit.

For the reader not familiar with electronics, it may be easier to review **Section 14.6.1.3** before reviewing the following paragraphs. The operation of the Node of Ranvier is simpler than that of the basic ganglion cells.

14.6.1.1 The Lead-lag network of the ganglion circuit

The waveform at location E' in [**Figure 14.5.4-2**] represents the output of the lead-lag network acting as a pre-emphasis circuit in the generic stage 3 circuit. The input to this circuit is represented by the input from Stage 2, nominally labeled E in this work. The waveform may take on the characteristics of a monopulse waveform associated with the luminance channel and be labeled E1. Alternately, it can be bipolar and be labeled E2, E3, or E4 when associated with the chrominace, polarization or appearance channels. The nominal performance of this circuit is illustrated in **Figure 14.7.1-1**. The upper frame illustrates the fact that the output of the circuit consists of a copy of the input added to a pedestal equal to a percentage of the slope of th waveform. As the slope of the input waveform increases, the output waveform becomes higher and steeper. For a given voltage at the output (as frequently introduced by a thresholding circuit), the equivalent input signal level is a function of the derivative of the input signal itself. This feature is a key to understanding the operation of many monopolar ganglion circuits because the input usually measured in the laboratory is either at the axoplasm of the previous neuron or at an earlier point in

---

[62]Fuortes, M. (1959) Initiation of impulses in visual cells of Limulus. *J. Physiol*. Vol. 48, pp 14-28

[63]Frank & Fuortes (1956) Xxx

[64]Barlow, H. & Levick, W. (1969) Three factors limiting the reliable detection of light by retinal ganglion cells of the cat. *J. Physiol*. vol. 200, pp 1-24

[65]Barlow, H. & Levick, W. (1969) Changes in the maintained discharge with adaptation level in the cat retina. *J. Physiol.* vol. 202, pp 699-718

[66]Purple, R. & Dodge, F. (1965) Interaction of excitation and inhibition in the eccentric cell in the eye of Limulus. Cold Spring Harbor, NY: Cold Spring Harbor Symp. Quant. Biol. vol. 30, pp 529-537

the signal chain.

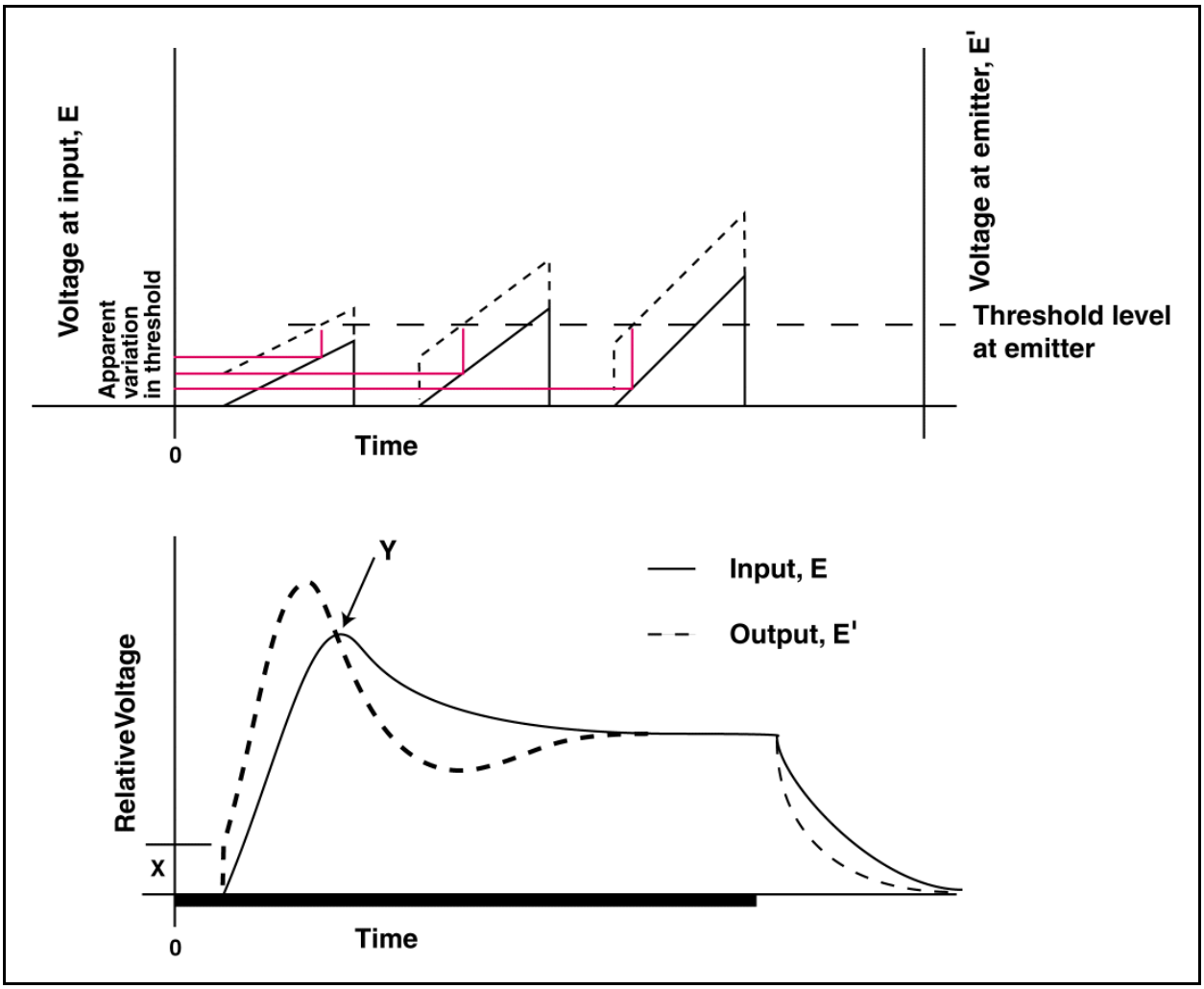

Figure 14.7.1-1 Conceptual and nominal performance of a lead-lag network. Upper frame shows the input (E, solid line) and output (E', dashed line) for a series of triangular pulses. For a given threshold at the output terminal of the network, there appears to be a variable threshold at the input terminal. Lower frame shows the dynamic performance of the network with a generator potential as the input (solid line). The solid bar represents the photon input stimulus creating the generator waveform. The output exhibits an initial pedestal, x, and rises faster than the input to a peak that occurs before the peak in the input waveform. If the rolloff in the original signal is significant, the voltage of the output waveform will become smaller than that of the input for a short period. Following termination of the stimulus, the output waveform will fall more rapidly than the generator waveform.

The dynamic character of the output signal compared to the input signal is illustrated in the lower frame. The output signal rises very quickly to the height of the pedestal, x, due to the differentiation process and then rises to an earlier peak than the input signal before beginning to decrease. At the point where the derivative of the input signal is zero, the two waveforms have the same value, Y. Following this value, the performance depends on whether the input exhibits a rolloff following the peak. If it does, the output will fall below the nominal value of the rolloff for an interval. Following termination of the stimulus creating the generator waveform, the output will decrease faster than the input as shown. These features are prominent in many recordings in the literature. They will be highlighted in the performance section to follow.

14.6.1.1.1 Background

[**Figure 14.6.1-1**] describes the operation of a lead-lag network with values chosen to provide a pre-emphasis function. A pre-emphasis circuit is designed to provide an output that consists of a true copy of the input signal plus a percentage of the derivative of the original signal. Using a triangular input waveform makes it easy to envision the output. Note how the amplitude of the output exceeds the input in Frame A by a constant voltage determined by the slope of the input waveform. Frame B predicts the output of such a circuit when excited by a pulse input. Note how the leading edge of the output of this circuit rises faster than, and peaks earlier than, the input waveform for the example shown. Note also how the trailing edge (following the cessation of stimulation) falls off faster than the input waveform. If the generator waveform applied to the input exhibits a falloff following the initial peak, note how the output falls **below** the nominal plateau amplitude of the pulse response. This feature is diagnostic for a pre-emphasis network.

Note point X in the figure. At this point, the input and output waveforms have the same amplitude because the slope (derivative) of the input waveform is zero. Note also that the steaper the rise in the leading edge of the input waveform, the farther to the left the peak in the output waveform occurs relative to the peak in the input waveform.

For more complex input signals, the output signal is difficult to describe except graphically.

14.6.1.2 The ganglion circuit as a driven monopulse oscillator

The literature has long focused on the concept that the axonal membrane of a neuron exhibited active behavior. It responded by producing an output that was significantly different from the input excitation. This concept has been supported by the early in-vitro experiments of Hodgkin, Huxley & Katz at the circuit level. Their work is reviewed in **Section 10.8.4.2**. There has been no verification of such behavior by a membrane in isolation, or explanation of how such an output is achieved after many years. This work employs an entirely different concept. This concept proposes that the active mechanism is the same as in man-made transistors and involves an equivalent biological device, the Activa. The Activa within a neuron is formed by the confluence of the dendritic, poditic and axonal tissue of the neuron. The Activa exhibits all of the characteristics of a man-made transistor as discussed in **Chapter 8**. Such a device can obviously be caused to oscillate, a fundamentally nonlinear phenomenon. The operation and structure of the ganglion cell as an oscillator is discussed in detail in **Chapter 9**.

To explain the operation of the ganglion cell (and any other circuit generating action potentials), the mechanisms involved require the cell be complete to insure its vitality. Removing of the dendrites (as in the work of Hodgkin, Huxley & Katz) is unacceptable.

Because of the small size of the individual dendrite structures, it is very difficult to penetrate them with a physical probe. An alternative is to penetrate the dendrolemma where it is within the volume of the soma. It is also possible to penetrate the podolemma in this region. It is important to be sure which lemma is penetrated in discussing the operation of cell producing action potentials.

Because of the electrical similarity of the axon and the dendrite, it is possible to interchange these elements and still form an Activa. Such an Activa is morphologically named a synapse (and more specifically a gap junction). The capability of electrolytically connecting a dendrite to an axon and an axon to a dendrite accounts for the ability to cascade neurons within the neural system. This similarity also leads to a structure called the axon segment that exhibits the electrical properties common to both a dendrite and an axon. By introducing the axon segment, it is possible to create a structure that can be replicated. This is the combination of a Node of Ranvier and an axon segment. The Node of Ranvier is a hybrid Activa circuit. It looks much like a gap junction under the electron microscope. However, it is found within a single structure known historically as the axon of a neuron. Replication of the Node of Ranvier and axon segment allows a single morphological neuron to grow to any desired length. The structure and operation of the Node of Ranvier is discussed in **Section 9.3**.

While there are many forms of electronic oscillators, at least two of these forms appear in biological (electrolytic) circuits. These are the driven monopulse oscillator and the driven free-running oscillator. In both cases, the basic circuit is that of a regenerative amplifier. In the first case, the circuit is biased so as to only individual pulses (action pulses) when the stimulus exceeds a threshold level. In the second case, the circuit oscillates continuously but the character of those oscillations changes in response to the stimulus.

The first case is commonly associated with the luminance channel of the visual system. There appears to be a close association of this type of oscillator with the morphologically designated parasol ganglion cell. The second type is generally associated with the chrominance, polarization and appearance channels of the visual system. These

oscillators appear to correlate well with the morphological designation, midget ganglion cells.

While the ganglion cells usually receive their excitation from neurons of Stage 2, there are evolutionary forms such as *Limulus* where the ganglion cells (morphologically labeled eccentric cells) appear to receive their stimulation from the photoreceptor cells of Stage 1. The eccentric cell is discussed in **Section 14.6.3.2**.

A fact not recognized in earlier work is that the electrical waveforms present in the dendroplasm, podoplasm and axoplasms are fundamentally different. While they contain some similar features, they exhibit different responses as a function of time. When recording waveforms from a ganglion cell, it is important to be topologically specific as to which plasma the probe contacted. When the probe is extracellular (in the INM), this fact should be carefully noted. Such a probe can sense a variety of waveforms through capacitive coupling in addition to sensing the local potential of the INM.

14.6.1.2.1 Routine operation of the driven monopulse oscillator

The operation of the driven monopulse oscillator is described in detail in **Section 9.3**. This type of oscillator is normally associated with the name pyramid ganglion cell. An important fact is that the operation of the circuit is not dependent on the potential of the emitter with respect to the INM. Nor is it dependent on the potential between the base and the INM. It is dependent on the potential between the emitter and the base. The emitter to INM potential is defied as E' and it is described in the previous figure. A probe of the dendroplasm may show some signs of action potentials on this waveform because of capacitive pickup. The more important waveform is Ep, the base potential, or the podoplasm potential. This potential is caused by the sum of the currents flowing within the Activa, the emitter current and the collector current. A typical base to INM potential is shown in **Figure 14.7.1-2** for a driven monopulse oscillator responding to a generator waveform, E. The analog portion of the waveform is a copy of the pre-emphasized signal, E'. It is smaller in absolute amplitude than the instantaneous emitter to INM potential. No action potentials are generated in the absence of a finite potential at E. When the emitter to base potential reaches the circuit threshold, the circuit goes into monopulse oscillation and the first action potential is created. The circuit exhibits a refractory period following the pulse that is proportional to the instantaneous emitter to base potential (in the absence of the oscillation). Thus, the period between pulses is proportional to the excitation. As the signal amplitude goes up, the pulses become closer together, and vice versa.

> While it is common to speak of the frequency of a pulse train, note that a frequency cannot be associated with one pulse and the concept is strained when speaking of two pulses. It can only be associated with three pulses if they are equally spaced, etc. In vision, the pulse train of action potentials only exhibits a constant frequency when the oscillator is free-running and not being modulated by an input signal. Under all other conditions, the pulse stream exhibits an instantaneous variation that is characteristic of a phase modulated carrier.

This composite waveform is the waveform usually reported after penetrating the soma of a ganglion or eccentric cell. The precise amplitude of the pulses compared to the analog waveform is determined by the specific parameters of the oscillator circuit, particularly the collector to base saturation voltage. This saturation potential introduces a maximum amplitude in the base to INM waveform and determines the maximum amplitude of the action potentials found in the axoplasm of the cell.

The pulses shown in the above figure are negative scaled copies of the action potentials that can be measured by penetrating the axoplasm of the ganglion (or eccentric) cell. They exhibit an essentially constant amplitude relative to the resting potential of the collector terminal of the circuit. The action potentials are positive going pulses originating at the quiescent axon potential (typically between 144 and 152 mV depending on location of the reference potential). The amplitude of these pulses is nominally 100 mV depending on the collector to base saturation potential of the oscillator circuit. The action potentials do not

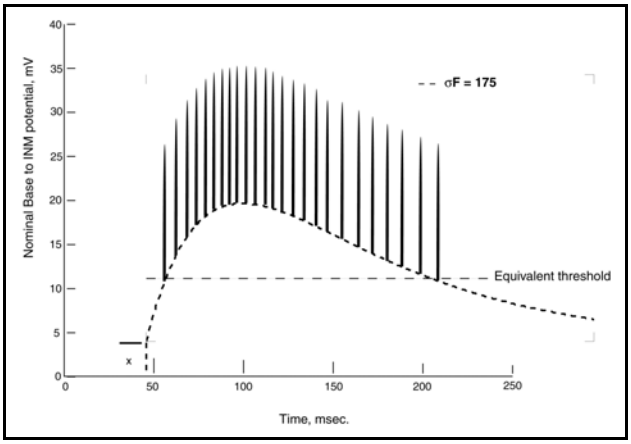

Figure 14.7.1-2 The potential at the base of a driven monopulse oscillator (pyramid type ganglion cell). The potentials shown are negative. Note vertical offset, x, in the analog portion of the waveform (dashed) due to the pre-emphasis network. Note how the spacing between the pulses varies with analog signal amplitude. The threshold level is a reflection of the emitter to base threshold.

become positive with respect to the INM as frequently suggested in the literature. These suggestions frequently rely on the assumption that the resting potential of the axon is near -70 mV. This is not correct for a ganglion or other oscillatory cell.

14.6.1.2.2 Routine operation of the driven free-running pulse oscillator

The driven free-running oscillator operates very similarly to the driven monopulse oscillator except it is normally biased to produce action potentials continuously. As in the above case, it is difficult to probe the dendroplasm of such a cell. However, the emitter potential, E' is similar to that for the driven monopulse oscillator. Also as above, the base potential (the podoplasm potential) is easier to obtain by probing. In the nominal case, the spacing between the pulses, in the absence of an input signal, is 33 msec. In pathological cases, this value varies. The variation is a major source of color vision abnormalities in humans (See discussion of Lakowski's work in **Section 18.1.5**).

Figure 14.7.1-3 illustrates the nominal podoplasm potential of a driven free-running pulse oscillator for a positive going input signal. The resulting waveform at the base is negative going relative to the INM. This is the condition normally defined in the experimental literature as an on-center waveform. This designation is usually inappropriate because xxx

The potential at the collector of the oscillator (at the axoplasm a), which may be contacted with a probe near the extreme of the hillock, is similar to the above waveform. However, it will be positive going starting from a resting potential near -152 mV. The ratio between the amplitudes of the analog and pulse components may be different.

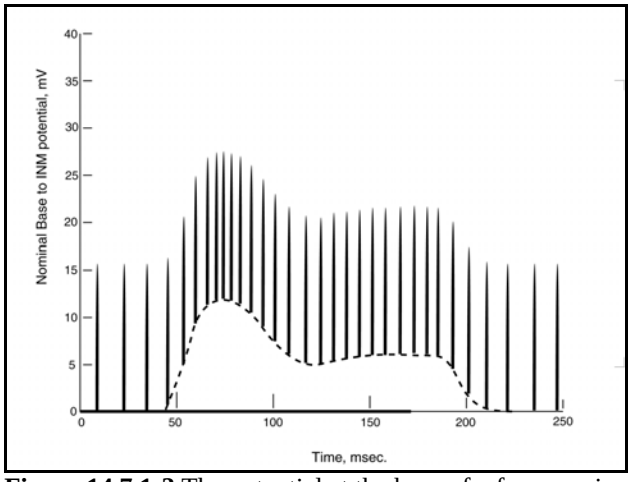

Figure 14.7.1-3 The potential at the base of a free-running monopulse oscillator (midget type ganglion cell). Only every fourth pulse is shown for clarity. The pulse train shown is for an "on-" type drive signal.

Figure 14.7.1-4 illustrates the output of a similar driven monopulse oscillator when the net signal applied between the emitter and the base is negative going relative to the quiescent condition. The quiescent value of the analog waveform at the base is still negative relative to the INM. However, the analog portion is positive relative to the quiescent level. The pulses remain negative going relative to the INM.

In the case of the driven monopulse oscillator, a negative going signal may be applied to the circuit in a variety of way depending on the signal path prior to the oscillator circuit. These options will be discussed below.

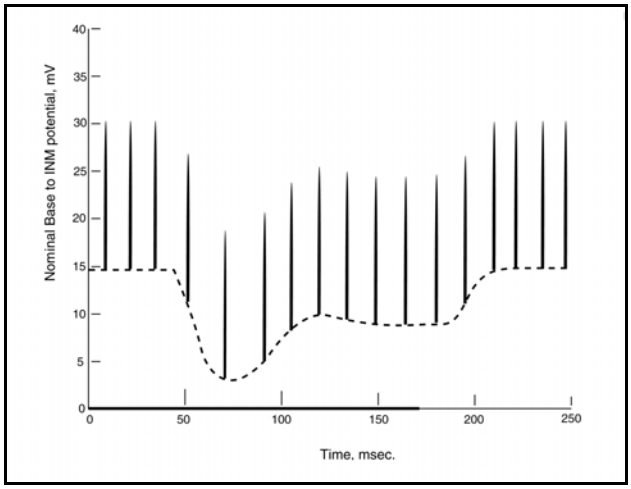

Figure 14.7.1-4 The waveform at the base terminal of a driven monopulse oscillator of the an "off-" type. The "off-" designation describes the polarity of the input stimulus. The vertical scale is negative going. The heavy bar at the horizontal axis denotes the photon excitation applied to the signal chain.

14.6.1.2.3 Nominal pulse intervals and frequencies

Figure 14.7.1-5 illustrates the range of pulse to pulse intervals, and equivalent instantaneous pulse frequencies obtainable from an action potential generator of the types described above. If a driven monopulse oscillator is operated at the bias labeled **B**, It will exhibit an infinitely long interval between output pulses in the absence of an input signal. For a positive going input signal, it will produce pulses at a pulse interval determined by the amplitude of that signal. If the circuit is biased to point **A**, the circuit will not respond until the input has reached the threshold labeled **B**. It will then generate pulses with a pulse interval determined by the signal amplitude above **B**. If biased at point **C**, the circuit will accept a bipolar input signal. Under quiescent conditions, it will generate a continuous series of pulses with an interval of 0.033 seconds. Upon excitation, it will change the pulse interval in response to the amplitude and polarity of the signal relative to the quiescent value. If biased too far from **C**, the circuit will not respond symmetrically with respect to the input signal. This will cause an offset, and is likely to also cause a distortion, in the recovered signal.

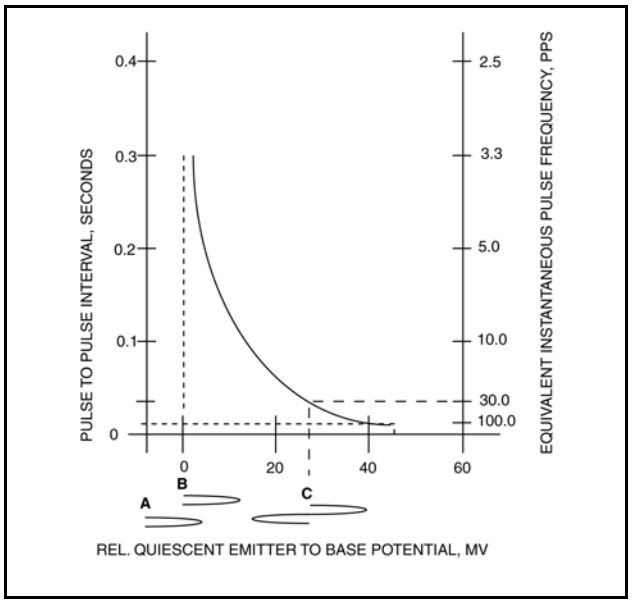

Figure 14.7.1-5 The output pulse environment of an action pulse generator. A generator with a bias at B exhibits no threshold for a monopolar input signal. If biased at A, it will exhibit a threshold to a monopolar input. If biased at C, it will accept a bipolar input signal.

14.6.1.2.4 Reported pulse intervals and frequencies

Figure 14.7.1-6 reproduces the lower portion of Figure 3 of a 1992 paper by van Essen, Anderson &

Felleman[67]. The paper presents a discussion of the character of the M and P channels of the optic nerve that provides excellent support for the circuit configurations identified in this work. *However, they offer no citations for the figure that lacks scales.* They note, "The primary role of P cells is to encode information about luminance contrast. They respond to low and moderate temporal frequencies (mainly 1 to 20 Hz) over the full range of spatial frequencies visible at a given eccentricity (with citations). M cells are optimized for higher temporal frequencies (mainly 5 to 40 Hz), but they provide only about one-third the spatial resolution because of their lower sampling density. Thus, the P and M systems cover partially overlapping regions of the spatiotemporal information space in the figure (with citations)." Based on the alternate vertical scale, the P signal would correspond to the response to a monopolar, typically brightness, signal in the previous figure (labeled A). The M signal would correspond to the response to a bipolar, typically chrominance, signal in the figure labeled C.

They continue by discussing in words secondary functions of the P and M cells without benefit of any circuit diagrams. The P cells actually encode the brightness contrast (the R–channel of this work) following normalization of the luminance stimulation level by the adaptation amplifiers and chromophores of the stage 1 sensory neurons.

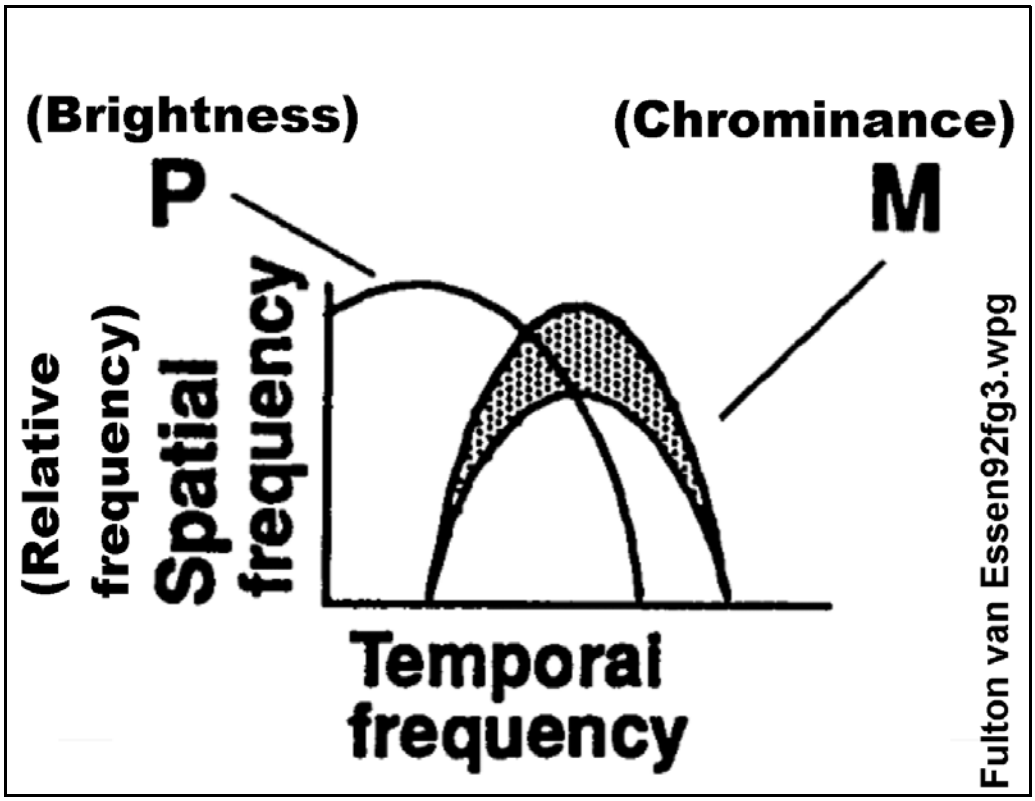

Figure 14.7.1-6 Histogram (spectrogram) of the P (brightness) and M (chrominance) channels of the optic nerve in monkey. The label "spatial frequency" appears to be extraneous. The vertical axis can be relabeled, relative frequency. See text. From van Essen et al. 1992.

The term spatial frequency is not defined in their text, nor is the location in the visual modality where the figure applies. As a general rule, the temporal frequency within the P and M channels is not related to the spatial frequency of stationary features within the image projected onto the retina. By rewording the label on the vertical scale to relative frequency of occurrence, the figure describes perfectly the spectral distributions of the stage 3 spectra of the pulse neurons delivering information from the ganglion cells of the retina to the LGN (**Section xxx**) within the biological visual system. It also exhibits the same spectral distributions (brightness and chrominance) to different

[67]Van Essen, D. Anderson, C. & Felleman, D. (jan 1992) Information processing in the primate visual system: an integrated systems perspective *Science, New Series* vol 255(5043) pp 419-423

scales) as found in the compatible color TV system used throughout the world from 1950 to 2010 (with the arrival of digital television broadcasting). Their comments about non-linearities associated with these channels (and specifically the shading in the figure) are superficial and contribute to the unintended obfuscation found in the biological literature about how the visual modality works.

They confuse their analysis by introducing subchannels. Their P-B channel focuses on spectral information while their P-I is focused on spatial information although they note, "But other types of information are multiplexed into these streams as well." These conceptual subchannels are the result of experimental extrapolations without the benefit of a circuit diagram. The P or parvocellular channel is fundamentally the summation of the spectral channels of the sensory neurons and equivalent to the R-channel of this work. It obviously includes spectral information. In fact, it contains virtually all of the information in the visual scene except color-difference information incorporated into the M channel. The M channel can be subdivided into the three color difference channels of this work; O–, P– & Q– .

The encoding within stage 3 involves logarithmic terms and the appropriate scales for the figure are logarithmic. In the absence of color information (monochromatic stimulation at either 494 or 572 nm) the M channel signals collapse to a nominal carrier frequency of 30 pulses per second. [This section is also found in **Section 15.6.7.3** of "The Neuron and Neural System: A 21st Century Paradigm" by this author[68].]

14.6.1.3 The Node or Ranvier as a driven monopulse oscillator

The operation of the Node of Ranvier as a regenerative oscillator is easiest to describe because it is not concerned with the analog characteristics of the input signal from the previous axon segment. Its performance is most easily correlated with the caricatures in the literature ostensibly describing the electrical performance of an excitable cell.

The detailed performance and waveforms of the Node of Ranvier are discussed in **Sections 10.4** & **10.8**. The expected waveforms are discussed beginning in **Section 108.2.6**.

14.6.1.3.1 The axon segment as a transmission line and filter

A comparison of the waveform predicted for location F2 versus that predicted for location F1 is instructive. The primary feature is the attenuation of the analog component of the waveform at F1 as the signal propagates along the axon segment beyond the hillock. In the actual circuit, it is very difficult to measure the potential waveform within the myelinated portion of the axon segment. The second most important feature is represented by the dispersion of the individual pulse waveforms as they travel along the axon segment. It is this signal dispersion that causes the loss in peak amplitude of the pulse (the total energy within the pulse remains essentially constant). The third feature is the relative delay in the pulse as it travels along the axon segment.

The axon segment is fundamentally a coaxial transmission line. Its characteristics are discussed in detail in **Section 10.3.4.1**. Such a line is represented by a filter consisting of a group of inductors in series that are shunted by a group of capacitors, one at the junction of each pair of inductors. In the case of the axon segment, the filter is largely loss free. However, it has a poor dispersion characteristic. As a result, the waveforms degenerate as they travel down the length of the segment as suggested by **Figure 14.7.1-7**.

[68]Fulton, J. (2012) The Neuron and Neural System: A 21st Century Paradigm. http://neuronresearch.net/neuron

14.6.1.3.2 The predicted waveforms at a Node of Ranvier

The purpose of a Node of Ranvier is to compensate for the loss of signal amplitude caused by the dispersion of the signal as it travels along an axon segment. It does this by acting as a driven monopulse oscillator. It generates a new action potential based on its circuit parameters in response to stimulation by a degraded action potential.

The input to the Node of Ranvier is essentially the waveform shown above at the end of the axon segment, F2. While the coupling between the axon segment and the emitter of the Node could include a lead-lag network, the cytology of the cell does not support such a circuit.

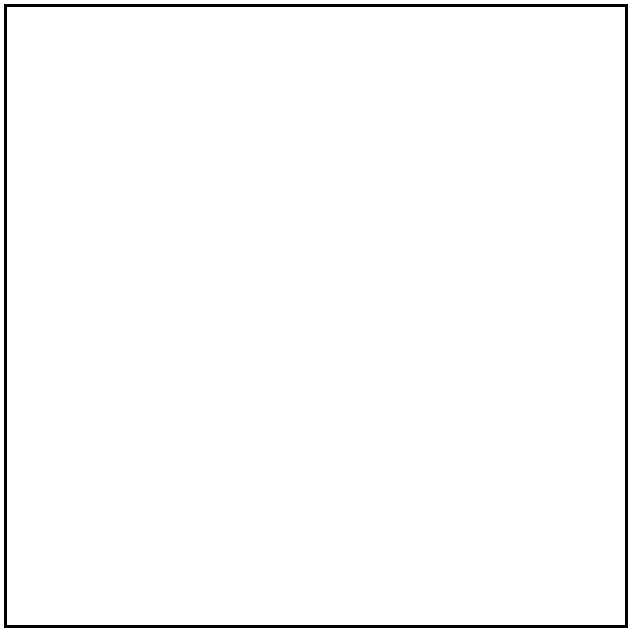

Figure 14.7.1-7 Caricature of a pulse traveling along an axon segment EMPTY.

Figure 14.7.1-8 shows the output waveform of the Node of Ranvier, F3, as it would appear to a probe in contact with the plasma in the post synaptic region of the following axon segment. This waveform does exhibit a small initial segment that represents the operation of the Activa as a linear amplifier prior to its transition into its nonlinear role as a pulse regenerator. The transition from this waveform to the action potential represents the amplified value of the threshold voltage at the input to the Activa of the Node. The voltage scale is positive going from the resting potential of the plasma (nominally a negative 144 mV relative to the surrounding INM). Note the asymmetry of these waveforms. The main action potential is the result of a switching function near the peak of the waveform. This is fundamentally different from the peak associated with a generator waveform of a photoreceptor cell which is continuous in this region.

The operation of the Node of Ranvier as a monopulse regenerator is discussed in detail in Chapter 9. xxx

14.6.1.3.3 The delay associated with the oscillator

The delay between the peak in the output of the Node of Ranvier, as well as the first oscillator in the ganglion cell, and when the input signal reaches the circuit threshold is relatively large. This delay is the primary delay controlling the apparent (or group) velocity associated with neural signaling. See **Section 9.3**.

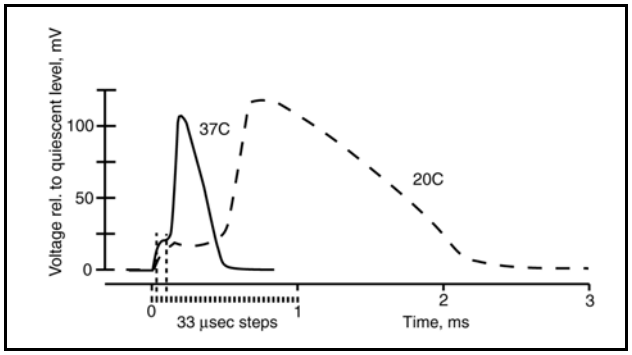

Figure 14.7.1-8 The action potential (collector waveform) at a Node of Ranvier of the rat. Shown at two different temperatures.

14.6.1.4 The waveforms at the pedicle of the ganglion cell

The waveform displayed at the pedicle of the ganglion cell , F4, is essentially the same whether the cell contains only a single long axon segment or multiple axon segments separated by multiple pulse regenerators (Nodes of Ranvier). This waveform is free of any analog component and consists of a series of action potentials with variable pulse-to-pulse spacing determined by the information being transmitted. The shape of the individual pulses is determined by the parameters of the last Node of Ranvier and may vary slightly due to the circuits parameters of the Node. In the absence of any nodes, the shape of the pulses is determined by the circuit parameters of the original oscillator circuit within the ganglion cell. Thus, the pulses may show slight differences. However, a discontinuity in the pulse waveform near its peak is frequently discernable (particularly when recording the waveform with an analog (still conventional) oscilloscope.

14.6.1.5 The waveforms at the pedicle of the stellate cell

Figure 14.7.1-9 shows the signals typically associated with the stellate cell. By varying the bias point associated with the circuit elements on the output side of its conexus, a variety of signals can be decoded. The output signals can be optimized for monopolar, bipolar or pulse operation.

[xxx The stellate cell can operate in close coordination with the orthodromic stage 4 signal processing neurons. To optimize this coordination, the stellate cell may act as an analog decoder or it can act as an event detector. In the later case, the output of the stellate cell may be a pulse that can be easily processed by a coincidence detector.

Konig et. al. have recently addressed the options available in stage 3 ganglion cells and other stage 4 signal

processing neurons without the availability of a detailed model[69]. Their work is necessarily abstract and attempts to draw conclusions from a series of simple psychophysical experiments. There thesis is intriguing. "Here, we argue that coincidence detection, rather than temporal integration, might be a prevalent operation mode of cortical neurons. We base our arguments on established biophysical properties of cortical neurons and on particular features of cortical dynamics." Their introduction suggests they only considered the operation of phasic neurons and performed little literary research before formulating their psychophysical concepts. They criticize their sources for suggesting that the cortical neural circuits operate on a time cycle of less than 15 ms, suggesting that their work indicates a time scale of a few milliseconds. This work, and a great deal of other work has shown that many cortical subsystems, particularly those concerned with ocular pointing operate on a time scale shorter than that in order to achieve close loop servo performance at 100 Hertz or better (including the delays associated with the oculomotor muscles). Thus, as many as 10,000 neurons may be operating simultaneously, in a combined series and parallel channel environment, that produces an output in less than a few milliseconds.

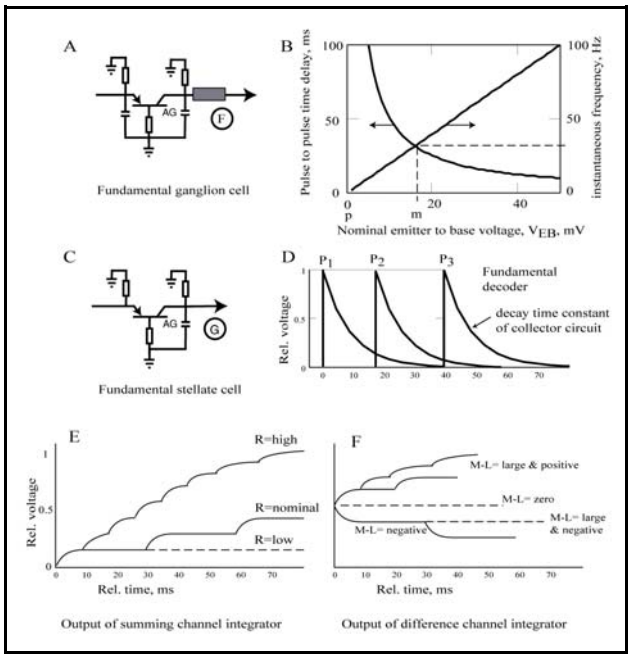

Figure 14.7.1-9 Signals recovered from the output of signal projection circuits.

Konig, et. al. use only simulated phasic neurons to present their case. While some of the cortical neurons undoubtedly operate in the coincidence mode, as suggested above for some of the stage 3 stellate cells, the vast majority of the cortical neurons do not do so using action potentials as input s signals. The coincidence function appears to occur after significant prior processing in the electrotonic mode. It is also likely to occur immediately before the process of memory implanting. Their sweeping proposal appears unsupportable. The subject of cortical signal processing will be addressed more fully in **Chapter 15**. **Chapter 7** has addressed the operation of the oculomotor servomechanisms in detail.

The symptom of "snowy vision" discussed in **Section 18.8.2** provides a rough estimate of the height of the individual steps in the recovered waveform shown in **D**, **E** and **F** of the above figure. Snowy vision appears to be caused by the generation of extraneous individual action potentials by the ganglion cells of the retina. When decoded at the brain, they result in an instantaneous change in amplitude estimated to be near 20% by only a few subjects. The sufferers describe the pulses as causing a "dark-going" noise pulse that is most obvious against a light background. The pulses appear to relate predominantly to the luminance channel as changes in color are reported much less frequently than changes in contrast. These suffers also confirm that the visual system operates as an AC coupled system. The noise pulses remain prominent in pitch darkness because of the neutral gray signal level achieved in the visual system (see Yarbus, 1967).

xxx

14.6.2 Predicted performance of the cascaded circuits

xxx

Note the difference in the signals presented to the dendrites of the ganglion cells (by the preceding circuits and labeled E) and the actual signals controlling the operation of the oscillator circuit within the ganglion cell (labeled E'). Note the difference in the signals recorded at the hillock of the typical ganglion cell (in the retina and labeled

[69]Konig, P. Engel, A. & Singer, W. (1996) Integrator or coincidence detector? The role of the cortical neuron revisited *TINS*, vol. 19, no. 4, pp 130-137

F1) and the signals at the actual pedicle of that nerve (located at the midbrain terminus and labeled F4). These waveforms are distinctly different. Note also the significant time delay between the signals recorded at the hillock of a ganglion cell and at its terminal pedicle, that may be separated by up to two meters in some peripheral neurons. They are typically separated by several centimeters in the visual system in the optic nerve. Laboratory investigators should recognize these differences when they are analyzing and interpreting their data. They need to be very specific about where they measured their signals.

Additional material comparing the bandwidth of the stage 3 and stage 1 neurons of vision is found in **Section 17.6.6**.

14.6.2.1 Problems with the "On--" and "Off--" signal nomenclature

There is a significant problems in semantics and nomenclature when discussing the electrophysiological signals recorded from the various appearances of Stage 3 signals. The problem is frequently protocol based. When beginning an experiment involving the recording of action potentials, there is a tendency to search for a signal that is continuous. The subject circuit is frequently described as supporting a maintained discharge. Statistically, this type of circuit may be more numerous than circuits generating pulses in response to a simple light stimulus. Those circuits exhibiting a maintained discharge may be associated with a variety of signal differencing channels. These circuits are generally associated with the differential signaling channels associated with chrominance, polarization and appearance. They are not associated with the luminance channels. The observed circuit may also be involved in diversity signal encoding. The presence of all of the above differencing channels varies with respect to position within the retina of a given species and with the species itself. Therefore to relate them to whether the stimulus is turned on or turned off is largely a matter of statistical chance. When they are associated with a chrominance channel, they may respond with an increase in pulse frequency in response to green light and with a decrease in pulse frequency in response to red or blue light. Many of the reports in the literature describing On-center results were obtained using "white" light of uncalibrated color temperature. The corresponding signal may actually change from an On–type to an Off–type by merely changing the center wavelength of the stimulus used.

In many experiments, the investigator has described an On–center and Off–surround situation using an arbitrary diameter stimulation disk surrounded by an arbitrary surround. The experiments were then performed without determining the spatial sensitivity of the system under examination to the diameter of the center disk or to the sensitivity of the system to the change in surround as a function of the distance from the edge of the central disk. In these experiments, it is rare to find any exploration of the impact of spectral content of the sources on the results.

If the nomenclature, On–center and Off-surround is to be used in experiments, it behooves the experimenter to demonstrate specifically what individual characteristics of the stimulus causes the circuit to increase or decrease in pulse frequency. The spectral parameters of th stimulus will frequently be found to be one of these characteristics.

Similar remarks apply to the measurement of the response to polarized stimuli. In many animals, the sensitivity to polarization varies with spectral band. Care must be taken that one is not measuring the difference between an input stimulus of one color and the input stimulus of only one polarization of a second color. In this case, the applicability of the designation On– may vary with the polarization of the stimulus.

Parkyn & Hawryshyn have introduced another variant although their semantics may be less than precise[70]. They choose to discuss the ON and OFF signals in terms of transient performance as measured within the optic nerve of salmonids. However, there transient may actually be the short term change associated with an intermittent stimulus. They note, "An ON-response in this study is defined as a transient voltage change at the level of the optic nerve following an increment of a light stimulus (e.g. the flash of reflected light from the side of another fish), while an OFF-response is a transient voltage change associated with the decrement of light (e.g. a passing shadow of an overhead predator)." They do not indicate whether the transient change is positive going or negative going. Nor do they indicate whether these changes begin from a more positive or a more negative excursion of the quiescent level. As a result, their terminology remains ambiguous. Further analysis of their data suggests they were using a very large electrical probe that averaged the data from multiple neurons and may not have actually penetrated any neurons (basically data from the INM). This assumption is consistent with the low amplitude of the recorded voltages. They also used a test probe amplifier with a 3 – 300 Hz passband. Such an amplifier would not support a step change in potential during the 750 ms duration of their stimuli (their figure 2D & 2E). The waveforms in these figures are

[70]Parkyn, D. & Hawryshyn, C. (2000) Spectral and ultraviolet-polarization sensitivity in juvenile salmonids: a comparative analysis using electrophysiology *J Exp Biol* vol. 203- pp 1173-1191

consistent with capacitive coupling between the probe and the signals within various electrotonic neurons.

14.6.2.2 Problems with the location of the probe within the system

As discussed in Chapter 15, the correlation between the recorded signals and the spatial, temporal, spectral and polarization characteristics of the stimuli causing them decreases with distance from the retina. Many of the signals emanating from the midbrain will show no correlation at all (in the absence of considerable more research into the signal processing associated with the LGN and pretectum) with the first order parameters of the incident radiation. The problem is acerbated significantly by the fact the visual system is a change detector and does not respond well to large diameter (greater than one degree) stationary stimuli in object space.

14.6.3 Reported Stage 3 performance

Section 14.6.1 and **14.6.2** have presented a great deal of information concerning the proposed theoretical waveforms based on the model of this work. This section will compare these waveforms to those measured over the years by many investigators.

There has been virtually no experimental work defining the performance of Stage 3 circuits in isolation. While several teams have traced the morphological extent of Stage 3 circuits in both the optic nerve and other commissure, they have not been able to interpret their results in terms of performance. Their problem has been complicated by their assumption that action potential pulses of the neural system are of primary importance. As late as 1988 Hubel was speaking almost entirely about the pulses he recorded from the LGN and other cortical locations, completely overlooking the importance of the analog waveforms within the feature extraction engines[71]. In fact, the pulse streams, made up of action potentials, are only a convenient method of propagating analog information. The actual information relating to the performance of the visual system is contained in the analog signal at the output of the stellate cells (typically found in layer 4c of the neural tissue of the brain) associated with Stage 3. Hubel describes the difficulty he and others have encountered in recording any signals in the primary visual cortex (pg 68-70) that responded to a specified light stimulus. This was partly because he was attempting to record action potentials generated at the output of a feature extraction engine. These only exist in the subsequent Stage 3 (commissure) circuit connecting the output of this engine to the next. In most cases, there are over a million neural circuits between the thousands of inputs to the engine being probed and its several hundred output circuits. Each of these output circuits (ganglion cells) feed commissure carrying different types and classes of information concerning the input signals. Correlating one of these outputs with a given image in object space is a challenging task that is well beyond current science.

Nowak & Bullier have provided a large amount of data related to the time delays associated with different circuits of the visual modality[72]. The data is presented without a top level block diagram or any more specific circuit diagrams. Thus, care must be used in interpreting the data. [xxx used in section on signal delays within the neural system]

Based on the model of this work, it is possible to correlate the pulse train of a Stage 3 signal path arriving at a stellate cell associated with the brain. However, there a variety of signal types carried by these paths. To interpret the pulse trains correctly, one must know the type of information being carried along that path. [It does little good to listen to an FM radio station using a radio designed to receive AM encoded signals.] In the absence of a very good model, it is very difficult to recognize the information being carried by a simple pulse train of action potentials obtained from probing the axoplasm of a nerve located morphologically. This will appear obvious from the data of Fukada referenced below.

Fortunately, there is a unique solution available to the problem of understanding the signals conveyed by each Stage 3 circuit. The podoplasm of each ganglion cell exhibits a composite waveform consisting of an analog portion describing the input to the circuit **and** a pulse portion describing the output of the circuit. It is the podoplasm of the ganglion cell soma that is frequently probed in attempts to record the output signals (action potentials) of the cell. Fortuitously, most investigators have recorded this composite waveform when they thought they were recording the signals associated with the axon of the cell. By examining the analog portion of these waveforms, recorded during a comprehensive experiment using well characterized input stimuli, it is much easier to determine the nature of the

---

[71]Hubel, D. (1988) Eye, Brain, and Vision. NY: W. H. Freeman, Chapter 2

[72]Nowak, L. & Bullier, J. (1997) The timing of information transfer in the visual system, Chapter 5 *in* Rockland et al. *eds*. Cerebral Cortex, Volume 12 NY: Plenum Press

signals being conveyed by a particular Stage 3 circuit.

While much of the data examined below was obtained under less than well designed experimental conditions, it is the best data available at this time for the purpose at hand.

14.6.3.1 Common measurement techniques

A variety of techniques have been used to accumulate the data in the literature. Most of them are invasive. As a result, there is very little data available on humans. There are several invasive, in-vivo, techniques. Some involve a high impedance (voltage) probe and some use a low impedance (current) probe. Some of the probes have penetrated the cell walls to provide intracellular measurements. Others have been limited to intercellular measurements. The latter may record the voltage of the relatively poorly conducting intercellular matrix or they may act as capacitance probes measuring the intracellular potential remotely. The most common in-vitro technique is to place a complete axon into a multi-chamber test cell that allows various portions of the cell to be electrically isolated from its other portions. This method has frequently suffered from the investigators limited knowledge of the topology, topography and internal cytology of the cell being examined.

As noted above, it is absolutely mandatory that the ganglion cell (and any other circuit generating action potentials) be complete to insure the vitality. Removing of the dendrites (as in the work of Hodgkin, Huxley & Katz) is unacceptable.

Because of the small size of the individual dendrite structures, it is very difficult to penetrate them with a physical probe. An alternative is to penetrate the dendrolemma where it is within the volume of the soma. It is also possible to penetrate the podolemma in this region. It is important to be sure which lemma is penetrated in discussing the operation of cell producing action potentials.

On occasion, probes have been arranged to move along the extracellular space adjacent to a single ganglion cell. When operating as current or voltage probes, they have collected useful information concerning the (ganglion and Node of Ranvier) amplifiers of the cell. When operated as capacitive probes, they have also been limited to collecting information near the amplifiers because of the effective shielding of the axon segments by the low capacitance of the myelination.

The choice of probe configuration and test set electronics introduces a degree of variation in the data collected by different investigators. The use of a capacitive probe necessarily overlooks the low frequency signal components of the Stage 3 waveforms. Similarly, the low frequency components in the output of the ganglion and Node of Ranvier amplifiers are not propagated well by the LC transmission lines of the axon segments.

14.6.3.2 Data from Limulus

Data collected from the eccentric cells of Limulus has been particularly easy to analyze. The data suggests that this cell acts as a conventional ganglion cell. Various data exists to show the Limulus eye is multi-spectral[73]. Chapman & Hall review the early literature suggesting that the median ocelli of Limulus are multispectral, UV– & M–channels, but that the lateral compound eye only exhibits UV sensitivity. It appears there data supports a broader interpretation, including the presence of a L–channel photoreceptor in the median ocellus (based on slope changes in figure 8). Borsellino, Fuortes & Smith have described the eccentric cell of Limulus[74]. Purple & Dodge and Behrens & Wulff both describe a cell known morphologically as the eccentric of the lateral eye of Limulus. It appears that Purple & Dodge have explored the properties of a summing type eccentric cell (with an input structure equivalent to a bipolar cell) while Behrens & Wulff discuss examples of differencing type eccentric cells and reference examples of two eccentric cells being found within the same ommitidium. Behrens & Wulff employed a simultaneous two-probe technique that appears to provide a number of definitive answers while demonstrating the complexity of exploring DC coupled combinations of retinula and eccentric cells.

---

[73]Chapman, R. & Lall, A. (1967) Electroretinograph characteristics and the spectral mechanisms of the median ocellus and the lateral eye in *Limulus polyphemus*. *J. Gen. Physiol*. vol. 50, pp 2267-2287

[74]Borsellino, A. Fuortes, M. & Smith, T. (1965) Visual responses in Limulus. Cold Spring Harbor Symposia on Quantitative Biology. vol XXX, pp 429-443

The role of Limulus as a transitionary form in evolution is generally recognized. While it shares the ommitidium cartridge structure with *Arthropoda*, at least one cell in each cartridge has been replace or extensively modified to form an "eccentric cell." This cell generates action potentials. These speciallized cells appear to be present in both the ocelli and the compound eyes of *Limulus*. As discussed in Chapter 9, this type of cell may have evolved along any one of three paths. It could be a modified photoreceptor cell, it could be a modified Stage 2 cell or it could be a stage 3 ganglion cell interfacing directly with the photoreceptor cells. Significantly more research would be needed to determine the correct evolutionary path. The need to generate action potentials is highlighted by the fact that the eyes of Limulus are not located on its head. They are located on its carapace. This location suggests a longer physical path between its eyes and its brain than typical of *Arthropoda*. The data of Behrens & Wulff suggest multiple spectral photoreceptors in the lateral eye of *Limulus*.

14.6.3.2.1 The summing type eccentric cell

Although it suffers from a number of oscillograph recording problems, **Figure 14.7.3-1** reproduces a figure from Fuortes that is in excellent agreement with the predicted performance for a summing type of eccentric cell. It appears to be due to probing of the output portion of the eccentric cell. There are no action potentials occurring before or significantly after the light stimulus. Note the delay in the output versus the stimulus shown by the black horizontal bars. Note the increase in "frequency" of the action potential stream as the illumination intensity is increasing. The fact the peak in the envelope of the pulse stream occurs prior to the peak in the analog waveform is indicative of the presence of a pre-emphasis circuit in the eccentric cell. Note also the undershoot in the analog generator potential waveform, for the maximum intensity stimulus, as it decreases from its peak value. This feature also supports the presence of a pre-emphasis circuit. In the middle frame, the reduction in the advance in the peak in the pulse envelope relative to the peak in the analog waveform is due to the reduction in the slope of the generator waveform. The disappearance of the undershoot following the analog peak is also indicative of a change in the shape of the generator waveform. In the lower frame, the effect of adaptation is clearly evident in the decrease in pulse frequency with time during the duration of the stimulus.

In the data of Purple & Dodge, it appears the signals from all of the photoreceptor cells within a given ommatidium cartridge are summed at its input. Thus, only monopolar data from a luminance channel is to be expected from an eccentric cell. There are no action potentials generated before or after the period of stimulation in the data of Purple & Dodge.

Purple & Dodge have collected very useful and illustrative data from the lateral eye of Limulus. Their figure 11 is reproduced as **Figure 14.7.3-2**. It represents electrical probe data from an impaled eccentric cell in response to stimulation of the visual system by light (lower frames) and the predicted data (upper frames) from their electrical model of the cell. They did not detail the actual model they used to create

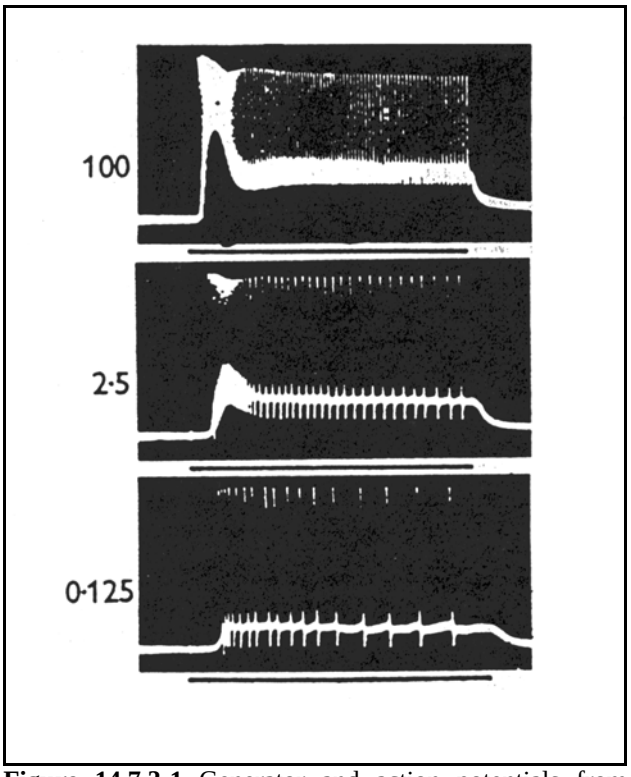

Figure 14.7.3-1 Generator and action potentials from impaled eccentric cell. Figures on left represent relative stimulus intensity. Figures appear to be adjusted in vertical height to accommodate the amplitude of the generator potential. All of the action potentials should be of equal height. From Fuortes, 1959.

the data. It may have been the model of Stevens[75]. Their electrical model is clearly different from the conceptual model of their figure 2. That model contained no capacitive elements.

There are many important features that can be extracted from the individual frames of this figure. Note the obvious undershoot in the voltage data following the termination of the light. Note also the similar undershoot in the frequency characteristic associated with the same data. This data strongly suggests the presence of a pre-emphasis circuit between the photoreceptor and the eccentric cell of Limulus.

Note the subtle difference in the phasic waveforms of the measured data and the calculated data. The tilt in the baseline between the individual phasic waveforms suggests a difference in frequency characteristics between the circuits generating the measured and calculated data. Note also the reduction in the amplitude of the phasic waveforms depending on their location in time. This variation is most likely due to the impedances involved in the oscillator circuit of the cell and the investigators test set. This difference is frequently encountered when the proper compensation is not provided for the probe capacitance. This reduction does not appear in the calculated waveforms of their figure 8 and would not be expected based on the model proposed by this work. When considering the

[75]Stevens, C. (1963) Input-output relation for Limulus receptor cells. In Biophysical Society, Abst. 7th ann. meeting, NY: 1963, item WF6.

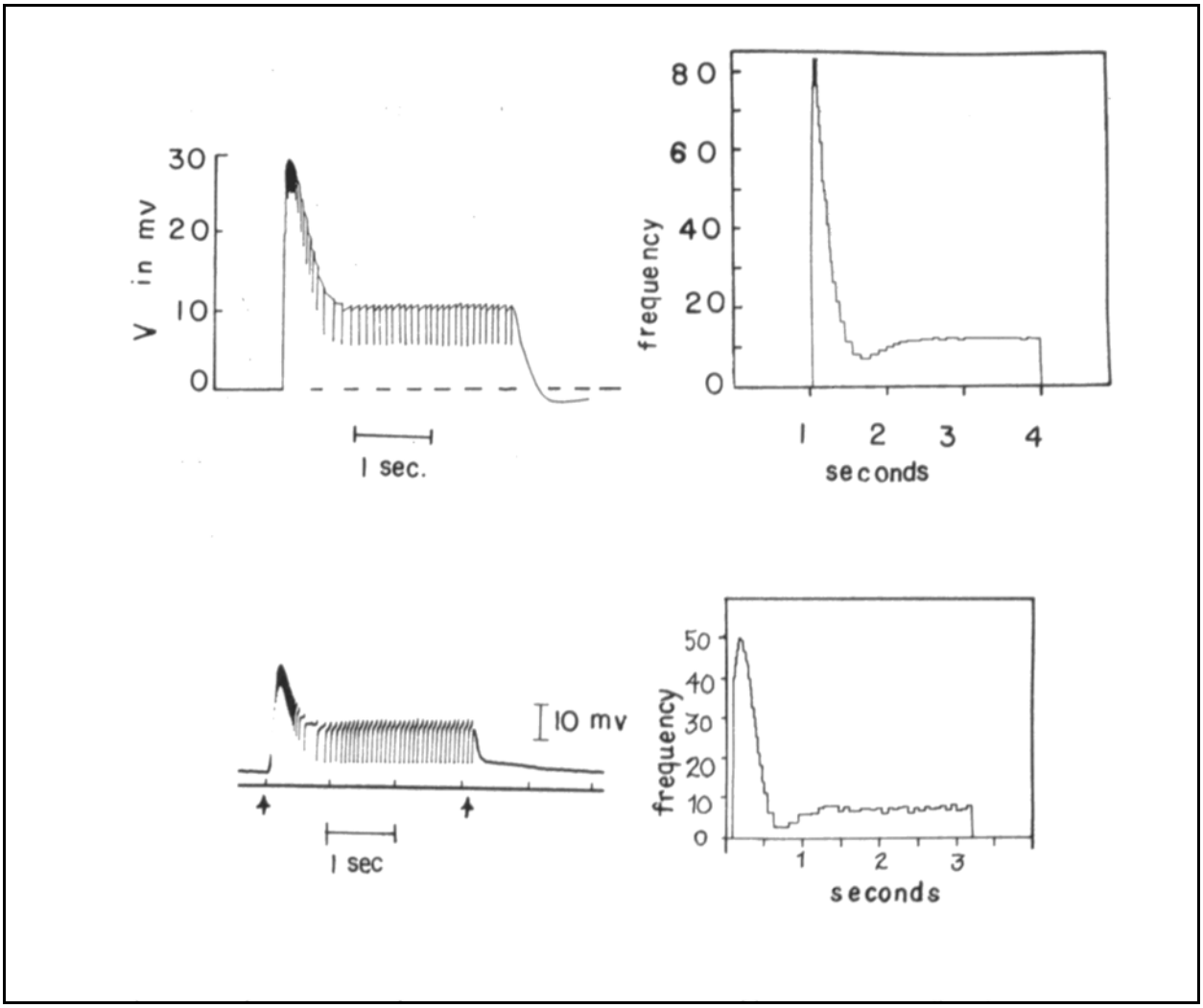

Figure 14.7.3-2 Measured data from eccentric cell of Limulus. Lower frames are measured data. Upper frames are projections from their proposed model. See text. From Purple & Dodge, 1965.

waveforms of figure 8 and figure 11, there is no undershoot in the frequency characteristics of figure 8. These waveforms are based on the introduction of a current pulse into the soma of the eccentric cell rather than the introduction of a light stimulus. Introducing current in this way would bypass any pre-emphasis circuit in the model associated with the synapses between the eccentric cell and the photoreceptor cells. This would also be the expected situation in the actual neural specimen based on this work. Introducing current into the soma would also bypass any variation in amplifier gain associated with the adaptation mechanism in the photoreceptor cells of Limulus.

The above features of the Purple & Dodge paper are in excellent agreement with the model proposed in this work. Many additional pieces of data can be mined from their paper.

14.6.3.2.2 The eccentric cells of Limulus

Behrens & Wulff have provided a different set of data for the lateral eye of Limulus[76]. The design of the *in-vitro* experiments appears to be good (except with regard to specifying the illuminant used for excitation). They have provided a comprehensive introduction reviewing the work of many others with this animal. These discussions highlight the criticality of where the electrical probe penetrates the eccentric cell. Their discussion and data are strikingly broader than that of Purple & Dodge. However, they were imprecise in describing the apparently broad band illumination used in their experiments. They did note the position of Ratliff, Miller, Wolbarsht & Wagner that some lateral eye cartridges contained two eccentric cells. Their figure 5 is particularly interesting. It is reproduced here as **Figure 14.7.3-3**

In each frame of this figure except the left middle frame, the lowest waveform records the light stimulus, the top waveform records the response of the retinula cell and the middle waveform records the response of the eccentric cell. The intermediate waveform is a timing trace. They noted the variability in the relative amplitudes of the various signals based on probe positioning. In the two lower right waveforms, the signals may be reversed due to probe positioning. There is a significant delay between the responses and changes in the light level due to the 10 +/- 2 degree Celsius temperature of the specimens.

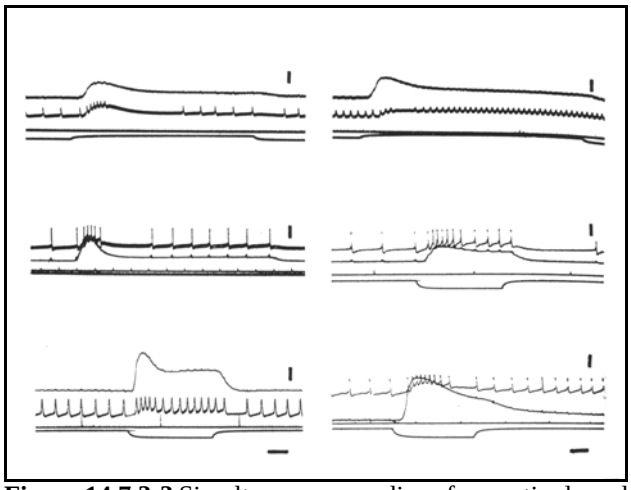

Figure 14.7.3-3 Simultaneous recordings from retinula and eccentric cells of Limulus. Vertical calibration bars represent deflection due to a 10 mv calibration signal. Horizontal bars represent 0.1 seconds. See text and original source for details. From Behrens & Wulff, 1965.

Note the presence of action potentials in the absence of light input to the visual system, both before and after stimulation. This situation suggests that the eccentric cell they examined was a free-running oscillator and its frequency increased with M–channel stimulation. This is the characteristic of a ganglion cell processing bipolar information derived from two different input circuits. Since the inputs come from photoreceptors in the same cartridge, they cannot represent spatial differences across the retina. However, they could be derived from spectrally distinct photoreceptors or from two different polarization sensitive channels in the same cartridge. Behrens & Wulff did not describe any polarization filter in their stimulation mechanism nor did they describe the spectral content of their source in detail.

Polarization sensitivity within a cartridge is a characteristic more highly developed in the cartridge of *Mollusca* than in *Arthropoda*. In any case, the conclusion can be drawn that the eccentric cell examined by Behrens & Wulff was of the type normally used to project bipolar signals derived from a differencing circuit prior to the oscillator.

Borsellino, Fuortes & Smith have provided a definitive picture of the generation of action potentials by the eccentric cell of *Limulus*. **Figure 14.7.3-4** is a reproduction of their figure 5. It provides an exceptionally good corroboration of the theory presented in this work from stimulation to the generation of action potentials in a simple system lacking any Stage 2 signal processing. The horizontal lines on the right point to the level of the peaks of the action potentials. These peaks did not reproduce well in the original publication and are difficult to see in this copy. The amplitude of the composite waveforms, and the ratio of the amplitude of the analog and pulse portions of the waveforms suggest that they were obtained by a probe contacting the podoplasm of the eccentric cell. The vertical scale for the figures appears to be a relative one. It does not start at the baseline for the signal waveforms of the lower frames. For some reason, it is drawn with zero conforming to the zero line of the stimulus. Borsellino, et. al. did not define the polarity of the waveforms, probably because to indicate they were negative going would interfere with their hypothesis. It is proposed that they are negative going. [Very few papers published during the 1960's defined the polarity of their recordings.] As discussed earlier, signals recorded at the base terminal of the monopulse oscillator within the eccentric cell are unique in providing a composite waveform consisting of an analog component describing the input to the circuit and a pulse component describing the output of the circuit. When combined with a

[76]Behrens, M. & Wulff, V. (1965) Light-initiated responses of retinula and eccentric cells in the *Limulus* lateral eye. *J. Gen. Physiol*. vol. 48, pp 1081-1093

graph describing the stimulus interval, a comprehensive view of the operation of the visual system is provided up to the point of action potential generation. If the data also provides the waveforms as a function of temperature (as in this case), a very complete picture is provided. The temperatures in Celsius, are marked adjacent to the individual frames.

Looking at the left frames first, the pulse to pulse intervals as a function of the underlying analog waveform are seen very clearly. However, the effect of the passband of their amplifier is clearly causing and undershoot in the composite waveform when each pulse ends. This is due to inadequate low frequency response in the amplifier. The intrinsic delay associated with the P/D mechanism is seen to vary indirectly with temperature. Similarly, the slope of the leading edge of the impulse responses are seen to increase with temperature. The time scales and the high threshold level in the case of the impulse responses suggest that all of the waveforms were obtained at very low photometric intensities. The threshold associated with the oscillator circuit is difficult to discern from the oscilloscope traces but it appears to be between 10 and 12 mV when measured in the podoplasm (at the base terminal). It is the highest level associated with the analog portion of the waveform prior to initiation of the first action potential. Following the initiation of the first pulse, the time interval prior to subsequent pulses is proportional to the height of the analog waveform. Note the difficulty in defining a frequency in the impulse response cases where only two or three pulses are generated. The action potential pulses are approximately 18 mV high in all cases within the figure. This is an appropriate amplitude for the pulses measured in the podoplasm. It would be expected to be larger, approximately 100 mV, and of opposite polarity if measured in the axoplasm.

The pulse responses on the right are presented on a different time scale. The effect of temperature is more difficult to see at this scale. However, the rise time of the leading edge and the fall time of the trailing edge of the analog waveform are clearly being reduced with a rise in temperature. Here again, there is very little sign of any overshoot. This is indicative of the low intensity of the stimulus. There is no sign of any pre-emphasis, probably because of the slow rise of the generator waveform produced by the photoreceptor cells. The analog waveform does not rise exceptionally fast and the peak in the pulse frequency appears to occur near the peak in the amplitude of the analog component. There is no sign of a drop below the plateau level following the initial rise as found in earlier cases. As expected, there is a finite intrinsic delay between the beginning of the stimulus and the rise of the analog waveform. The delay between the end of the stimulus and the drop in the analog waveform is less than the initial delay. The falloff of the analog waveform following the end of the stimulus appears to be exponential with no sign of an enhanced falloff due to a lead-lag network. There are no action potentials generated prior to the start of the analog waveform or following the end of the analog waveform. The output is fully compatible with a designation of a luminance channel signal as defined in this work.

Every feature in this figure corroborates the theory of this work!

The shape of the impulse responses on the left suggest a $\sigma \cdot F \cdot \tau$ value of about six. This value was obtained by overlaying the impulse function with a template of the P/D Equation for different values of $\sigma \cdot F \cdot \tau$. This template is found in Section A.4.2. of Appendix A. The type of light source used to collect the data was not specified. However, it appears it was quite noisy (compared to that used in the following figure). As a result, the pulse to pulse intervals in the right-hand frames are not uniform. The average pulse frequency for the

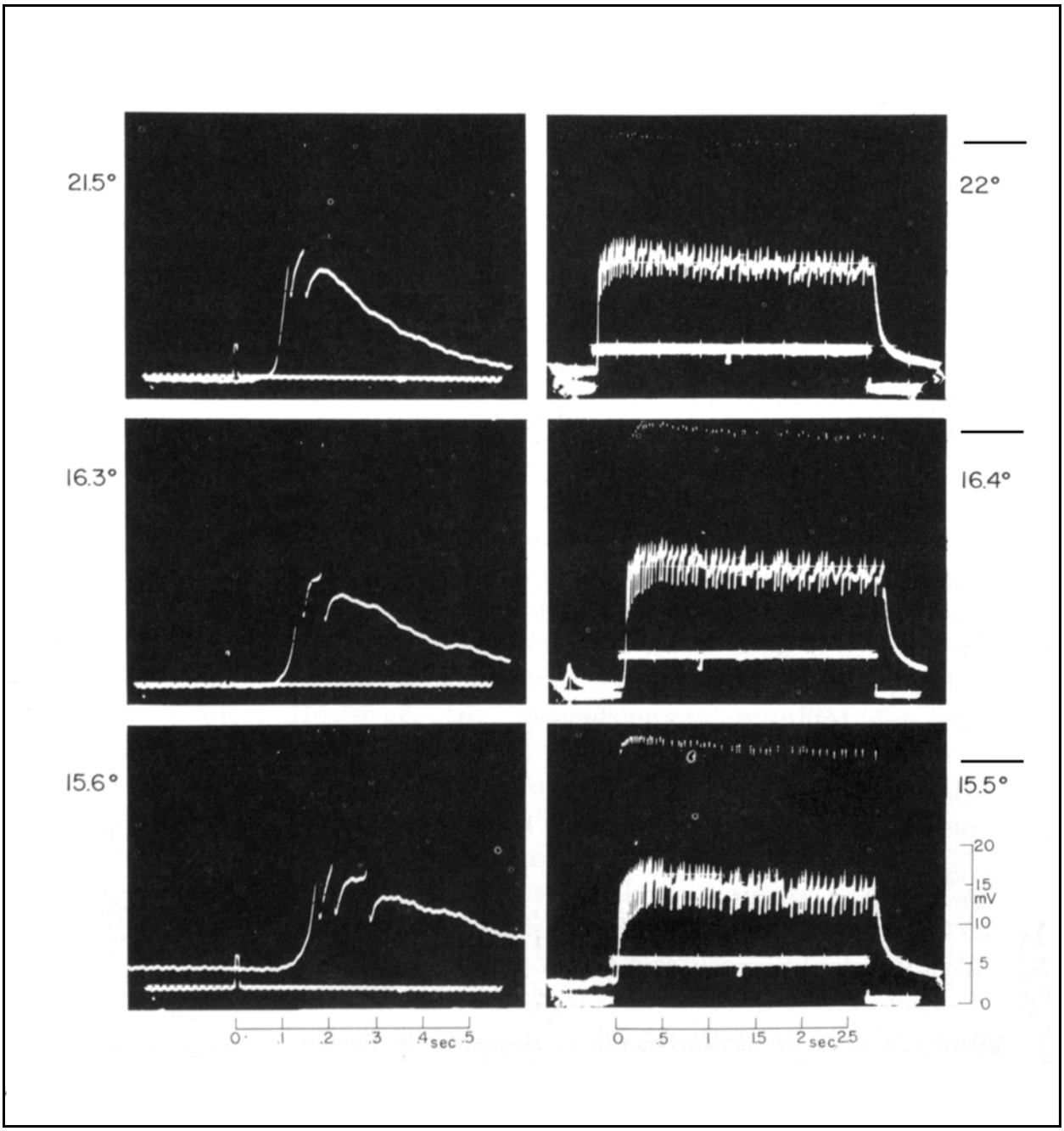

Figure 14.7.3-4 Responses evoked by flashes of light versus temperature in Limulus.

22 Celsius data is about 13.5 pps.

Fuortes & Poggio have provided additional data on what they "presumed" to be the eccentric cell. It provides additional insight that builds on the above discussion. While the above figure focused on low excitation levels at a variety of temperatures, Their figure 2, reproduced here as **Figure 14.7.3-5,** concentrates on varying the stimulus intensity over a large range and extends the time interval of recording out to almost 20 seconds while maintaining the temperature at 18 Celsius.

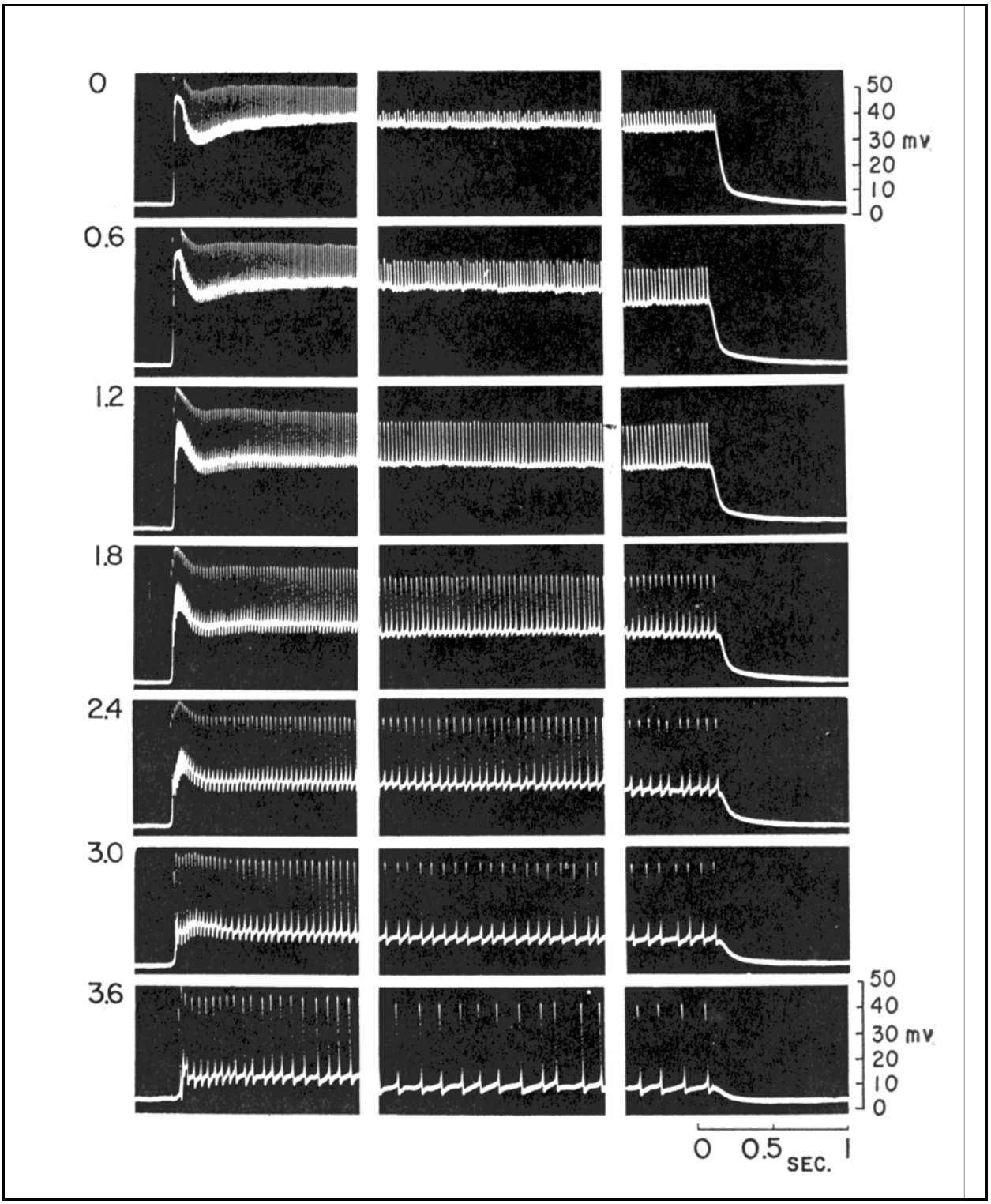

Figure 14.7.3-5 Long responses to steps of light in Limulus. Unit 3358. Temperature 18 Celsius. Stimuli applied in order of increasing intensity with 20 seconds between intensities. Each intensity held for 20 seconds. Samples separated by 8.4 seconds. See text. From Fuortes & Poggio, 1962.

Each of the individual traces in the figure last for less than two seconds and there are 8.4 seconds between the traces in a given row. The numbers on the left indicate the attenuation of the stimulus applied to the visual system in logarithmic units. The voltage scale at the lower right applies to each row of data.

The fact that a pre-emphasis circuit is present in Limulus is apparent from looking at the left-most part of the left hand frames. As the stimulus level rises in intensity, the leading edge of the P/D response steepens. This places more of the energy of the waveform in the temporal frequency band that the pre-emphasis circuit emphasizes. Similarly, the trailing edge following the peak in the P/D response is seen to drop below the plateau level of the long term response to stimulation as the stimulation is increased. Finally, the simple exponential fall in the analog waveform following the termination of the stimulus shows an exponential character at the lower stimulus levels but a less exponential character as the effect of the pre-emphasis circuit on the P/D response becomes more significant. Unfortunately, the delay between the start of the rise of the analog response and the start of the stimulation is not shown. This data would show a distinct reduction in delay as the stimulus rose. The relationship between the interval between the action potentials and the amplitude of the analog waveform is also seen clearly in the figures. The higher the amplitude of the analog waveform, which reflects the signal amplitude applied to the dendroplasm of the cell, the higher the frequency of the action potential stream. For comparison purposes, the pulse rate in the 22 Celsius frame of the previous figure was approximately the same as the middle frame at the 3.0 log unit level.

The frames at different intensity levels show a significant compression between the analog waveform amplitude and the stimulus intensity. This compression can be explained in terms of two functions, the compression factor associated with the P/D Equation and the compression due to the adaptation amplifiers of the photoreceptor cells. Based on the similarity in the pulse rates between this figure and the previous one, it can be assumed that the $\sigma \cdot F \cdot \tau$ value of the analog waveform at the intensity level of 3.0 is also about six. This would suggest that the compression factor in the P/D Equation can be ignored for stimuli of higher intensity than this value but becomes significant for lower values. The template for the scale factor of the P/D Equation, which describes this compression, can be found in Section A.4.1 of Appendix A. If true, the compression factor related to the P/D Equation would dominate in these frames and the adaptation mechanism would contribute a small factor. This may well be the case here since most of the change in amplitude with stimulus intensity appears to occur in the lower three rows of the figure. The compression factor in those frames is about a factor of 3 for a change in intensity of 1.2 log units. The compression in the upper five frames is much lower at about a factor of 2 for a change in intensity of 2.4 log units.

By counting the number of pulses per unit time in the middle and right-most frames, it is possible to define the nominal frequency of the action potentials as a function of the input stimulus under steady state conditions. The pulses are seen to vary from this nominal frequency in the left most frames. This variation, combined with the precise location of the initial pulse relative to the leading edge of the analog waveform are indicative of the time interval type of phase modulation (as opposed to frequency modulation) used in the visual system. Fuortes & Poggio counted these pulses and provided graphs of both the instantaneous frequency at intervals of about 20 msec and the average frequency during the steady state portion of the response to the stimulus. Their peak instantaneous frequency was about 115 impulses per second at the highest light level.

Note the consistency in the height of the combined analog and pulse waveforms in the center and right frames. It is nearly constant at about 38 mV. [The trimming of the individual photographs leaves the false impression that it is lower in the upper frames. A second potential scale has been added to overcome this impression.] This constancy is representative of the saturation voltage of the monopulse oscillator. The level of 38 mV would be expected to be very near the positive-most voltage reached by the action potentials of the axoplasm. Note the fact that the initial peak in the waveforms is slightly higher than 38 mV. [The pictures in the upper left were cropped and do not show the precise shape of the pulses occurring near the peak.]. This is indicative of a fall in the saturation voltage. The saturation voltage in a semiconductor device is a function of the maximum collector supply potential. This fact would suggest that the maximum axoplasm potential (provided by an electrostenolytic mechanism) exhibits one or more time constants. The actual potential reached at a given time appears to be proportional to the current drawn from the electrostenolytic supply. At higher pulse frequencies, more average current is drawn from the supply (since the individual pulses do not change in shape) and its output voltage would be expected to drop.

This figure provides considerable more corroboration of additional elements of the model proposed in this work! The figure can be interpreted much better using the electrolytic model that Fuortes & Poggio were able to do in their discussion which relied upon a chemical model. They had particular difficulty explaining the pre-emphasis circuit.

14.6.3.2.3 The next steps in *Limulus* research

The available data, the model of this work and the above analysis provide a very comprehensive description of the luminance (or fundamental path) performance of Limulus from the point of stimulation up to the action potentials of

Stage 3. A complete end to end electrophysiological circuit can be described up to the axons of the Stage 3 circuits and the values of the relevant circuit elements cab be annotated (For more detail, see Appendix D). There remain some unknowns and some questions.

1. There is a need to explore the stellate cells at the end of the eccentric cell axon, to record the signals at their podoplasm and axoplasm under similar stimulus conditions to that used to acquire the available data.

2. While the literature suggests the lateral compound eye is only sensitive to one spectral channel, the structure of the cartridge of the ommatidium would suggest otherwise. The grouping of multiple photoreceptor cells around a common region consisting of multiple Outer Segments within a single pixel strongly suggests the cells are sensing different characteristics of the incident light. The differences between the cells may relate to their chromatic or polarization sensitivity. The fact that each of the cells appears to exhibit a distinct axon proceeding from the caricature needs to be confirmed. These would be expected to carry analog waveforms to Stage 2 signal processing elements or directly to Stage 4 signal processing elements within the brain of the animal. The difference between Stage 2 and Stage 4 may be academic in such a simple system.

3. There is a need to explore the nature of the second eccentric cell associated with at least some ommatidium of the lateral compound eye. Does the podoplasm of this eccentric cell exhibit a bipolar analog waveform ? If so, does it represent the difference between two spectral channels or between two polarization channels?

14.6.3.3 Data from rat

Schwarz & Eikhof have provided a variety of action potential waveforms recorded in- vitro from the rat under several pathological conditions[77]. The test configuration was that ascribed to Nonner. Their data conforms to the predicted waveforms of the previous paragraphs. The nonlinear current-voltage relationship they present was used in this work to calibrate the regenerative feedback circuit of **Section 8.5.3.4**.

14.6.3.4 Data from cat

Barlow & Levick have provided data on the maintained and "on demand" action potential streams of cat[78,79]. The first paper concentrated on the recorded action potential streams by calculating the ratio of the average number of quantal absorptions required to elicit one extra impulse in the action potential train. The paper concentrated more on technique development than it did on obtaining clear results. It did not present a model of the portion of the visual system they were attempting to explore. It learned more about the adaptation process than it did about the processes related to action potentials. The second paper concentrated more on the type of ganglion cells producing continuous streams of action potentials. They appear to be unaware of the functional distinction between ganglion cells producing "maintained" pulse discharges and those generating pulses on demand. Their stimuli were not designed to differentiate between these two classes of ganglion cells. Their data is primarily statistical and lacks the waveforms as a function of time like those available for *Limulus*. Lacking a model of the system, they engaged in considerable discussion containing a significant degree of speculation.

Fukada, et. al. have provided interesting electrophysiological data for the cat[80]. The data in their Figure 1 can be easily separated into monopolar channels exhibiting no action potentials during the off interval (left and right columns) and bipolar channels exhibiting action potentials during both the "off" and "on" intervals (center two columns). Further, the two center columns can be further differentiated into the left column where the pulse frequency increases with incident illumination and the right column where the pulse frequency decreases with incident illumination. The incident illumination was not characterized beyond saying it was a glow modulator tube

---

[77]Schwarz, J. & Eikhof, G. (1987) Na currents and action potentials in rat myelinated nerve fibres at 20 and 37 Celsius. *Pflugers Arch*. vol. 409, pp. 569-577

[78]Barlow, H. & Levick, W. (1969) Three factors limiting the reliable detection of light by retinal ganglion cells of the cat. *J. Physiol*. vol. 200, pp 1-24

[79]Barlow, H. & Levick, W. (1969) Changes in the maintained discharge with adaptation level in the cat retina. *J. Physiol*. vol. 202, pp 699-718

[80]Fukada, Y. Motokawa, K. Norton, A. & Tasaki, K. (1966) Functional significance of conduction velocity in the transfer of flicker information in the optic nerve of the cat. *J. Neurophysiol*. vol. 29, pp 698-714

of a given manufacturer. The authors noted in the caption that the figure had been retouched.

Figure 1 contains a lot more information than discussed by the authors when interpreted in terms of this model. The authors note that minimum signals were used relative to a threshold. This can cause the rate of onset of the light to have a significant impact on any pre-emphasis circuit in the signal path. This may be part of the cause of the unexplained behavior in the right hand column during the flickering pulses compared to the steady light. It is also noted that the waveforms show no sign of any analog pattern associated with their pulse trains. No analog waveform has been propagated from the first Activa of the ganglion cell to the location of the recording at either a pedicle or at a Node of Ranvier more than 30 mm away.

Of more interest is the second column. The column shows an initial group of action potentials associated with the start of the stimulus (whether steady [for one half second] or pulsing rapidly). Second, there is a distinct pause in the action pulse train following cessation of the stimulus. This cessation is followed by an action pulse train at the quiescent frequency of the ganglion cell. This is precisely the mode of operation proposed for a ganglion cell accommodating a bipolar input signal.

While the performance summarized in column three is clearly different from that in column two, note the pause in the action pulse train immediately following the cessation of the long pulse. This is also likely to be the normal response to the cessation of the stimulus.

Their findings with regard to the average velocity of action potentials between the optic disk and the entrance to the midbrain are similar to earlier investigators. Their data contains too many uncontrolled or uncharacterized variables to allow firm conclusions. The major peak in their bimodal distribution near 40 meters/sec is compatible with most of the data cited in this work.

Their discussion of flicker could be expanded considerably based on the model of this work. The experiments of Fukada, et. al. deserve to be repeated using modern instrumentation and a more carefully differentiated series of experiments within the overall experiment design.

Sherman & Guillery have provided excellent data showing the response of a chrominance channel of vision in cat[81]. **Figure 14.7.3-6** reproduces their figure using terminology consistent with this work. No parameters of the specific test configuration (particularly the stimulus intensity during the tests) were was provided. However, it appears current was injected into the dendroplasm cavity of ganglion cell associated with the LGN in order to change the operating bias of the cell under otherwise *in-vivo* conditions. As a result the mode of oscillation changed from free-running to driven even though the cell was originally conveying a chrominance channel signal. In A, the pulse rate in the absence of stimulation was a nominal 33 Hz. Under stimulation, the output pulse rate varied from 10 to 60 Hz as expected. When the bias point was raised to – 65 mV, the quiescent pulse rate fell to an average of 6-7 Hz. When the same stimulus was applied, the output exhibited a pulse rate as high as 60 Hz for short portions of the stimulus cycle but was cutoff during a majority of the cycle. These results are in excellent agreement with the electrolytic theory and proposed three terminal neuron configuration of this work.

[81]Sherman, M. & Guillery, R. (1996) Functional organization of thalamocortical relays J. Neurophysiol. vol 96, no. 3, pp 1367-1395

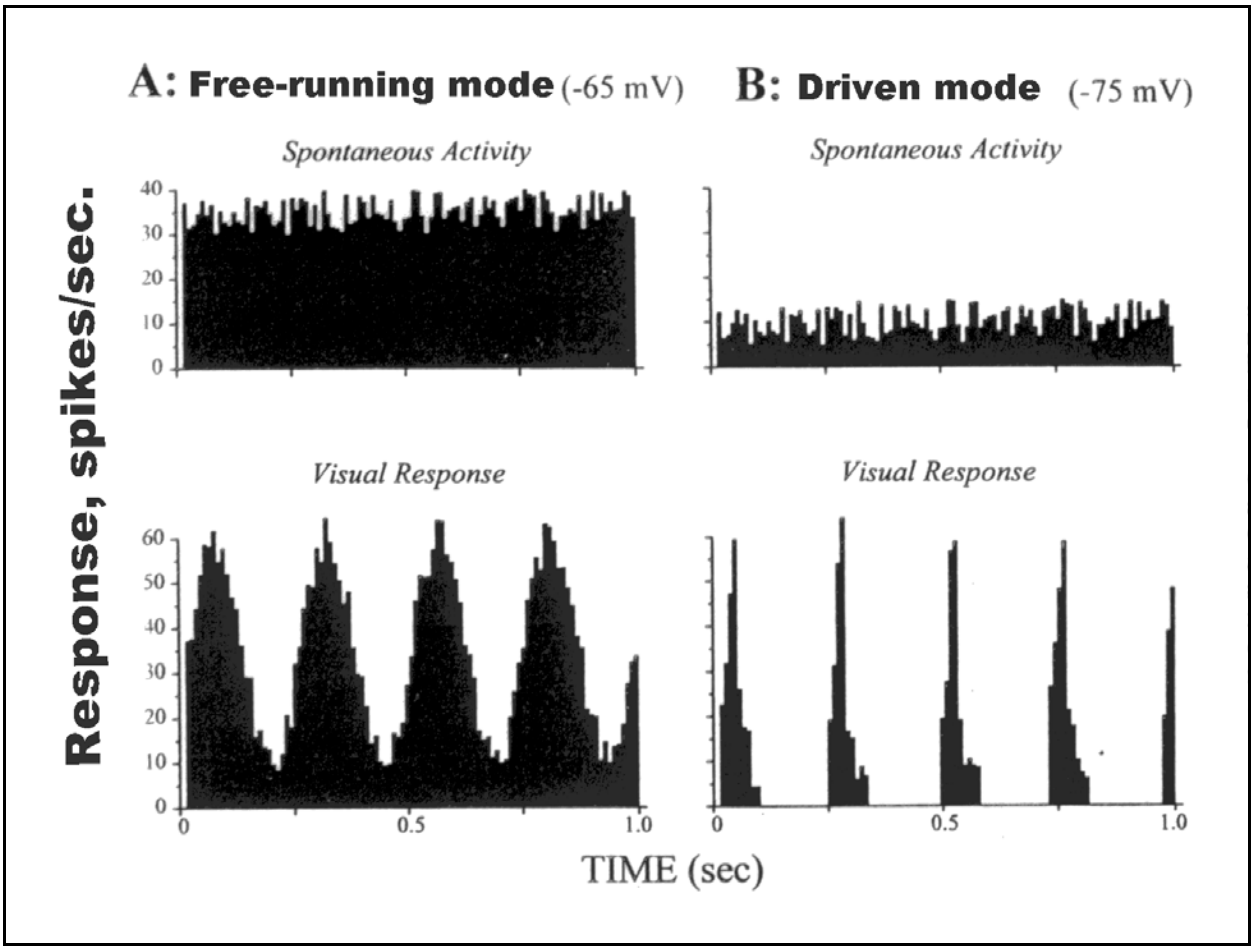

Figure 14.7.3-6 Spontaneous and visually driven responses of cat geniculate cell *in-vivo*. Top, histograms showing spontaneous activity. Bottom, histograms showing response to four cycles of a drifting sinusoidal grating. Current injected into (apparently the dendroplasm of) the cell to achieve the given bias potential. Reinterpreted from Sherman & Guillery, 1996.

14.6.3.5 Data from macaque monkeys

Lee & Sun have recently provided valuable data in the absence of an adequate model[82]. They made intracellular measurements within the in-vivo retina of macaque monkeys, *M fascicularis*. They assert they measured PC and MC cells based on the following criteria; "PC cells can generally be identified by their tonic responses and spectral opponency, and MC cells by their phasic responses and lack of spectral opponency." The MC cells were described as associated with the magnocellular pathway. They failed to elucidate, but it appears, the PC cells were associated with the parvocellular pathway. In spite of these definitions, they attribute most of their spectral opponency results to MC cells. While stating they employed standard tests, they did not demonstrate that any of their recordings were actually present in the parvocellular or magnocellular pathways or the appropriate layers of the lateral geniculate nuclei (LGN).

They provided "A simple model" in their figure 1A which they discounted in its caption. The model consisted of a

[82]Lee, B. B., & Sun, H. (2009). The chromatic input to cells of the magnocellular pathway of primates *J Vision* vol 9(2):15, pp1–18, http://journalofvision.org/9/2/15/, doi:10.1167/9.2.15.

set of waveforms showing distortion when plotted using a linear ordinate. Their more complex model of figure 1B was actually a conceptual block diagram mixing achromatic and chromatic receptive fields following a nonlinearity..

They speak of a 1st harmonic (1F) chromatic response given by |M-L| , that is taken in this work as one of the two primary chromatic responses (the Q-channel of the parvocellular channel). They also speak of a 1F luminance response given by |M+L| and taken as part of the actual S+M+L luminance response of this work (with or without the absolute bars). The luminance information (R-channel) is passed to the brain by the magnocellular channel in this work. Empiricists bear the responsibility of showing that signals attributed to the magnocellular pathway actually go to the magnocellular layers of the LGN. Lee & Sun also speak of a frequency doubled (2F) response but this appears to be primarily due to the distortion they encounter when using a linear ordinate to plot a fundamentally exponential response following stage 3 encoding.

They performed most of their experiments in the peripheral retina (4-12° eccentricity). Many experiments included center-surround tests. They note in the second paragraph of their results section, "The results were unexpected." When plotting their work on a linear ordinate, they show a distortion from the expected sinusoidal response to a sinusoidal stimulus. The model of this work (**Section 14.3**) shows stage 3 encoding is exponential. This model would suggest their results in the right column of figure 2 would be clearer if plotted using a logarithmic ordinate. Similarly for all of the graphs in figure 11. When they plotted their data using a logarithmic ordinate, as in figures 3A & 3B, their data is easier to interpret.

The distortions they encounter using a linear ordinate are not present in the data delivered to stage 4 because the stage 3 demodulating circuits, like the modulating circuits, are exponentially based. As a result, the overall stage 3 performance is linear and transparent to the rest of the neural system within its operating range.

14.6.3.6 Data from humans

The operation of Stage 3 neurons in humans is virtually the same as in other species at the same temperature (at least outside the CNS). However, there have been important measurements made in humans that are not particularly significant. Action potentials occurring at repetition rates of 800-1000 Hz have been reported for projection neurons within the cortex[83]. These may well be associated with short projection circuits where the requirement to complete the associated analog computations rapidly may justify the higher power requirements needed to achieve such high phasic clock rates.

14.6.3.7 The comprehensive review by Destexhe et al.

> Destexhe et al[84]. provided a comprehensive paper describing a wide range of experiments and models that portend the transition of the neuron research community to a more sophisticated level based on electrolytic processes and mechanisms within the neural system of the animal kingdom. Several supporting papers have subsequently appeared from this group[85],[86],[87]. Unfortunately, they all are based on the Hodgkin & Huxley model of a neuron from the 1940's. On the other hand, they point out many problems with this 2-terminal model of a neuron and describe many experiments that suggest a 3-terminal neuron would be a better model for both *in-vivo* and *in-vitro* experiments. This work provides that 3-terminal model (**Chapters 8** & **9**).

The papers of Destexhe et al., Alvado, et al., Rudolph et al. and Gomes et al. can not be addressed in their entirety in the space available. As a group, they are *revolutionary support* to the thesis of this work. Only selected sections and conclusions of these papers will be discussed here.

---

[83]Steriade, M. Jones, E. & McCormick, D. (1997) Thalamus vol. 1, NY: Elsevier, pg 73

[84]Destexhe, A. Rudolph, M. & Pare, D. (2003) The high-conductance of neocortical neurons *in vivo. Nature Rev: Neurosci* vol 4, pp 739-751

[85]Alvado, L. Tomasa, J. Saighia , S. et al. (2004) Hardware computation of conductance-based neuron models *Neurocomputing* vol 58–60, pp 109 – 115

[86]Rudolph, M. & Destexhe, A. (2007) How much can we trust neural simulation strategies? *Neurocomputing* vol 70, pp 1966–1969

[87]Gomes, J-M. Bédard, C. Valtcheva, S. et al. (2015, *in press*) Intracellular impedance measurements reveal non-ohmic properties of the extracellular medium around neurons

14.6.3.7.1 The 2003 Destexhe et al. paper

The Destexhe et al. paper is based almost entirely on electrophysiological measurements, with a majority of those measurements involving intracellular recording techniques. Many of the experiments involved multiple simultaneous intracellular recordings showing both analog signals in one cytoplasmic chamber and phasic signals in a different cytoplasmic chamber. These measurements are not compatible with a single chamber, two-terminal model neuron as envisioned and described by Hodgkin & Huxley et al.

Destexhe et al. also stressed the fact that an *in-vivo* neuron operates in a totally different environment than the same neuron *in-vitro*. The *in-vivo* neuron typically receives input signals from up to 1000 other neurons simultaneously, whereas, the *in-vitro* neuron receives at most one artificial input signal. The great majority of the individual inputs *in-vivo* involve analog signals.

The recognition that a great many of the input signals to a stage 3A encoding neuron are analog in form highlights the crucial fact that the central neural system (CNS) in particular is not a pulse domain based computer (typically described as a digital computer). The CNS is in fact a very large scale analog computer. Relatively simple analog computers were widely used during the Second World War before the extensive development of the digital computer and digital integrated circuits.

Destexhe et al. provide a variety of critically important definitions in side-bars scatter throughout the paper. Most of these are very important in understanding what they are describing. A few miss their mark because they are based on a 2-terminal model of a neuron. As an example, the term transconductance, a term used to describe the performance of active semiconductive devices, does not appear in their paper. The term conductance, however, referring to the impedance of a membrane is present generally. The conductance is defined as the reciprocal of the impedance. Destexhe struggle with some of the terms because of their model. They speak of a leak conductance as "A constitutively active conductance, the reversal potential of which is called the leak reversal." What is "a constitutively active conductance"? Is it a non-linear conductance like that of a diode? Is it a conductance that is only defined over a limited voltage range. Is it a conductance associated with an active semiconductor device? Incorporating an active 3-terminal electrolytic semiconductor device, an Activa, within each neuron changes the entire conceptual environment. All of the highly developed terminology of the Institute of Electrical and Electronic Engineers (IEEE) becomes available to the biophysical community.

Their figure 3b is reproduced here at **Figure 14.7.3-7**. Their figure is actually an adaptation of a 2000 figure of Hausser et al[88]. that was reproduced from a 1997 figure in Stuart et al. There is a difficulty with the captions associated with this figure. The caption of the 2003 paper implies all of the recordings were from the same neuron and it says, "Active propagation of dendritic action potentials. Left: low-intensity stimuli applied at distal dendritic levels generate an action potential that is initiated in the axosomatic region (green and blue) and then back-propagates into the dendrite (orange). Right: simultaneous recordings from dendrites (orange, 400 μm from soma; pink, 920 μm from soma) and soma reveal both subthreshold and suprathreshold responses to distal synaptic stimulation." The 2000 paper notes in the caption, "All recordings are from different neocortical layer 5 pyramidal neurons, with the recording locations indicated schematically on a typical morphology." The earlier title appears to be more forthright. Following a brief introduction, the 2000 paper uses the title "A Renaissance in Dendrite Research" to describe the major changes in simultaneous probing and imaging that occurred during the 1990's. The figure is similar to an earlier figure in Stuart et al.[89] that shows when they actually recorded waveforms simultaneously. Here again, the precision of the time delays is low and detailed voltage and time scales were not provided. They confirm "These studies show that the site of action potential initiation is in the axon, even when synaptic activation is powerful enough to elicit dendritic electrogenesis" where they more specifically identify the axon hillock as the ultimate source. Destexhe et al., and Hausser et al are associated with the same laboratory, as are Alvado et al., Rudolph & Destexhe & Gomes et al. None of the papers cited provide a circuit diagram of the neuron they are investigating. Figure 1 of Stuart et al. provides a simple cartoon describing potential sites of an action potential generator. Neither do the papers describe the character of the synapse (or group of synapses) stimulating their neuron.

---

[88]Häusser, M. Spruston, N.& Stuart, G. (2000) Diversity and Dynamics of Dendritic Signaling *Science* vol 290, pp 739-744

[89]Stuart, G. Spruston, N. Sakmann, B. & Häusser, M. (1997) Action potential initiation and backpropagation in neurons of the mammalian CNS *Trends Neurosci* Vol 20, pp 125–131

The axon monopulse waveforms are relatively low in amplitude. This may have been due to their attempt to employ semi-*in-vivo* conditions where their target neuron remained in a slice of tissue and the traget axon may have still been connected via synapse with multiple orthodromic neurites (thereby loading the axonal circuit from an impedance perspective).

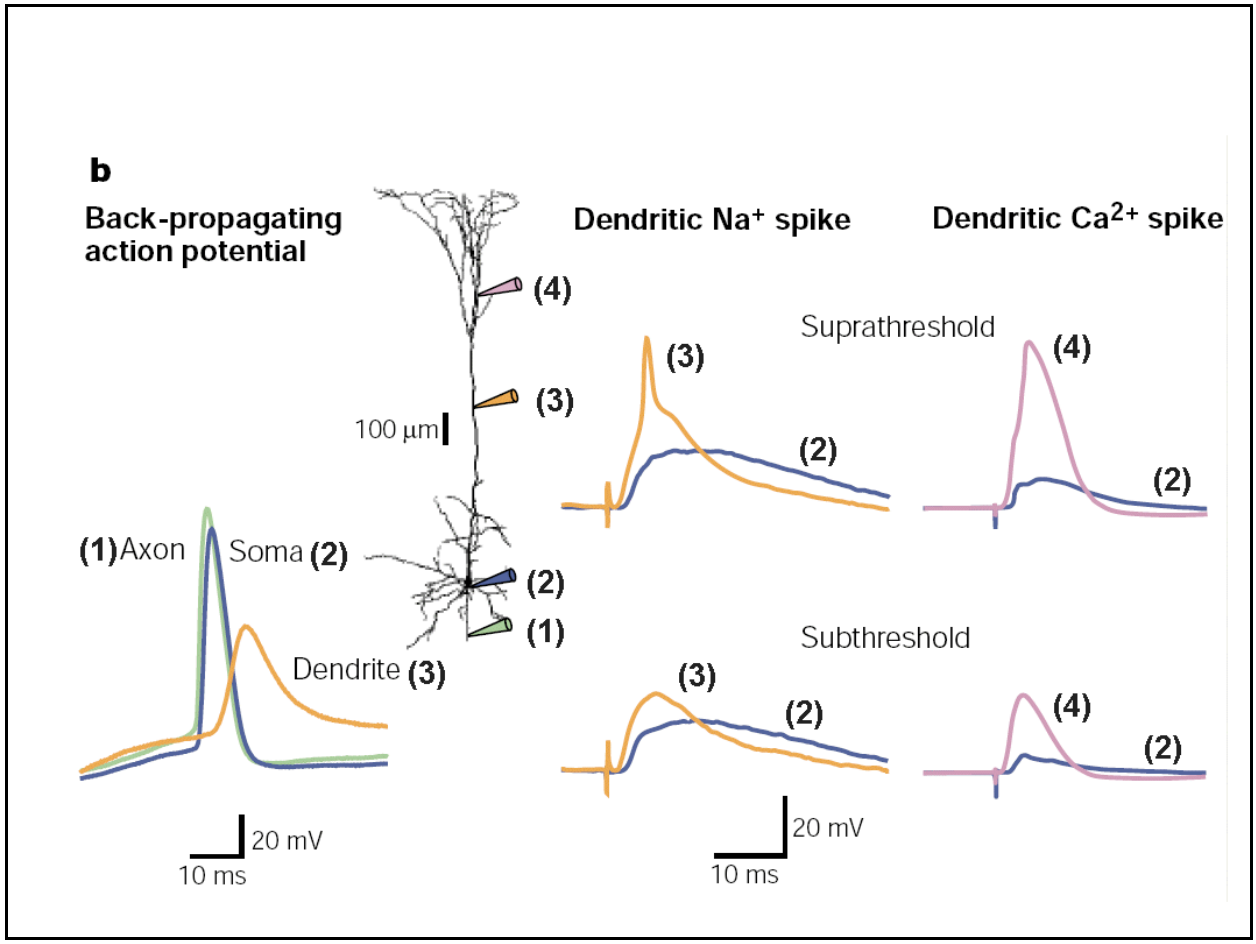

Figure 14.7.3-7 Waveforms from Destexhe et al. of a stage 3A neuron. The probes are color-coded to match the color of the waveforms. The axon probe is at the very bottom of the camera lucida representation of the neuron. The original labeling and discussion reflects the concept of the neuron as a 2-terminal device. No probing of the podoplasm of the radial portion of the bistratified neuritic (historically dendritic) tree was reported. Numbers have been added as labels to facilitate easier discussion. See text. Panel b adapted from Stuart et al., 2000 by Destexhe et al., 2003. The 2000 variant was adapted from an earlier 1997 version by Hausser et al., 1997.

All three of the authors cited above describe their neuron as a pyramidal neuron. However, they fail to describe the functional significance of the bistratified character of such neurons; the fact that the top arborization is a dendritic tree and the lower arborization is a poditic tree typically emanating radially from the soma. Destexhe et al. does recognize the potential for a functional difference on page 743. The pyramid neuron is a classic example of a three-terminal neuron as illustrated in **Section 9.2.2**. The dendritic arborization forms a stage 2 summing network feeding into the non-inverting input of the stage 3A encoding neuron. The poditic arborization forms a stage 2 summing network feeding into the inverting input of the stage 3A encoding neuron. This functional arrangement is described in **Figure 14.2.2-2** of **Section 14.2.2** under the label, “differential input from two synapses” without detailing the stage 2 summing functions. The internal structure and electronic model of a single ended ganglion neuron is developed in **Section 9.3.5**.

The label “back-propagating action potential” is reasonable if it is recognized that a portion of the axonal voltage waveform may be connected to the dendroplasm via the axoplasmn-to-dendroplasm capacitance. Such a signal

introduced into the dendroplasm cannot propagate beyond the synapses of the dendrite because of the synapses operating as nearly perfect "active diodes." Such diodes exhibit an essentially zero reverse transconductance along with their very high orthodromic transconductance.

The labels "dendritic Na+ spike" and "dendritic Ca^{2+} spike" are euphemisms for an allocation of the actual voltages recorded from the dendroplasm between two voltages defined in the Hodgkin & Huxley two terminal (single compartment) model of a neuron. In there model, the conceptual Na^{+} and Ca^{2+} currents were so named because of the concentration of their ions in the surrounding matrix. It is now known these ions do not exist alone in the matrix but only highly complexed with water. These complexed molecules are incapable of passing through the hollow core of any known pore or voltage controlled gate in the external lemma of a neuron. In there concept, the Na^{+} ions moved quickly and the Ca^{2+} ions more slowly through the lemma. The authors of the figure did not record the flow of any ions through the lemma in their experiments. They only recorded voltages and currents that they inferred involved positive ions instead of negative electrons (the conventional electrical current). They did not describe the actual voltage they recorded from the dendroplasm of their target neuron. In the absence of the actual voltage waveforms Destexhe et al. recorded, the actual Suprathreshold and Subthreshold waveforms of their pyramidal neuron can not be interpreted. The reader is referred to Section 14.3.2 for a discussion of similar waveforms in Stage 3A neurons of the pyramid type.

The original investigators did not report that they probed any of the podites of their pyramid neuron. If they had, they would have recorded relatively small amplitude waveforms of the opposite polarity of the axon waveforms. Their amplitude would be a result of the same current flowing out of the axoplasm and into the podoplasm but the much lower impedance connected between the podaplasm and the external ground circuit of their instrumentation. The more detailed relationships between the voltages in the figure can be displayed on a single serape showing each of the relevant voltages and currents and their inter-relationship, as a function of time. [xxx figs Myocyte serape.wpg, myocyte stressed serape.wpg & Neuron w poda supply param stim serape.wpg could not locate any text in WhNeuron folder. See Appendix O]

Frame 3a of the above three papers display a group of "conductance densities" as a function of distance along the trunk of the dendritic tree of the pyramid neuron of frame 3b. The functions do not show significant variations in these conductance densities. As a result, these functions are inconsequential. The actual functions reflect the fact that the actual quantities measured were currents. They are labeled as currents (using the conventional symbol for current, I, not conductances. Their right most function is labeled I_h and cites Migliore & Shepherd. The title of their paper is intriguing but the paper is not enlightening, "Emerging rules for the distributions of active dendritic conductances." The paper is based on the archaic 2-terminal neuron concept, relies upon the NEURON software program of that time, and does not draw a set of succinct findings or definitions. They define an α-conductance in generic terms, " The functional form, $G(t) = (t/\alpha)\exp(-\alpha t)$ is known as the α-function, and is widely used to represent the time course of a synaptic conductance. The value of α determines the rise and decay times."

> This α–function is the Poisson equation that Hodgkin & Huxley struggled unsuccessfully to apply to the neuron beginning in the 1940's. It only allows for a single time constant for both rise and decay times. Most measurements of the dendroplasm potential do not exhibit symmetrical time constants because of the character of the synaptic transconductance; it is assymetrical because the synapse incorporates an "active diode."

The conductance of the individual trunk of the dendritic tree is not particularly relevant to the operation of the neuron, the total current flowing along that conductance is a key parameter. When discussing the *in-vivo* condition, Destexhe et al. have offered the following definition, "In epochs of irregular fast EEG activity, as seen in waking and the up state of KX anaesthesia, cortical neurons have a low input resistance, are depolarized, experience continuous membrane potential fluctuations and fire spontaneously at rest. We will refer to this condition as the 'high-conductance' state of cortical neurons. This state differs markedly from that seen *in vitro*, where cortical cells lack spontaneous firing, and have a high input resistance and a hyperpolarized membrane potential, showing only discrete synaptic events." Since both the synapses and the pyramidal neurons are current mode devices, the above definition does describe a high current in the neurite circuitry leading to the relatively continuous generation of monopulses (action potentials). Their discussion and the data in their Figure 3 supports the conclusion, they are actually speaking of the total current injected into the dendritic tree of the pyramid neuron leading to the generation of multiple monopulse waveforms (a stream of action potentials). It can be assumed their term conductance refers to the conductance (the reciprocal of resistance) of an individual putative open pore or gate in the dendritic lemma. The conductance density is then a measure of the number of pores or gates per unit area of the lemma. Cytological documentation of the existence of such pores and gates in significant numbers has not been provided for any neural

lemma as of 2016. Destexhe et al. cited DeFelipe & Farinas[90]. While the DeFelipe & Farinas paper is a major work of significance, it is histological in perspective and does not include the word pore or the word gate in its 44 pages. Neither does it address the sodium ion, Na^+, or Calcium ion, Ca^{2+}. The cartoon of the synapse they display is that of the chemical neurotransmitter community. Their chemical neurotransmitter approach is in considerable conflict with the electronic stimulation via the synapse, involving the Na^+ and Ca^{2+} ions. Defelipe & Farinas treat GABA in the context of a GABAergic (inhibitory) synapse. While they do deal with the density of synapses associated with a large variety of neurons, they do not discuss the density of conductances. As in the case of the above terms, the term conductance does not appear in their 44 page presentation.

> Destexhe et al. continued their discussions (page 743) by deviating from the single compartment model of Hodgkin & Huxley into multiple-compartment models. The noted that the currently popular computer program, NEURON, also allowed users to postulate multiple compartments within a single neuron and "using a set of isopotential compartments." Requiring a small number of compartments to be isopotential is not consistent with actual neuron measurements (**Section 5.8.4**) or the more sophisticated discussions of signal propagation within myelinated axon segments (**Section 6.3.1**). Herman recognized this fact during the mid-19th Century. Destexhe et al. provide very useful potential values in their text but continue to avoid discussing the internal cytological structures of neurons. Their Box 1, frames a and d do illustrate the nominal axoplasm potential under *in-vivo* conditions (their high conductance condition) with the axoplasm quiescent potential near -60 mv compared to the more typical *in-vitro* (low stimulation condition) of about –154 mv. They offer two potential models satisfying their measurements but do not define them cytologically. Their amplitude distributions shown in the middle column of Box 1 do not appear to relate to the membrane potentials of the first column without additional interpretation.

Beginning on page 745, Destexhe et al. begin to interpret their data based on their "high conductance" state. They assert, "The impact of high-conductance states on the integrative properties of cortical neurons has been investigated using computational models. However, they make no effort to demonstrate that their computational models are sufficiently precise and sophisticated to be relied upon. Their models lead them to conclude that cortical neurons respond stochastically to a given stimulus. In fact, their behavior is best described by probability functions." ***This can be shown to be untrue in multiple cases where the response is totally deterministic given a sufficiently clear electrolytic (not computational) model of the neuron***. They proceed to introduce several dilemma that result from their analyses and potential conceptual solutions. The remainder of the paper discusses various hypothetical solutions without significant supporting data. The first paragraph of their conclusions asserts, "Experiments and models indicate that the intense synaptic activity seen in vivo is not detrimental, but can confer advantageous computational properties on neocortical neurons." This appears to be a valid conclusion but it does not rely upon their models. Subsequent paragraphs are considerably more argumentive and dependent on a wide variety of largely conceptual assumption.

The 1997 Stuart et al. paper sought to determine the location of the action potential generator in a cytologically and electronically undefined stage 3 neuron. They make it clear their term conductance refers to the conductance of an individual putative open pore or gate in the dendritic lemma based on the chemical theory of the neuron. It is presumed that this pore or gate is an integral feature of the synaptic process. They begin, "Three scenarios of synaptic integration and action potential initiation can therefore be envisioned: (1) passive synaptic integration followed by axonal action potential initiation; (2) active synaptic integration with dendritic action potential initiation; and (3) active synaptic integration with axonal action potential initiation. The pattern of action potential firing of a neuron in response to synaptic input will differ depending on which one of these scenarios holds. Knowledge of where action potentials are initiated and how they spread in neurons is therefore crucial for understanding how neurons transform synaptic input into axonal output." The Stuart et al. paper offers many different speculative options but converge most closely to the assertion that the action potential is generated most likely in the region where the dendroplasm and axoplasm meet, typically in the hillock of the axon. The tentativeness of their conclusions is suggested by their statement, "Some analyses of extracellular field potentials during synchronized synaptic activation of populations of hippocampal pyramidal and cerebellar Purkinje neurons *in vivo* have led to the conclusion that action potentials can be initiated in the dendrites before the soma. The interpretation of these experiments, however, is complicated as the recorded extracellular field depends on the geometric arrangement of the activated cells, their degree of synchronization of activation, the shape and possible in-homogeneity of the extracellular space, and the location of both the recording and reference (ground) electrodes." The tentative nature of their paper is indicated by the heading of one section ending in a question mark, "Why are action potentials

---

[90]DeFelipe. J & Farinas, I (1992) The pyramidal neuron of the cerebral cortex: morphological and chemical characteristic of the synaptic inputs *Progr Neurobiol* vol 39, pp 563-607

initiated in the axon?" Their next paragraph is again speculative and not based on any data in their paper. "Propagation of action potentials back into the dendritic tree—Once initiated in the axon, action potentials will propagate into the dendritic tree in a retrograde fashion. The extent of this action potential backpropagation has been found to vary depending on the type of neuron (3 citations). Lacking a schematic of their neuron, none of these parties can explain what mechanisms contribute to these observations. After additional discussion, they note, "Experiments like this, and others, show that action potentials propagate actively into the dendrites of neocortical and hippocampal pyramidal, hippocampal granule, substantia nigra and spinal cord neurons (5 citations) whereas backpropagation is largely passive in cerebellar Purkinje neurons (2 citations). They conclude the discussion portion of their paper with, "What does a backpropagating action potential do?— Some neurons have backpropagating action potentials, while others do not. This cell-specific difference suggests that active backpropagation of action potentials into the dendritic tree is functionally important in those neurons where it occurs. But what is the point of a backpropagating action potential?" The above actions and where they occur are readily explained by the Electrolytic Theory of the Neuron.

The complete theory of the electrolytic neuron is presented in Chapter 8. The morphological arrangement of one or more neurons in tandem are shown at the simplest level in **Section 10.1.5** and in additional detail in **Section 8.4.4**. It is common in the peripheral portion of the hearing modality of the nervous system to find stage 3A encoding neurons where the soma is not between the neuritic inputs and the axonal outputs. The Activa is formed conventionally at this junction but the soma is located orthodromic to the first myelinated axon segment. xxx Such a neuron might be considered a more complex morphologically monopolar neuron. Stuart et al. have noted that in some pyramid neurons, an action potential can be generated in a portion of a myelinated axon that occurs on the same side of the soma as the neuritic tree (either a dendritic tree, a poditic tree or both tree types in a bistratified configuration. They note, "These experiments show that fast, Na^+ action potentials are always initiated in the axon before the soma, independent of whether slower, dendritic regenerative responses occur or not (Stuart & Sakmann, 1996)." As shown in **Section xxx**, the soma plays no operational role in neural signaling. The pulse forming capability of a neuron occurs at the junction between the dendroplasm, the podaplasm and the axoplasm. The physical lemma associated with these plasmas come together in a specific configuration that constitutes an active semiconducting device labeled an Activa. The soma only contributes to the homeostasis of the overall neuron.

The electrical and semiconducting properties of the 3-terminal active device (the Activa) within a simple 3-terminal neuron is developed in **Section. 8.5**. The operation of a neuron as a stage 3A monopulse generator is described in detail in **Section 8.5.4**.

14.6.4 Asymmetry in Stage 3 performance

[**Figure 14.6.1-8**] exhibits a major asymmetry between recovered positive-going signals and recovered negative-going signals. Positive-going signals exhibit a considerably higher sampling rate (that is proportional to the magnitude of the underlying signal). The quality of the recovered negative-going signal is much poorer. This quality is inversely proportional to the magnitude of the underlying signal. In theory, a very deep red or a very deep blue stimulus of high magnitude can drive the pulse rate in the Stage 3 circuits to zero. For the duration of this situation, the output of the Stage 3 circuit will not change at all.

The literature has not reported the asymmetric performance of the signal projection circuits. However, this asymmetry is well known to magicians and has actually been recognized in the design of color television systems. The magician is well aware of the longer time to perceive a scene in the deep red and the deep blue regions relative to the green region. These facts were incorporated into the design of the NTSC color television system (and the subsequent PAL system).

14.6.5 The lead-lag network and the putative chemical synapse

The ability of the electrolytic synapse hypothesis to explain in detail the operation of the lead-lag networks associated with the circuits of Stage 3 forms a significant challenge to the concept of the chemical synapse.

The details of how a putative chemical synapse operates has never appeared in the literature. It has only been described generally as involving "chemical neurotransmitters" crossing the gap between the pre-- and post synaptic junction. The crossing has generally been assumed to be by diffusion. Such diffusion may be in the presence of an external density gradient, or a self-induced gradient. Such diffusion has not been shown capable of functioning as a complex transfer impedance involving both a resistive and a reactive component. A resistive impedance

(representative of a resistance or a diode) and a reactive impedance (representative of a capacitor) in parallel are needed to explain the role of the synapse in the lead-lag function. In fact, the diffusion of neurotransmitters has not been shown to exhibit the characteristics of a diode. The diffusion rate is normally proportional to the difference in field strength (whether electrically induced or due to a density gradient)

While the synapse is frequently described as having the characteristics of a diode, this is an oversimplification. The actual current delivered to the post-synaptic dendroplasm is not a function of the potential between the pre- and post synaptic terminals. It is a function of the potential between the pre-synaptic terminal and the inter neural matrix (INM). The underlying mechanism employs a three-terminal device. Such a semiconductor device is normally called an Activa (biological) or a transistor (man-made).

Section 2.4 of Chapter 2 of the author's work, "The Neuron and Neural System" addresses the multiple roles of the synapse and the Node of Ranvier in detail[91]. Section 14.8 of this chapter provides introductiory remarks relative to the subject of electrolytic versus chemical synapses.

The existence of a lead-lag network in the Stage 3 neural circuits of vision is strong evidence for the synapse relying upon an electrolytic as opposed to a chemical mechanism. Furthermore, the fact that the current through the synapse is not a function of the potential between the axoplasm and the dendroplasm confirms the three-terminal nature of the underlying mechanism. No description of a purely chemical mechanism exhibiting these properties has appeared. As Shown in Chapter 7, the materials labeled neurotransmitters are actually consitituents used on, or antagonists to, the electrostenolytic mechanism used to provide electrical power to the individual neurons of then neural system. These materials impact the operation of the overall neurons on a time scale of seconds but do not impadt the more rapid operation of the circuits related to signaling (within milliseconds) .

While the circuit diagrams shown in this work are proposed to be the actual circuits of neurology and not merely emulations, some readers may not be willing to accept the electrolytic nature of the synapse. They may wish to consider the above circuits only emulations of a yet undiscovered chemical mechanism supporting the synapse. They should recognize that the discovery of such a mechanism is not likely.

14.7 Analyses of Stage 3 data and cumulative data to Stage 3 EMPTY

14.7.1 Direct analyses of Stage 3 data and cumulative data to Stage 3

[xxx Look at Smoorenburg, et al. in detail Is it really R channel data or difference channel?]
[xxx details should be here with summary in Chapter 9]

Palmer & Evans have provided good data that can be used to quantify the performance of the Stage 3 projection neurons in the cat[92]. The data was recorded at either the cochlear nerve or the cochlear nucleus in response to a node A stimulus. While they did not specify whether their data applied to the Stage 3 neurons at the input or the output of the cochlear nucleus, it can be assumed it applied to the input because of its simple relationship to the stimulus.

They showed data for the number of action potential "spikes" during a 500 ms duration constant amplitude stimulus (rise and fall times of 5 ms) at various frequencies. The dashed lines in their figures represented tonal responses measured at the CF of the fiber in the absence of any applied masking noise. Each curve was the result of averaging 20 responses at that frequency. By overlaying the dashed lines in their figures 2, 3, 4 & 5, and re-scaling figure 4 for a 500 ms stimulus duration, **Figure 14.7.4-1** is obtained. The curves are the result of averaging

[91]Fulton, J. (20012) The Neuron and Neural System. *Published on line.* http://neuronresearch.net/neuron/

[92]Palmer, A. & Evans, E. (1982) Intensity coding in the auditory periphery of the cat: responses of cochlear nerve and cochlear nucleus neurons to signals in the presence of bandstop masking noise *Hear Res* vol. 7, pp 305-323

It can be seen that the maximum pulse rate of the ganglion neurons was between 200 and 250 pulses per second. This is similar to the maximum rate found in visual Stage 3 ganglion neurons. The re-scaling of figure 4 (fiber 829_{03}) assumed no affect of adaptation between these time sequences. The linearity of the responses within their operational range on semi-logarithmic coordinates suggests linear encoding by the ganglion neurons following logarithmic compression by the Stage 1 tonal sensor neurons (OHC). The uniformity of the histograms of the ganglion neurons also suggest linear encoding and little adaptation by the sensory neurons during the pulse duration. The spikes/bin in their figure 6 also suggest linear encoding following logarithmic compression by the sensory neurons. There is an indication of some short term adaptation during the pulse interval compatible with a time constant of xxx ms. Alternately, the initial overshoot could be due to a small amount of Stage 2 pre-emphasis.

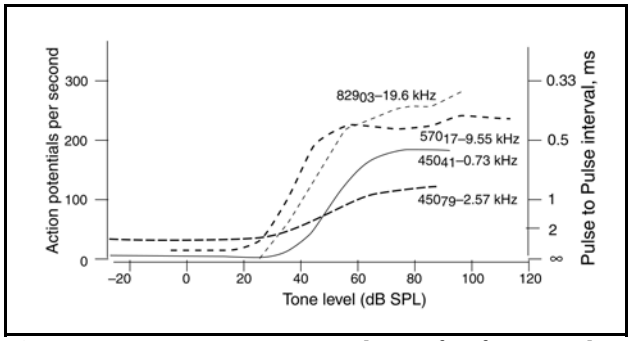

Figure 14.7.4-1 Action potential rate for four ganglion neurons, three from the auditory nerve and one from the dorsal cochlear nucleus (570_{17}). See text.

The low spontaneous rate for three of these ganglion encoders suggests they are driven oscillators (operating like the parasol ganglions of the retina). The spontaneous rates are primarily due to background acoustic energy. The smooth transition from a low spontaneous rate to the operational range suggests there was no significant thresholding at the input to the Stage 3 ganglion neurons. The relatively high spontaneous rate of fiber 450_{79} and its relatively low maximum pulse rate suggests this signal may have been created by a free-running ganglion neuron. Such neurons are found frequently in the visual system where they are labeled midget ganglion cells. They exhibit a differential input structure (with the signal in this case representing the positive-going, non-inverting input). For the free-running ganglion neurons, the method of encoding uses time delay modulation and not frequency modulation. This is a form of phase modulation where the pulse-to-pulse interval is varied. Thus the scale on the right would be appropriate for exploring this possibility further. Within the operating range, the response remains a straight line when plotted using log-log coordinates. It is nearly a straight line when using semi-log coordinates.

The protocol used by Palmer & Evans is open to question. They note, During the analysis there was visual feedback to the experimenter consisting of an updated plot of average spikes/stimulus versus signal level, on an oscilloscope slaved to the computer display." "The analysis was terminated when inspection of the updated display indicated that consistent averages had been obtained." This wording suggested that adaptation was encountered at the start of individual test sequences and eliminated in the final recorded data. The dynamic range of at least the three upper responses is on the order of 30 dB. This is consistent with the nominal dynamic range of 26 dB used elsewhere in this work. This is the "instantaneous" dynamic range in the absence of adaptation.

The histograms for dorsal cochlear neuron 323_{10} exposed to a pure tone at 8.7 kHz (their figure 6) show an infinitesimal spontaneous firing rate under their protocol for stimulus levels between102 and 32 dB SPL. Below 32 dB SPL, the firing rate in the absence of a tone begins to rise and essentially equals the rate during the tone at 12 dB SPL. Below 12 dB SPL, the firing rate is nominally equal to the background rate with or without the presence of the stimulus. On the other hand, the spikes/bin (and also the total number of spikes per stimulus interval) remains essentially constant for stimulus ranges of 62 to 102 dB SPL. These numbers suggest the kaumotopic audio regime (equivalent to scotopic regime in vision) extends up to 12–22 dB for this specimen. The mesotopic regime extends from this value up to 52–62 dB SPL. The phonotopic regime, of constant performance in spite of amplitude changes, extends from this value up to at least 92 dB SPL. It is clear from that figure and these values that a single tonal signaling channel can accommodate the required dynamic range when adaptation is allowed to occur.

When the dynamic range contributed by adaptation within the sensory neurons is introduced (40–50 dB), the paradox introduced by Palmer & Evans, and at the heart of their paper, is resolved. There is no need to consider a "population theory" of hearing operation (where multiple neurons are required in parallel to accommodate the observed dynamic range of a stimulus). Such theories have also been called volley theories.

[xxx see also Kiang 65 fig 6.10 and Rose 71 fig 9]

14.7.1.1 The biochemistry of the Stage 3 neurons

Wenthold & Martin have provided material on the biochemistry of the Stage 3 neurons with particular emphasis on the role of glutamate and aspartate in their operation[93]. Although their discussion is based on the chemical theory of the neuron, the data is compatible with the Electrolytic Theory of the Neuron relied upon here. Their extensive list of references shows a clear role of glutamate and aspartate in the operation of these neurons and the lack of such participation by acetylcholine. Glutamate and Aspartate are the primary sources of electrostenolytic (electrical) power to operate the neurons. They operate as neuro-facilitators rather than the conventional view that they are neurotransmitters, a role filled by electrons rather than chemicals.

Wenthold & Martin also discuss the role of GABA and glycine, and their relatively high concentrations within the cochlear nucleus. Their position is in agreement with this work in describing both GABA and glycine as neuro-inhibitors. Normally, they are the residue of the electrostenolytic process powering the neurons. The excessive buildup of these neuro-inhibitors near a neuron is a clear source of inhibition.

14.7.1.2 Limitations on rate encoding and discrimination

The majority of the ganglion neurons of Stage 3 are rate limited to less than 300 action potential pulses per second. This is true of both the auditory and visual systems. On the other hand, Johnson and others have recorded pulse rates of up to at least 550 AP/sec in cats responding to low frequencies (less than one kHz). Since 300 AP/sec is the highest clock frequency to be expected in-vivo, the stellate decoding neurons have been optimized to accept up to this pulse rate. This limitation on the maximum acceptable rate of about 300 Hz for stimulating the stellate cells has been well documented[94]. Carlyon & Deeks even note that this rate cannot be exceeded by direct electrical stimulation in the course of research with implanted hearing aids. They provide a variety of additional references. [xxx May have to rewrite or clarify –Carlyon & Deeks were not measuring AP but were apparently pulsing the nodes of Ranvier within the system]

14.7.2 Indirect analyses of cumulative data to Stage 3

Liberman & Kiang have noted “abnormal” signals in the optic nerve of cat[95]. These signals can be interpreted in several ways. They can be differentiated into those exhibiting a broadband response with no narrowband content and those characterized by a narrowband peak frequently associated with a lower level broadband content. They can also be divided into those waveforms exhibiting a near zero spontaneous rate and those exhibiting a nominal spontaneous rate. The broadband responses with no narrowband content will be defined as intensity signals here. They will be defined as developed from signals originating in the IHCs. Most of the broadband signals are found in channels with a near zero spontaneous rate. The narrowband peak signals will be defined as chromatic signals originating in the OHCs. The narrowband signals are occasionally found associated with channels exhibiting near zero spontaneous rates. Alternately, they are often found associated with high spontaneous rate channels. [xxx prepare a matrix]

Figure 14.7.4-2 shows the typical pattern of action potential generation within the auditory nerve of cat. Note the significant number of units exhibiting a zero spontaneous rate of action potential generation (over 16%). The absolute background level during these experiments was not specified. It can be assumed that some of the units with very low spontaneous rates should be classified as zero rate units in the absence of background sound. This would bring the population of zero spontaneous rate units to about 20%. The units with a finite spontaneous rate is generally monomodal, although many authors have defined it as bimodal. While not clearly identified, the mean spontaneous rate is on the order of 60 spikes/sec. Other studies have provided a mean rate closer to 30-50 spikes/sec.

---

[93]Wenthold, R. & Martin, M. (1984) Neurotransmitters of the auditory nerve and central auditory system *In* Berlin, C. Hearing Science. Philadelphia, Pa: Taylor & Francis Chapter 10, pp 342-369

[94]Carlyon, R. & Deeks, J. (2002) Limitations on rate discrimination *J Acoust Soc Am* vol. 112(3), pt 1, pp 1009-1014

[95]Liberman, M. & Kiang, N. (1978) Acoustic trauma in cats *Acta Oto-laryngol suppl* 358 pp 1-63

The measurement of signals associated with the auditory nerve are frequently performed over very large stimulus ranges (greater than 60 dB). Based on similar circuits in the visual system, it can be concluded that the instantaneous dynamic range of stage 2, 3 and 4 neural circuits is usually less than 45 dB. Based on this analogy, it can be assumed that the large dynamic ranges measured are due partly to adaptation within the stage 1 neurons. Individual protocols need to be examined very carefully to determine if the investigator performed his measurements over time intervals long with respect to the adaptation time constants. In general, the test stimulus durations were longer than the adaptation time constant. As a result, the recorded signals represent a dynamic situation exhibiting a larger dynamic range than expected from a static circuit. This provides a partial explanation for the frequently encountered waveforms containing a narrow peak and a broad low level background. Such diagrams are frequently characterized as containing a "tip" and "xxx."

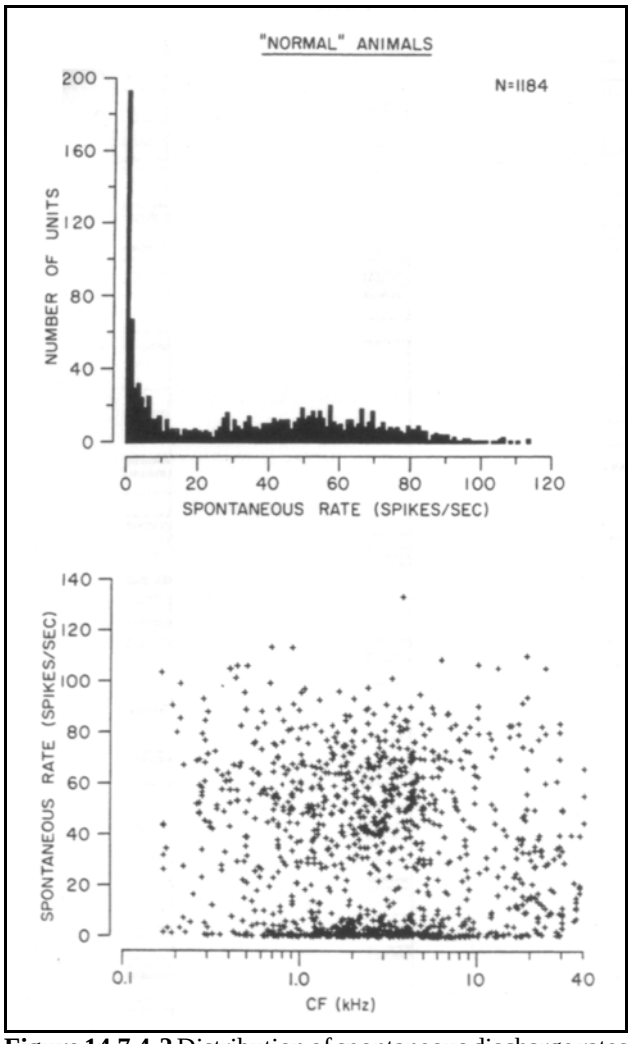

Figure 14.7.4-2 Distribution of spontaneous discharge rates for normal cats (n = 11). From Liberman & Kiang, 1978.

Figure 14.7.4-3 provides a wealth of background information concerning stage 3 signal projection. The upper frame shows two waveforms typical of the chromatic channels (on the left) and two waveforms typical of the intensity channels (on the right). Unit 66-69 shows a significant loss of sensitivity compared to unit 81-62 (these were obtained during traumatic acoustic experiments).

The lower frames of the figure illustrates the time constant problem in auditory nerve measurements. The use of histograms introduces a host of problems related to the technique itself (**Section 1.xxx**). However, it is a source of considerable information in the current literature. The overall sample interval was 30 seconds. The length of the individual test stimuli was not stated explicitly. However, the change in the pulse rate with time is clear. A time constant of about 50 milliseconds can be associated with the three samples on the left. A time constant of about 25 to 35 milliseconds can be associated with unit 72-33. All of these units showed nominal spontaneous rates of action potential generation. However, the background acoustic level was not specified for these experiments (it was stated that the sound level in the unexplored ear was typically 40 dB below that of the ear under evaluation).

These time constants are compatible with other measurements. They suggest that the auditory system of cat adapts very quickly to changes in stimulus level. As a result, the length of the stimulus used in virtually all laboratory measurements must be considered longer than the adaptation interval.

It is proposed that frequency spectrum of unit 81-62 represents the narrowband frequency spectrum associated with the chromatic channels (lowest 45 dB of the pressure range) plus a broadband component due to leakage of broadband signal from Hensen's Stripe into the OHC sensors. This assertion will be explored more fully in the remainder of this Chapter.

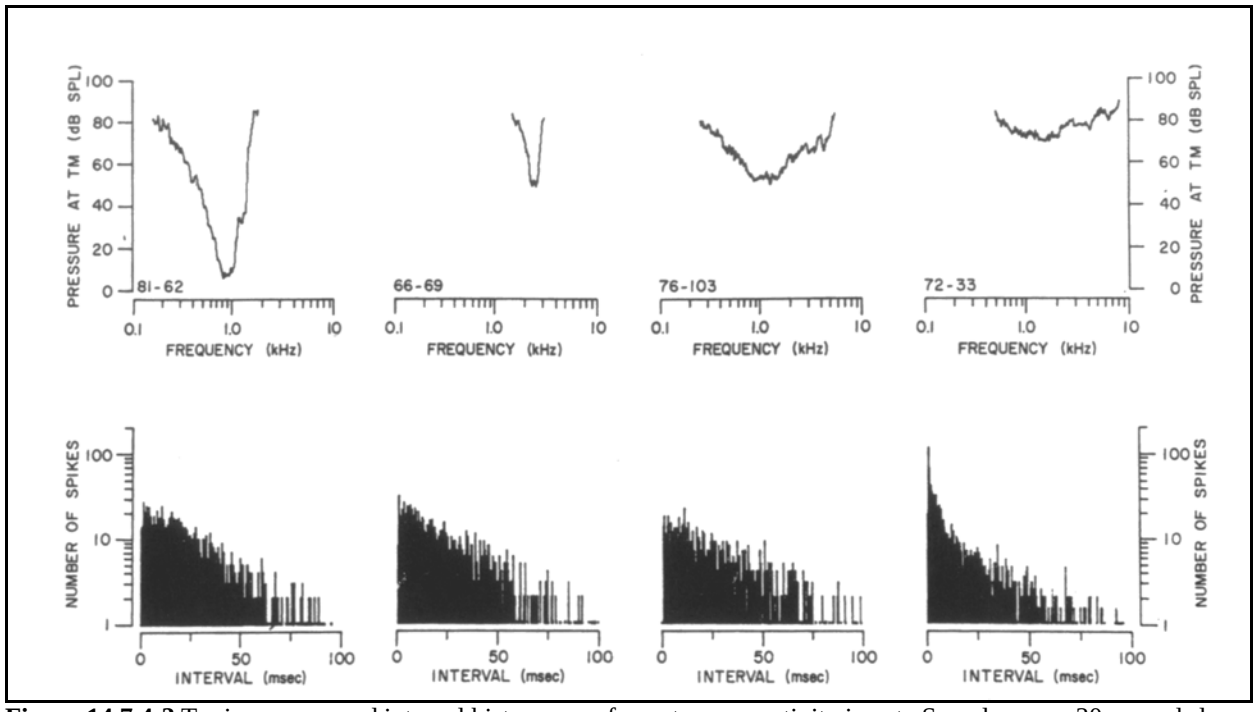

Figure 14.7.4-3 Tuning curves and interval histograms of spontaneous activity in cat. Samples were 30 seconds long. Bin width on each measurement was 500 microseconds. The average rate of discharge for these four units were, from left to right, 41, 40, 32 and 37 spikes/per second. From Liberman & Kiang, 1978.

14.7.1.1 Signals associated with the differencing channels

Gelfand provided a caricature of the action potential stream generated in the auditory nerve in response to a variable amplitude stimulus[96]. While reasonable, it only applies to the action potential stream associated with a finite "spontaneous rate." Such a spontaneous rate is characteristic of a midget ganglion cell of the spiral ganglia. Midget ganglia react to electrically bipolar input signals. While he shows the pulse rate increasing in the presence of a stimulus, he does not show the equivalent decrease in the rate in the presence of the stimulus of opposite polarity.

14.7.1.2 Signals associated with the summing channels

Parasol ganglion cells are found in vision associated with action potential streams that respond to electrically monopolar signals. The exhibit a negligible "spontaneous rate." The rate of action potentials is due to the phase modulation of the pulses in response to stimulus amplitude. An absence of pulses (infinite duration between pulses) is indicative of no stimulation. Duration is reduced in proportion to the amplitude of the stimulus.

14.8 The synapse in functional context

As noted earlier, there are two major functional roles for synapses;
• the transfer of information from an axon or axon segment to the next orthodromic axon segment or neurite of the neural modality and of the electrolytic type or,
• the transfer of commands to activate a muscle or gland from a stage 6 neuron to a muscle or gland and of the chemical type.

[96]Gelfand, S. (1998) Hearing NY: Marcel Dekker pg 184

In some contexts of this chapter and in all contexts of chapter 2 of the more recent work designated below, a modified stage 6 neuron, capable of emitting a range of chemicals at its pedicle, has been designated a stage 7 neuron.

The vast majority, probably exceeding 99% of neurons are involved in signal transfer *within* the neural modality (stages 1 through 6) and are of the *electrolytic* type. Less than 1% of neurons are involved in the release of chemical substances (primarily at the muscle/glandular interfaces of stage 7) and therefore of the *chemical* type.

The vast majority, probably exceeding 95% of neurons are involved in analog signal transfer *within* the neural modality (stages 1 through 6). Less than 5% of neurons exhibit myelinated axons, output phasic signals and thus generate action potentials (**Section 10.1.1.2**).

> It is difficult to calculate the 95% value because the total number of neurons in a given animal neural system remains unknown. The number for the human neural system appears to increase by a factor of ten about every decade or two as the available instrumentation improves.

All known morphologically defined Nodes of Ranvier involve the transfer of signals between axon segments without involving any chemicals directly in the transfer. They are all of the *electrolytic* type.

Section 2.4 of Chapter 2 of the author's work, "The Neuron and Neural System" addresses the multiple roles of the synapse and the Node of Ranvier in detail[97].

14.9 Summary

[xxx 7.5.3 SUMMARY of the properties of the Stage 2 & 3 signaling neurons]

[xxx prepare table like but different from Kim in Berlin pgs 243,245 257, expand]

14.9.1 Form of the signals presented to the brain

Although this work will not proceed beyond the signaling related to the "straight through" path and the associated chrominance and geometrical paths, the general nature of the signals presented to the higher perceptual centers of the brain can be defined. Without knowing the degree of convergence related to a given ganglion cell and its associated signaling channels, the retinal area related to this ganglion cell can be defined as a zone. The signals presented to the higher perceptual centers associated with this zone can be defined approximately. They consist of:

> + some form of time and retinal location tags
>
> + a single luminance field normally providing geometric position information (for $\delta\phi < K$) and illumination level information (for $\delta\phi > K$).
>
> + two chrominance fields, one containing a biphase value providing L - M hue information and one containing a biphase value providing S - M hue information.

In the man made environment of today, the luminance field value for $\delta\phi < K$ may actually relate to a sudden temporal change in brightness rather than (or as well as) geometric position data.

For $\delta\phi < K$ in the luminance channel, it is probable that the chrominance field information is discarded as extraneous. This avoids a problem encountered by man in early day multi-spectral earth resources satellites; the satellite would sense a road going through a farm field in terms of illuminance. It would report a chrominance value in each spectral channel for the edge of the road that averaged the value for the road surface and the adjacent field; on the ground, a look up table was used to determine the crop growing in each pixel of the imagery--the result was a report that the road through a corn field was lined with peas. See the comments regarding the analogy with color television below.

---

[97] Fulton, J. (20012) The Neuron and Neural System. *Published on line*. http://neuronresearch.net/neuron/

Because of the limited amplitude of the continuous tremor, the distortion of the physiological optical system, the variation in the size of photoreceptors with retinal location, and the level of convergence/divergence in the retinal signal processing; the detailed content of the zone records defined above and the manner in which they are used in the higher cortical processing may be different than for the “straight through” path signals.

14.9.2 Analogies with color television

[[Expand to include digital television and full frame memory]]

The form of the data passed from the decoding circuitry to the perception centers of the brain can now be compared with the form of this data surmised by the National Television Standards Committee (NTSC) in the 1950’s. This committee was charged with the development of the color television system used (with a variety of minor modifications to meet practical constraints) in most of the world to this day. One of the primary tasks of that committee was to ascertain the physiological parameters of human color vision. It ascertained three principle facts;

+ in areas of fine detail, a chrominance signal was not required, the eye would perceive the area as containing the same color as the surrounding area.

+ it was important to transmit the L-channel minus M-channel difference information in a wider frequency channel than the S-channel minus M-channel difference information. This insured that any large scene elements would be perceived as of uniform hue, even in the regions near sharp luminance transitions or fine detail.

+ the human eye was not able to distinguish absolute hues or luminances. A color image would be perceived in an acceptable manner even if the absolute color range was translated over a significant part of the visual spectrum, unless there was a local reference available to the viewer for comparison. If there was a local reference available, the visual system was then very discerning of any differences between the television picture and the local reference.

+ it was important to transmit spectral information that was accurate in the region between **XXX and XXX.** This wide range was a problem for early color display devices which did not provide a L-channel phosphor with a response far enough into the red region of the spectrum. Current display devices utilize phosphors with a peak response remarkably close to the absorption peaks of the human eye, XXX, XXX, and XXX.

The resultant NTSC specification called for the widest possible bandwidth luminance channel in order to provide faithful reproduction of high contrast edges and two asymmetric chrominance channels of more limited bandwidth; with the L-channel wider than the S-channel, a system that came to be known as the “mixed highs”. In order to optimize transmission channel capacity, the modulation system chosen was such as to transmit both spatial (luminance) and chrominance information in a complex synchronous phase modulation technique utilizing a temporal reference pulse in order to reconstruct the image at the receiver.

The conceptual comparison between the NTSC color television system and the human visual system it was meant to serve is satisfying. The engineering decisions made at that time based on physiological testing resulted in a system that is very similar to the system it was designed to serve in an optimum manner.

14.9.3 Analogies with digital television

With the explosion in the capabilities of micro-electronics, it has become possible to provide a full frame memory store, of about 360,000 digital words, that can be refreshed every one-thirtieth of a second inexpensively. Furthermore, this refresh process can introduce a different digital word in individual address locations within the complete memory. This capability was first used in the 1980's to provide real time conversion between European and North American television transmissions. In the 1990's, it became so inexpensive that it is used in every television broadcast satellite, as opposed to television relay satellites. In the 2000's, all terrestrial television transmissions will also adopt a full frame memory at each receiver.

The above capability is architecturally the same as the vision system in animals with one principle difference. Whereas, digital television employs a scanning process to convert a two dimension image into a serial word (and bit) stream, the eye employs an n-wide parallel word stream.

14.9.4 Background with respect to the optic nerve in chordata

The purpose of Stage 3 signal processing is straight forward--encode all of the information received by the retina in as compact a form as possible compatible with efficient recovery of the data using simple realizable circuits, while providing adequate reliability over the life span of the animal.

The problem includes two principle aspects; providing an addressing scheme that allows the information to be properly interpreted in the brain, and providing simple coding schemes for the actual data. There are a great variety of addressing and coding schemes that could be used.

----------xxx
In the higher vertebrates, the brain uses the signal sent to the muscles of the eye to cause this tremor as a reference signal for purposes of demodulating, i. e. decoding, the signals received over the optic nerve. Thus the visual process employs a synchronous demodulator and there is a closed loop in the visual system which consists of :

+ the oscillator in the brain that controls the continuous tremor of the eye.
+ the muscles of the eye which causes a continuous scanning motion
+ the product of the scene presented to the photoreceptors of the eye and the angular motion of the photoreceptors caused by the muscles
+ the modulation performed by the ganglion cells in what appears to be an asynchronous manner
+ the synchronous demodulation performed in the brain to recover the information related to the scene through the multiplication of the signals received from the ganglion cells by the original oscillator signal.
+ the delivery of the demodulated information to the higher levels of the brain for perceptual processing and recognition

There is a considerable delay in this servo loop due to the relatively low transport velocity associated with the electrolytic nature of the neural pathways compared to that found in metallic circuits. This delay is apparently measured by the brain and compensated for at a very early age, during what might be called the boot-up operation in computer language .

----------xxx
In the lower animals, the absence of the continuous tremor leads to a different mode of operation of the visual system. The system relies on motion in the scene itself to generate changes in the output of the photoreceptors for transmission to the brain. These changes are modulated by the ganglion cells, where necessary due to distance, and transmitted to the brain for demodulation. In the very simplest animals, where the eye is immediately adjacent to the "brain", the modulation and demodulation steps may be omitted. In either of these cases, the only information received at the brain is due to the motion of parts of the external scene. In the absence of motion, or rapid changes in illumination, the animal is blind.

----------xxx
There are a number of intermediate modes related to the modulation/demodulation process outlined above, including a variety of hybrids.

14.9.4.1 Hybrid #1, higher vertebrates xxx

With the rotational flexibility of the eye in the chordate animals, several hybrid operating modes must be examined. The simplest is to consider how the eye operates during periods of rapid angular movement, versus how it operates once fixation has been achieved with respect to a given scene element.
When the eye commands a change in the point of visual fixation, it ceases to generate signals calling for continuous tremor and issues a command for mor gross muscular activity associated with rapid angular eye movement. In the human, the data received by the brain during rapid motion of the eye is essentially useless and the brain usually commands the eyelid closed during this interval to avoid contamination of the visual database. Since the eye operates in an open loop manner during the rapid angular eye movements, the brain commands the eyelid open based on a calculated time for the eye to arrive at the desired fixation coordinates. New data is then collected by the brain, after reinstituting continuous tremor, and if necessary further corrections are made in pointing. Although the brain has access to inputs from other sensory elements in order to command the motions of the eyes, the system is subject to a number of errors which can lead to the condition known as vertigo, where the visual perception system is confused by the information it receives and essentially tells the higher perceptual centers that it is in trouble.

14.9.4.2 Hybrid #1, the cat XXX

It appears that the cat family, including the common house cat, use the continuous tremor of the eye when they are operating in the "navigation mode" to see their environment and where they are going; but suppress the continuous tremor, at least to a degree, after they have located their prey and go into the "feeding mode". By suppressing the continuous tremor, either totally or partially, the visual system of the cat suppresses other imagery in its perceptual field in order to concentrate on the motions of the prey. And as is well known, once the prey stops moving, the cat loses its interest in it rapidly unless its taste and smell receptors tell it to eat the prey. The cat seems to change character completely as it returns to the "navigation mode", showing increased interest in its surroundings.

14.9.5 Future test equipment configurations

[xxx broaden to include all test configurations and address analog versus phasic components meeting the needs of the cochlear microphonic, section 4.1.3 in hearing Emphasize that the OHC and IHC channels are fundamentally different]
The significant variation in neural system performance as a function of temperature must not be overlooked in future investigations. Variations of a factor of xxx are encountered between 20 C and 37 C. Failing to control, or at least record, temperature to a precision of ±0.1 C will limit the utility of the data obtained.

Future investigators should plan to incorporate the appropriate modulation decoding circuits in their test equipment to augment their histogram generating software. When examining the broadband channels, at node F of Stage 3, a simple delta-modulation circuit is adequate. When examining the tonal channels, at node F of Stage 3, a phase (not frequency) demodulator should be used. Both of these circuits can be as simple as those biological circuits described within this chapter.

When recording voltage waveforms at the output of the propagation neurons, it is important to measure the DC potential of the signal before after and during the signal. Otherwise the operating parameters of the circuit cannot be properly described. If the tests are performed *in-vivo*, the local potential of the inter-neural matrix, INM, should be used as a reference. These are especially important protocol steps if AC amplifiers and waveform summation procedures are adopted to recover the signals in the presence of stray noise. Recording the DC potential will also aid in differentiating between signals recorded in the initial segment and subsequent axonal segments of a single neuron versus those recorded from the dendroplasm of the encoding neuron or a Node of Ranvier.

[xxx talk about two types of decoders]
Care must be taken to distinguish between a time-delay modulation decoder and an FM decoder. An FM decoder will generate gibberish when supplied with a time-delay encoded signal.

14.9.6 Introduction of a revised rate histogram EMPTY

[xxx discuss and reference **Section xxx** where it is used]
[xxx differentiate between summation channel scales and differencing channel scales]

Chapter 14 Table of Contents (20 November 2018)

14.1 Introduction 1
14.1.1 Original perspective of chapter 2
14.1.2 Plan of discussion EXPAND 2
14.1.3 Background (using vision as a framework) 3
14.1.3.1 Fundamental physical architectures of the Phylogenic Tree 3
14.1.3.1.1 Architecture of Arthropoda 3
14.1.3.1.2 Architecture of *Mollusca* 5
14.1.3.1.3 Architecture of *Chordata* 6
14.1.3.3.2 Description of the signal projection paths in *Chordata* 6
14.1.4 Introduction focused on hearing 8
14.1.4.1 Background literature from hearing 10
14.1.4.2 Importance of synchronous data recording 12
14.1.5 Requirements in future test protocols and equipment configurations 12
14.2 Neural coding: architecture, modes & mechanisms 13
14.2.1 The utility of conformal transforms in information analysis 13
14.2.1.1 The arrangement of planes for purposes of coincidence detection and correlation 15
14.2.1.2 The more complex conformal transformations used in vision 15
14.2.1.3 The more complex Riemann conformal transform in hearing 15
14.2.2 Route conservation as a major tool in neural systems 16
14.2.3 The translation of the analog information into the phasic domain by encoding 16
14.3 The actual codes used in signal propagation 17
14.3.1 The Neural Code used in the magnacellular (brightness) and other monopolar pathways 18
14.3.1.1 The IRIG description of the code 19
14.3.1.1.1 An IRIG encoder compatible with a stage 3A neuron 20
14.3.2 The Neural Code used in the parvocellular (chrominance) and other bipolar pathways . . 21
14.3.3 The Transfer Functions for the Sum & Difference Neural Codes 21
14.3.4 Examples of sound encoding 22
XXX Vision related stuff 23
14.2.1 Field mapping in vision 24
14.2.1.2 Retinal field mapping 24
14.2.1.2.1 Retinal mapping requirements in man 25
14.2.1.2.2 Retinal mapping requirements of the awareness mode 26
14.2.1.2.3 Retinal mapping requirements of the analytical mode 27
14.2.1.2.5 The role of color data in the awareness and analytical modes 28
14.2.1.3 Mapping theory 28
14.2.1.3.1 Background 28
14.2.1.3.2 Nominal architecture 29
14.2.1.4 Role of physiological optics in retinal mapping 30
14.2.1.5 Delay as a factor in retinal mapping 30
14.2.1.5.1 Delay associated with Meyer's loop EMPTY 30
14.2.2 Signal coding 30
14.2.2.1 Introduction to signal encoding and modulation 32
14.2.2.1.1 Frequency versus phase modulation 33
14.2.2.1 Luminance coding 33
14.2.2.1.2 Luminance coding at the LGN 33
14.2.2.2 Chrominance coding EMPTY 34
14.2.2.2.1 Chrominance coding in the optic nerve 35
14.2.2.2.2 Chrominance coding at the LGN 36
14.2.3 Coding theory applicable to neural systems 36
14.2.3.1 The unique features of the action potential EMPTY 37
14.2.3.2 The driven stream of action potentials 37
14.2.3.3 The free-running stream of action potentials 38
14.2.3.4 Relevant data EMPTY 38
14.2.4 Functional Encoding 38

14.3.2 Encoding 38
14.3.2.1 Details of the encoding of the monophase signal EMPTY 39
14.3.2.2 Details of the encoding of the biphase signal EMPTY 39
14.3.3 Transmission 39
14.3.4 Decoding 39
14.3.4.1 Linear versus antilogarithmic decoding 40
14.3.4.2 Details of the decoding of the monophase signal 40
14.3.4.3 Details of the decoding of the biphase signal 41
14.3.5 Form of the decoded information 41
14.3.5.1 Luminance related signals 41
14.3.5.1.1 Form EMPTY 41
14.3.5.1.2 Motion EMPTY 41
14.3.5.1.3 Brightness EMPTY 41
14.3.5.2 Chrominance related signals 41
14.3.5.2.1 Hue 41
14.3.5.2.2 Saturation 42
14.3.5.3 Composite information map in vector space 42
14.3 Overview of Stage 3 operation and performance norms 42
14.3.1 Types of encoding used in vision, hearing, etc. 43
14.3.1.1 Evidence of differential encoding in hearing 43
14.3.2 Details of the projection neuron circuits EMPTY 43
14.3.2.1 Details of the stage 3 encoding circuits EMPTY 43
14.3.2.2 The action potential (AP) versus pseudo-action potentials 44
14.3.2.2 Details of the stages 3B & 3BP decoding circuits EDIT 47
14.6.1.6 The waveforms at the pedicle of the stellate cell 49
14.3.2.3 The end-to-end transfer function for a Stage 3 circuit 50
14.3.2.3.1 The transfer function supporting the Alarm mode 54
14.3.2.3.2 The transfer function supporting the Awareness mode 54
14.3.3 The quiescent operating conditions associated with Stage 3 EMPTY 54
14.3.3.1 The quiescent DC potential at the Stage 3 Alarm mode EMPTY 54
14.3.3.1.1 The quiescent DC potential at the Stage 3 Alarm mode EMPTY . 54
14.3.3.1.1 The quiescent DC potential at the Stage 3 Awareness mode EMPTY 54
14.3.3.2 The quiescent noise conditions associated with stage 3 EMPTY 54
14.3.3.2.1 Comparison of the noise in the visual and hearing systems EMPTY 54
14.3.4 How temporal signal asymmetry is handled in vision 54
14.4 Specific coding applications by sensor modality 54
14.4.1 Coding architectures used by all sensory modalities 55
14.4.1.1 Spatial encoding for purposes of temporal (frequency filtering) 55
14.4.1.2 Spatial encoding for purposes of Optic Nerve minimization–Phantom circuits 55
14.4.1.3 Many to one versus many to a few 56
14.4.2 The architecture of spatial encoding relative to vision 56
14.4.2.1 The architecture of spatial encoding relative to the retina EMPTY . 57
14.4.2.2 The spatial encoding as presented to the LGN EMPTY 57
14.4.2.3 The spatial encoding as presented to the pretectum EMPTY 57
14.4.2.4 Spatial encoding remote from the retina 57
14.4.3 The architecture of acoustic frequency encoding relative to hearing EMPTY 57
14.4.3.1 The coding of neural signals in hearing EMPTY 57
14.4.3.1.1 Coding concepts applicable to hearing 57
14.4.3.2 The coding of simple signals within stage 3 EMPTY 58
14.4.3.3 The coding of complex signals within stage 3 EMPTY 58
14.4.3.4 Ensemble coding 59
14.4.4 The architecture of spatial encoding relative to somatosensory performance RESERVED 59
14.4.5 The architecture of spatial encoding relative to taste and smell RESERVED 59
14.4.6 The use of histograms to interpret neurological signals BRIEF 59
14.4.6.1 The use of histograms to interpret auditory data 59
14.4.6.2 A new, revised histogram for hearing research BRIEF 62
14.4.6.3 Transformation of older histograms to the revised format EDIT 63

14.4.6.4 Theoretical and real tone-test representations using the revised histogram . . . 67
14.4.6.4.1 Test data applicable to the primary signaling channels 67
14.4.6.4.2 Test data applicable to the additive signal processing channels . . . 67
MERGE Two-tone test data shown in histograms of additive channels 68
14.4.6.4.3 Test data applicable to the subtractive processing channels 68
MERGE Two-tone test data shown in histograms of subtractive channels . . . 68
14.4.6.5 More complex signal processing prior to node F 68
14.4.6.6 Three-tone test data shown in histograms 68
14.4.6.7 The use of histograms to interpret cumulative data in mammals SHOW 68
14.4.6.7.1 Background EMPTY 68
14.4.6.7.2 Examples from squirrel monkey (showing phase shift) 68
14.4.6.7.3 Examples from cat 68
14.4.6.7.4 Examples from guinea-pig 69
14.5 Operation of the Stage 3, Signal Projection circuits 69
14.5.1 The Activa within a neuron 69
14.5.1.1 DC potentials within a ganglion cell 71
14.5.1.2 AC potentials within a ganglion cell 73
14.5.2 Block diagrams for the Stage 3, Signal Projection circuits 74
14.5.3 Circuit elements critical to Stage 3, Signal Projection circuits 74
14.5.4 Circuit diagrams for the Stage 3, Signal Projection circuits 79
14.5.4.1 Circuits for conveying monopolar (primarily luminance) signals 83
14.5.4.2 Circuits for conveying bipolar (primarily chrominance) signals 83
14.5.4.3 Signals recovered from the projection circuits 83
14.5.4.4 Commissure circuits EDIT 85
14.5.4.4.1 Commissure histograms EMPTY 88
14.5.4.5 Other efferent neural circuits 88
14.5.5 Transfer functions for Stage 3 Circuits 88
14.6 Performance of Stage 3 circuits 89
14.6.1 Predicted performance of the individual circuits 90
14.6.1.1 The Lead-lag network of the ganglion circuit 90
14.6.1.1.1 Background 91
14.6.1.2 The ganglion circuit as a driven monopulse oscillator 92
14.6.1.2.1 Routine operation of the driven monopulse oscillator 93
14.6.1.2.2 Routine operation of the driven free-running pulse oscillator 94
14.6.1.2.3 Nominal pulse intervals and frequencies 96
14.6.1.2.4 Reported pulse intervals and frequencies 96
14.6.1.3 The Node or Ranvier as a driven monopulse oscillator 98
14.6.1.3.1 The axon segment as a transmission line and filter 98
14.6.1.3.2 The predicted waveforms at a Node of Ranvier 99
14.6.1.3.3 The delay associated with the oscillator 100
14.6.1.4 The waveforms at the pedicle of the ganglion cell 100
14.6.1.5 The waveforms at the pedicle of the stellate cell 100
14.6.2 Predicted performance of the cascaded circuits 101
14.6.2.1 Problems with the “On--” and “Off--” signal nomenclature 102
14.6.2.2 Problems with the location of the probe within the system 103
14.6.3 Reported Stage 3 performance 103
14.6.3.1 Common measurement techniques 104
14.6.3.2 Data from Limulus 104
14.6.3.2.1 The summing type eccentric cell 105
14.6.3.2.2 The eccentric cells of Limulus 107
14.6.3.2.3 The next steps in *Limulus* research 113
14.6.3.3 Data from rat 114
14.6.3.4 Data from cat 114
14.6.3.5 Data from macaque monkeys 116
14.6.3.6 Data from humans 117
14.6.3.7 The comprehensive review by Destexhe et al. 117
14.6.3.7.1 The 2003 Destexhe et al. paper 118
14.6.4 Asymmetry in Stage 3 performance 122
14.6.5 The lead-lag network and the putative chemical synapse 122
14.7 Analyses of Stage 3 data and cumulative data to Stage 3 EMPTY 123

14.7.1 Direct analyses of Stage 3 data and cumulative data to Stage 3 123
14.7.1.1 The biochemistry of the Stage 3 neurons 124
14.7.1.2 Limitations on rate encoding and discrimination 125
14.7.2 Indirect analyses of cumulative data to Stage 3 125
14.7.1.1 Signals associated with the differencing channels 127
14.7.1.2 Signals associated with the summing channels 127
14.8 The synapse in functional context 127
14.9 Summary 128
14.9.1 Form of the signals presented to the brain 128
14.9.2 Analogies with color television 129
14.9.3 Analogies with digital television 129
14.9.4 Background with respect to the optic nerve in chordata 129
14.9.4.1 Hybrid #1, higher vertebrates 130
14.9.4.2 Hybrid #1, the cat XXX 130
14.9.5 Future test equipment configurations 131
14.9.6 Introduction of a revised rate histogram EMPTY 131

List of Figures (20 November 2018)

Figure 14.1.3-1 Architecture of the visual system of *Arthropoda* 4
Figure 14.1.3-2 Architecture of the visual system of *Mollusca.* 5
Figure 14.1.3-3 Architecture of the visual system of *Chordata*. Empty 6
Figure 14.1.3-4 Top neural block diagram of the visual system of Chordata 7
Figure 14.1.3-5 Fundamental architecture of the signal projection paths of chordate vision EXPAND 8
Figure 14.1.3-6 Stage 3 afferent signal projection overview. 9
Figure 14.1.3-7 Fundamental circuit diagram of hearing EDIT 10
Figure 14.2.1-1 Top level description of tertiary signaling 14
Figure 14.2.1-2 Top level description of the Stage 3 signal path 17
Figure 14.3.1-1 A typical encoder circuit satisfying the IRIG Standard 106-96 20
Figure 14.3.3-1 The steady state transfer functions of the stage 3A encoding neurons 22
Figure 14.3.3-2 Examples of the place code used in the neural system 23
Figure 14.3.4-1 Fundamental coding architectures used in the peripheral retina 31
Figure 14.3.4-2 Details of the coding architecture used in the retinas 32
Figure 14.3.9-1 XXX XXX 40
Figure 14.3.9-2 XXX XXX 42
Figure 14.4.1-1 Basic structure of a ganglion projection neuron as found in the auditory system 43
Figure 14.4.2-1 The nominal transfer function of a ganglion neuron 44
Figure 14.4.2-2 The Action Potential (AP) versus the pseudo AP SCREWED 45
Figure 14.4.2-3 Generic stage 3B decoding circuit of the neurological system EXPAND 48
Figure 14.4.2-4 Generic stage 3BP decoding circuit with isolated reference source 49
Figure 14.4.2-5 Signals recovered from the output of signal projection circuits 50
Figure 14.4.2-6 The performance of a combined ganglion cell and stellate cell of stage 3 52
Figure 14.4.2-7 The overall transfer function of a Stage 3 projection circuit 53
Figure 14.5.1-1 Intracortical circuits at the cerebral cortex 55
Figure 14.5.1-2 Diversity summing in time to achieve spatial filtering 55
Figure 14.5.6-1 The form of a simple histogram ADD 60
Figure 14.5.6-2 A period histogram prepared from the discharge pattern of a ganglion cell 61
Figure 14.5.7-1 The revised rate histogram applicable to auditory research 63
Figure 14.5.7-2 The conversion of a discharge rate histogram to a inter-pulse time interval histogram 66
Figure 14.5.8-1 Using the revised histogram for type B (IHC) and type N (OHC) 67
Figure 14.6.1-1 Electron micrograph of a pyramidal cell in the visual cortex of the rat 69
Figure 14.6.1-2 Caricature of the rat pyramidal cell 70
Figure 14.6.3-1 The fundamental structure of stage 3 neural circuitry 75
Figure 14.6.3-2 EMPTY The simple concept of a ganglion neuron as a series of conduits 76
Figure 14.6.3-3 The morphology and topology of an axon segment ADD 77
Figure 14.6.3-4 The topography and topology of an axon segment 77
Figure 14.6.4-1 The fundamental circuit configuration of the visual system xxx 80
Figure 14.6.4-2 Optional circuit diagram 81
Figure 14.6.4-3 Generic Stage 3 circuit diagram 82
Figure 14.6.4-4 Alternate signal recovery circuits of Stage 3 84
Figure 14.6.4-5 The major neural paths of the human brain based on diffusion MRI 86
Figure 14.6.4-6 Difference in myelination between neurons of the commissure of the CNS and nerves ADD . . . 87
Figure 14.6.5-1 The nominal transfer function of Stage 3 ganglion & stellate neurons ADD 89
Figure 14.7.1-1 Conceptual and nominal performance of a lead-lag network 91
Figure 14.7.1-2 The potential at the base of a driven monopulse oscillator (pyramid type ganglion cell) 93
Figure 14.7.1-3 The potential at the base of a free-running monopulse oscillator (midget type ganglion cell) 95
Figure 14.7.1-4 The waveform at the base terminal of a driven monopulse oscillator of the an “off-” type 96
Figure 14.7.1-5 The output pulse environment of an action pulse generator 96
Figure 14.7.1-6 Histogram (spectrogram) of the P (brightness) and M (chrominance) channels of the optic nerve 97
Figure 14.7.1-7 Caricature of a pulse traveling along an axon segment EMPTY 98
Figure 14.7.1-8 The action potential (collector waveform) at a Node of Ranvier of the rat 100
Figure 14.7.1-9 Signals recovered from the output of signal projection circuits 101
Figure 14.7.3-1 Generator and action potentials from impaled eccentric cell 105
Figure 14.7.3-2 Measured data from eccentric cell of Limulus 106

Figure 14.7.3-3 Simultaneous recordings from retinula and eccentric cells 108
Figure 14.7.3-4 Responses evoked by flashes of light versus temperature in Limulus 110
Figure 14.7.3-5 Long responses to steps of light in Limulus 112
Figure 14.7.3-6 Spontaneous and visually driven responses of cat geniculate cell *in-vivo* 116
Figure 14.7.3-7 Waveforms from Destexhe et al. of a stage 3A neuron 119
Figure 14.7.4-1 Action potential rate for four ganglion neurons 123
Figure 14.7.4-2 Distribution of spontaneous discharge rates for normal cats (n = 11) 125

(Active) SUBJECT INDEX (using advanced indexing option)

95% 128
99% 128
acetylcholine 125
action potential . . 2, 10-12, 17, 19, 21-23, 27, 31, 36-38, 40, 44-46, 53, 57, 62, 65, 67, 76, 83, 84, 88, 90, 93, 96, 99, 100, 103, 105, 109, 113, 114, 118, 119, 121-123, 125-127
Activa 8, 17, 19, 31, 32, 35, 38, 40, 45, 46, 48, 69-71, 73-77, 81-83, 92, 93, 100, 115, 118, 122, 123
active diode 31, 32, 120
acuity 29
acupuncture 16
adaptation 26, 33, 35, 42, 56, 65, 90, 97, 105, 107, 113, 114, 118, 124, 126
afterimage 35
alarm mode 10, 19, 37, 38, 54
amplification 31, 40, 73
analytical mode 25-27
arborization 28, 56, 119
association areas 48
astrocyte 30, 86, 87
attention 2, 16, 18, 35
auditory nerve 10, 11, 43, 62, 64, 65, 68, 123, 125-127
autocorrelation 18
average velocity 17, 115
awareness mode 10, 16, 25-27, 54
axon segment 18, 31, 71, 75-77, 82, 92, 98-100, 122, 127
axoplasm 3, 40, 45, 46, 70, 77, 90, 93, 95, 103, 109, 113, 114, 120-123
bilayer 45
bipolar 1, 2, 11, 21, 22, 26, 31, 33-35, 38, 39, 44, 49, 53, 56, 71, 80, 83, 84, 89, 90, 96, 97, 100, 104, 108, 114, 115, 127
bistratified 119, 122
bit serial 47
broadband 11, 68, 125, 126, 131
calibration 108
Central Nervous System 1, 2, 16, 47
cerebellum 27, 28
cerebrum 48, 49, 57
circadian rhythm 3
clock 117, 125
coaxial cable 17, 20, 77
cochlear microphonic 131
cochlear nucleus 10, 11, 123, 125
cochlear partition 15, 16
cochleotopic 13
colliculus 6, 16, 27
commissure 2, 6, 24, 47, 57, 74, 85-88, 103
compensation 106
compound eye 26, 104, 114
computation 26, 58, 117
computational 1, 13, 15, 16, 58, 121
computational anatomy 1, 13, 15, 16, 58
conduction velocity 114
conexus 49, 100
cross-section 11
cuticular plate 44
database 42, 130
decoder 13, 49, 53, 100, 131
dendrolemma 92, 104
diencephalon 16
diode 31, 32, 40, 81, 82, 118, 120, 123

dynamic range 12, 18, 21, 124, 126
eccentric cell 89, 90, 93, 104-108, 110, 114
Electrolytic Theory of the Neuron 122, 125
electrostenolytic process 125
encoder 20, 53
evolution 105
expanded 37, 63, 80, 115
feedback 40, 114, 124
Fourier transform 1, 16
free-running 11, 31, 37, 38, 80, 83, 92-95, 108, 115, 124
frequency of occurrence 97
fusion frequency 25
GABA 121, 125
ganglion neuron 10, 16-19, 21, 31, 32, 43-45, 53, 60, 76, 88, 89, 119, 124
glia 30
glutamate 125
group velocity 74
Hensen's stripe 126
hydronium 71
ice 16
impedance measurements 117
inferior colliculus 16
inflated 87
instantaneous velocity 17
intelligence 18
interp 15, 16
inverting 20, 31, 71, 90, 119, 124
IRIG 19, 20
kaumotopic 66, 124
latency 10, 11, 68
lateral geniculate 14, 15, 41, 116
layer 4C 103
lgn/occipital 30, 31
light adaptation 35
Limulus 3, 89, 90, 93, 104-108, 110, 112-114
locomotion 27
LOT 115
masking 123
Medulla 4
mesotopic 66, 124
Meyer's loop 30
midbrain 6, 27, 80, 82, 83, 102, 103, 115
modulation 3, 12, 13, 19, 29, 32, 33, 36-39, 43, 59, 60, 62, 65, 113, 124, 127, 129-131
monopolar 1, 10, 11, 18, 19, 21, 22, 31, 33, 37, 44, 49, 53, 80, 83, 84, 89, 90, 96, 97, 100, 105, 114, 122, 127
monopulse 80, 83, 90, 92-96, 98-100, 108, 113, 119, 120, 122
monopulse oscillator 80, 92-96, 98, 99, 108, 113
MRI 86
multi-dimensional 48
myelin 42, 69, 77, 86
myelinated 1, 5, 6, 11, 12, 17, 18, 20, 30, 47, 85, 86, 98, 114, 121, 122, 128
Myelination 5, 30, 82, 85, 87, 104
narrow band 35
navigation 56, 131
neural coding 13, 36
neurite 31, 120, 127
neurites 69, 71, 73, 119
neurotransmitter 121
node A 123
node E 60
node E' 8
Node of Ranvier 2, 11, 20, 43, 75, 77, 82, 83, 90, 92, 98-100, 104, 115, 123, 128, 131

noise 11, 18, 19, 23, 33, 37, 48, 50, 54, 63, 66, 101, 123, 131
non-inverting 31, 71, 119, 124
n- 25, 29, 56, 129
OHC 11, 44, 64, 65, 67, 68, 124, 126, 131
oligodendroglia 86
P/D equation 109, 113
parametric 19, 23
parvocellular 21, 31, 35, 98, 116, 117
pedestal 67, 90, 91
perigeniculate 15
perilymph 46
pgn/pulvinar 30, 31
phase velocity 30
phase-locking 59
phylogenic tree 3, 23
place code 19, 21, 23
pnp 20
poda 120
podites 74, 120
poditic 40, 48, 71, 73, 92, 119, 122
POS 27
Pretectum 25, 27, 29, 57, 103
probabilistic 17
propagation velocity 77, 82
protocol 18, 60, 102, 124, 131
pseudo-action potential 46
pulse-to-pulse 30, 31, 83, 100, 124
pulvinar 15, 16, 30, 31, 36, 41, 48
Pulvinar pathway 36
pyramid neuron 119, 120
rate code 18, 19
rectifier 40, 63, 76
refractory period 93
residue 125
resonance 86
saliency map 27, 28, 48
serape 120
servo loop 25, 130
short term memory 25
spatial dispersion 26
spectrogram 97
spinal cord 85, 122
spiral ganglia 8, 10, 11, 16, 127
SPL 61, 66, 124
stage 1 . . . . . 2, 12, 30, 31, 89, 93, 97, 102, 124, 126
stage 2 . . . . . 2, 12, 31, 39, 41, 50, 62, 67, 68, 74, 81, 88-90, 93, 105, 108, 114, 119, 124, 126, 128
stage 3 . . 2-4, 6-13, 17-19, 21, 24, 26, 30-33, 37, 38, 41-47, 49, 50, 52-54, 57-61, 64, 66, 67, 69, 74, 75, 79, 81-86, 88-90, 97, 98, 100-105, 114, 117, 121-126, 130, 131
stage 3A 20, 22, 30-32, 52, 88, 118-120, 122
stage 3B 30-32, 47, 48, 52, 88
stage 3BP 47, 49
stage 4 . . . . . 2, 10, 11, 19, 49, 68, 81, 84, 88, 100, 114, 117
stage 5 10
stage 6 . . . . . 127, 128
stage 7 128
stellate 2, 9, 10, 16-18, 31, 40, 43, 44, 49-53, 57, 74-76, 79, 80, 82-84, 88, 89, 100, 101, 103, 114, 125
stellate cell 10, 31, 49, 52, 57, 74-76, 80, 83, 84, 100, 103
stellate neuron 16-18, 31, 52, 88, 89
stellite 23
stress 56, 68

superior colliculus 6, 27
synaesthesia 48
synapse 1, 3, 12, 19, 31, 32, 40, 71, 73, 75, 76, 79, 81-84, 92, 118-123, 127, 128
telemetry 20
thalamus 41, 49, 85, 86, 117
three-terminal 32, 119, 123
threshold 19, 27, 39-41, 45, 60, 83, 91-93, 96, 100, 109, 115
tinnitus 48
tonotopic 11, 13, 14
topography 69, 77, 104
topology 2, 8, 69, 77, 104
tractography 86
translation 16, 32
trapezoidal body 9, 16
tremor 5, 26, 27, 33, 40, 41, 56, 129-131
type B 11, 67
type I 11
type II 11
type N 9, 11, 38, 67
verification 92
visual cortex 69, 103
volition mode 28
volley theory 58
white matter 85, 86
Wikipedia 18, 85
word serial 47-49
word serial/bit parallel 47-49
xxx . . 5, 6, 11-17, 20, 23, 30-32, 34, 39, 40, 42, 46, 48, 49, 55-57, 59, 62, 68, 69, 71, 80, 85, 87, 88, 90, 94, 97, 100, 101, 104, 122, 124, 126, 128-131
[xxx 1, 3, 9-12, 30, 33, 36, 39, 40, 43, 44, 47, 57-59, 62, 63, 66-69, 83, 85, 86, 103, 120, 123-125, 128, 131